

BEHAVIOUR OF REINFORCED CONCRETE JOINTS

BEHAVIOUR OF REINFORCED CONCRETE JOINTS

by

SAAD E.A. SALLAM, B.Sc., M.Eng.

A Thesis

Submitted to the Faculty of Graduate Studies

in Partial Fulfillment of the Requirements

for the Degree

Doctor of Philosophy

© SAAD E.A. SALLAM 1978

McMaster University

April, 1978

To My Dear Wife SANAA

whose

Patience, Understanding, and Assistance

are deeply appreciated.

DOCTOR OF PHILOSOPHY (1978) .

McMASTER UNIVERSITY

(Civil Engineering)

Hamilton, Ontario

TITLE: Behaviour of Reinforced Concrete Joints

AUTHOR: Saad Eldin Abdalla Sallam, B.Sc. (Cairo Univ.)

M.Eng. (McMaster Univ.)

SUPERVISOR: Dr. R.G. Drysdale

NUMBER OF PAGES: xvii, 308

ACKNOWLEDGEMENTS

I wish to express my sincere gratitude to Dr. R.G. Drysdale for his guidance and interest during the course of this study. It has been a privilege and a pleasure to work under his supervision.

I am also indebted to the members of my supervisory committee, Dr. A.C. Heidebrecht, Dr. J. Morrison, Dr. G.AE. Oravas, and Dr. H. Robinson for their valuable suggestions.

I would like to take this opportunity to thank McMaster University, and the National Research Council of Canada for financial support, and Dr. J.J. Emery for lending his computer subroutines.

Last but not the least, I must mention my deepest appreciation to my parents, without whose help and encouragement this thesis would have been difficult to complete.

ABSTRACT

No rigorous explanation exists for the behaviour of reinforced concrete joints. The lack of understanding the complex interaction may account for continued use of inadequate joint details particularly for knee joints subjected to opening moments. The object of this research was to provide a better understanding of joint behaviour through a combined experimental and analytical investigation.

In the experimental program, 6 specimens with different types of joint details were tested under opening moment. These details reflected recent recommendations by other investigators and some adaptations of their ideas. The results served as evidence of the ability to produce effective and simple details as well as serving as a basis for evaluating the reliability of the analytical model.

A method of analysis has been developed using the finite element method to model the behaviour of reinforced concrete including the interactions between concrete and steel in the form of bond and dowel forces. One of the principle features of this method of analysis is the built in ability to trace the propagation, location and orientation of cracking. This feature was tested by comparing predicted behaviour of beams failing in shear and flexure with test results. Very good agreement with the well documented phenomena of various

modes of cracking and failure provided evidence of the validity of the analytical method.

The analyses of the joints reproduced cracking patterns and sequences as well as capacities which are quite close to the test results. The analytical information helped to identify the primary causes of failure or premature failure and thereby provided a more rational basis for suggesting alternate joint details which will behave much better than inadequate details which are currently recommended.

TABLE OF CONTENTS

	PAGE
CHAPTER 1: INTRODUCTION	
1.1 Foreward	1
1.2 Definitions	2
1.3 Purpose and Scope	4
1.3.1 Scope of the Experimental Progam	4
1.3.2 Scope of the Analytical Investigation	5
1.4 Outline and Resume of the Thesis	6
CHAPTER 2: LITERATURE REVIEW	
2.1 Introduction	8
2.2 Current and Previous Joint Detailing Practice	9
2.3 Experimental Research on Joints	13
2.3.1 Joints Subjected to Negative Bending Moment	13
2.3.2 Early Research on Corner Joints Subjected to Positive Bending Moment	14
2.3.3 Recent Research on Corner Joints Subjected to Positive Bending Moment	16
2.4 Development of the Finite Element Method in the Analysis of Reinforced Concrete Members	31
2.4.1 General Background	31
2.4.2 Development of the Finite Element Method	34

2.4.3	Analysis of Reinforced Concrete Using the Finite Element Method	36
2.5	The Force-Displacement Relationships for the Finite Element Analysis of Reinforced Concrete	39
2.5.1	The Bond-Slip Relationship	39
2.5.2	Dowel Action	45
2.5.3	Aggregate Interlock	47
2.6	Summary	50
CHAPTER 3: MATERIAL PROPERTIES, TEST SPECIMEN, AND EQUIPMENT AND INSTRUMENTATION.		
3.1	Introduction	51
3.2	Material Properties	52
3.2.1	Concrete Mix and Batching Procedure	52
3.2.2	Curing of the Concrete	55
3.2.3	Concrete Stress-Strain Relationship	55
3.2.4	Concrete In Tension	62
3.2.5	Reinforcing Steel	63
3.3	Development of the Shape of the Test Specimen	65
3.4	Preparations and Equipment for Joint Tests	67
3.4.1	Forms and Steel Reinforcing Cages	69
3.4.2	Preparation of the Specimens for Testing	69
3.5	Summary	74
CHAPTER 4: McMASTER UNIVERSITY JOINT TEST RESULTS		
4.1	Introduction	76
4.2	Requirements for Satisfactory Details	76

4.3	Choice of Different Details to be Tested	78
4.3.1	General	78
4.3.2	Descriptions of the Joint Details Tested	80
4.3.2.1	Detail (1)	80
4.3.2.2	Detail (2)	82
4.3.2.3	Detail (3)	83
4.3.2.4	Detail (4)	84
4.3.2.5	Detail (5)	85
4.3.2.6	Detail (6)	85
4.4	Test Procedure	86
4.4.1	Incrementally Increasing Load Tests	86
4.4.2	Test Procedure for Joints Subjected to Load Reversals, Details (5) and (6)	87
4.5	Test Results	89
4.5.1	General Behaviour	89
4.5.2	Cracking Patterns	95
4.6	Observations	110
CHAPTER 5: ANALYTICAL METHOD AND DESCRIPTION OF THE COMPUTER PROGRAM		
5.1	Introduction	112
5.2	Idealizations Introduced in the Finite Element Method of Analysis	113
5.3	Mathematical Formulation	116
5.3.1	Concrete and Steel Elements	116
5.3.2	Cracked Concrete Elements	120
5.3.3	Stirrup Elements	125
5.3.4	Joint Elements	127

5.4	Program Description	130
5.4.1	General	130
5.4.2	Function of the Main Program and the Sub- routines	131
5.4.3	Program Logic and Operation	133
5.4.4	Some Problems Associated with Finite Element Analysis for Reinforced Concrete	136
5.5	Additional Information	139
CHAPTER 6: APPLICATION OF THE FINITE ELEMENT METHOD TO SIMPLE REINFORCED CONCRETE BEAMS.		
6.1	Introduction	141
6.2	Test Data and Description of the Analyzed Beams	142
6.3	Summary of Test Results	148
6.4	Failure Criteria for Beams	151
6.4.1	General	151
6.4.2	Criteria of Failure for Concrete in Compression	152
6.4.3	Failure criteria for Concrete in Tension	153
6.4.4	Failure criteria for Bond Elements	154
6.4.5	Failure Criteria for Dowel action	156
6.4.6	Definition of Modes of Failure for Beams	158
6.5	Comparison of Experimental and Analytical Results	161
6.5.1	General	161
6.5.2	General Observations on Load-Deflection Results	161
6.5.3	Cracking Patterns and Failure Modes	166
6.5.3.1	Beam (4)	167

6.5.3.2	Beam (7/1)	171
6.5.3.3	Beam (9/1)	173
6.5.3.4	Beams EA1 & EB1	176
6.5.4	Detailed Behaviour of Beam (7/1) at different Loading Steps	181
6.6	Conclusion	194
CHAPTER 7: APPLICATION OF THE FINITE ELEMENT METHOD TO REINFORCED CONCRETE JOINTS		
7.1	Introduction	195
7.2	Failure Modes for Joints	197
7.3	Presentation of Analytical Results and Comparison with Test Results	199
7.3.1	General	199
7.3.2	Load-deflection Results	199
7.3.3	Moment-rotation Results	209
7.3.4	Discussion of Behaviour of Each Detail	216
7.3.4.1	Detail (1)	221
7.3.4.2	Detail (2)	224
7.3.4.3	Detail (3)	228
7.3.4.4	Details (4 & 5)	232
7.3.4.5	Detail (6)	246
7.4	Summary	248
CHAPTER 8: SUMMARY AND CONCLUSIONS		
8.1	Introduction	250
8.2	Summary of the Experimental Investigation	251

8.3	Summary of the Analytical Investigation	252
8.4	Final Conclusions	253
8.5	Suggestions for Future Research	255
APPENDIX A:	Computer Program Listing and Description of Subroutines	257

LIST OF FIGURES

FIGURE		PAGE
1.1	Definition of Reinforcing Steel Types in Joints	3
2.1	Detail Proposed by Robinson	10
2.2	Detail Proposed by Boughton for Tanks	10
2.3	Detail Proposed by Boughton for Frames	10
2.4	Details Suggested by The Institution of Structural Engineers in London	12
2.5	Detail Recommended by ACI 315-74	12
2.6	Wästlund Test Set-Up	15
2.7	Test Arrangement by Gumensky	15
2.8	Detail Suggested by Posey and Kofoid	15
2.9	Details of Corner Connection Reinforcement Tested by Beaufait and Williams	19
2.10	Details of Corner Connection Reinforcement Tested by Swann.	21
2.11	Test Arrangement and Dimensions of Test Specimens by Mayfield et.al.	23
2.12	Details of Corner Reinforcement by Mayfield et.al.	23
2.13	Details of Corner Reinforcement by Mayfield et.al.	25
2.14	Corner Details Suggested by Balint and Taylor	28
2.15	Unit Bond Stress vs Unit Slip	44
3.1	Typical Experimental Concrete Stress-Strain Diagram	57
3.2	Typical Axial Stress-Strain Diagram for Tension Tests of Number 6 Bar Specimens	64

3.3	Idealized Stress-Strain Curve for Steel Reinforcing Bars	66
3.4	Sketches of Possible Types of Test Specimens	68
3.5	Schematic Drawing of The Joint Specimen and Test Arrangement	71
3.6	Photograph showing Specimen Prepared for Testing	72
4.1	Steel Reinforcement Details Used in the Test Program	79
4.2	Load-Deflection Results for Tested Joint Details	90
4.3	Moment-Rotation Results for Tested Joint Details	92
4.4	Load-Deflection Results for 4 Cycles of Loading, Detail (5)	93
4.5	Load-Deflection Results for 4 Cycles of Loading, Detail (6)	94
4.6	Experimental Cracking Pattern at Failure for Detail (1)	96
4.7	Experimental Cracking Pattern at Failure for Detail (2)	97
4.8	Experimental Cracking Pattern at Failure for Detail (3)	98
4.9	Experimental Cracking Pattern at Failure for Detail (4)	99
4.10	Experimental Cracking Pattern after first Cycle of Loading with Opening Moment for Detail (5)	100
4.11	Experimental Cracking Pattern after first Cycle of Loading with Opening Moment for Detail (6)	101
4.12	Joint Detail (3) after Failure	103
4.13	Joint Detail (4) after Failure	104
4.14	Joint Detail (5) after Failure	105
4.15	Joint Detail (6) after Failure	106
4.16	Possible Crack Types in Joint Region	108

5.1	Finite Element Idealization of a Simple Beam	115
5.2	Idealization of a Cracked Concrete Element	123
5.3	Idealization of Stirrup Elements	126
5.4	Joint Element Representation	129
5.5.	Computer Program Organization of the Main Program and the Subroutine	132
5.6	Pure Bending of the Beam Solved by a Coarse Sub-Division	137
6.1a	Dimensions of the Analyzed Beams	147
6.1b	Stress-Strain Diagram for Steel Used in Leonhardt and Walther's Beams	147
6.2	Crack and Failure Pictures for Leonhardt and Walther's Beams	149
6.3	Dowel Stresses in Beams	157
6.4	Load-Deflection Results of Beams (7/1)	162
6.5	Load-Deflection Results of Beam (9/1)	163
6.6	Load-Deflection Results of Beam EA1	164
6.7	Load-Deflection Results of Beam EB1 and EB2	165
6.8	Cracking Pattern Results for Beam (4)	168
6.9	Cracking Pattern Results for Beam(7/1)	172
6.10	Cracking Pattern Results for Beam (9/1)	174
6.11	Cracking Pattern Results for Beam (EA1)	178
6.12	Cracking Pattern Results for Beam (EB1)	179
6.13 - 6.35	Details of Crack Propagation and Concrete, Steel and Bond-Stress Distributions for Beam (7/1) at Different Stages of Loading	182-193

7.1	Finite Element Mesh Used for Analysis of Detail (2).	201
7.2	Finite Element Mesh Used for Analysis of Detail (3)	202
7.3	Finite Element Mesh Used for Analysis of Details (1, 5, and 6)	203
7.4	Load-Deflection Results for Detail (2)	205
7.5	Load-Deflection Results for Detail (3)	207
7.6	Experimental and Analytical Moment-Rotation Results for Detail (1)	210
7.7	Experimental and Analytical Moment-Rotation Results for Detail (2)	211
7.8	Experimental and Analytical Moment-Rotation Results for Detail (3)	212
7.9	Experimental and Analytical Moment-Rotation Results for Detail (4 & 5)	213
7.10	Experimental and Analytical Moment-Rotation Results for Detail (6)	214
7.11	Predicted Cracking pattern for Detail (1)	222
7.12	Predicted Cracking Pattern for Detail (2), Using the Same Amount of Diagonal Stirrups as that for the test	225
7.13	Predicted Cracking Pattern for Detail (2'), Same as Detail (2), but Using Heavier Diagonal Stirrups	227
7.14	Predicted Cracking Pattern for Detail (3), Diagonal Bar Properly Anchored in the Compression Zones.	229

7.15	Predicted Cracking Pattern for Detail (3'), Same as Detail (3) but with Poor Anchorage of the Diagonal Bar Ends.	231
7.16	Predicted Cracking Patterns for Details (4 & 5)	234
7.17	Experimental vs Analytical Strain Diagrams before Cracking	237
7.18	Strain Diagrams at Different Sections in the Constant Moment Region for Details (4 & 5)	239
7.19	Concrete Strain Distribution in the Normal and Tangent Directions to the Corner Diagonals for Details (4 & 5)	241
7.20	Localized Steel Stresses at Different Load Levels From the Analysis of Details (4 & 5)	243
7.21	Stresses in Diagonal Bar at Different Load Levels for Details (4 & 5)	244
7.22	Bond Stresses at Different Loading Stages along the Main Reinforcement for Details (4 & 5)	245
7.23	Predicted Cracking Patterns for Detail (6)	247

CHAPTER 1
INTRODUCTION

1.1 Foreword

This thesis deals with a field of concrete research on which relatively little previous work has been done. The topic of this investigation is the behaviour of the joint between reinforced concrete beams and columns or between other intersecting members.

The advantages of modern design theories including the ultimate strength design method may be negated to a certain extent by the apparent lack of information on joint behaviour and joint detailing. In fact, it has been shown (50, 58, 74, 91, 97) that in many cases the capacity of members cannot be utilized because of inadequate capacity of joints. The lack of adequate information about the interaction of beams and columns at their intersections is reflected by the omission of this topic in textbooks (96) and by the rather noncommittal recommendations contained in Section 7.11 of ACI 318-71, "Building Code Requirements for Reinforced Concrete" (69).

Recently ACI-ASCE Committee 352 published "Recommendations for Design of Beam-Column Joints in Monolithic Reinforced Concrete Structures" (104). However, these recommendations are restricted to joints other than knee joints which is the particular subject of this dissertation. Considering the possible range

of variables, the inapplicability of the traditional analytical methods, and the complexity of behaviour, it is not surprising that no comprehensive evaluation of this problem is available.

Many parameters may influence the behaviour of reinforced concrete joints. The effects of altering some of these parameters are not known. Some important parameters to be considered are:

- (1) details of the steel reinforcing bars used in the joint region,
- (2) properties of the materials used,
- (3) physical dimensions of the intersecting members,
- (4) steel percentage used for both the intersecting members and the joint region,¹
- (5) anchorage length provided for reinforcing bars in the joint region,
- (6) number and size of stirrups used, if any, and their shape.

The large number of parameters involved and the inherent complexity of a theoretical solution have so far precluded a thorough study of the effects of the above parameters.

1.2 Definitions

The definitions listed below are provided to avoid the need for repeating lengthy descriptions or explanations in the text.

Diagonal Bar is a reinforcing bar which is placed diagonally as close to the inside corner of the joint as the cover will allow (see Fig. 1.1). The cross-sectional area of this type of reinforcement will be denoted as A_{sd} .

Diagonal Stirrups are stirrups placed diagonally to join the inside and outside corners of the joint, as shown in Fig. 1.1.

Their cross-sectional area is denoted as A_{st} .

Joint, unless otherwise stated, the word, "Joint" will be used in place of "knee or corner beam-column connection subjected to positive movement which tends to open the angle between the intersecting members".

Joint Efficiency is the ratio between an experimentally or analytically obtained capacity and the theoretical flexural capacity of the larger of the two intersecting members.

Joint Element is an element which joins steel and concrete elements at their interface in the finite element analysis and which represents bond-slip and dowel action. The same joint element may be called a bond and/or a dowel element (linkage).

Positive or Negative Moments are bending moments which tends to open or close the angle at the joint respectively.

Theoretical Capacity is the flexural capacity calculated using statics and the Whitney stress block (96) representation for concrete in compression.

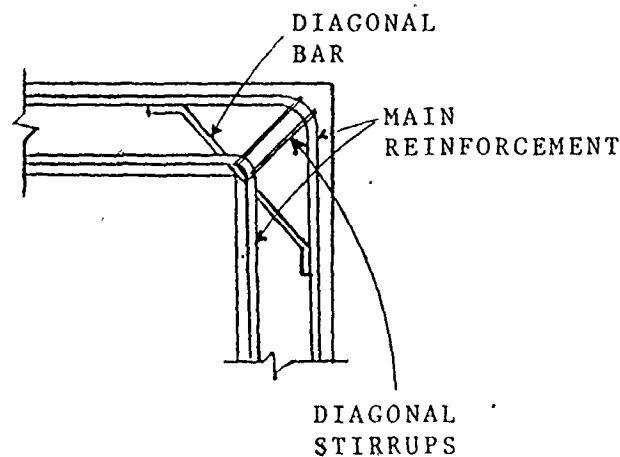


Fig. 1.1 DEFINITION OF REINFORCING STEEL TYPES IN JOINTS

1.3 Purpose and Scope

The primary objective of this investigation was to contribute to the knowledge of the behaviour of reinforced concrete joints. In a more restrictive sense the major area of investigation was concerned with the behaviour of joints subjected to positive moment. It was decided that both experimental and analytical studies would be undertaken. The experimental program would provide personal experience with testing joints and would help to gain a physical appreciation of their behaviour as well as providing well documented data for comparison with results from the analytical study. Because of the range of the range of the parameters involved, development of an analytical method was necessary in order to compliment the experimental program and provide a means for extending the study in the future.

1.3.1 Scope of the Experimental Program

An extensive experimental program was not within the scope of this investigation. Other investigators (74,97) who have done extensive testing with relatively little theoretical interpretation have not been able to provide a thorough explanation of the behaviour of joints. Therefore, the major emphasis of the experimental part of this study was to provide reliable data which could be used to confirm the adequacy of the analytical model. However, an important consideration was also to try to develop a simple and more efficient detail which could improve current practice.

The test specimen, loading conditions, method of testing and range of variables were chosen so that the test results would be

as informative in themselves as possible, and the number of tests would be minimized while still providing a reasonable basis for comparison with the analytical results. It was preferred that the specimen dimensions be as large as was practical in order to reduce doubts concerning size effects when relating test values to actual structures. In addition, fabrication tolerances would be less significant for larger overall dimensions.

1.3.2 Scope of the Analytical Investigation

The main objectives of the analytical investigation was to develop an analytical model to predict the behaviour of reinforced concrete joints. (However, it was anticipated that this would be a useful tool for studying other structural elements.) This analytical model should take into account the important aspects which affect the behaviour of reinforced concrete structures.

A review of the major factors involved in the behaviour of reinforced concrete will help to identify difficulties associated with developing such a method of analysis. Ngo and Scordelis (39) indicated that some of these difficulties are as follows:

1. Non-homogeneity of concrete and its non-linear stress-strain relationship.
2. Intricate interaction of steel and concrete relative to bond-slip characteristics and dowel action.
3. Time-dependent deformation of concrete.
4. Cracking and crack propagation with accompanying changes in stiffness.
5. Aggregate interlock and dowel effects varying with crack propagation.
6. Limited knowledge of the response of concrete

subjected to biaxial and triaxial states of stress.

Earlier studies of these aspects and the experience of others (68,99), indicated that conventional methods of analysis would not adequately accommodate inclusion of these aspects. That is, use of plane section behaviour with assumed elastic or elastic-plastic materials would not be acceptable for developing an envisioned analytical procedure which could more adequately incorporate the influences of the above effects. Thus, it was concluded that the nature of reinforced concrete, coupled with the complexities of the joint behaviour itself, required adaptation and development of more sophisticated analytical methods to facilitate a more detailed and accurate investigation.

The development of high speed digital computers and the formulation of the finite element method permit the development of an efficient analytical model which can result in a more realistic evaluation of the behaviour of reinforced concrete structures.

It was intended that the development of this analytical tool would contribute to the knowledge of joints and that this tool would also help in the development of rules for the design of efficient joints. It was thought that particular emphasis should be placed on the modelling of cracking and crack propagation as a means of evaluating effects of different joint details on the behaviour of joints.

1.4 Outline and Resume of the Thesis

To help the reader follow the organization of the material in this thesis, the following outline is presented.

Chapter 2 contains a review of selected literature covering the following:

1. Testing and detailing of reinforced concrete joints.
2. Development and use of the finite element method.
3. Load-deformation characteristics for materials used in connection with the analytical method.

Chapter 3 contains a description of the test specimen and the test set-up. Also the basic material properties which are required in the analysis are reported and discussed. The experimental results of the six joints tested are reported in Chapter 4 and general observations on the behaviour and relative merits of different joint details are made. In Chapter 5, the description of the method of analysis and the development of the computer program are given. To provide an alternate method for evaluating the reliability of the computer program, analytical results for simply supported reinforced concrete beams are presented and compared with test results in Chapter 6. An evaluation of these results including the effects of variations of different parameters were discussed because of the interesting nature of the findings. The analytical results for joints are presented and compared with the experimental data in Chapter 7. In all these chapters pertinent observations and conclusions are made as they become apparent. Finally in Chapter 8, a brief summary of the results of the experimental and analytical work and the final conclusions are presented along with some recommendations for future research.

CHAPTER 2

LITERATURE REVIEW

2.1 Introduction

As discussed in Chapter 1, study of the problem under consideration requires a basic understanding of behaviour of reinforced concrete members and the properties of the materials. These aspects will be discussed in the chapters where they are used. This chapter will be devoted to a review of the pertinent literature dealing with the particular problems focused-on in this thesis.

The literature review is organized into three major groupings, each dealing with information related to specific aspects of this investigation. These are:

- a. Details of tests on Beam-Column joints.
- b. Theoretical Modelling of reinforced concrete structures using the finite element method.
- c. Description of Force-Displacement relationships for use in the finite element analysis of reinforced concrete.

Other literature which is relevant but more commonly used is not reviewed here but is referenced throughout the text. Some of the references reported in the following sections were

not directly available to the author. Summaries or translations of these were found in other publications. Reference to the original publication is included in the review for the sake of completeness. These references are identified with square brackets in the Bibliography and the publications in which they were summarized are shown at the end of each reference.

2.2 Current and Previous Joint Detailing Practice:

In this section a selection of the most frequently used reinforcing details for corner joints subjected to positive bending are reported. (1, 2, 3, 4, 6, 19, 20, 52, 63, 74, 91, 97, 100, 103). Some of these details as well as some others were investigated by the author.

In 1964, Robinson (20) suggested the reinforcements detail shown in Fig. 2.1 for piers, ~~abutments~~ for bridges.

Boughton proposed the detail shown in Fig. 2.2 for square water tanks in the design aid, "Reinforced Concrete Detailers' Manual", (52) London 1969. He also suggests the detail in Fig. 2.3, for corners in frames subjected to positive moment.

For corners subjected to positive moment the report, "Standard Method of Detailing Reinforced Concrete", by the Concrete Society in conjunction with the Institution of Structural Engineers in London, 1970 (63), provides the following recommendations for corner reinforcing details

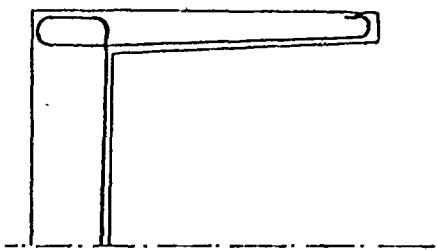


Fig 2.1 DETAIL PROPOSED BY ROBINSON (20)

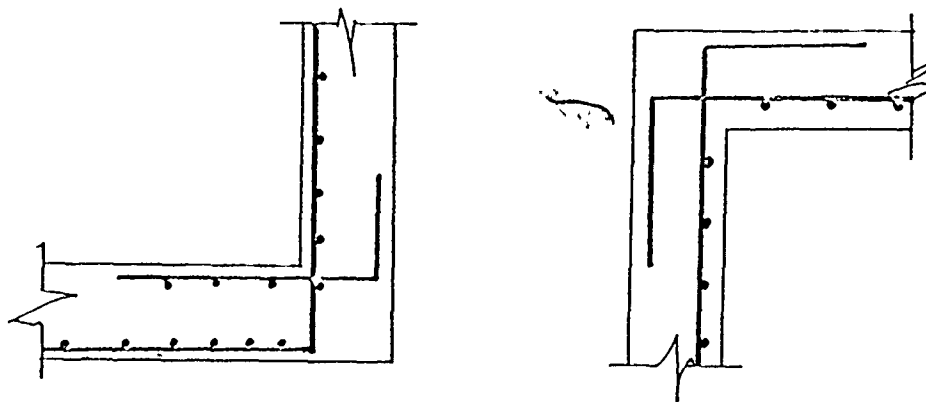


Fig. 2.2 DETAIL PROPOSED BY BOUGHTON (52)
FOR TANKS.

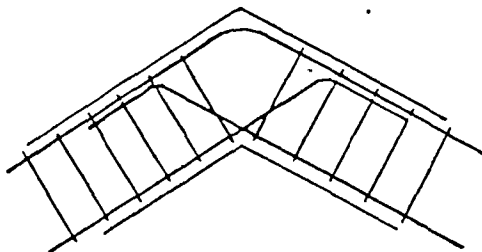


Fig. 2.3 DETAIL PROPOSED BY BOUGHTON (52)
FOR FRAMES.

as indicated in Fig. 2.4: "Looped bars as shown in figure (a) should be avoided. Better arrangements consist of two straight bars with right-angle bends sufficient to provide proper anchorage (figure (b)) or two hairpin bars (figure (c))".

The simple corner detail shown in Fig. 2.5 was recommended in 1974 by ACI Committee 315, "Manual of Standard Practice for Detailing Reinforced Concrete Structures" (100).

In 1976, the ACI-ASCE Joint Committee 352 report "Recommendations for Design of Beam-Column Joints in Monolithic Reinforced Concrete Structures" (104) provided tentative recommendations for proportioning and detailing of beam-column joints in monolithic reinforced concrete structures. Several limitations were imposed on the recommendations. The following paragraph, probably represents the most noteworthy restriction relative to this research investigation: "It should be noted that shear provisions cited above may not be applicable to joints in which only two members meet, such as knee joints or where the column above the joint is considerably smaller than the one below. All data cited above were obtained from tests of joints with columns above and below the core. Special problems often arise with corner or knee joints. Knee and corner joints require special reinforcement to prevent failures produced by bursting or spalling stresses in the joint. Results of tests of corner and knee joints are reported in the literature, and methods for reinforcing such joints are presented therein."

Looped bars as shown in figure (a) should be avoided. Better arrangements consist of two straight bars with right-angle bends sufficient to provide proper anchorage (figure (b)) or two halfpin bars (figure (c)).

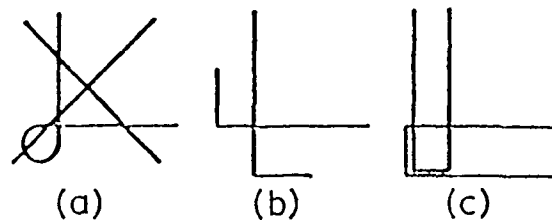
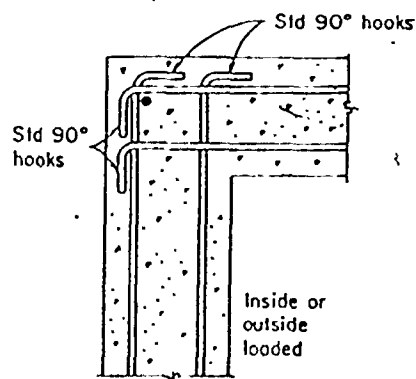


Fig. 2.4. DETAILS SUGGESTED BY THE INSTITUTION OF STRUCTURAL ENGINEERS IN LONDON.
(Reproduced from Reference 63)



Typical corner detail

Fig. 2.5. DETAIL RECOMMENDED BY ACI 315-74.
(Reproduced from Reference 100)

The above certainly indicates the difficulty in understanding and detailing corner joints. In addition it should be mentioned here that the above statement that methods for reinforcing are available should be qualified to indicate that not all of the suggestions are adequate.

2.3 Experimental Research on Joints.

In this section both early (pre 1945) and more recent research on corner joints are summarized. Special attention is given to joints subjected to positive bending moment.

2.3.1 Joints subjected to Negative Bending Moment:

In 1934 (1) and more recently (4, 19, 74, 91, 97), it has been shown that when a corner is subjected to a negative bending moment, detailing presents no major difficulties. It was shown (91, 97) that when the tension reinforcement is detailed, as is commonly done, so that it passes around the outside of the corner joint, no serious loss of efficiency should be anticipated. One reason for premature failures in corner joints subjected to negative bending moment is the possibility of a splitting failure under the bend of the reinforcing bar (Fig: 1.I). Experimental investigations (1, 2, 3) showed that the ability to develop higher steel stress prior to splitting failure in the concrete increased with the radius of curvature of the bend, but not in direct proportion. However, it was shown (65) that no such splitting failure should be expected if the current codes' (63, 69)

recommendations regulating the bend radii for reinforcing bars are observed.

This brief review was included to indicate that there are no major problems with these joints under negative moments.

2.3.2 Early Research on Corner Joints Subjected to Positive Bending Moment:

Pioneer studies of corners subjected to positive bending moment dealt mainly with looped patterns of reinforcement. Use of loops was regarded as the most obvious way of placing the reinforcement in a corner. Wästlund (1, 2, 3) systematically investigated the capacity of concrete to resist bearing stresses caused by such reinforcing loops. This large number of tests demonstrated that understanding the behaviour of these corners was not a simple problem. In order to try to determine the possible influences of the various factors, a number of test series were carried out in which the concrete quality, the radius of curvature of the loop, the width of the concrete specimen perpendicular to the plane of the loop and the model scale was systematically varied. Fig. 2.6 illustrates the type of angle beam specimen which was used in this investigation. Concrete having a cube strength of 190 kg/cm^2 (2700 psi) and plain bars were used in most of the tests. Steel stresses at failure were reported to be from 2,000 to 3,000 kg/cm^2 (28.5 to 42.5 ksi). These values are appreciably below the strengths of the presently used steel and concrete. Another essential difference is that the currently used deformed bars have different bond characteristics than the plain bars which were used for

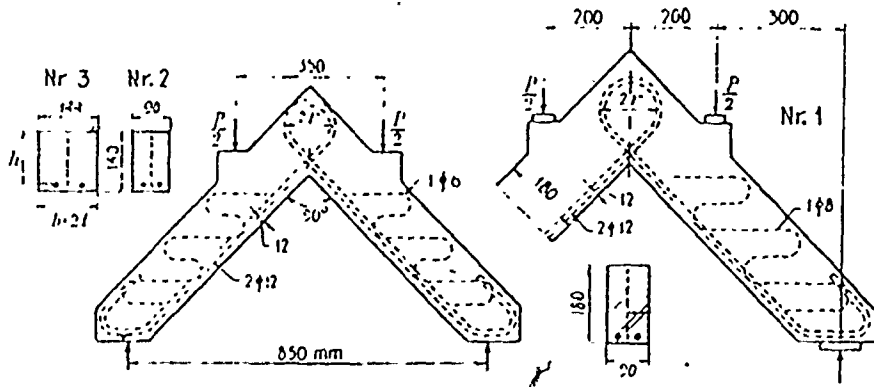


Fig. 2-6. WÄSTLUND TEST SET-UP (1)
 (Reproduced from Reference 97)

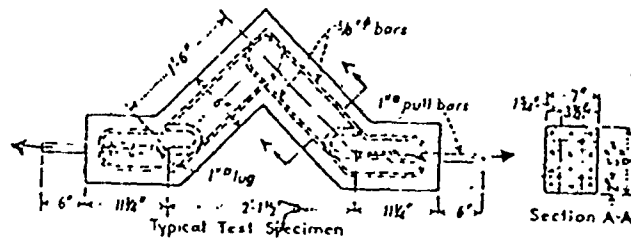


Fig. 2-7. TEST ARRANGEMENT BY GUMENSKY (4)
 (Reproduced from Reference 97)

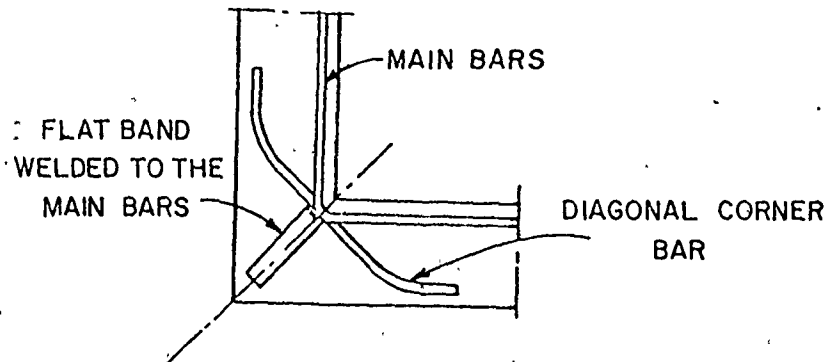


Fig. 2-8. DETAIL SUGGESTED BY POSEY AND KOFOID.
 (Reproduced from Reference 6)

these tests. As a result of Wästlund's experimental work, some empirical equations were derived to obtain the steel stresses on failure of the concrete. However, the applicability of these equations to current conditions is limited.

Gumensky, (4) in the U.S.A. carried out tests in 1939 on concrete corners in tension. He used the simple test specimen and loading arrangement sketched in Fig. 2.7. Five reinforcing patterns were compared. It was found advantageous to use reinforcing loops in combination with a cross bar in a fillet. In 1943, Posey and Kofoed (6), carried out tests on concrete corners with a test method similar to that of Gumensky (4). They developed the corner detail reproduced in Fig. 2.8. It consisted of main bars which were bent very tightly around the inner corner and which were supplemented by diagonal corner bars, and flat bands welded to the main reinforcement. They found this detail to be superior to using loops. Although the detail looks different the same general idea was developed in the 1970's by Mayfield, et. al. (74, 91).

The pioneering work reported in this section was of a great value. The problems and difficulties in detailing joints subjected to positive moment were pointed out. However, none of the details developed 100% efficiency even with the low concrete and steel strengths used at the time of these investigations.

2.3.3 Recent Research on Corner Joints Subjected to Positive Bending Moment:

Relatively few researchers have reported studies on the particular subject of this thesis, reinforced concrete joints. The main purpose here is to gather the available information on corner joints subjected to positive moment. This information is included to provide a broader background for understanding of the problem. In this section an overall review of the subject is presented. Then special concentration on corner joints subjected to positive bending moment follows to assist in understanding how these results influenced the course of this study.

Although little information on the actual behaviour of joints in buildings was available, Hanson and Connor (41) in 1967 commented that, "Where unsatisfactory performance during earthquake shocks is observed, it can usually be attributed to quality of materials or construction, or to poor reinforcement details in the structural joints." They considered that unsatisfactory details of joint reinforcement were not limited to seismic design, but that good design practice requires that joints be designed to be as strong as the adjoining members.

In 1968, Beaufait and Williams (50), in a preliminary investigation on the behaviour of reinforced concrete frames, also considered reinforcing details which were later (65) described as "classic" detailing errors. Beaufait and Williams tested a series of pin-supported portal frames subjected to

either a repeated, reversible, horizontal sway force, or a single horizontal sway force, at the level of the beam. The objectives of their preliminary project were to study the effects of the loading on the ultimate strength of the concrete frame, and to investigate the influence of different patterns of reinforcement at the corner joints. The three corner details tested are shown in Fig. 2.9. Their results showed that the distribution of the reinforcement at the joint influenced the response of the structure. Detail (a) resulted in a rather sudden collapse of the frame due to the lack of continuity of the reinforcement. Detail (b) exhibited more ductility than (a). Detail (c) had the highest load capacity of those frames which were loaded to failure by a single horizontal force. It had less than 39% efficiency and failed due to the tendency of the tension bars to straighten out. The details tested were not examples of good design. However, the tests clearly indicated what kind of corner details should be avoided. Beaufait and Williams concluded that "the placement of reinforcement at the joints is critical and the manner in which continuity of the reinforcement is developed at the joints can and does have a very definite influence on the behaviour of the structure."

Swann (58, 66), in 1969 and 1970, found that some detailing arrangements in current practice were not as strong as other, less conventional joint details. The object of his preliminary investigation was to obtain data on details in common use and to develop more efficient ones.

Specimens representing the right-angle bend of a

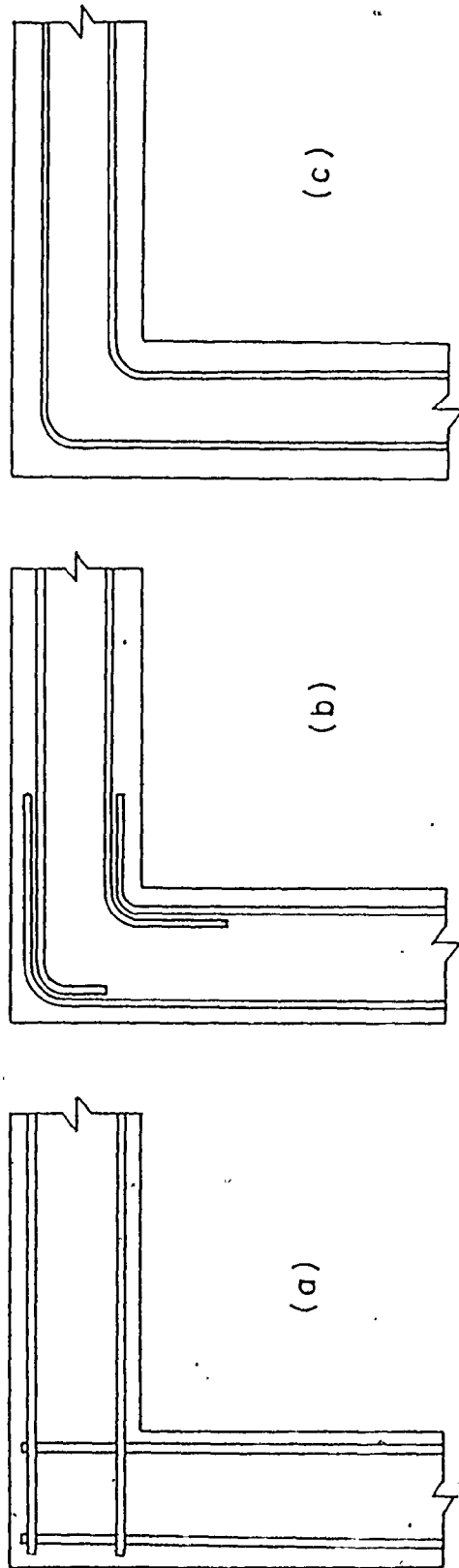


Fig.2.9 DETAILS OF CORNER CONNECTION-REINFORCEMENT
TESTED BY BEAUFIT AND WILLIAMS (50)

portal frame were tested with both positive and negative bending moment. The detailing arrangements shown in Fig. 2.10, range, as Swann indicated from the simplest possible arrangements, Details (1) and (2), through details having varying degrees of popularity, Details (3), (4), (5), (6) and (7), to innovations specifically designed to resist the anticipated forces such as Details (8), (9) and (10).

For positive bending moments, Swann found that Details (9) and (10) performed significantly better than the others. In cases where the bending moment tended to close the right angle, bearing failure of the concrete occurred at the bends of the main reinforcement. Swann's specimens had at least 3% tension reinforcement ratios. This may in part explain why some of the low joint efficiencies were obtained. The work by Swann pointed out deficiencies in detailing practice but did not result in any new detailing proposals.

In 1970 Mayfield et al. (74, 91) started an extensive experimental program at the University of Nottingham, England. Devoted mainly to investigating the effects of corner detailing on lightweight concrete, the program was carried out in two stages. In the first stage 48 reinforced lightweight concrete corners were tested. The effects of 12 types of reinforcement details on ultimate strength, stiffness and cracking were studied. The test results were reported jointly by Mayfield, Kong, Bennison and Davies (74). The test arrangement and dimensions of the test specimen as well as the 12 details

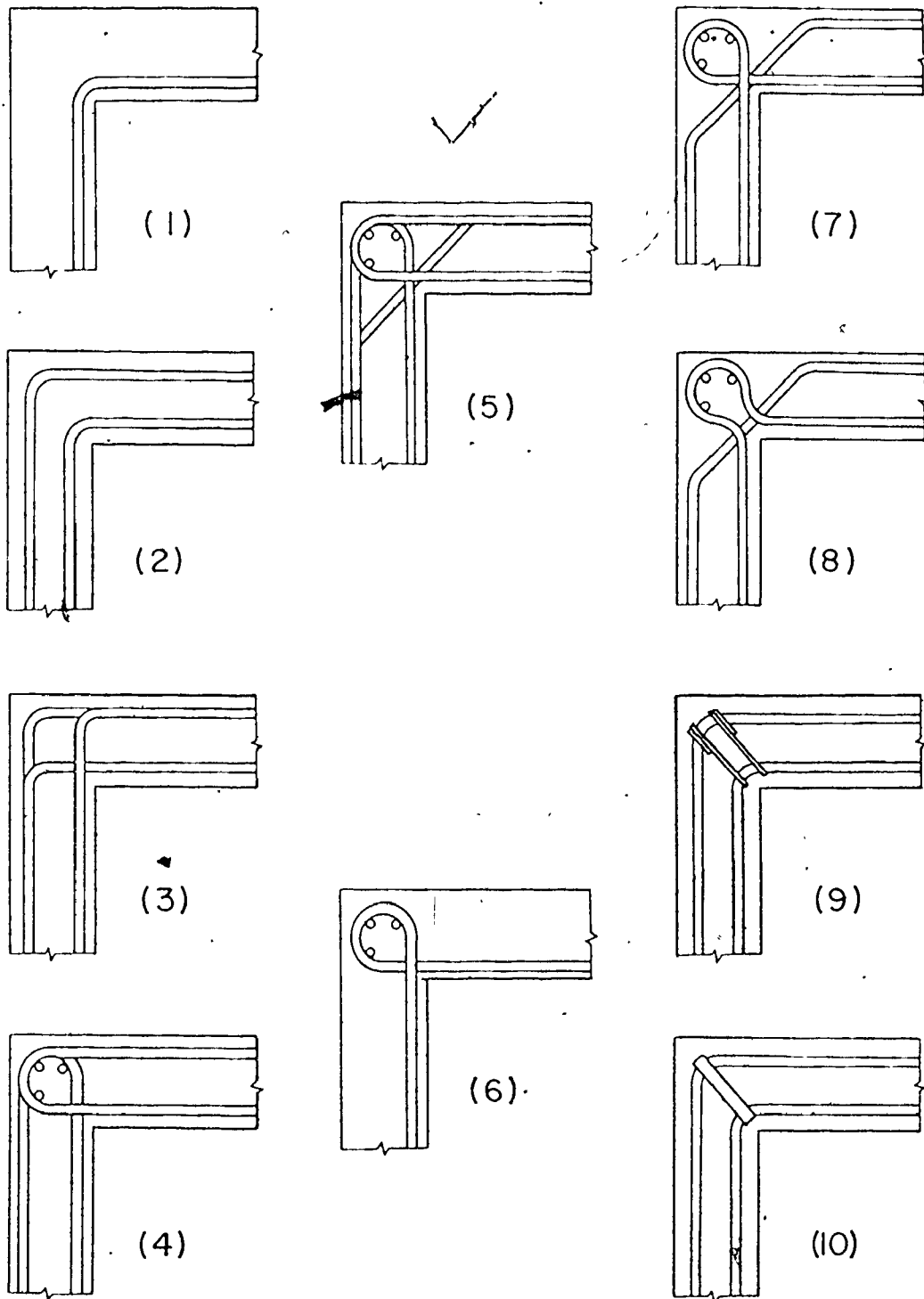


Fig. 2.10 DETAILS OF CORNER CONNECTION REINFORCEMENT
TESTED BY SWANN(58)

of corner reinforcement are reproduced in Figs. 2.11 and 2.12. The details were tested for both negative and positive bending moments. They concluded that no major difficulties when a negative moment was applied should be expected. However, when positive moment was applied, the best detail was found to be Detail (6) shown in Fig. 2.12. Its efficiency was only 75% of the capacity of the intersecting members. It was also concluded that some corner details (1 & 2) commonly used in practice were not as efficient as other less conventional (Detail 6), but simpler details. Tables, 2.1, 2.2 and 2.3, reproduced from reference (74), summarize the details of reinforcement sizes and concrete strengths, test results for negative and for positive bending moments respectively. These results constitute a major source of data and for positive moment indicate efficiencies ranging from 17% to 75%.

Having identified the problems involved with corners subjected to positive bending moment a second stage was reported by the same team (91) in 1972. Fifty-four reinforced lightweight concrete corners subjected to positive bending moment were tested. The effects of 28 different types of reinforcing details (Fig. 2.13) on ultimate flexural strength, stiffness, and cracking were studied.

Tables 2.4 and 2.5 were reproduced from reference (91) to show the details of reinforcement sizes and concrete strengths, and the test results respectively. It was found that the use of two sets of mutually perpendicular diagonal reinforcement was a promising method for developing flexural strength, reducing crack widths and producing reasonably

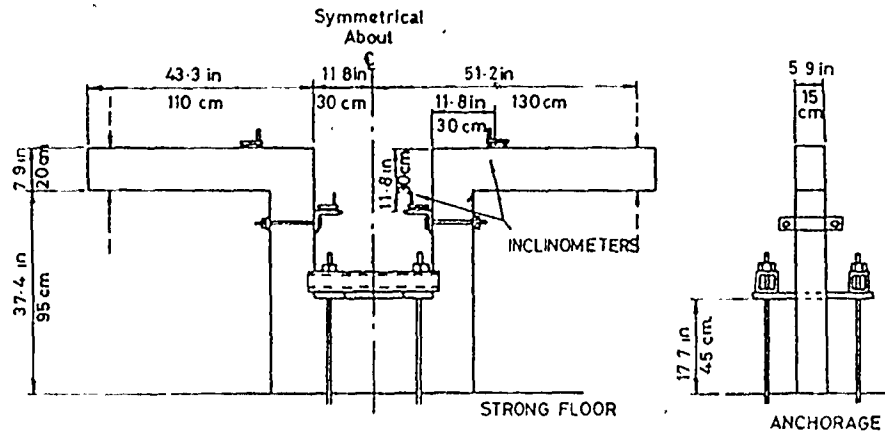


Fig. 2.11. Test arrangement and dimensions of test specimens

Reproduced from Reference 74

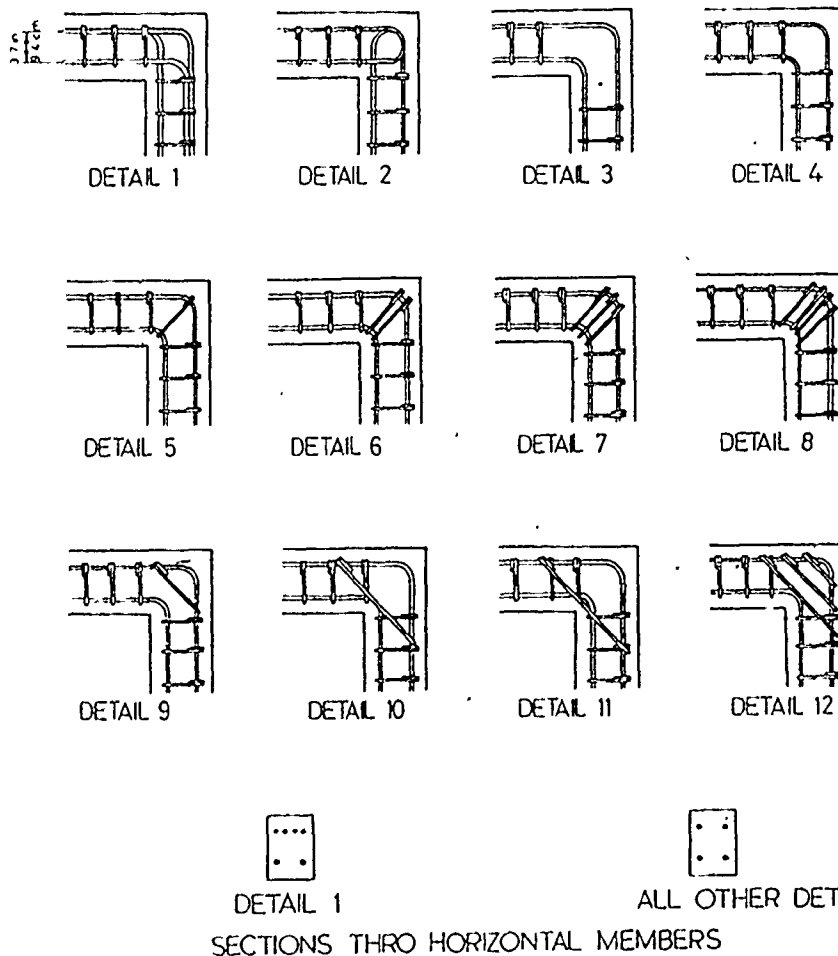


Fig. 2.12. Details of corner reinforcement (The longitudinal steel extends to the end of the flexural member in all details, and is terminated by a standard hook)

Reproduced from Reference 74

Table 2.1 (Reproduced from Reference 74)
 DETAILS OF REINFORCEMENT SIZES AND CONCRETE STRENGTHS

Detail Reference No.	Corner Reference No.*	Diameters of			Concrete Cylinder Strength, psi (kN/cm ²)
		Main bars in (cm)	Diagonal stirrups (cm)	Other stirrups (cm)	
1	1-1, 1-2	0.47(1.2)	None	0.24(0.6)	3000 (210)
	1-3, 1-4	0.47(1.2)	None	0.24(0.6)	
	2-1, 2-2	0.47(1.2)	None	0.24(0.6)	
2	2-3, 2-4	0.47(1.2)	None	0.24(0.6)	2700 (190)
	3-1, 3-2	0.47(1.2)	None	0.24(0.6)	
	4A-1, 4A-2	0.47(1.2)	None	0.24(0.6)	
3	4B	0.47(1.2)	None	0.22(0.6)	3400 (240)
	4C	0.47(1.2)	None	0.22(0.6)	
	4D	0.47(1.2)	None	0.22(0.6)	
4	5A-1, 5A-2	0.47(1.2)	0.47(1.2)	0.24(0.6)	2500 (175)
	5A-3, 5A-4	0.47(1.2)	0.47(1.2)	0.24(0.6)	
	5B-1, 5B-2	0.47(1.2)	0.24(0.6)	0.24(0.6)	
	5B-3, 5B-4	0.47(1.2)	0.24(0.6)	0.24(0.6)	
	5C-11, 5C-21	0.47(1.2)	0.47(1.2)	0.24(0.6)	
	5D-11, 5D-21	0.47(1.2)	0.24(0.6)	0.24(0.6)	
	5E-1, 5E-2	0.47(1.2)	0.21(0.6)	0.24(0.6)	
	5F-1, 5F-2	0.32(0.8)	0.24(0.6)	0.24(0.6)	
	6A-1, 6A-2	0.47(1.2)	0.24(0.6)	0.24(0.6)	
	6B-1, 6B-2	0.47(1.2)	0.32(0.8)	0.24(0.6)	
	6C-1, 6C-2	0.47(1.2)	0.47(1.2)	0.24(0.6)	
	7-1, 7-2	0.47(1.2)	0.24(0.6)	0.24(0.6)	
8	8-1, 8-2	0.47(1.2)	0.24(0.6)	0.24(0.6)	3000 (210)
	9-1, 9-2	0.47(1.2)	0.24(0.6)	0.24(0.6)	
9	10A-1, 10A-2	0.47(1.2)	0.24(0.6)	0.24(0.6)	2450 (175)
	10B	0.32(0.8)	0.24(0.6)	0.24(0.6)	
10	11	0.32(0.8)	0.24(0.6)	0.24(0.6)	2500 (175)
	12-1, 12-2	0.47(1.2)	0.34(0.8)	0.24(0.6)	

*Notation for corner reference number. The figure before the hyphen indicates the type of corner detail (Fig. 2), and the figure after the hyphen indicates the specimen number. Thus 3-2 represents Detail 3-Corner, Specimen 2. Where different bar sizes were used for the same type of corner detail, distinguishing letters, A, B, C, etc. are used.
 †Diagonal stirrups in these corners were deliberately misplaced by 10 deg to observe the effect of inaccurate bar placing.

Table 2.2 (Reproduced from Reference 74)
 TEST RESULTS (LOAD-CLOSING CORNERS)

Corner Reference No.	M _c [*]	At 40 percent M _c				At 80 percent M _c		
		Rotation, radians x 10 ⁻²	Crack widths		Rotation, radians x 10 ⁻²	Crack widths		
			Average, mm	Maximum, mm		Average, mm	Maximum, mm	
1-3	1.25	2.1	0.1	0.1	7.1	0.2	0.3	
1-4	1.27	1.5	NV*	NV*	4.3	0.2	0.2	
2-3	0.94	3.4	0.2	0.2	11.7	0.6	1.1	
2-4	1.17	3.2	0.3	0.25	13.2	0.8	1.2	
3-2	1.27	2.6	0.2	0.2	9.2	0.4	0.65	
4A-2	1.24	2.8	0.2	0.2	8.2	0.4	0.5	
5A-3	1.17	3.7	0.1	0.1	10.0	0.2	0.25	
5A-4	1.22	2.5	0.1	0.1	9.7	0.2	0.25	
5B-3	1.25	3.1	0.1	0.15	8.7	0.3	0.4	
5B-4	1.29	4.9	0.1	0.15	9.9	0.2	0.4	
5C-2	1.20	2.3	0.15	0.25	7.3	0.4	0.6	
5D-3	1.24	2.9	0.1	0.1	7.2	0.25	0.2	
5E-2	0.89	4.5	0.2	0.2	12.9	0.45	0.8	
5F-2	1.45	2.2	NV*	0.2	7.4	0.4	0.4	
12-2	1.22	1.9	0.2	0.15	7.6	0.4	0.5	

*NV = none visible.
 †Corner notation as in Table 1.

Table 2.3 (Reproduced from Reference 74)
 TEST RESULTS (LOAD-OPENING CORNERS)

Corner Reference No.	M _c [*]	At 20 percent M _c				At 40 percent M _c		
		Rotation, radians x 10 ⁻²	Crack widths		Rotation, radians x 10 ⁻²	Crack widths		
			Average, mm	Maximum, mm		Average, mm	Maximum, mm	
1-1	0.19	F	F	F	F	F	F	
1-2	0.19	F	F	F	F	F	F	
2-1	0.44	0.2	NV†	NV	NF‡	NF	NF	
2-2	0.43	0.2	NV	NV	8.5	0.3	1.4	
2-3	0.16	F	F	F	F	F	F	
4A-1	0.29	1.2	0.1	0.2	F	F	F	
4B	0.22	2.4	0.2	0.2	F	F	F	
4C	0.24	1.9	0.1	0.2	F	F	F	
5A-1	0.32	1.2	0.1	0.1	6.1	0.4	0.7	
5A-2	0.42	2.1	NV	NV	11.7	0.2	0.2	
5B-1	0.41	1.7	0.1	0.2	NF	NF	NF	
5B-2	0.46	4.0	0.1	0.1	12.9	0.6	1.0	
5C-4	0.43	1.1	0.1	0.1	9.2	0.7	1.0	
5D-4	0.42	1.9	0.1	0.2	NF	NF	NF	
5D-4	0.26	2.5	0.2	0.4	F	F	F	
5F-1	0.62	2.6	NV	NV	4.8	0.2	0.2	
6A-1	0.42	0.8	0.1	0.1	1.2	0.2	1.4	
6A-2	0.48	0.9	0.1	0.1	7.1	0.2	1.0	
5B-1	0.60	0.7	NV	NV	4.0	0.2	0.2	
5B-2	0.52	0.7	NV	NV	1.8	0.2	0.4	
6C-1	0.60	1.2	0.1	0.1	3.1	0.4	0.6	
6C-2	0.75	0.8	NV	NV	2.6	0.2	0.4	
7-1	0.58	0.7	NV	NV	4.3	0.2	0.2	
7-2	0.60	0.8	NV	NV	2.1	0.1	0.2	
8-1	0.20	0.2	0.1	0.1	5.6	0.2	0.6	
8-2	0.45	0.2	NV	NV	2.4	0.4	0.2	
8-3	0.28	0.7	NV	NV	F	F	F	
8-4	0.21	2.2	0.2	0.2	F	F	F	
10A-1	0.24	1.7	NV	NV	F	F	F	
10A-2	0.22	2.6	NV	NV	F	F	F	
10B	0.66	0.2	NV	NV	10.9	NV	NV	
11	0.72	0.2	NV	NV	0.3	NV	NV	
12-2	0.27	0.2	NV	NV	F	F	F	

*F = Failed, (NV) = None visible, (NF) = Near failure.
 †Corner notation as in Table 1.

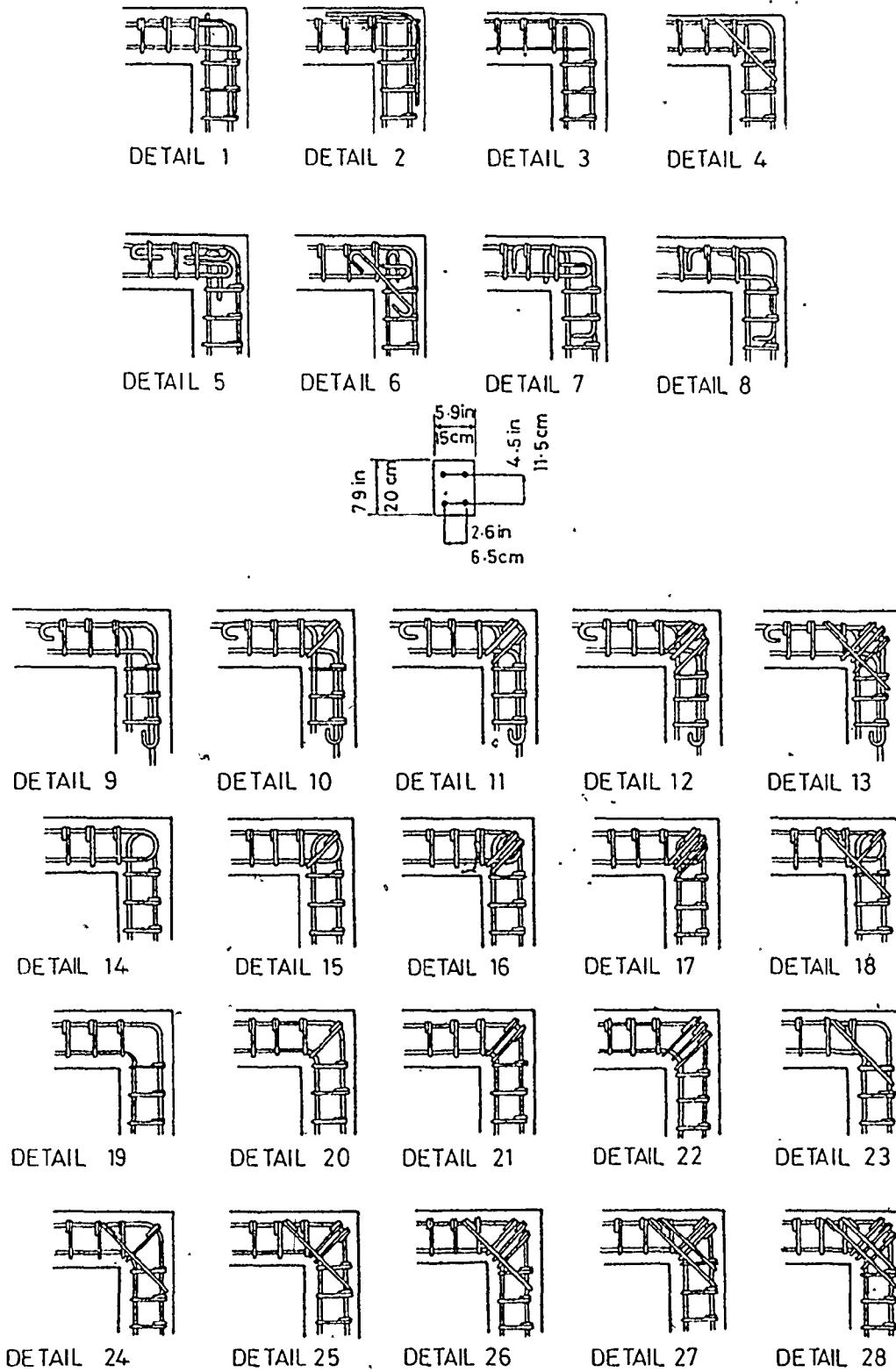


Fig. 2.13. Details of corner reinforcement (main longitudinal bars extend to end of flexural member and are terminated by a standard hook)

Reproduced from Reference 91

ductile behaviour. Of all the details tested, Detail 26 gave the best overall performance. ✓ This was the only detail to exceed 100% corner efficiency. It is apparent however, that this detail is only good for low percentages of reinforcement. The efficiency ranged from 99% to 130% for a tension steel percentage of 0.52. When the percentage of tension steel was increased to 1.34, the efficiency dropped dramatically down to 38%.

In 1972, Balint and Taylor (85) in England made the following recommendation: "The provision of a splay adds greatly to the strength of opening flexural corners and should be provided whenever possible". They suggested that the detail reproduced in Fig. 2.14 may be used for tensile steel reinforcement ratios up to 1%. The reinforcement detail consists of hair pins and splay bars. Balint and Taylor (85) and also Nilsson (97) concluded that sufficient corner strength can always be obtained by using a haunch.

In 1973, Nilsson documented in a comprehensive report (97) published by the National Swedish Building Research the results and conclusions of a research program in which he tested 78 corner and joint specimens tested from 1965 to 1973.

The following causes of failure in corner joints were discussed:

1. Diagonal tension failure.

Table 2.4 (Reproduced from Reference 91)
 DETAILS OF REINFORCEMENT SIZES AND CONCRETE STRENGTHS

Detail reference no.	Corner reference no.	Diameters in (cm)			Concrete cylinder strength psi (kgf/cm ²)
		Main bars	Diagonal reinforcement Type (i)	Type (ii)	
1	1-1, 1-2	0.25(1.0)	None	None	2500 (175)
2	2-1, 2-2	0.25(1.0)	None	None	2750 (195)
3	3	0.25(1.0)	None	None	2550 (180)
4	4	0.25(1.0)	None	0.75(3.0)	2550 (180)
5	5-1, 5-2	0.25(1.0)	None	None	2100 (150)
6	6-1, 6-2	0.25(1.0)	None	0.25(1.0)	2700 (195)
7	7-1, 7-2	0.25(1.0)	None	None	2700 (195)
8	8-1, 8-2	0.25(1.0)	None	None	2500 (175)
9	9	0.25(1.0)	None	None	2500 (175)
10	10	0.25(1.0)	0.25(1.0)	None	2500 (175)
11	11	0.25(1.0)	0.25(1.0)	None	2400 (170)
12	12	0.25(1.0)	0.25(1.0)	None	2400 (170)
13	13A	0.25(1.0)	0.25(1.0)	0.25(1.0)	2500 (175)
14	14	0.25(1.0)	None	None	2300 (165)
15	15	0.25(1.0)	0.25(1.0)	None	2300 (165)
16	16	0.25(1.0)	0.25(1.0)	None	2150 (155)
17	17	0.25(1.0)	0.25(1.0)	None	2150 (155)
18	18A	0.25(1.0)	0.25(1.0)	0.25(1.0)	2500 (175)
19	19	0.25(1.0)	0.25(1.0)	0.25(1.0)	2500 (175)
20	20-1, 20-2	0.25(1.0)	None	None	2750 (195)
21	21A, 21A-1	0.25(1.0)	0.25(1.0)	None	2600 (185)
22	22B	0.25(1.0)	0.25(1.0)	None	1900 (135)
23	23A-1, 23A-2	0.25(1.0)	0.25(1.0)	None	2750 (195)
24	24	0.25(1.0)	0.25(1.0)	None	1800 (130)
25	25C	0.25(1.0)	0.25(1.0)	None	2300 (165)
26	26A	0.25(1.0)	0.25(1.0)	0.25(1.0)	2300 (165)
27	27	0.25(1.0)	0.25(1.0)	0.25(1.0)	2300 (165)
28	28	0.25(1.0)	0.25(1.0)	0.25(1.0)	2300 (165)
29	29A	0.25(1.0)	0.25(1.0)	0.25(1.0)	2500 (175)
30	30A	0.25(1.0)	0.25(1.0)	0.25(1.0)	2500 (175)
31	31A	0.25(1.0)	0.25(1.0)	0.25(1.0)	2500 (175)
32	32C	0.25(1.0)	0.25(1.0)	0.25(1.0)	2500 (175)
33	33A	0.25(1.0)	0.25(1.0)	0.25(1.0)	2500 (175)
34	34A	0.25(1.0)	0.25(1.0)	0.25(1.0)	2500 (175)
35	35A	0.25(1.0)	0.25(1.0)	0.25(1.0)	2500 (175)
36	36A	0.25(1.0)	0.25(1.0)	0.25(1.0)	2500 (175)
37	37	0.25(1.0)	0.25(1.0)	0.25(1.0)	2500 (175)
38	38	0.25(1.0)	0.25(1.0)	0.25(1.0)	2500 (175)

* Notation for corner reference number: The figure before the hyphen indicates the type of corner detail (Fig. 1) and the figure after the hyphen indicates the type of specimen number. e.g. 5-2 represents Detail 5 - Corner Specimen 2. Where different bar sizes were used for the (i) or (ii) bar at corner detail distinguishing letters A, B, C etc. are used. (Diagonal reinforcement Type (i) is along the line from the inside reentrant angle to the outside of the corner as in Detail 1; Diagonal reinforcement Type (ii) is perpendicular to Type (i) as in Detail 2.)

Table 2.5 (Reproduced from Reference 91)
 TEST RESULTS (LOAD OPENING CORNER)

Corner reference no.	M _c	At 70 percent M _c		At 40 percent M _c		At 60 percent M _c	
		Net rotation radians x 10 ⁻³	Maximum crack width mm	Net rotation radians x 10 ⁻³	Maximum crack width mm	Net rotation radians x 10 ⁻³	Maximum crack width mm
1-1	0.42	-0.11	NV	0.47	0.1	F	F
1-2	0.20	-0.04	NV	0.13	0.12	F	F
2-1	0.45	-0.25	NV	0.11	0.3	F	F
3-2	0.40	-0.08	NV	0.21	0.1	F	F
3	0.43	-0.4	NV	-0.22	0.1	F	F
4	0.50	-0.24	NV	0.2	0.1	NT	NT
5-1	0.61	-0.20	NV	0.3	0.1	NT	NT
5-2	0.61	-0.41	NV	0.24	0.1	NT	NT
6-1	0.42	-0.04	NV	-0.12	0.1	0.75	0.3
6-2	0.61	-0.7	NV	0.22	0.1	1.00	0.1
7-1	0.51	-0.23	NV	0.2	0.2	F	F
7-2	0.61	-0.06	NV	0.43	0.1	NT	NT
8-1	0.45	-0.06	NV	0.22	0.1	F	F
8-2	0.61	-0.07	NV	-0.23	-0.1	F	F
9	0.52	-0.12	NV	0.4	0.1	F	F
10	0.63	-0.23	NV	0.4	0.1	NT	NT
11	0.62	0.43	NV	1.24	0.13	0.64	0.3
12	0.62	0.00	NV	0.00	0.1	1.10	0.20
13A	0.66	0.00	NV	0.72	0.15	1.4	0.4
13B	0.95	-0.20	NV	-0.23	0.15	0.89	0.3
14	0.72	-0.04	NV	0.8	0.2	1.27	0.3
15	0.60	-0.23	NV	0.23	0.1	1.22	0.3
16	0.62	0.19	NV	0.5	0.2	1.07	0.3
17	0.75	0.43	NV	0.14	0.1	1.00	0.4
18A	0.94	-0.40	NV	0.8	0.1	2.04	0.25
18B	1.02	-0.8	NV	-0.23	0.1	0.84	0.18
19-1	0.42	-0.28	NV	NT	NT	F	F
19-2	0.21	-0.13	NV	1.20	0.2	F	F
20-1	0.28	0.00	NV	1.00	0.2	F	F
20-2	0.40	0.20	NV	1.14	0.2	F	F
21A-1	0.62	-0.23	NV	1.00	0.2	0.9	1.1
21A-2	0.61	0.01	NV	0.47	0.1	NT	NT
21B	0.77	-0.00	NV	0.00	0.1	2.14	0.6
22A-1	0.42	-0.13	NV	1.4	0.15	NT	NT
22A-2	0.42	-0.25	0.00	1.10	0.15	NT	NT
22B	0.60	-0.23	NV	0.9	0.2	1.62	0.6
22C	0.65	0.1	0.1	0.8	0.2	1.8	0.6
23	0.45	0.00	NV	1.2	0.1	F	F
24A	0.61	0.13	NV	0.8	0.1	1.50	0.5
24B	0.25	0.00	NV	0.7	0.1	F	F
25A	0.60	-0.23	NV	0.00	0.1	1.03	0.25
25B	0.91	-0.15	NV	-0.17	0.00	1.50	0.3
25C	0.60	0.00	NV	0.2	0.2	NT	NT
25D	0.62	-0.25	NV	0.2	0.00	1.62	0.30
25E	0.90	-0.19	NV	0.1	0.1	1.70	0.3
26A	1.00	0.23	NV	0.15	0.00	0.47	0.2
26B-1	1.15	0.00	NV	0.10	0.1	1.1	0.25
26B-2	1.05	0.00	NV	0.42	0.1	2.04	0.3
26C	0.95	-0.10	NV	0.00	0.00	1.73	0.3
26D	1.20	-0.19	NV	-0.1	NT	0.52	0.1
26E	0.29	0.01	0.1	F	F	F	F
26F	0.27	0.10	0.1	F	F	F	F
27	0.90	-0.15	NV	0.22	NT	0.73	0.1
28	0.61	-0.07	NV	0.8	1.0	1.17	0.3

* Corner notation as in Table 1
 NV - None Visible
 F - Failed
 NT - Near failure

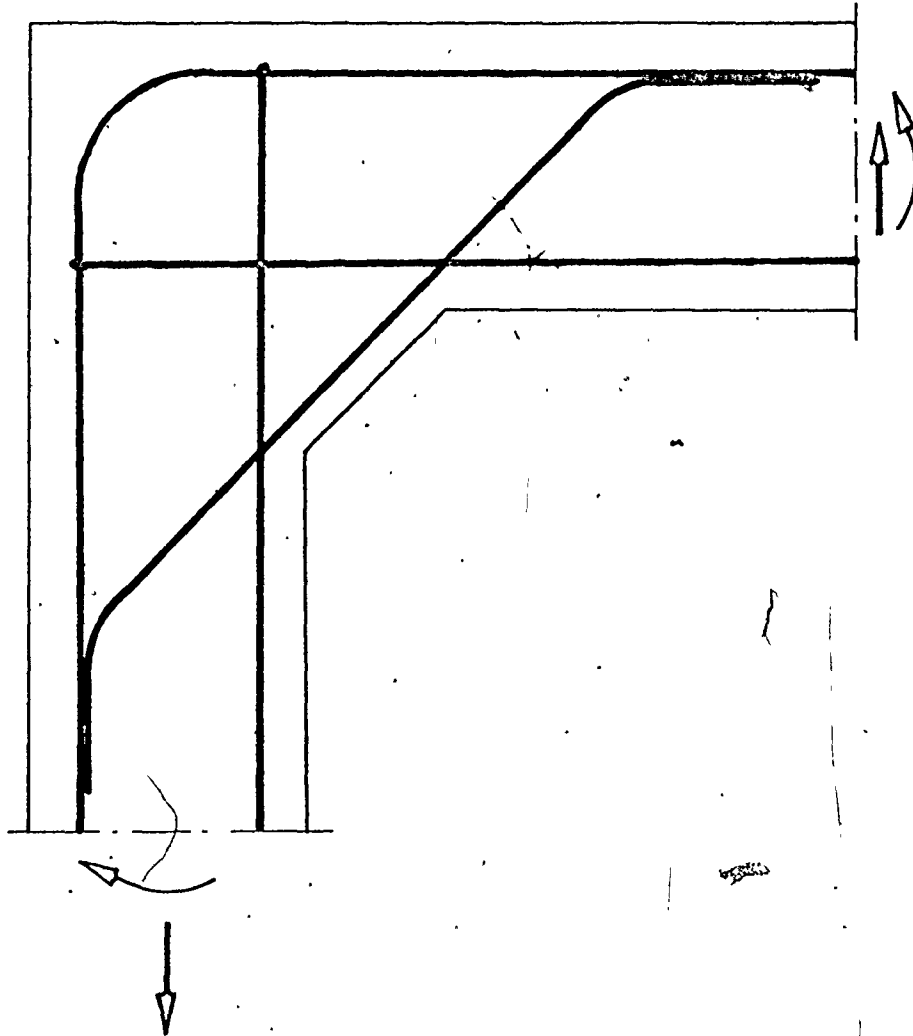


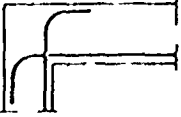
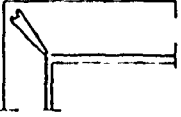
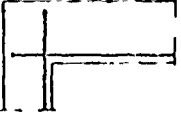
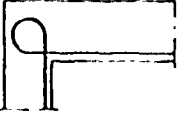
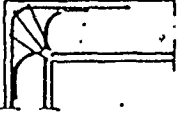
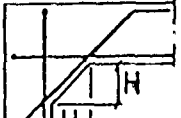
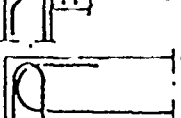
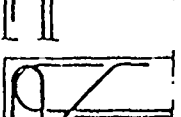

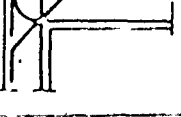


Fig. 2.14 CORNER DETAIL SUGGESTED BY
BALINT AND TAYLOR (85).

2. Splitting failure.
3. Failure due primarily to yielding of the reinforcement.
4. Anchorage failure.
5. Failure due primarily to crushing of concrete.

Of these causes of failure, special attention was devoted to diagonal tension failure. Simple expressions based on truss analogies were derived for the analysis of this type of failure. The emphasis of the experimental work centred on corners subjected to positive moment (tension on the inside). Some solutions for reinforcing such joints were offered in his document (97). Other types of joints with similar problems, such as corners in retaining walls, T-joints, and X-joints were also studied by Nilsson.

Proposals were put forward (97) for simple and functional reinforcement layouts for corners and some other common types of joints in reinforced concrete structures subjected to bending. Nilsson restricted the percentage of reinforcement in his details to certain amounts depending on the steel grade. However, he recognized the fact that much is still to be done in this field in order to more clearly understand the behaviour of reinforced concrete beam-column connections. Nilsson's work appears to be very thorough and his design recommendations are very beneficial. Document D7: 1973 (97), along with his other reports and publications listed in reference (97) can be of great help as detailing

Table 2.6 (Reproduced from Reference 97)
 Nilsson's Joint Details and Test Results

Specimen number	Haunch size H cm	Concrete strength		Failure moment M_{ut} kgfm	Calculated ultimate moment M_{uc} kgfm	$\frac{M_{ut}}{M_{uc}}$ %	Inside corner crack width at $M_{uc}/1.8$ mm
		σ_c kgf/cm ²	σ_{sp} kgf/cm ²				
 U 21		339	27.3	990	3135	32	Failed
 U 27		277	21.1	1840	2990	61	0.60
 U 15		289	25.6	2227	3290	68	0.70
 U 12		335	31.2	2474	3220	77	0.27
 U 28		272	20.5	2540	3185	79	0.26
 UV 1	15	305	23.7	3160			
 UV 2	5	345	25.2	3120			
 U 24		398	25.9	2804	3240	87	0.34
 UV 3	10	318	24.1	3712			0.08
 UV 4	5	277	22.3	3505			0.06
 UV 5		335	26.2	3629	3180	114	0.11
 UV 6		292	24.3	3505	3040	115	0.13
UV 7		339	18.4	3773	3070	123	0.13

references. In Table 2.6, his test results are reproduced (97). Details UV5, UV6, and UV7 were found to be the most efficient.

Although the behaviour of beam-column connections under cyclic loading is beyond the scope of this investigation, a list of references is included in the Bibliography to assist future investigators in the subject.

Example of valuable work on T-joints subjected to reversible loading were conducted at the University of Toronto by Uzumeri et. al. (101) and at the University of Canterbury in New Zealand, by Park and Paulay, (95, 103). Among other variables, different placement patterns of tension steel and of stirrups were studied. Both studies contain efficient detailing examples and contributed to a more complete understanding of the subject.

2.4 Development of the Finite Element Method in the Analysis of Reinforced Concrete Members:

2.4.1 General Background

Significant improvements and developments of the methods of reinforced concrete design were achieved as a result of continued research over the years. Design theories were proposed as early as 1850 with the application of reinforced concrete slab construction which appeared in France and England. (10, 14).

Working stress and ultimate strength design methods gained varying degrees of acceptance between 1900 and 1970. These two methods have been derived from

extensive experimental and analytical research work by many investigators. From this vast body of research data, building codes have adopted these two simplified methods which were proved to be adequate for a large proportion of the problems encountered in practice. However, the simplifying assumptions associated with these methods are not adequate for some of the complex interaction in reinforced concrete such as those outlined in Section 1.3.2. Designers are often confronted with special cases where conventional methods are ineffective. A common design solution where cost is low, is to make sections larger and/or more heavily reinforced to eliminate any possibility of failure. In problems where failure can lead to catastrophic results, such as loss of life, damage to costly equipment etc., load tests on prototypes and models must be carried out even if they are expensive and time consuming.

Researchers also need more sophisticated methods of analysis to be able to describe more accurately the behaviour of reinforced concrete and thereby be in a position to suggest better design formulae for the building codes.

The development of high speed digital computers and the formulation of the finite element method has

provided a means for the development of analytical models which can lead to a realistic evaluation of the behaviour of reinforced concrete. As a result it is possible to focus on the state of internal stresses and displacements in a manner which seems necessary if the detailed behaviour of reinforced concrete is to be properly investigated (39).

Formulation of a sophisticated form of such an analysis can be a difficult task not only in terms of the numerical solution of the non-linear problem arising from material properties but also in terms of the definition of realistic relationships governing material and structural behaviour. Considering that prediction of the behaviour of a single homogeneous isotropic material is commonly based on approximations such as idealized elasto-plastic stress-strain properties and empirical yield criteria, it may be easy to understand why the modelling of the behaviour of such a complex composite material as reinforced concrete has been subjected to many approximations and assumptions.

Existing experimental evidence and the corresponding

empirical or semi-empirical relationships for each individual material (steel and concrete) offer reasonable guidelines for modelling of their behaviour. However, as will be discussed later, interaction of concrete and steel has not been studied sufficiently to have the same degree of confidence. Interactions between the two materials such as bond-slip behaviour and dowel action, and also aggregate interlock between two concrete interfaces are important aspects which require considerably more study.

In this investigation what is judged to be the most reliable data (as documented in Sections 2.5 and 3.2) on each subject is used. To minimize the inaccuracies involved in the analysis, material properties were kept as close as possible to those from which the above relationships were developed.

2.4.2 Development of the Finite Element Method

The gradual trend toward representation of a continuum by an aggregation of discrete elements seems to have resulted from recognition that this idealization is more amenable to a numerical solution. The resulting structure is analyzed as a highly indeterminate structure using either the force or the displacement approach. The difference between these approaches lies in the selection of the unknowns to be initially solved and in the variation in the matrix quantities associated with their formulation.

The basic concept of the displacement method is that any structural member may be considered as an assemblage of individual elements interconnected at a finite number of nodal points. By placing certain constraints on displacements, conformity is assured between elements. It is the finite nature of the connectivity which makes it possible to formulate simultaneous algebraic equations and which distinguishes the method from continuum mechanics.

Displacement methods have been shown (90) to be more versatile than force methods since their formulation is simpler for a majority of structural analysis problems. One of the earliest representations of a continuum by discrete elements appears to have originated in the early 1940's with Hrennikoff (5) and McHenry (7). Besides inaccuracies due to the bar element chosen, the method gave rise to very large arrays of equations which could not easily be solved due to the lack of electronic digital computers.

Matrix formulations and the use of electronic digital computers developed rapidly in the air-craft industry. Further development of the finite element method from approximately 1955 to 1965 was reported mostly in the journals of aeronautical societies.

Turner and Clough (15) in 1956 introduced a two-dimensional plate element in the analysis of air-craft structure. Rectangular and triangular plane element stiffness derivations for plane stress condition were presented in 1960 by Clough (17).

With the increased availability of faster computers with larger core storage capacities, and because of its apparent potential, the finite element method has undergone a very rapid development in the last decade. New families of 2 and 3 dimensional elements have been developed to solve linear and non-linear problems in plates, shells, arches and solids and hundreds of papers have been published. Special conferences entirely devoted to the subject have been held, such as those held at Wright-Patterson Air Force Base (25, 42), in Japan, (55) at Nashville (57), and in Montreal (89). Development of such elements and methods have been summarized in books published by Zienkiewicz (37), Prezemienieki (43), Holand and Bell (59), and Desai and Abel (80). Books dealing with the matrix formulation have also been published by numerous authors among whom are Gere and Weaver (26), Rubinstein (31), and Meek (70).

2.4.3. Analysis of Reinforced Concrete Using the Finite Element Method:

Comparatively few publications in the ever growing reference list on finite element method have been devoted to the analysis of reinforced concrete. One of the first applications of the Finite Element Method to concrete was reported by Clough, Wilson, Sims and Rhodes (21, 23) who studied the behaviour of a gravity dam in which deep cracking had been observed. The crack was represented in the finite element

system by separation of elements along the crack line where independent nodal points were assumed for the elements on each side of the crack. Concrete was assumed to behave elastically under all applied loads.

Zienkiewicz and Cheung (37) described a simple way to simulate crack formation in low tensile capacity materials such as rocks and concrete by changing the overstressed element into an element with a zero stiffness in the direction perpendicular to the crack. Ngo and Scordelis (39) introduced in 1967 special elements to model the interaction between steel and concrete. In their study, simple beams with tensile reinforcement only were represented by triangular finite elements and the concrete-steel interaction was idealized by springs of zero length having constant stiffnesses for both bond-slip and dowel force-dowel displacement relationships. A number of beams with various predefined crack patterns were analyzed to evaluate concrete and steel stresses, bond stresses and deflections. The influence of decreasing stiffness due to various crack lengths was studied. Both steel and concrete were assumed to exhibit linear elastic behaviour.

Nilson (51) extended these studies by defining a non-linear bond-slip relationship and by introducing non-linear behaviour of concrete in the analysis of tension specimens which were axially or eccentrically loaded. Incremental loading procedures were used to follow the non-linearities of the materials. The concrete elements were considered to have failed when the principal tensile stress reached the modulus of

rupture. Execution of the program was then halted and the cracked element was replaced by two smaller elements with new node numbers on each side of the crack. A completely new topology was thus defined and this new structure was reloaded from zero load until another element cracked.

Franklin (60) extended the previous work by developing nonlinear analysis capable of redistributing stresses after cracking by iterating at each load increment. Triangular, rectangular, quadrilateral and rod elements were used with and without bond links. It was observed that the bond phenomenon was important for modelling beams to predict failure loads.

In 1970, Ngo, Franklin and Scordelis (68) formulated a more refined model of a reinforced concrete beam in which they introduced aggregate interlock linkages along, predefined diagonal tension cracks of various lengths. Linear behaviour of materials was retained. Beams with and without stirrups were analyzed. One of the significant results was that they determined the horizontal and vertical spring forces simulating bond and dowel forces which have no counter-part in experimental data.

A limit analysis of reinforced concrete slabs using a mixed finite element model with both force and displacement variables was reported by Backlund (79). Mufti et. al. (72), Spokowski (88), and Houde (93) using non-linear material

properties and bond-slip relations derived by Nilson (51) and Houde (93), developed computer programs with incremental loading procedures which delete the cracked element's stiffness and redistribute the strain energy to the adjacent uncracked elements. Looy (94) in 1972 directed particular attention towards problems associated with cracking. Initiation and propagation of cracks were considered to occur through elements rather than being restricted to following the element boundaries.

2.5 The Force-Displacement Relationships for the Finite Element Analysis of Reinforced Concrete

In this section the state-of-the art for the development of the following three important force-displacement relationships are discussed:

1. Bond-slip relationship
2. Dowel Action
3. Aggregate Interlock.

The stress-strain relationships for concrete and steel are discussed in the next chapter where data from the experimental program are also presented.

2.5.1 The Bond-Slip Relationship

Bond stress is the unit shearing force parallel to the axis of the reinforcing bar and on the steel-concrete interface. The bond stresses transfer the force from the steel bar to the surrounding concrete and vice versa.

Bishara (8), Brice (9), Mains (11), Bresler and Bertero (30), Perry and Thompson (35) and more recently, Nilson (48, 78, 92), and Houde (93) have studied the bond-slip problem.

The work of the first four researchers was pioneering work concentrating on the techniques to measure bond and slip. No specific bond-slip relationships were developed.

In 1966 Bresler and Bertero (30) tested concentrically reinforced specimens having one number 9 bar. They measured the end slip versus the bond stress. They reported results on both the bond stress distribution and the measured end slips.

Nilson (48) used Bresler and Bertero's results to derive a tentative local bond stress-slip relationship. He calculated the bond stress distribution along the length of the bar from the values of the steel stresses determined at closely spaced locations (1-2 inches). Slip between concrete and steel was defined as the difference between the steel displacement and the concrete displacement at particular locations, since it was difficult to measure the actual value of slip experimentally. Although there was considerable scatter, Nilson fitted the results of the experiments into the following third degree polynomial.

$$\bar{u} = 3.606 \times 10^6 d - 5.356 \times 10^9 d^2 + 1.986 \times 10^{12} d^3$$

.....(2.1)

where U is the nominal bond stress (psi) and d is the local bond slip (inch).

More recently, Nilson (78, 92) measured the steel strain along the length of an embedded reinforcing bar to provide the basis for calculation of bond stress variation. He measured the internal strains in the concrete close to the interface at a number of locations along the embedded length. By numerical integration of both the steel strains and the concrete strains, displacement and slip were determined. Nilson used the method he described to investigate the bond stress versus slip relations for a No. 8 standard deformed reinforcing bar in two types of specimens, using concrete strengths in the range of 4000 psi.

He proposed a bilinear bond stress-slip relation as follows

$$U = 3100(1.43S + 1.50)\sqrt{f'_c} d \dots\dots\dots(2.2)$$

and $U_u \leq (1.43S + 1.5)\sqrt{f'_c} \dots\dots\dots(2.3)$

where,

S = distance from the loaded end face of specimens tested (and by analogy, the distance from a crack face in typical members).

U = bond stress (psi)

U_u = peak bond stress (psi)

d = slip

f'_c = cylinder strength of concrete (psi)

Nilson found that both the peak local bond stress and the bond stress-slip modulus vary with distance from the loaded end of the specimens tested. He gave representative equations for peak bond stress and for bond stress as a function of slip. However, he claimed no generality for his results because the data were available only for a limited range of variables. He reported that some of the variables that may have an effect on the relationship are size, type, number and spacing of bars, concrete strength, type of specimen, and type and duration of loading.

In 1974 Haude and Mirza (99) tested two types of specimens; tension and anchorage (Beam-ends). Sixty two concentric tension tests were conducted on specimens with varying cross-sections and reinforced with a single steel bar (either No. 4, 6, or 8). They measured the steel strain and the end slip in twelve of the concentric tension tests with No. 8 bars and in six of the twenty-four beam-end tests. Concrete strength was varied from 3,000 to 7,000 psi. They found that the average crack spacing in the tension specimen to be equal to three times the concrete cover thickness. They proposed that the slip can be expressed by the following empirical expression,

$$d = k f_s^{1.1} (A_c/A_s)^{1/3} \dots\dots\dots(2.4)$$

where

- f_s = the applied steel stress at the face (ksi)
 A_s, A_c = area of steel bar and concrete in tension
 respectively
 k = experimental constant (in/ksi) with an
 average value of 0.19

Houde and Mirza found that the bond forces are dependent on the embedment length, the concrete cross-section and the concrete strength.

For the series of tests with No. 8 bars, local bond stresses at known points along the bar were calculated at various load levels using the bar forces. Slip was evaluated from eqn. (2.4). All results were then normalized to a concrete strength of 5,000 psi using the factor $(f'_c / 5,000)^{1/2}$. For slip up to the point where the peak bond force is reached the following fourth degree polynomial was proposed to relate the local bond stress U and the local bond slip d ,

$$U = 1.95E + 06d - 2.35E + 09d^2 + 1.39E + 12d^3 - .33E + 15d^4 \dots\dots\dots(2.5)$$

The initial bond-slip modulus (dU/dd) was seen to be close to 2.0×10^6 psi. A similar value is obtainable from Nilson's bilinear relationship, equation (2.2), when $f'_c = 5000$ psi and $S = 5.33$ inch. Figure (2.15) shows the curve obtained from Houde and Mirza's (93) mathematical expression versus his test results.

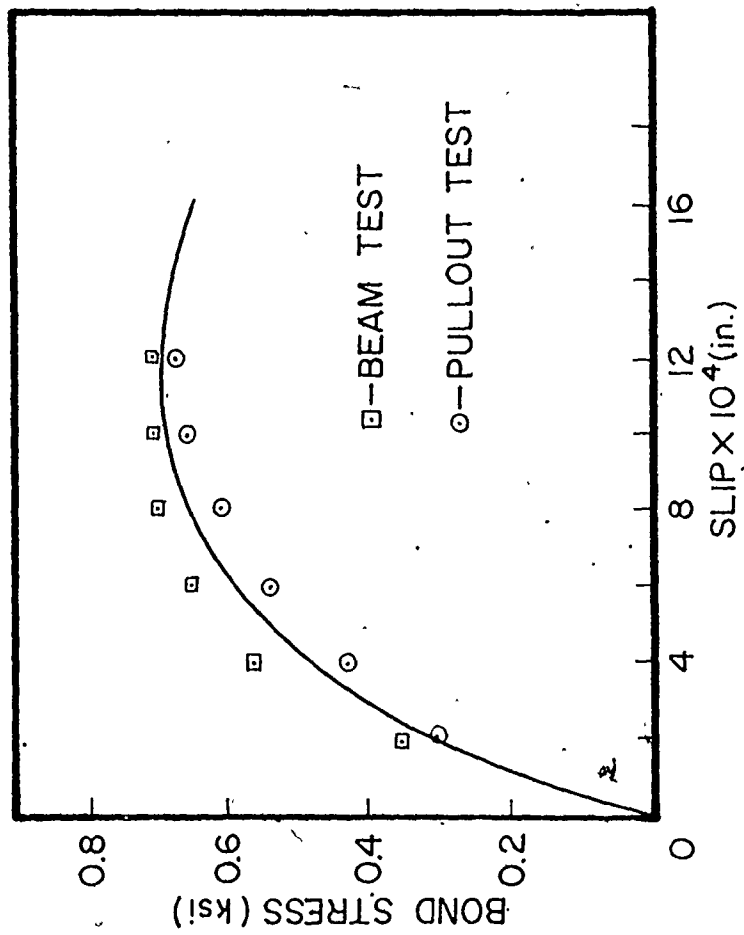


Fig. 2.15 UNIT BOND STRESS vs. UNIT SLIP
 REPRODUCED FROM REFERENCE (93)

Although Nilson found the peak bond stress to be proportional to the distance from the crack face, Houde and Mirza did not observe such a relationship in their investigation.

In this study, Houde and Mirza's equations are used. It was thought that adding the distance to the crack face as a variable which effects the bond-slip relationship would add to the complexity of the numerical solution without either theoretical justification or strong experimental evidence.

It seems evident that the current knowledge of the bond stress-slip relationship is still very limited. Some of the important factors that may affect this relationship have yet to be studied. Some of these variables were reported by Nilson (92) as mentioned earlier.

2.5.2 Dowel Action

Dowel action describes a mechanism by which shear is transferred across cracks in reinforced concrete members. In addition to longitudinal forces, the reinforcement is required to carry dowel forces which are perpendicular to its axis.

Krefeld and Thurston (33, 34), Fenwick and Paulay (49), Taylor (44, 64) and Houde (93) studied the dowel phenomenon.

Krefeld and Thurston (33, 34) tested divided beams which were joined by reinforcing bars of different sizes. Beam width, concrete cover and distance of the preformed crack from

the support were varied. They proposed a force-displacement relationship which takes all of the above mentioned variables in addition to the concrete strength into consideration. Their work is valuable. However, the inclusion of the distance from the crack to the beam support as a parameter restricts the use of their equations to beam applications.

Fenwick and Paulay (49) reported that effects of embedment length, number, diameter, arrangement and bond properties of bars, shear displacement across the crack and the tensile stress in reinforcing bars, are most important. Using direct shear testing models, they studied the effect of embedment length in addition to the parameters studied by Krefeld and Thurston (33, 34). However, the steel reinforcements were not subjected to tension in these experiments.

Taylor (44, 64) adopted the same specimens as developed by Krefeld and Thurston. He studied the effects of concrete strength, number and layout of reinforcing bars, shear span, cover, and beam width. He did not study the effect of bar diameters. Taylor suggested a force-displacement relationship which contained a large constant value term which made his equation insensitive to changes in net beam width and in tensile strength of concrete which he had found to be the most important factors associated with this phenomena.

Houde (93) recently developed equations for the dowel cracking loads and the dowel load-displacement relationship which take beam net width and concrete strength into account.

He developed the equations using his own test results and test data from others (44, 49, 64). This formed part of an extensive program to derive force-displacement relationships to be used in finite element analyses of reinforced concrete members. All his test results for dowel action were normalized to a common concrete strength level of 4,300 psi using the multiplier $(f'_c/4300)^{1/2}$. The following equations which he proposed are used in this investigation to describe the dowel phenomena.

$$V_d = 2,000 D_f \Delta_{\text{crack}} \dots\dots\dots(2.6)$$

where $D_f = 40 b_n (f'_c)^{1/3} \text{ (lb.)} \dots\dots\dots(2.7)$

$$V_d = \text{dowel load (lbs)}$$

$$\Delta_{\text{crack}} = \text{dowel displacement (in)}$$

$$= 5 \times 10^{-4} \text{ in.}$$

$$D_f = \text{dowel cracking load (lbs)}$$

$$b_n = \text{net width of beam (in)}$$

therefore $v_{d \text{ crack}} = 40 b_n (f'_c)^{1/3} \dots\dots\dots(2.8)$

2.5.3 Aggregate Interlock:

Aggregate interlock describes another mechanism for transferring shear across cracks. When concrete cracks, the surfaces of cracks are usually rough and irregular. Relative displacement along the crack is necessary to cause shear transfer by aggregate interlock.

Aggregate interlock was studied by Nowlen (47) Fenwick (49), Gergely (53), Loeber (61) Taylor (67) and Houde (93).

Nowlen (47) concluded from tests under dynamic loading that maximum aggregate size is important especially for wide cracks. He did not give any specific values or equations to represent his conclusions.

Gergely (53) concluded from his direct shear tests that the contribution of aggregate interlock in the shear capacity of a cracked member can be as high as 40%.

Fenwick (49) using direct shear tests, developed a shear stress-shear displacement equation which takes crack width and concrete compressive strength into account. The expression developed by Fenwick gives results essentially equivalent to the ones obtainable from the equations derived recently by Houde (93).

Loeber (61) reported that the effect of aggregate size is not important.

Taylor (67) using beam-end type and direct shear tests found that concrete strength, aggregate type and displacement ratio (or inclination of crack) have sizeable effects on the phenomenon. He also implied that his equations could only be used in the analysis of beams similar to the limited number he tested, and did not claim the generality of his equation.

Houde (93) tested 32 specimens similar to Fenwick's where he studied the effects of crack width, concrete strengths,

and maximum aggregate size. The shear displacements were always measured along a 45 degree crack line. Houde developed with a relatively simple equation that relates shear stress and displacement per unit crack length with crack width and concrete strength as variables.

The equation developed by Houde (93) to determine the shear stress transmitted by aggregate interlock action is expressed as follows:

$$f_{a_i} = 57 (1/c)^{3/2} (f'_c/5,000)^{1/2} \Delta_s \text{ (psi)} \dots\dots(2.9)$$

where,

f_{a_i} is the shearing stress (psi)

c is the crack width (inch)

Δ_s is the shear displacement along the crack
(inch/inch)

This expression gives results essentially equivalent to the ones derived by Fenwick from tests on specimens similar to those of Houde.

The study of the effects of aggregate size greater than 3/4" or less than 3/8", the effects of the actual problem of progressive crack opening has not been found in the literature. Due to computer core storage limitations and to the fact that aggregate interlock is only effective for a limited range of structural elements for which the shear crack widths maintain fairly small values during the

loading to failure , this phenomena was not included in the present analysis.

2.6 Summary

In this chapter, the literature review was organized into three major groupings, each dealing with information related to specific aspects of this investigation. These were:

- a. Details of tests of Beam-Column joints.
- b. Theoretical modelling of reinforced concrete structures using the finite element method.
- c. Description of Force-Displacement relationships for use in the finite element analysis of reinforced concrete.

Other literature which is relevant but more commonly used was not reviewed in this Chapter, but is referenced throughout the text.

CHAPTER 3
MATERIAL PROPERTIES, TEST SPECIMEN, AND EQUIPMENT
AND INSTRUMENTATION

3.1 Introduction

This chapter provides information about the materials used in the experimental test program. Included are the experimental stress-strain results for the concrete which was used to fabricate the joint test specimens described later. The correlation of these results with a general stress-strain equation is also presented. In addition the stress-strain relationship for the reinforcing steel used in the joint test specimens is described. This data and its mathematical representation provide necessary information for the numerical analyses of the joint test specimens which are presented in Chapter 7.

This chapter also provides explanations for the choice of test specimen shape and contains information on details of the specimens such as dimensions, tolerances, and fabrication methods. In addition the instrumentation and measurements to be taken and the test set-up and equipment are described and discussed. The joint test procedure is included in Chapter 4, with the joint test results.

3.2 Material Properties

Only one predesigned (36) concrete mix was used in this testing program. Many variables and the corresponding uncertainties pertaining to these were eliminated by using a standard mix. This mix was used in most research on concrete structures done in McMaster University. Such properties of concrete as the stress-strain relationship, increased strength with age, creep, and shrinkage were readily available. The use of this predesigned mix necessitated checking the accuracy of the predetermined stress-strain relationship. Tests to determine this relationship were performed for each specimen.

3.2.1 Concrete Mix and Batching Procedure

Table 3.1 lists the proportions by weight of the concrete mix as well as the weights required for each batch. The weight of the aggregate was for the air-dried condition. Concrete slump and aggregate types are also included, in Table 3.1.

Three batches of concrete were required to complete the casting of each test specimen. One concrete pour consisted of the following group of specimens:

- a) One rectangular frame (described in Section 3.3).
- b) 6 standard 6 inch diameter by 12 inch long cylinders.

Immediately preceding mixing of the first batch, a "butter" batch of one quarter the regular batch was mixed to condition the nine cubic feet horizontal drum mixer. This

concrete was then thrown out. Subsequent batches were mixed in rapid succession to avoid drying out of the mixer between batches. Each batch was allowed to mix for five minutes after the last of the water had been added. The complete mixing and concrete placing operation took about 40 minutes.

The horizontally cast frame and the standard cylinders were poured in three equal layers corresponding to the three concrete batches. Each layer was then placed and vibrated as soon as it was removed from the mixer. The concrete was internally vibrated using a 1 1/4 inch diameter poker type vibrator. For the top layer, the forms were filled so that the concrete was about one half of an inch over the top of the form after vibrating. The excess was then trowelled off level with the top of the form. It was believed that by following this procedure any tendency for the formation of a weaker top surface layer of concrete associated with migration of water due to vibration would be avoided.

Component	Percent By Weight	Weight in pounds per Batch
Portland Cement Type 1	14.0	127.37
Water	9.1	82.55
Fine aggregate (Washed pit run sand, fineness Modulus = 2.51)	46.6	423.61
Coarse Aggregate (3/8" max. size crushed limestone)	30.3	275.28
TOTAL	100.00	908.81
Slump for a standard 12 inch slump cone = 2.25 inch		
Volume per batch = 6.0 cubic feet (approximately)		

Table 3.1 Concrete Mix Data

3.2.2 Curing of the Concrete

About five hours after placing, when the concrete had begun to harden, wet burlap was placed over the specimens and kept moist. The curing continued to the age of 21 days at which time the specimens were moved to the structural testing floor to facilitate instrumentation and other preparations for testing. After 28 days from casting, the testing was begun.

3.2.3 Concrete Stress-Strain Relationship

The concrete cylinders were cast to provide individual and collective strength and stress-strain information for the specimens. At least 4 cylinders were tested at 28 days to determine the concrete strength and the stress-strain curve. Two or more of each were instrumented to provide the stress-strain information. The cylinders were instrumented with two sets of gauge points placed on opposite sides of the cylinder. These gauge points were centred on the concrete cylinders with an eight inch gauge length. A Demec Strain Indicator, which is a demountable mechanical strain indicator, was used to measure the strains. This instrument was calibrated into divisions of 0.00001 inches per inch and could be read accurately to one division as determined by repeated readings.

The cylinders were capped with a molten sulphur compound and were tested in a 300 kip capacity hydraulic "Tinius Olson" testing machine. Readings were taken at 10 kip intervals up to about 80 percent of the cylinder strength. After

exceeding 80% of the cylinder strength, strain measurements were taken on one side of the cylinder without stopping loading until material failure was imminent. Comparison of the strengths of cylinders used for the stress-strain measurements with companion cylinders tested only to determine strength indicated that there was no apparent loss of strength due to the incremental loading required to take strain measurements.

The average of the strains from the cylinder tests were used for plotting the stress-strain curve. Although it was not possible to obtain reliable strain readings at strains beyond the ultimate strength of the cylinders (too much energy release), the measurements taken indicated a gradual decrease of stress up to about 0.0025 inches/inch. This data agreed reasonably well with Saenz's (24) equation. This equation for the concrete stress-strain relationship has been used in other studies (51, 88, 93) and is accepted as a good generalization for a wide range of concrete strengths. Therefore, it was adopted to facilitate use of the analytical model for concrete properties other than those used in the experimental program.

The concrete stress-strain curve was used to determine values for the moduli of elasticities used in the numerical analysis. The curve represented by Saenz's (24) equation was plotted in Fig. 3.1, along with the actual curve obtained experimentally. Saenz's equation (24) is

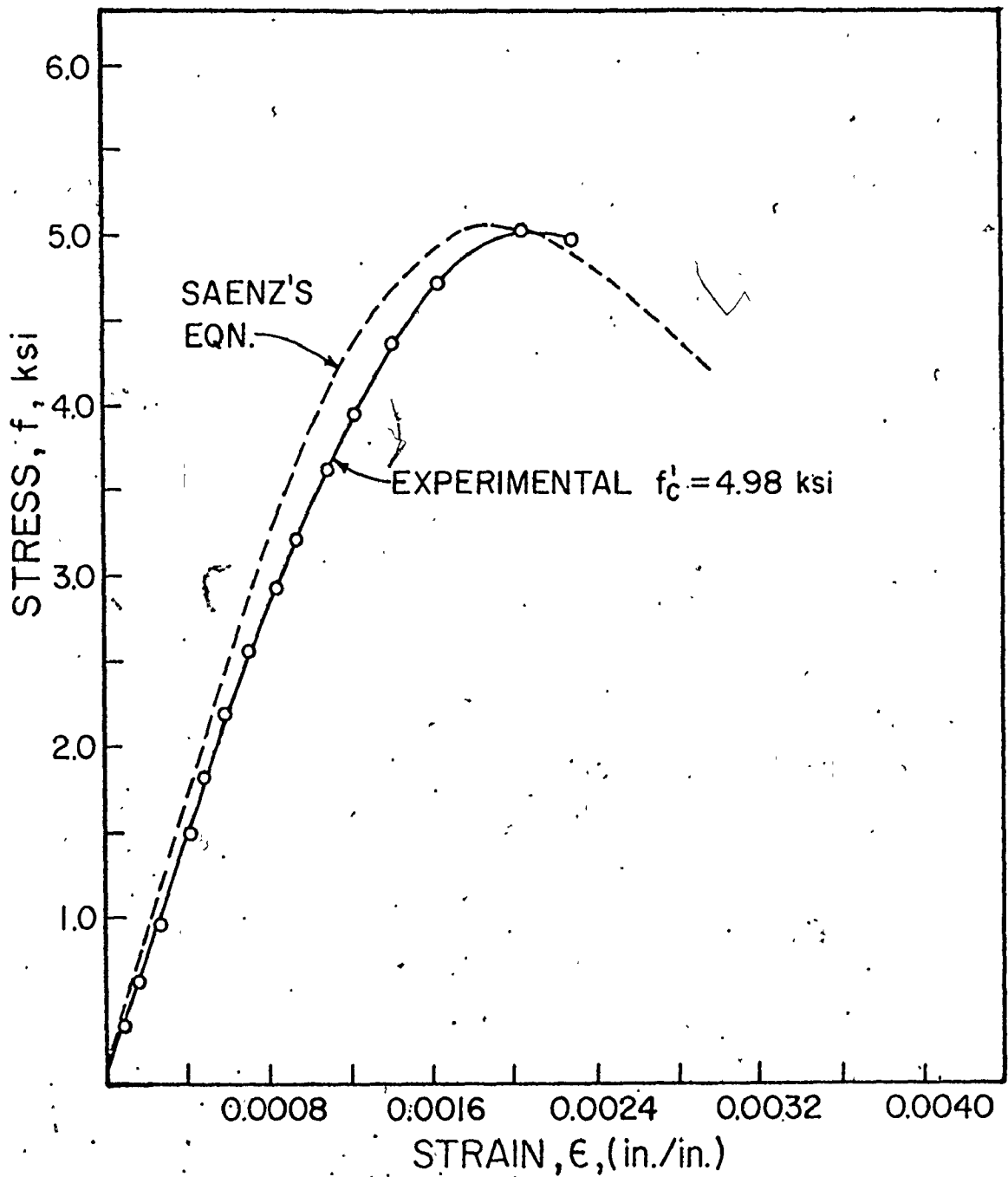


Fig. 3.1. TYPICAL EXPERIMENTAL CONCRETE STRESS-STRAIN DIAGRAM AS COMPARED WITH SAENZ'S EQUATION.⁽²⁴⁾

$$f = \frac{E_c \epsilon}{1 + (R + R_E - 2) \frac{\epsilon}{\epsilon_0} - (2R-1) \left(\frac{\epsilon}{\epsilon_0}\right)^2 + R \left(\frac{\epsilon}{\epsilon_0}\right)^3} \quad \dots \dots \dots (3.1)$$

where

$$R = \frac{R_E (R_f - 1)}{(R_E - 1)^2} - \frac{1}{R_E} \quad \dots \dots \dots (3.2)$$

$$R_E = \frac{E_c}{E_0} \quad \dots \dots \dots (3.3)$$

$$R_f = \frac{f'_c}{f_f} \quad \dots \dots \dots (3.4)$$

$$R_E = \frac{\epsilon_f}{\epsilon_0} \quad \dots \dots \dots (3.5)$$

and where

f = concrete stress

ϵ = concrete strain

ϵ_0 = concrete strain corresponding to maximum stress

f'_c = maximum concrete stress

ϵ_f = maximum concrete strain at failure

f_f = concrete stress at maximum strain

E_c = initial tangent modulus of Elasticity

$$E_0 = \frac{f'_c}{\epsilon_0}$$

From equation (3.1) both the tangent modulus of elasticity, E_t ,

and the secant modulus, E_s , have been derived as follows:

$$E_t = \frac{df}{d\epsilon} = \frac{E_c (1 + C_1 (\frac{\epsilon}{\epsilon_0})^2 - 2C_2 (\frac{\epsilon}{\epsilon_0})^3)}{(1 + C_3 (\frac{\epsilon}{\epsilon_0}) - C_1 (\frac{\epsilon}{\epsilon_0})^2 + C_2 (\frac{\epsilon}{\epsilon_0})^3)^2} \quad (3.6)$$

$$E_s = \frac{f}{\epsilon} = \frac{E_c}{1 + C_3 \frac{\epsilon}{\epsilon_0} - C_1 (\frac{\epsilon}{\epsilon_0})^2 + C_2 (\frac{\epsilon}{\epsilon_0})^3} \quad (3.7)$$

where,

$$\begin{aligned} C_1 &= 2R - 1 \\ C_2 &= R \\ C_3 &= R + R_E - 2 \end{aligned}$$

Saenz suggested the following values for ϵ_0 , ϵ_f , f_f and E_c from the analysis of test results of Desayi and Krishnan (11).

$$\epsilon_0 = 10^{-5} (f'_c)^{.25} [31.5 - (f'_c)^{.25}] \text{ in./in., } f'_c \text{ in psi} \quad \dots\dots\dots (3.8)$$

$$E_c = 10^5 (f'_c)^{.5} / [1.0 + 0.006 (f'_c)^{.5}] \text{ psi, with } f'_c \text{ in psi} \quad \dots\dots\dots (3.9)$$

The values of ϵ_f and f_f suggested by Saenz to be used in his equation are as follows:

f'_c (psi)	ϵ_f (in./in.)	f_f (psi)
1275	.0035	1060
3005	.0030	2700
4440	.0025	4190
7180	.0025	6800

Since all of the concrete strengths used in this investigation were in the vicinity of 5000 psi, ϵ_f was set at .0025 and f_f was approximated to $0.94 f'_c$ which is fairly close to the actual suggested values for f'_c over 4440 psi. The values of E_c from eqn. (3.9) were found to be higher than those reported elsewhere (61, 86) for concrete in this strength range. The ACI (61) equation for E_c was found to agree better with the experimental values obtained in this investigation.

$$E_c = 33(w)^{1.5} (f'_c)^{1/2} \dots\dots\dots(3.10)$$

where, $w = 145$ pcf for normal weight concrete.

This substitution for equation (3.9) is also appropriate for various concrete strengths. Although the validity of equation (3.9) is questioned, it does not affect the general validity of Saenz's equation (3.1). Therefore equation (3.10) was used in the analysis in place of Saenz's equation (3.9). The curve shown in Fig. 3.1 which represents Saenz's equation was plotted using the value of E_c obtained using equation (3.10).

The validity of using the stress-strain relationships derived from a concentric compression test in eccentric compression analysis has been questioned by numerous researchers. Rüşh (16) and Struman et.al. (29) reported that strain gradient retards cracking and stated explicitly that much higher stress-strain peaks can be expected in eccentric compression. As much as 70% higher stress and 50% higher strain peaks were suggested by Struman et.al. (29). Many other researchers, Clark et.al. (40) and Hognestad et.al. (13)) illustrated more conclusively that the strain gradient has minimal effect on the stress value but tends to increase the maximum strain attained before cracking occurs. The effect of the strain gradient, in addition to crack retardation, is to introduce a different strain rate in the various fibres. Assuming a plane section to remain plane, at least at a certain distance from the beam supports, each fiber is deformed at a different rate proportional to their distance from the neutral axis. The increased deformability of concrete with time (creep) is well known to be a function of the level of sustained stress and may explain some of the differences already noted (40).

The maximum strains at failure suggested by Saenz (24) were obtained from uniaxial (concentric) compression tests. Although these values were incorporated in the representation of the stress-strain relationship, they were not used as the limiting compressive strain which determines the criteria of failure for concrete in compression. This limiting strain was set at

0.003 in./in. for the range of concrete strengths used in the test program. This value is higher than that suggested by Saenz by 20% as proposed by Lui et.al. (86,87). Further discussion on the criteria of failure of concrete in compression is included in Chapter 6.

3.2.4 Concrete In Tension

The tensile strength of concrete is usually neglected in reinforced concrete structural design. This slightly conservative practice has been adopted because of the relative weakness of concrete in tension as compared with compressive strength. The purpose for which the finite element analysis in this investigation is intended, requires recognition of the importance of including the tension properties of concrete. The extent of the propagation of cracking in a reinforced concrete member depends largely on the tensile strength of concrete.

The level of the tensile strength obtained by testing is dependent on the type of the test and on the specimen size. Examples of tensile strengths reported in the literature (32, 93, 98) were $4.5 \sqrt{f'_c}$, $7.0 \sqrt{f'_c}$ and $9.6 \sqrt{f'_c}$ for axial tensile tests, splitting (Brazilian) test, and flexure tests, respectively.

Although, there is some indication in the literature that some small amounts of yielding may occur prior to failure (98), the stress-strain relationship of concrete in tension can be represented by a straight line without serious loss of accuracy (32). A modulus of elasticity in tension equal to the

initial tangent modulus of concrete in compression is used in this investigation up to the value of the ultimate tensile strength.

3.2.5 Reinforcing Steel

High grade deformed reinforcing steel was used in the experimental part of this investigation. The minimum nominal yield stress of 60 ksi specified by the manufacturer was always obtained. Unfortunately the flat yield plateau was not evident in the stress-strain curve for the main steel reinforcement. The transition from elastic behaviour to the strain hardening region occurred between 65 and 72 ksi. A typical ultimate tensile strength of over 115 ksi was obtained from the average of several test specimens. Relevant details of these test results which were required for the numerical analyses are reported in Chapter 4. Figure 3.2 shows a typical stress-strain curve for the number 6 bars used to reinforce the joint specimens.

Twenty-two inch test lengths were randomly cut from some of the bars to determine the stress-strain properties of the reinforcement. A 120 kip capacity hydraulically operated "Tinius-Olson" Testing Machine was used to perform the tests. Reference holes for the Demec Strain Indicator were drilled on opposite sides of the test lengths and located on the bar deformations. Strain measurements were taken at 2500 lb. increments and at approximately 500 lb. increments after yielding.

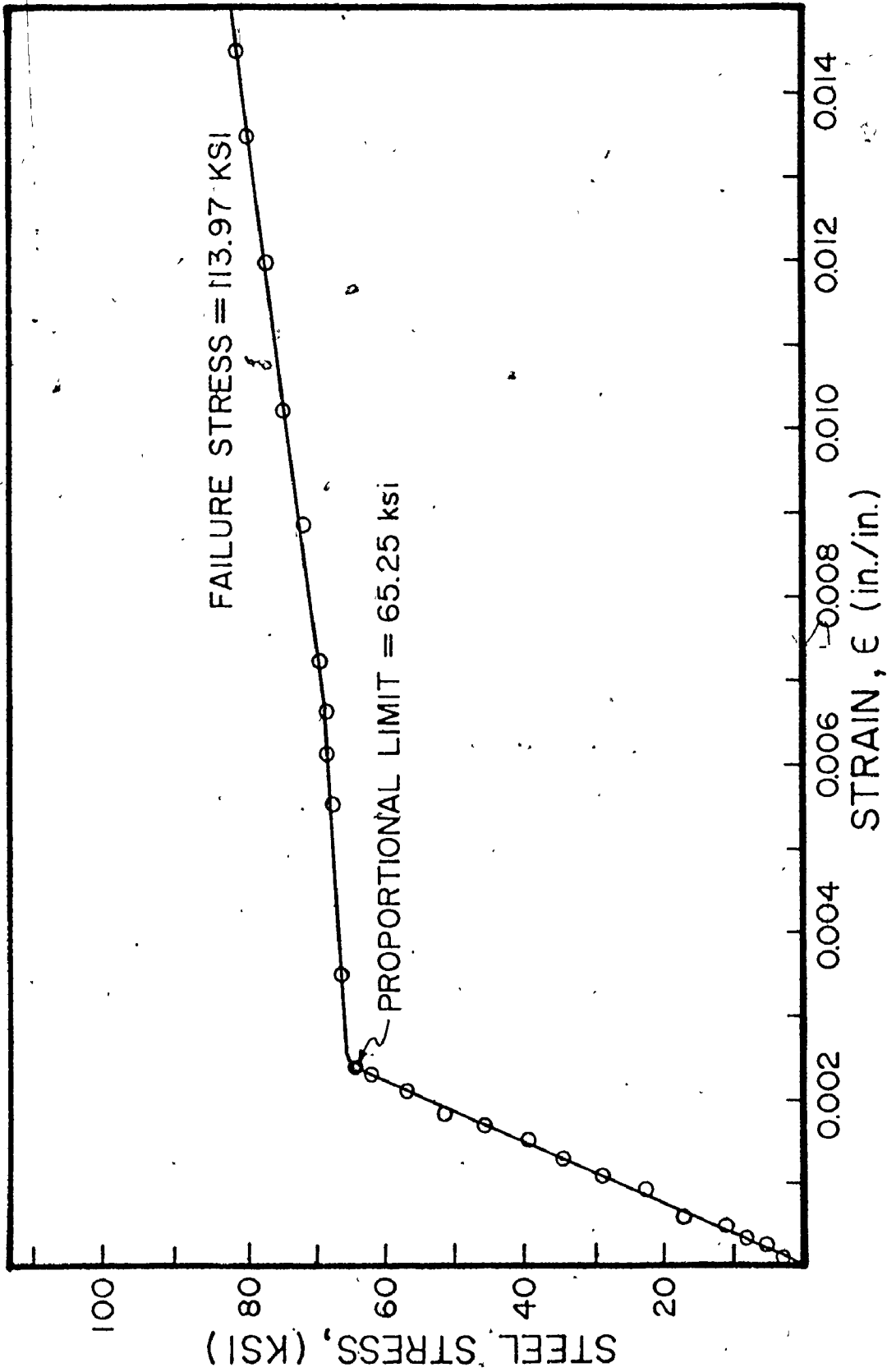


Fig. 3.2 TYPICAL AXIAL STRESS-STRAIN DIAGRAM FOR TENSION TESTS OF No. 6 BAR SPECIMENS.

The actual average areas of the bars were found by weighing the samples and measuring their lengths. It was felt that the extra complexities of trying to mathematically model the ill-defined yield region of the stress-strain curve for the steel reinforcement was not justified. Therefore, a well defined yield point followed by a short yield plateau leading to a strain hardening region as shown in Fig. 3.3 was adopted in the analysis.

3.3 Development of the Shape of the Test Specimen

A major consideration in the design of the joint test specimen was that it should be large enough to incorporate a wide range of reinforcing details and to be representative of dimensions encountered in current practice, but also small enough to facilitate handling and testing. A typical type of specimen, which was considered to fulfil these requirements, consisted of two members meeting at right angle as shown in Fig. 3.4.a and used by Swann (58, 66). The simplicity of the design was offset by the many envisaged disadvantages. The 'L' shape, with a centre of gravity situated outside the members, would cause lifting and handling problems. In addition, a sophisticated base fixing attachment would be necessary to provide the required stability for testing.

Figure 3.4.b shows the shape of the specimen used by Nilsson (97) which appeared to produce a design with few handling or stability problems. However, the joint not being

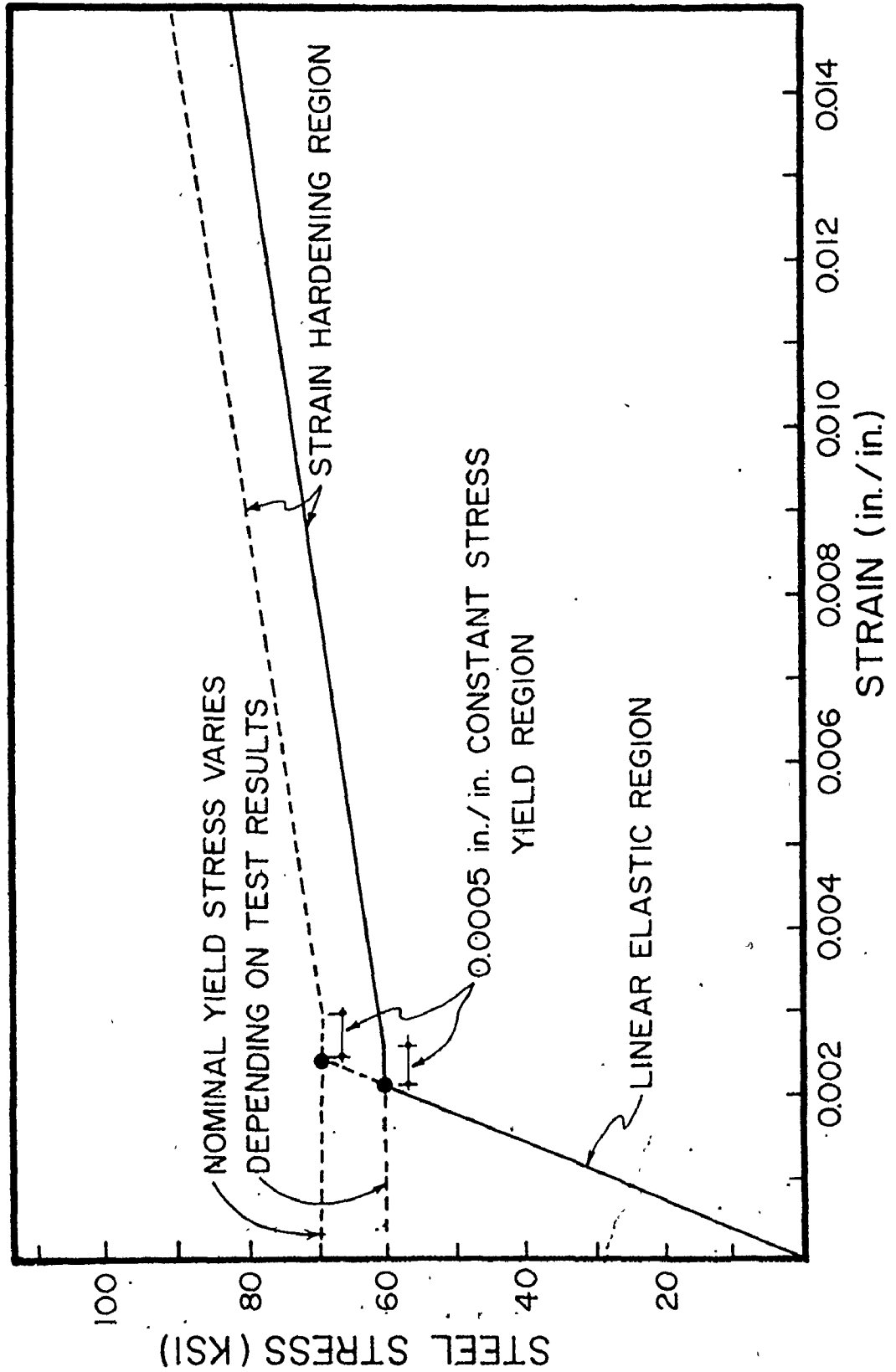


Fig. 3.3 IDEALIZED STRESS-STRAIN CURVE FOR STEEL REINFORCING BARS.

tested still requires restraint of some form if each joint is to be tested individually. As an alternative it was thought that a specimen with a large base member, arranged as shown in Fig. 3.4.c would give stability and enable the load to be applied either from above or below. However, this arrangement would yield only one test joint per specimen.

Mayfield et.al. (91) combined two specimens of the type shown in Fig. 3.4.c to form a specimen similar to the one shown in Fig. 3.4.d. The excess weight and bulk of this specimen and the relatively complex reinforcing required if smaller dimensions were used led to the modified shape developed for this investigation.

Figure 3.4.e shows the shape of the test specimen adopted for this experimental program. It was a relatively simple matter to fix the test specimen to the laboratory floor in a way which would ensure the independent testing of each corner joint.

The dimensions chosen were considered to meet the demands previously outlined. Detailed dimensions on a schematic drawing of the joint specimen and a photograph for the test setup are included in Section 3.4.2.

3.4 Preparations and Equipment for Joint Tests:

This section briefly describes the procedures and equipment used to prepare the joints for testing. In addition, the test equipment and measuring devices are described.

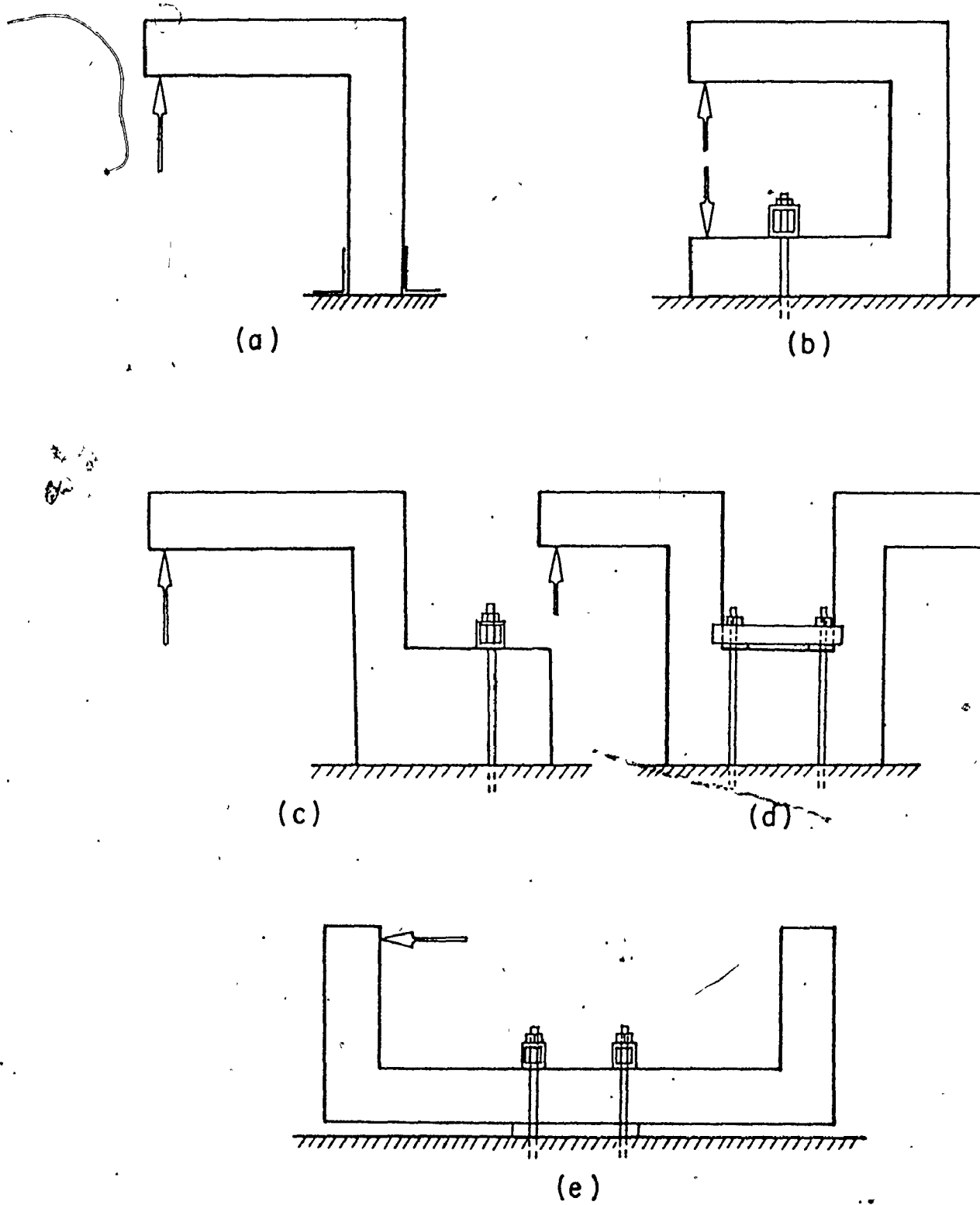


Fig. 3.4 SKETCHES OF POSSIBLE TYPES OF TEST SPECIMENS.

3.4.1 Forms and Steel Reinforcing Cages:

As was mentioned in Section 3.2.1, one specimen having two joints and six cylinders were cast at one time. Steel forms available from previous concrete research in the Applied Dynamics Laboratory were used to fabricate the test specimens. The use of the steel forms permitted fabrication to close dimensional tolerances (approximately $\pm 1/16$ in.)

The reinforcing steel cages for the joints were made by tying the bars to 1/4 inch diameter stirrups spaced at 6 inch intervals. These stirrups were accurately produced on a specially designed bending device. The reinforcement was firmly wired into each corner of the stirrups. After each cage was completed, the spacing of the reinforcing steel was rechecked. If necessary, adjustments were made by prying apart with a lever system, and re-wiring the bars to the ties. Small steel seats were used to correctly position and hold the cage in place in the form. These seats were kept out of the joint region to avoid any complicating effects in this critical region.

3.4.2 Preparation of the Specimens for Testing

After curing of the concrete, the specimens were moved to the test floor where they were prepared for testing. The following steps were required:

(a) Fixing the Specimen to the Test Floor:

The frame was accurately positioned between the two columns which had been prestressed to the floor. Figures 3.5 and 3.6, show two 8 in. by 8 in. hollow structural sections (C and D) 3' - 0" apart which were used to fix the specimen to the floor. The specimen was kept six inches above the floor level by resting it on a 6 in. by 9 in. H.S.S. (E). The length of the elevating H.S.S. was made 3' - 8" to match the outside dimension between the other two H.S.S.'s which were placed on the top as shown in Figs. 3.5 and 3.6. Using four, 2 1/2 inch diameter bolts the 2 top H.S.S.s were then tightened to the specimen. The amount of tightening was determined so that the bearing stress in the concrete under the H.S.S.s was approximately 500 psi.

(b) Installation of Loading Equipment:

Two hydraulic jacks (20 and 50 kip) capacity were installed as shown in Figs. 3.5 and 3.6. The top jack was mounted on a sliding plate and was continuously lowered during loading at amounts equal to the vertical deflections measured by the dial gauge designated with the letter A in Fig. 3.5. The sliding plate was bolted to a channel which spanned between the two columns and was in turn bolted to each of them with six 1 inch diameter bolts as shown in Fig. 3.6. A roller bearing plate was mounted on the frame opposite to the loading cell, using two 3 inch angles joined by two 1/4 inch diameter threaded rods which were tightened around the vertical member of the specimen, to fix the angles in place. The bearing plate

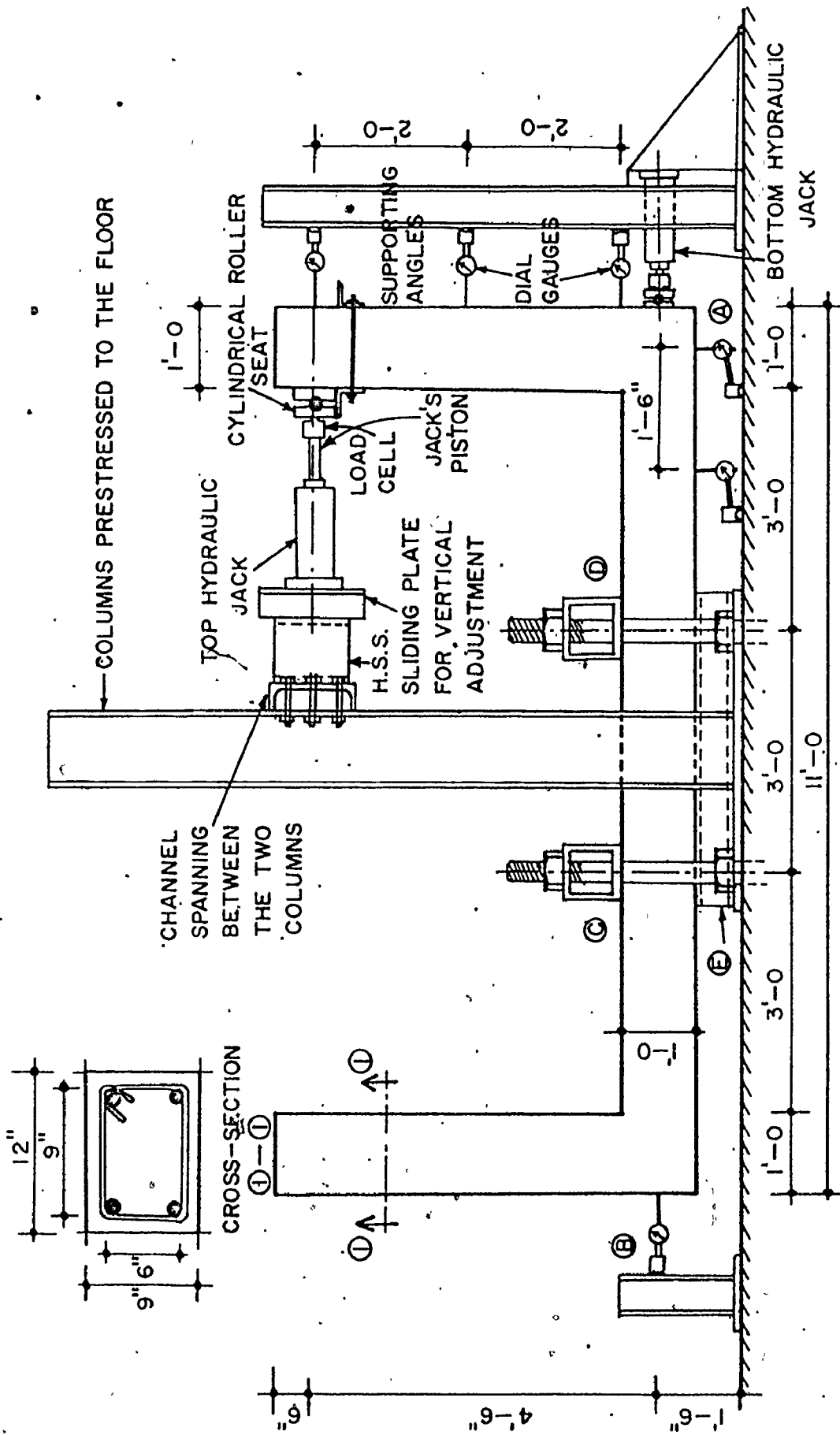


Fig. 3.5 SCHEMATIC DRAWING OF THE JOINT SPECIMEN AND TEST ARRANGEMENT.



FIG 36 PHOTOGRAPH SHOWING SPECIMEN PREPARED FOR TESTING

was then simply rested on the projecting leg of the angle.

The bottom jack was mounted directly on a channel reinforced with three brackets. This arrangement was bolted to the floor using two, 2 1/2" diameter bolts. A roller bearing was then placed against the frame and was used to transfer the jack's force from the load cell to the frame.

Calibrated load cells were used to accurately control the applied loads. These were placed between the end of the piston and the bearing plate for both locations. During testing the load levels for both jacks were always maintained at the same value. This created a pure bending moment region in the horizontal member of the specimen. (The increase or decrease of the load level in the bottom jack to apply axial compression or tension on the horizontal member to simulate columns in actual structures is possible with this same arrangement.). However, to eliminate variation of this parameter, the testing program was confined to cases with pure bending moment in the horizontal member.

(c) Instrumentation for Deflection and Strain Measurements:

For each test, six dial gauges were positioned at the locations shown in Fig. 3.5. The precision with which the dial gauges could be read was one half of a division which represents 1/1000' of an inch. The three gauges mounted opposite the vertical member were installed to facilitate reading the horizontal deflection of the vertical member. The two dial

gauges placed underneath the horizontal member were installed for vertical deflection measurements. All gauge readings were then used to calculate joint rotations. The gauge which was positioned at the joint not being tested (designated by letter B in Fig. 3.5, was provided to detect any sliding of the specimen. Since the loads applied by both top and bottom jacks were intended to be kept very close to being balanced no sliding was expected.

The Demec Strain Indicator, which is a demountable mechanical strain gauge, referred to in section 3.2.3, was also used for measuring the joint strains.

Demec points were installed as can be seen on the right hand side of the specimen shown in Fig. 3.6. The points were spaced at 8 inches, some of which were overlapped to get several readings at distances less than 8 inches apart. Two rows of Demec points were installed in the compression zone and one row was used at the level of the tension reinforcement. In the joint region several additional points were used to measure the strains at 45 and 135 degrees from the horizontal.

3.5 Summary

In this chapter, the basic material properties for the concrete and the steel used in the fabrication of the test specimens, the choice of the shape of the specimen, and the preparations and equipment along with description of the test setup for joint testing were discussed. Care was taken in the fabrication and testing of the joints and other test specimens

in order to reduce the influence of test variability. This was especially important because of the limited number of test specimens planned for this investigation. Additional aspects related to the testing procedure will be discussed in Chapter 4.

CHAPTER 4

MCMASTER UNIVERSITY JOINT TEST RESULTS

4.1 Introduction

The fabrication and instrumentation of the test joints, the materials used and their properties, and the joint test equipment were described in Chapter 3. The details of the joints tested, the test procedure and the basic test results are presented in this chapter. The test results are compared with results from the numerical analysis method in Chapter 7. Based simply on observations from the tests some preliminary observations regarding joint detailing were possible and are presented at the end of this chapter.

4.2 Requirements for Satisfactory Details:

At present there is no recognized procedure for the design of reinforced concrete joints and there are no comprehensive detailing standards to be complied with other than those associated with the general design of the intersecting members. A designer normally arranges the steel around the corner according to the existing practice of his company, or may be guided by the various publications of technical bodies, or by available detailing manuals which in fact do not specifically address the problem of joints. Some of the more popular corner details were discussed in Chapter 2. An

illustration of the speculative nature of this area of design is the fact that some of the details preferred in the past are now specifically described as details to be avoided (20, 63). It is apparent from Fig. 2.4 that the reinforcement was not specifically designed to resist the anticipated forces. Indeed, little distinction was made between corners with applied load tending to open the angle and those with the applied load tending to close it. It appears that ease of construction was considered to be of overriding importance.

One of the aims of this investigation was to establish experimentally joint details which would perform satisfactorily when positive bending moment is applied.

In order for a reinforcing layout to be considered satisfactory, reinforcement should be placed in such a way that the joint meets certain fundamental requirements. These are summarized as follows:

1. The joint should be capable of developing a moment at least as large as the maximum calculated failure moment in the intersecting members. Flexural failure may in this case occur outside the joint, which, then does not limit the load bearing capacity of the remainder of the structure.

2. If the first requirement is not met, then the joint should satisfy the ductility necessary for redistribution of forces in the structure without brittle failure of the joints.

3. Cracks preferentially occur on the inside of joints subjected to tension. The widths of corner cracks should therefore be limited to an acceptable value under service loads.

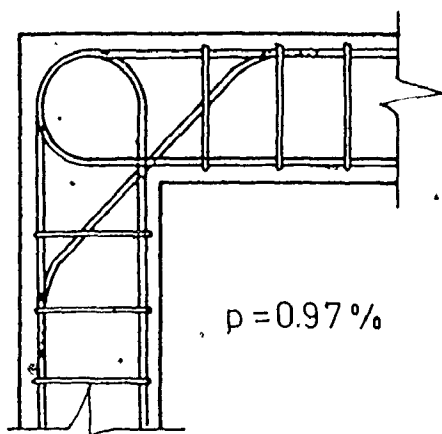
4. The reinforcement should be easy to fabricate and to fix in place. One measure of the ultimate worth of this investigation will be its influence on design practice where practical considerations and simplicity in construction are important requirements.

The experimental contribution towards finding this satisfactory layout consisted of tests on six corner joints comprising four different details. Two of these were reproduced arrangements reported to be satisfactory by Mayfield et al. (74,91) and Nilsson (97). Three of the four details tested were considered satisfactory, (two of these were developed by the author). One of the details was considered to be superior to the others. Two more tests were performed on this same detail; one to confirm the original behaviour and the other to determine the influence of increasing the ratio of steel reinforcement on the behaviour of the joint.

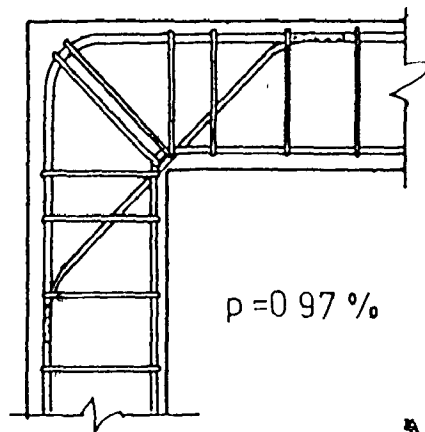
4.3 Choice of Different Details to be Tested

4.3.1 General

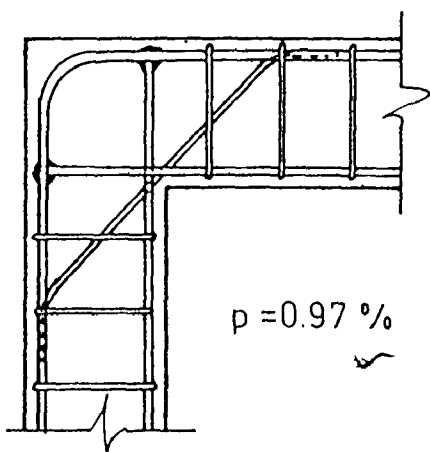
The corner details studied in this investigation are shown in Fig. 4.1. As was described in Chapter 3, two joint specimens were cast at the same time. Initially, the



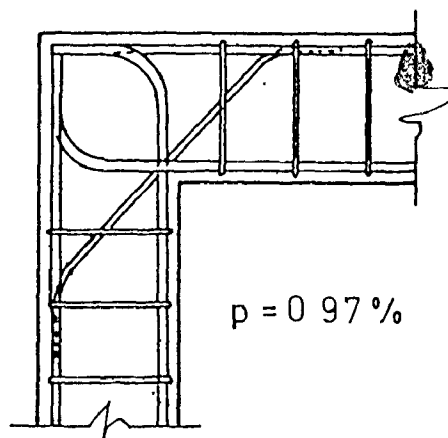
(a) DETAIL (1)
(from Reference 97)



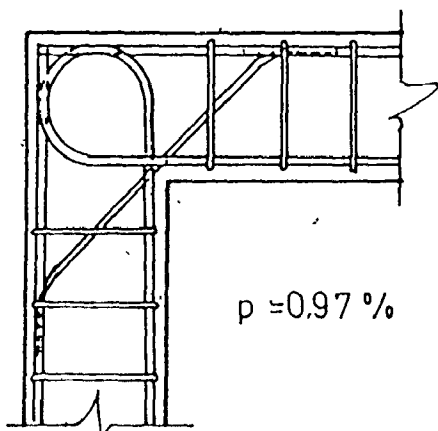
(b) DETAIL (2)
(from Reference 91)



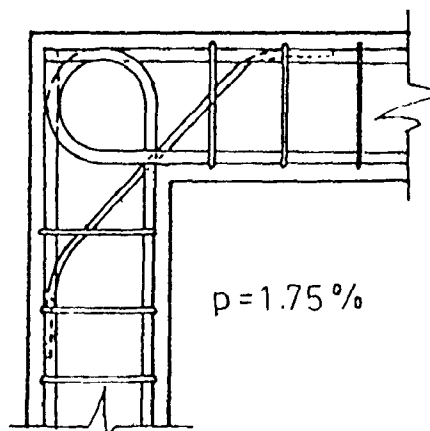
(c) DETAIL (3)



(d) DETAIL (4)



(e) DETAIL (5)



(f) DETAIL (6)

Fig. 4.1 STEEL REINFORCEMENT DETAILS USED IN THE TEST PROGRAM.

experimental program studied two corner joint details which were reported in the literature (91, 97) as being highly efficient details. Some progress toward the development of new details was then made using a series of four tests. The reasons for the choice of each of the details is discussed in this section.

In the experimental part of this study, details which had been shown to be inadequate in other experimental programs (74, 91, 97), were avoided. It is relevant to mention again that some of these inadequate details are widely used and are recommended in some manuals (63, 100) for reinforced concrete detailing practice. Some of these details were shown in Fig. 2.1 to 2.5.

4.3.2 Descriptions of the Joint Details Tested:

4.3.2.1 Detail (1):

Detail (1) was proposed as the result of one of the most comprehensive experimental programs on the subject of joint detailing. The detail developed by Nilsson (97) in Sweden, as shown in Fig. 4.1a, is governed by the following recommendations. "The main reinforcement from the inside tension face is to be extended out into the joint, from where it is to return into the compression zone of the same cross-section to the same level as the inclined reinforcement. The main reinforcement is to be laid as near to the face as the cover specified in the standards will allow. The main

reinforcement is to be designed on the basis of the forces and moments in the intersecting members. The sections are to be regarded as singly reinforced and the calculations can be carried out by elementary bending theory, the effect of the inclined reinforcement being ignored. The spacing of the bars should be the same at both sections. The inclined reinforcement is to have an area approximately 50% of that of the largest main reinforcement. The spacing of the inclined bars should be the same as for the main reinforcement in the intersecting members."

This detail is now adopted by the building authorities in Sweden and thought of as a very efficient detail.

The upper limit on the reinforcement percentage was set at 1.2% for 57 ksi (Grade Ks 40) steel and 0.8% for 85 ksi (Grade Ks 60) steel where these are all based on using around 4500 psi concrete.

In the current investigation, the amount of steel chosen for the main reinforcement was 2 No. 6 bars having an area of 0.884 in.² or $p = 0.97\%$. The inclined bars were 2 No. 4 bars having an area = 0.393 in.², or 44.4% of the area of the main reinforcement. The quality of the high strength steel and concrete were discussed in the previous Chapter.

The results of testing this detail are discussed in Section 4.5.

4.3.2.2 Detail (2) :

Detail (2) was the second detail tested in this investigation which was developed by other researchers. The detail shown in Fig. 4.1. (b) , proposed by Mayfield et.al. (91) was found to be the most efficient detail as a result of testing over one hundred joints. The joints tested by Mayfield et.al. were reported in Chapter 2 and the details were reproduced in Fig. 2.12 and 2.13. They adopted an obvious method of using stirrups to strengthen some of the simple yet deficient reinforcement details.

As shown in Fig. 4.1.b the main tension reinforcement had to be bent very tightly around the inner corner. It was found very difficult to get adequate concrete cover in the corner when the bending radii rules specified by the current codes were observed. Mayfield et.al. did not recommend any specific amount of steel for stirrups. Instead they concluded that a suitable combination of stirrups and inclined reinforcement according to Details 13, 18, 26, in Fig. 2.13 provides a promising method for reducing crack widths and achieving reasonable ductility, and that this detail will be capable of producing corner efficiencies exceeding 100%.

One shortcoming of using stirrups in corners is that the practical use of such a layout would likely be restricted to beam-column joints. For joint corners in retaining walls for example, stirrups could be difficult to place.

In this investigation Detail (2), was very similar to detail (26) by Mayfield et.al. The only change was that the (inclined) diagonal stirrups were replaced by 2 No. 4 bars, the area of which was 0.393 in.^2 . The main tension reinforcement was maintained at 2 No. 6 bars as for Detail (1) ($p = 0.97\%$).

Two No. 3 two-branch stirrups having an area of 0.44 in.^2 (or stirrup to main tensile reinforcement ratio of 0.5) were used to join the tension and compression reinforcement along the line from the inside to the outside of the corner. It was anticipated that the stirrup area might be low. However, it was used as an initial guideline for the behaviour of this detail. Increasing the amount of stirrups in the corner would have made the placing of concrete such a difficult process that incomplete compaction in the joint region would have been quite possible. Discussion of the effect of increasing the stirrup area on the behaviour of the corner joint is included in Chapter 7.

4.3.2.3 Detail (3):

Detail (3) was the first of a series of four details which were tested in an attempt to develop an efficient and simple detail. A few difficulties were encountered in fabricating the steel for Detail (1). The exact spacing required between tension and compression reinforcement was not easy to obtain. Bending steel 180° was found to be impractical. Also fitting beam and column stirrups was rather difficult.

The area of stirrups which would be required using Detail (2) to obtain reasonable efficiency was anticipated to be large. This would be particularly true considering the crowding of the steel in the joint region.

It was thought that Detail (3), shown in Fig. 4.1.c could be a step towards simplifying the joint detail without sacrificing the desired efficiency.

From review of other tests (97) it appeared to be of prime importance to confine the core of the joint region to avoid diagonal tension failures, hence the detail was designed as follows:

1. The tension reinforcement was composed of 2 No. 6 straight bars in each of the two intersecting members. These were extended to meet and were welded to the compression reinforcement near the outer faces.

2. The compression reinforcement consisted of two No. 6 bars bent at 90 degrees as shown in Figure 4.1.c.

3. The diagonal (inclined) reinforcement of 2 No. 4 bars were also added. This type of reinforcement was common to all the tests performed in this investigation and as it is discussed in Chapter 7, was found to be necessary.

Detail (3) was simple to fabricate. However, the availability of welding equipment is essential.

4.3.2.4 Detail (4) :

Detail (4), shown in Fig. 4.1.d was developed to avoid either welding the reinforcing steel or bending the

steel more than 90° , or using stirrups. The tension reinforcement consists of 2 No. 6 bars in each intersecting member, each bent at 90° degrees. The steel is placed in the cage so that the end of the 90° hook reaches the outer corner of the joint (with the appropriate cover). The addition of concrete stubs to one or both of the intersecting members would be beneficial for providing end anchorage especially for larger steel sizes or smaller member dimensions (95). Compression steel was simply 2 No. 6 straight bars stopped at the outer corner of the joint. Obviously this arrangement is not adequate for loads tending to close the joint. Inclined diagonal bars of the same size for the three previous details were added.

4.3.2.5 Detail (5) :

Detail (5) was made essentially the same as detail (4). The main purpose was to confirm the results obtained from the test on detail (4). One change made to accommodate the possibility of load reversals was that compression steel was made continuous using 90° bent bar as shown in Fig. 4.1.e. This detail was also suggested by Park and Paulay, for joints with large intersecting members, in their text (103) which was published after this experimental program was conducted.

4.3.2.6 Detail (6) :

The effect of higher percentage of reinforcement on the behaviour of the joint was examined by testing Detail (6). The layout was exactly the same as that for Detail (5), with only the amount of reinforcement changed. Two No. 8 bars were used for tension reinforcement in each member with

of compression steel ($p = p' = 1.75\%$). The

inclined diagonal bars were made of 2 No. 6 bars, with an area ratio of 56%, of the area of the main tension reinforcement.

4.4 Test Procedure

The testing rig described in Chapter 3, was used to load the test specimens to failure. The test procedures for Details (1), (2), (3), & (4) were identical, but different from those for Details (5) and (6) which were subjected to 4 cycles of load reversals before loading to failure. Test procedures for the two groups are described in this section.

4.4.1 Incrementally Increasing Load Tests

In this group of tests the two jacks (top and bottom) shown in Fig. 3.5 were activated simultaneously. The jacks were both in compression and were acting in opposite directions. The top jack pushed the vertical member to open the corner. This resulted in a constant shearing force and linearly changing bending moment on the vertical member. The bottom jack applied the same amount of force as the top one to eliminate the tension from the horizontal member which is, therefore subjected to pure bending moment only.

Initial readings were taken, then the loads were applied in increments. After each 1.0 kip increment, dial gauge readings and Demec readings were taken to measure deflection and strains. Also the cracks were traced using a magnifying flashlight and were marked to show the crack propagation at the different load levels. The 1.0 kip increments were decreased to .5 kip increments near the failure loads. The load levels for both

jacks were continuously monitored and adjusted to maintain constant loads during the process of taking measurements.

After all the measurements were taken, the load was increased to the next load level and the whole procedure was repeated. This process was continued until failure of the specimen.

Strain measurements were not taken after the joint region was cracked or spalled in a way that measurements would no longer represent strains.

Dial gauges placed under the specimen to facilitate the calculations of joint rotations were removed when the joint was judged to be quite near failure. This precautionary measure was taken to avoid damage to the gauges.

Details of test results are discussed in the following sections of this chapter.

4.4.2 Test Procedure for Joints Subjected to Load Reversals,

Details (5) and (6) :

After the completion of the first four tests it was decided that the next two specimens would be subjected to load reversals before the joint was loaded to failure. It was thought that this type of information would provide a worthwhile additional aspect for the evaluation of the adequacy of the detail. In addition to evaluating behaviour for bending in both directions, it could provide some indication of the joints' capabilities for withstanding cyclic effects.

Since cyclic loading was not within the original scope of this investigation and was included only to provide an indication of overall suitability of this detail, the test procedure was designed so that damage to the specimen during cyclic loading would be minimal. The precaution taken was to limit the inelastic deformations and thereby minimize damage, unless it happened that a defective detail was used which exhibits unfavourable characteristics.

Discussions with Tso* and Paulay** helped to clarify the author's ideas on this matter. It was decided that an arbitrary deflection be chosen and the joint be opened then closed to get a specified deflection in both directions. This procedure was to be repeated for four cycles, then the specimen was to be loaded to failure with the load opening the joint.

The criterion by which the joint would be judged to be adequate was to maintain at least 85% of the original load after 4 cycles of loading to the specified deflection, and to maintain its ultimate capacity when finally loaded to failure.

* Private communication with W.K. Tso, Professor & Chairman Department of Civil Engineering, McMaster University, Hamilton Ontario, Canada.

** Private communication with T. Paulay, Professor, Department of Civil Engineering, University of Canterbury, New Zealand.

An arbitrary deflection of 1.00 inch was chosen for both joints (5) and (6). This amount of deflection, which represented nearly four times the measured deflection for Detail (5) at the theoretical working load level, was chosen so that the main reinforcement would be in the vicinity of yielding. This precaution was taken to avoid any possibility of severe damage during load reversals. This aspect was of great concern to the author because of the limited number of tests which were planned for this investigation.

When the top jack was pushing to open the joint, the test procedure was the same as that discussed in the previous section for Details(1), (2), (3) and (4). However, when the top jack was pulling to close the joint, the bottom jack was not activated thereby allowing a compressive force equal to the load applied by the top jack to be transferred to the horizontal member. Strain measurements were not taken after the first cycle of loading was completed.

4.5 Test Results

4.5.1 General Behaviour

The test procedure and arrangements of steel reinforcement were discussed in the previous sections. In this section and the following sections the test results and some preliminary observations are presented.

The load-deflection curves for the six joints are shown in Fig. 4.2. Load-deflection or moment-rotation curves are considered to be reliable bases for comparisons of

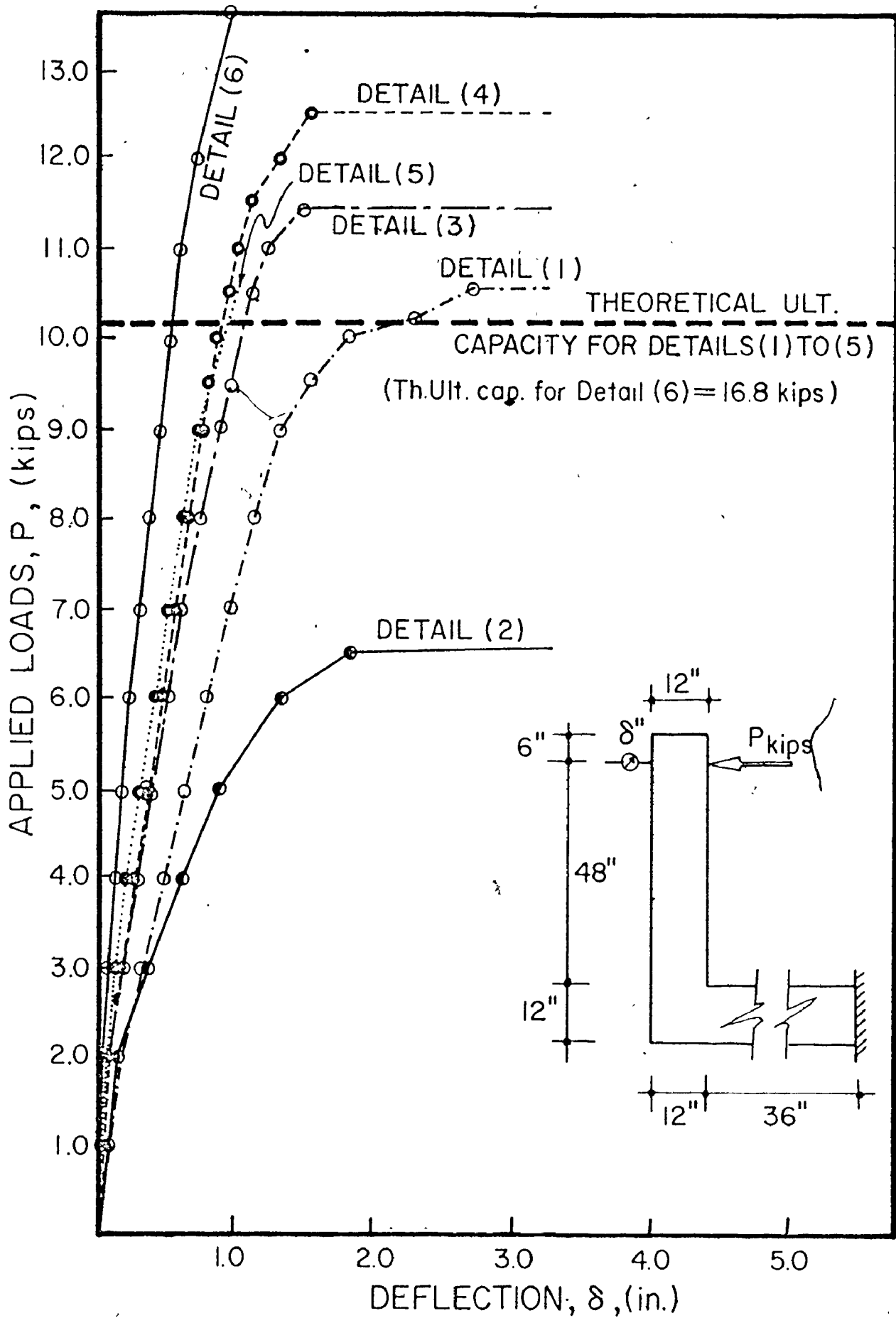


Fig 4 2

FCTION S TESTED T DETA

behaviour of structures since the basic test measurements are used.

From Figure 4.2, it can be seen that the results are divided into four distinct behaviour groups. Detail (2) has a very low load capacity and comparatively unfavourable load-deflection characteristics. Detail (1) which has an intermediate load capacity also has an improved load-deflection characteristic. Details (3), (4) and (5) have capacities which are higher than Detail (1) and the load-deflection curves are quite consistent. Detail (6) was the only joint tested with a different percentage of reinforcement. A direct comparison between the capacity of this joint and of the others is not valid. However, the joint capacity was close to the calculated capacity of the intersecting members according to the ultimate strength theory using the Whitney Stress Block (96).

Figure 4.3 shows the moment-rotation curves for all the details. The same general characteristics as for the load-deflection curves were observed except that the behaviour of Detail (1) was closer to that of Detail (3), (4) and (5).

The load-deflection curves for Details (5), and (6), shown in Fig. 4.2 are for the opening part of first loading cycle only. The full load-deflection curves for all cycles of loading for these details are shown in Figs. 4.4 and 4.5 respectively.

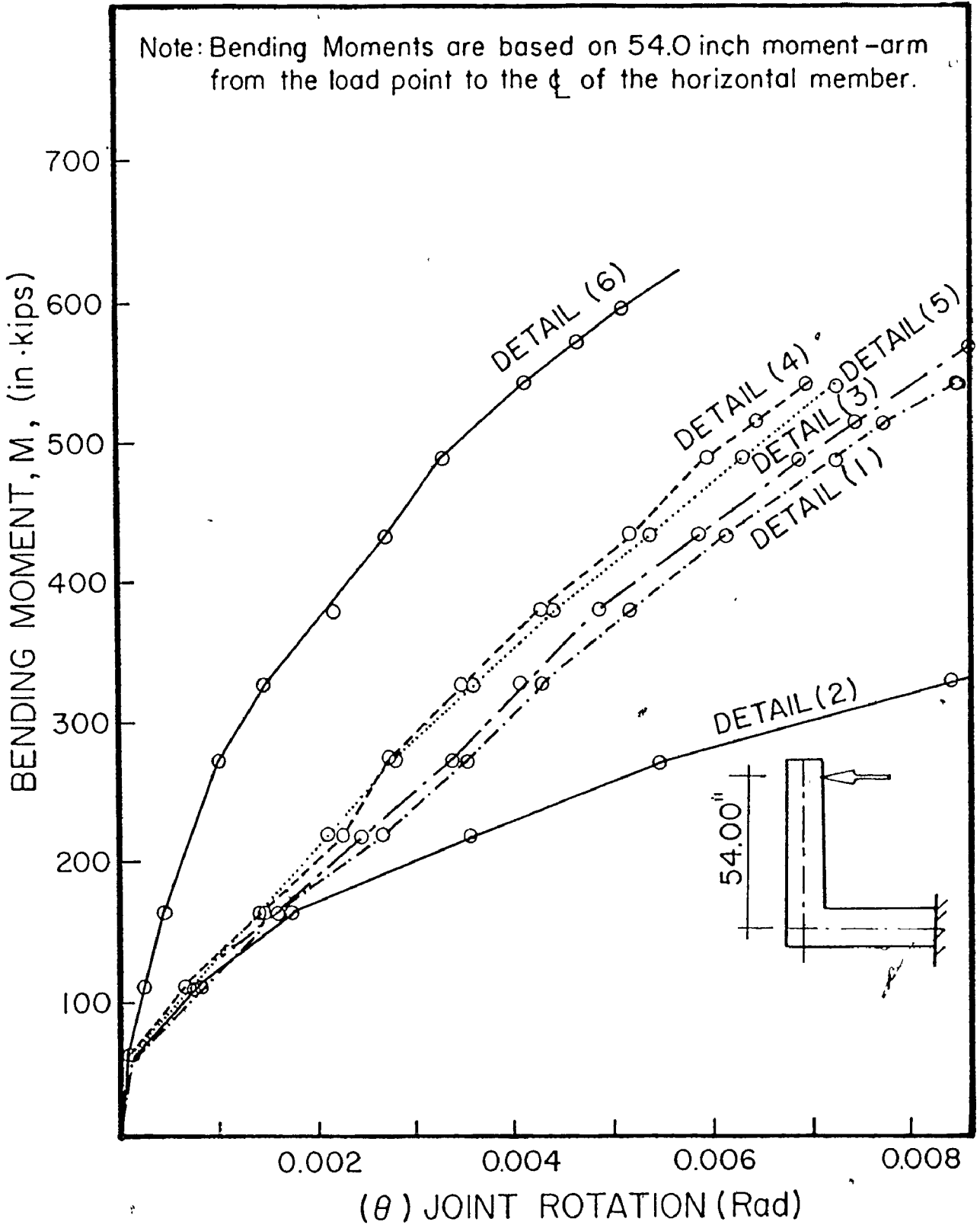


Fig. 4.3 MOMENT-ROTATION RESULTS FOR TESTED JOINT DETAILS

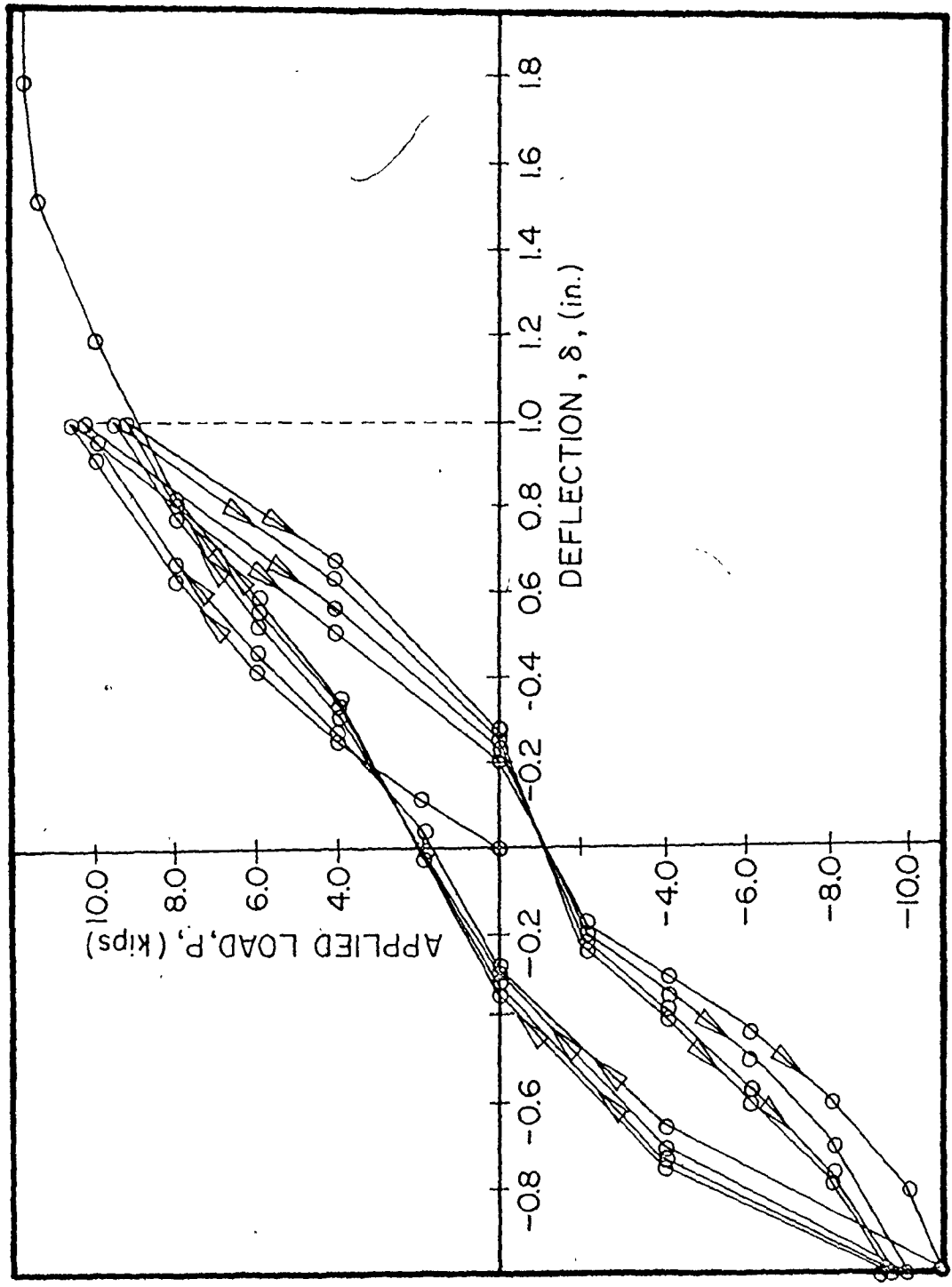


Fig. 4.4 LOAD-DEFLECTION RESULTS FOR 4 CYCLES OF LOADING, DETAIL (5)

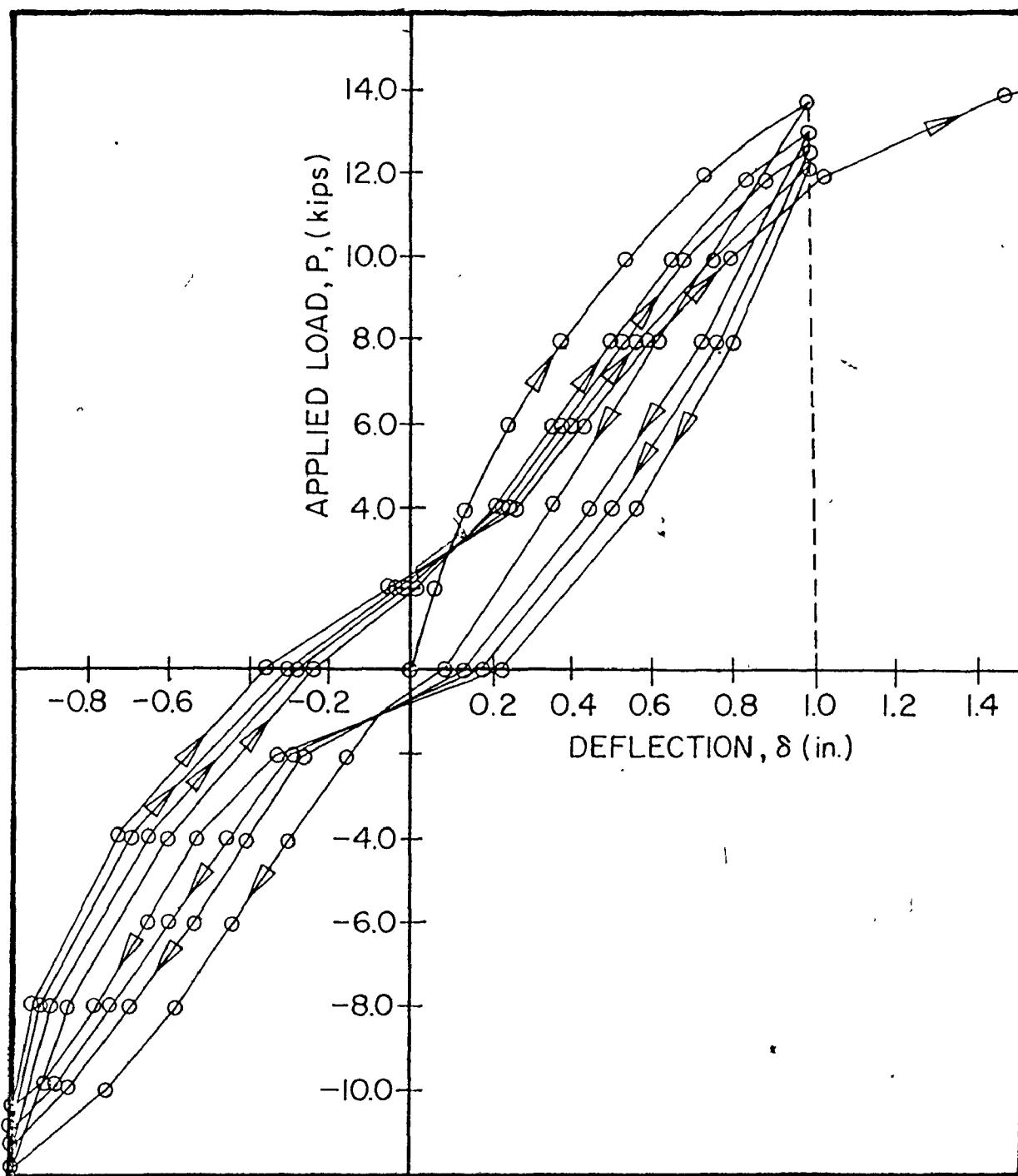


Fig. 4.5 LOAD-DEFLECTION RESULTS FOR 4 CYCLES OF LOADING, DETAIL (6)

4.5.2 Cracking Patterns

The cracking patterns at failure for Details (1) to (4) and after the first cycle of loading for Details (5) and (6) are presented in Figures 4.6 through 4.11. These drawings are scaled reductions of tracings made on the tested specimens.

The numbers shown beside the cracks represent the load levels at which the cracks had propagated to the points where the numbers are written.

From Figures 4.6 to 4.11 it is clear that the flexural cracks in the two intersecting members are not identical for all the tested specimens having equal amounts of steel reinforcement. However, crack spacing and crack propagation are fairly consistent.

Crack widths were not measured in this investigation but visual observations didn't show any great differences between different specimens for regions outside of the joint. However, major differences for cracking in the joint region between some of the details were observed.

Table 4.1 shows the measured crack spacings outside the joint region for each test specimen. Average, minimum and maximum crack spacing are given for every specimen. The mean and standard deviation of all the crack spacings of the specimens with equal amounts of steel reinforcement are also given.

Fig. 4.10 EXPERIMENTAL CRACKING PATTERN
 AFTER FIRST CYCLE OF LOADING
 WITH OPENING MOMENT FOR DETAIL (5).
 ($A_s = A_s' = 2 \# 6$ bars, $A_{sd} = 2 \# 4$ bars,
 $b = 9''$, $t = 12''$)

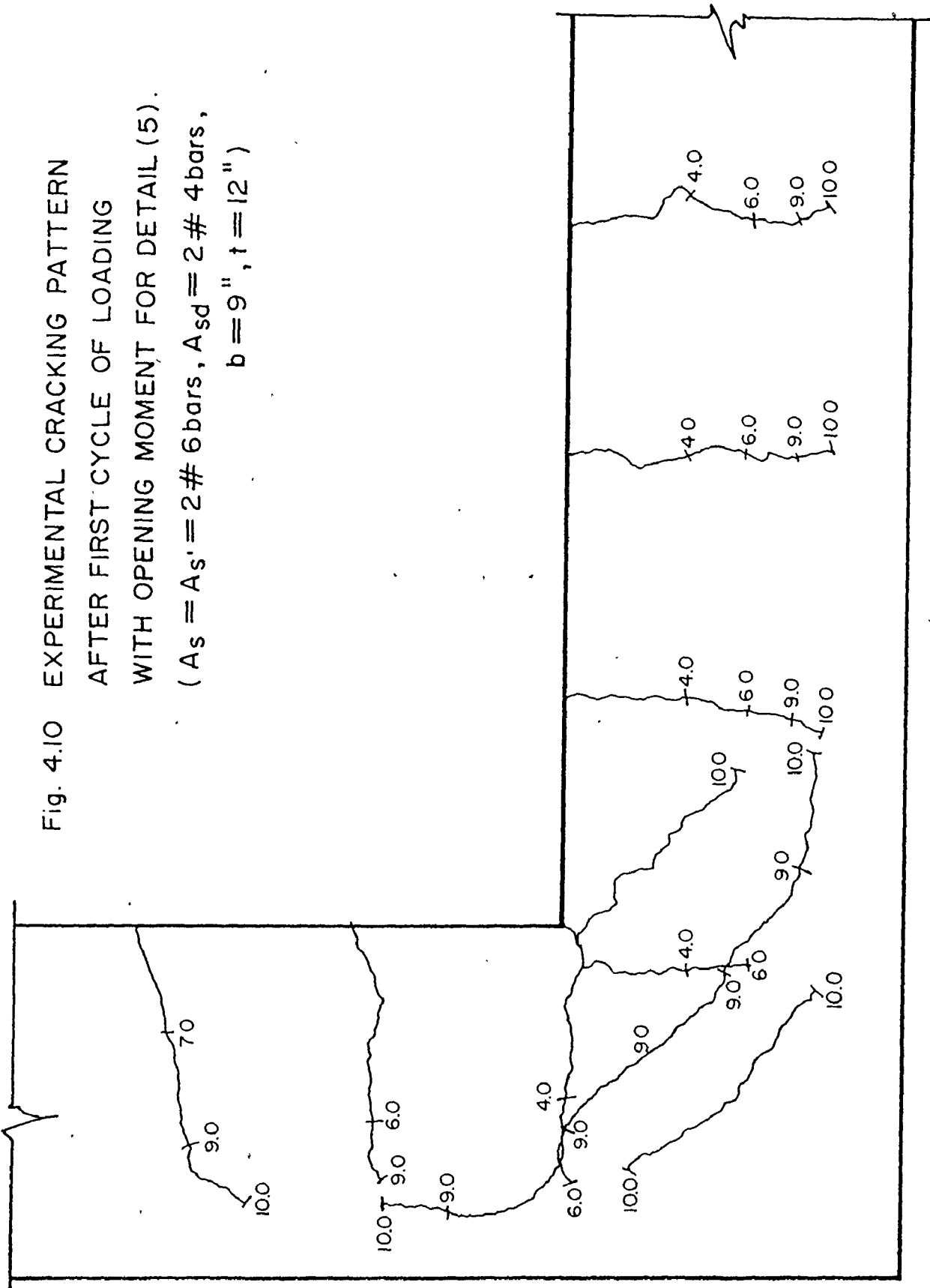


Fig. 4.11 EXPERIMENTAL CRACKING PATTERN

AFTER 1st CYCLE OF LOADING WITH OPENING MOMENT FOR DETAIL (6).

($A_s = A_{s'} = 2\#8$ bars, $A_{sd} = 2\#6$ bars,

$b = 9"$, $t = 12"$)

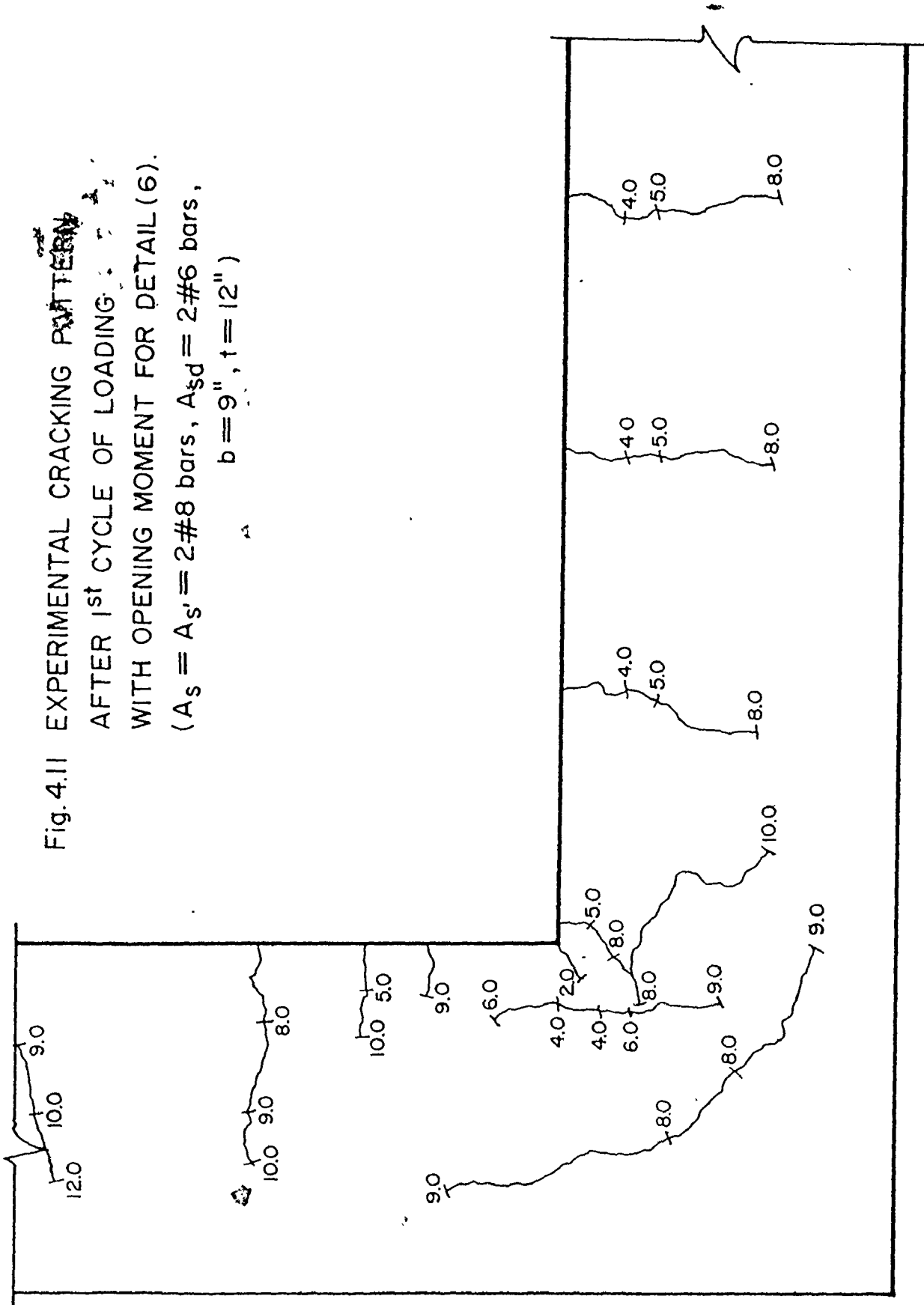


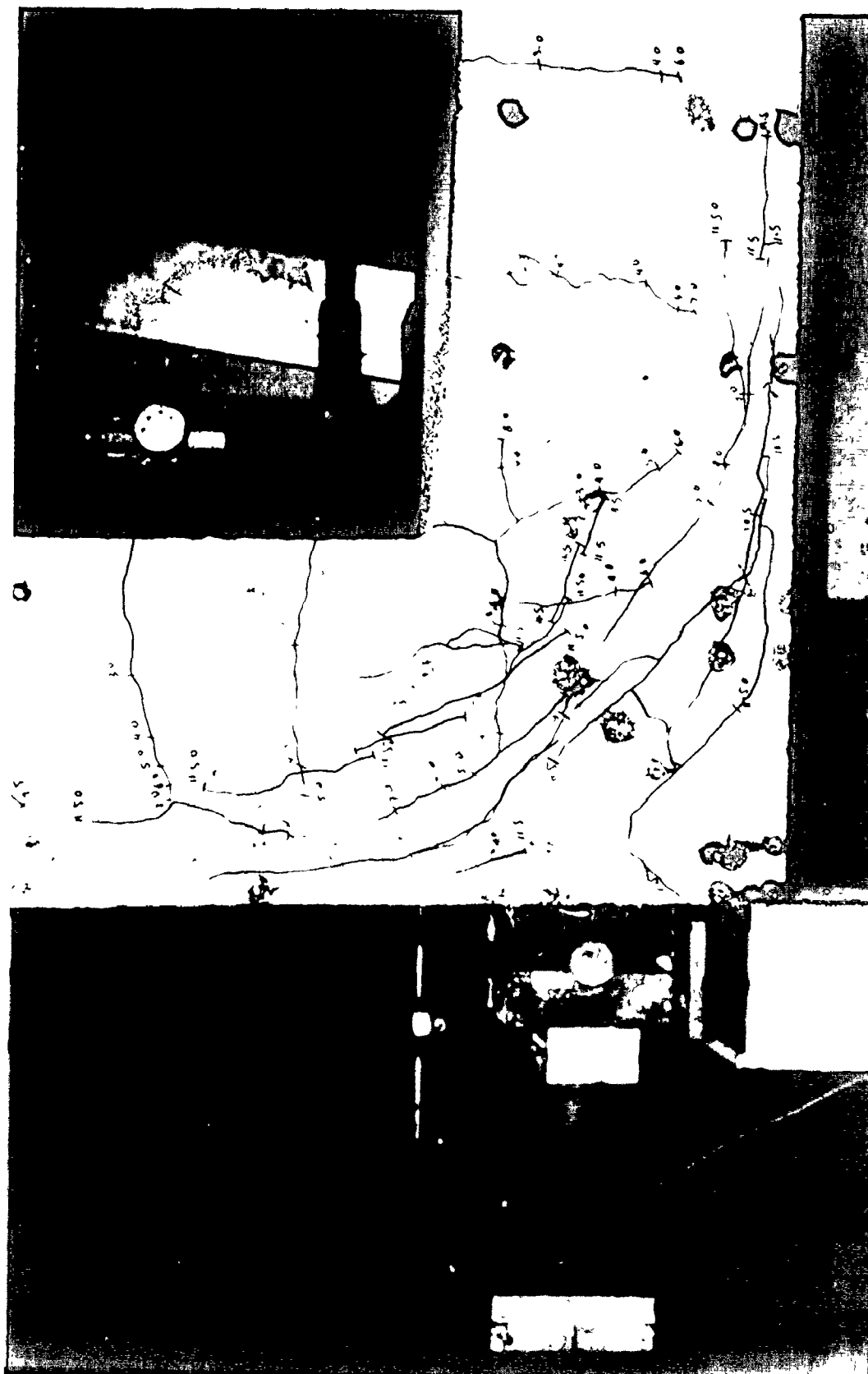
Table 4.1 Measured Crack Spacing Outside the Joint Region.

Crack Spacing (inches)			
Joint Detail	Average	Maximum	Minimum
(1)	4.9	6.0	3.6
(2)	5.1	5.8	3.6
(3)	7.15	8.8	6.6
(4)	6.27	6.4	5.6
(5)	7.8	8.4	7.6
(6)	7.67	9.5	6.2
MEAN* = 6.24"		Standard Deviation* = 1.26	
*Excluding detail (6) (different reinforcement ratio)			

Figures 4.12 to 4.15 show photographs for Details (3), (4), (5) and (6) at failure respectively.

Large differences in the cracking patterns at the joints regions of the different specimens can be observed from Figures 4.6 to 4.11. Diagonal cracking which is considered to be the main concern in the joint regions varies considerably. It is generally acceptable that the more the diagonal crack propagation is delayed, the stronger the joint will be (74, 97). Three types of cracks in the joint region have been identified and are illustrated in Figure 4.16. These are:

1. Flexural Cracks designated as type (a)



NT DETAIL (3) AFTER FAILURE

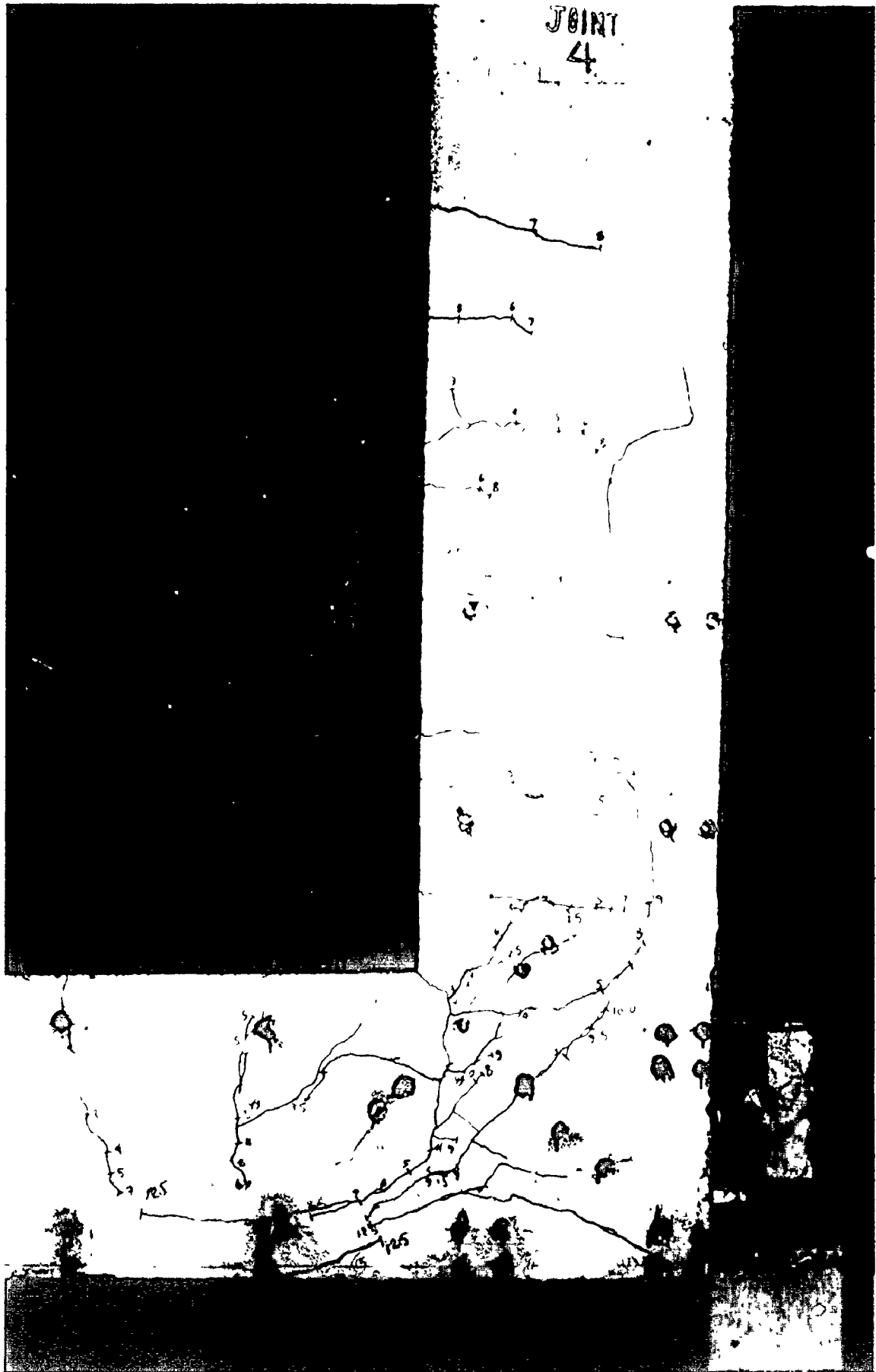


FIG. 4.13 JOINT DETAIL (4) AFTER FAILURE

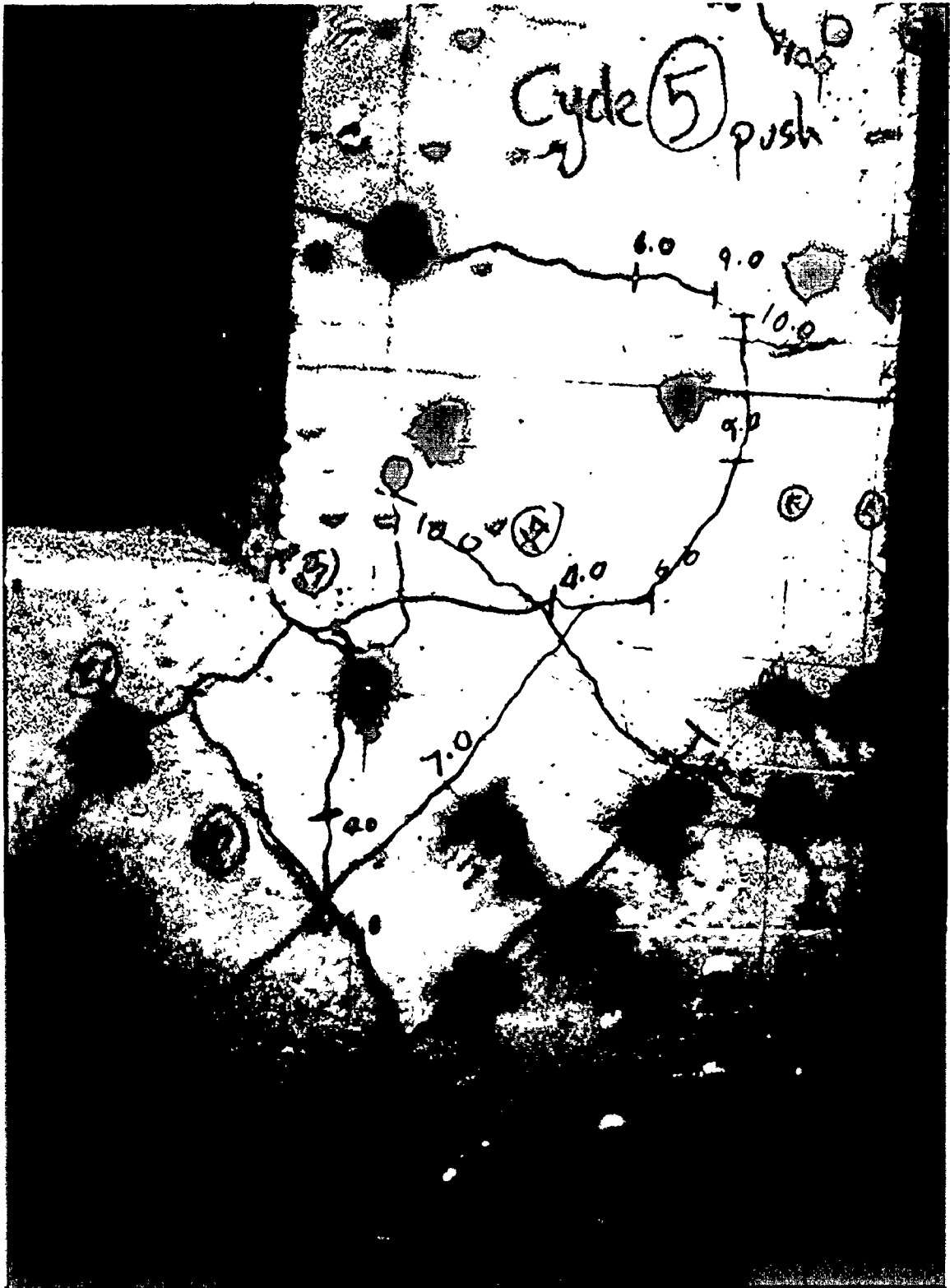
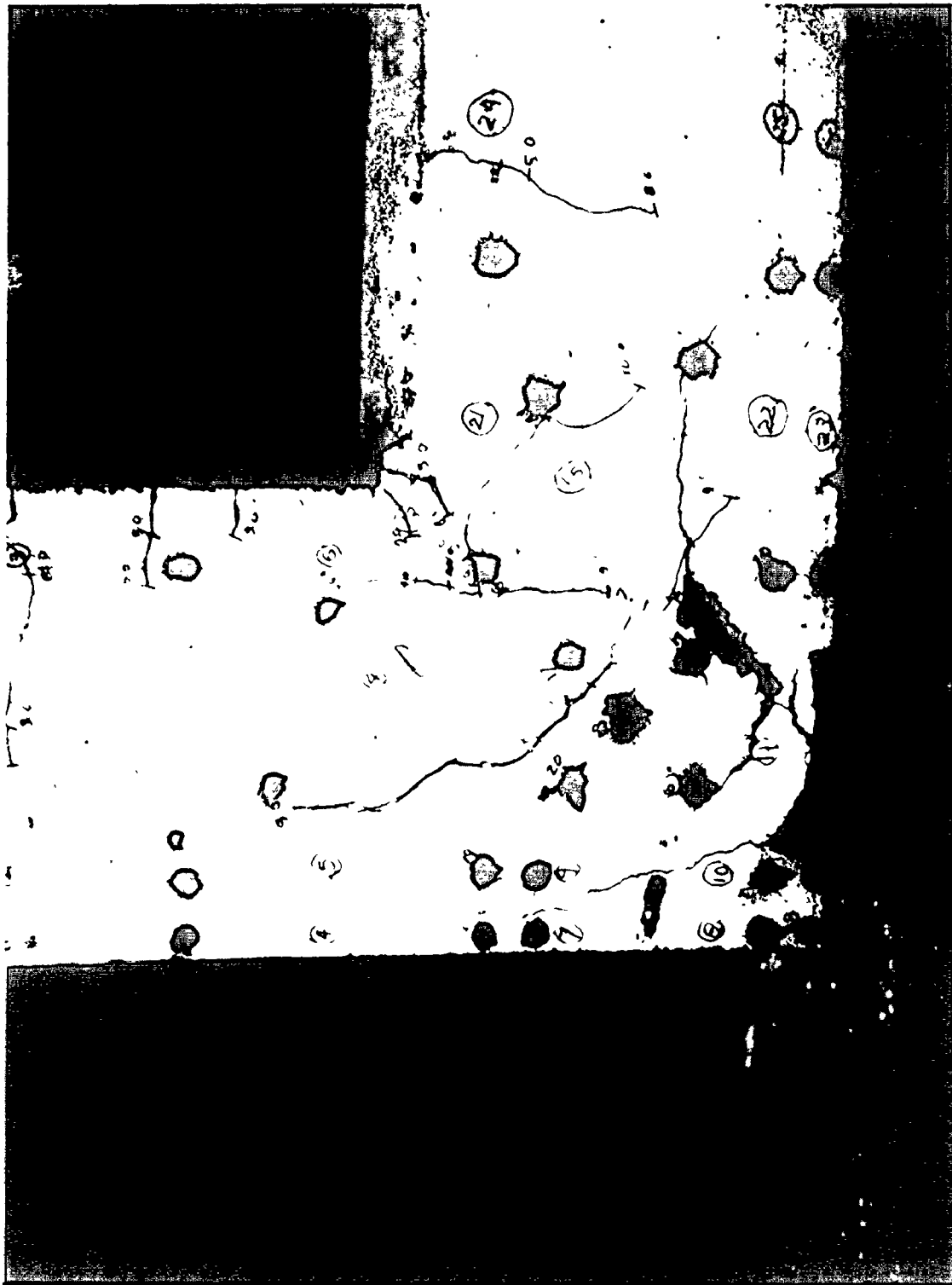


FIG. 4.14

JOINT DETAIL (5) AFTER FAILURE



JOINT DETAIL (6) AFTER FAILURE

(2) Corner tension cracks designated as type (b)

(3) Diagonal tension cracks designated as type (c)

Crack type (b) is inevitable in any corner joint subjected to moment tending to open the angle. Diagonal reinforcement was provided in all the specimens to limit the width and the propagation of this type of crack.

Crack type (a) can be seen at the joint region in all the specimens except for Detail (2) where premature yielding of the stirrups diagonally joining the compression and tension reinforcement (as shown in Fig. 4.1.b) caused the cracks to propagate diagonally in both directions instead of being controlled vertically and horizontally.

The formation of type (c) cracks signifies the main differences between one joint detail and another. Also cracks of type (a) will usually propagate diagonally as designated by type (d) in Fig. 4.16. These cracks may eventually cause a diagonal tension failure of the joint if stirrups were not provided at these locations in the two intersecting members. Type (d) cracks shall be regarded as different from type (c) although their directions are usually the same. They form at different locations and they may form even in the presence of positive confinement for the joint core.

The approximate load levels at which cracks of types (a), (b), (c) and (d) were first observed expressed as percentages of the calculated ultimate load capacities of the intersecting members using the Whitney Stress Block (96) are presented

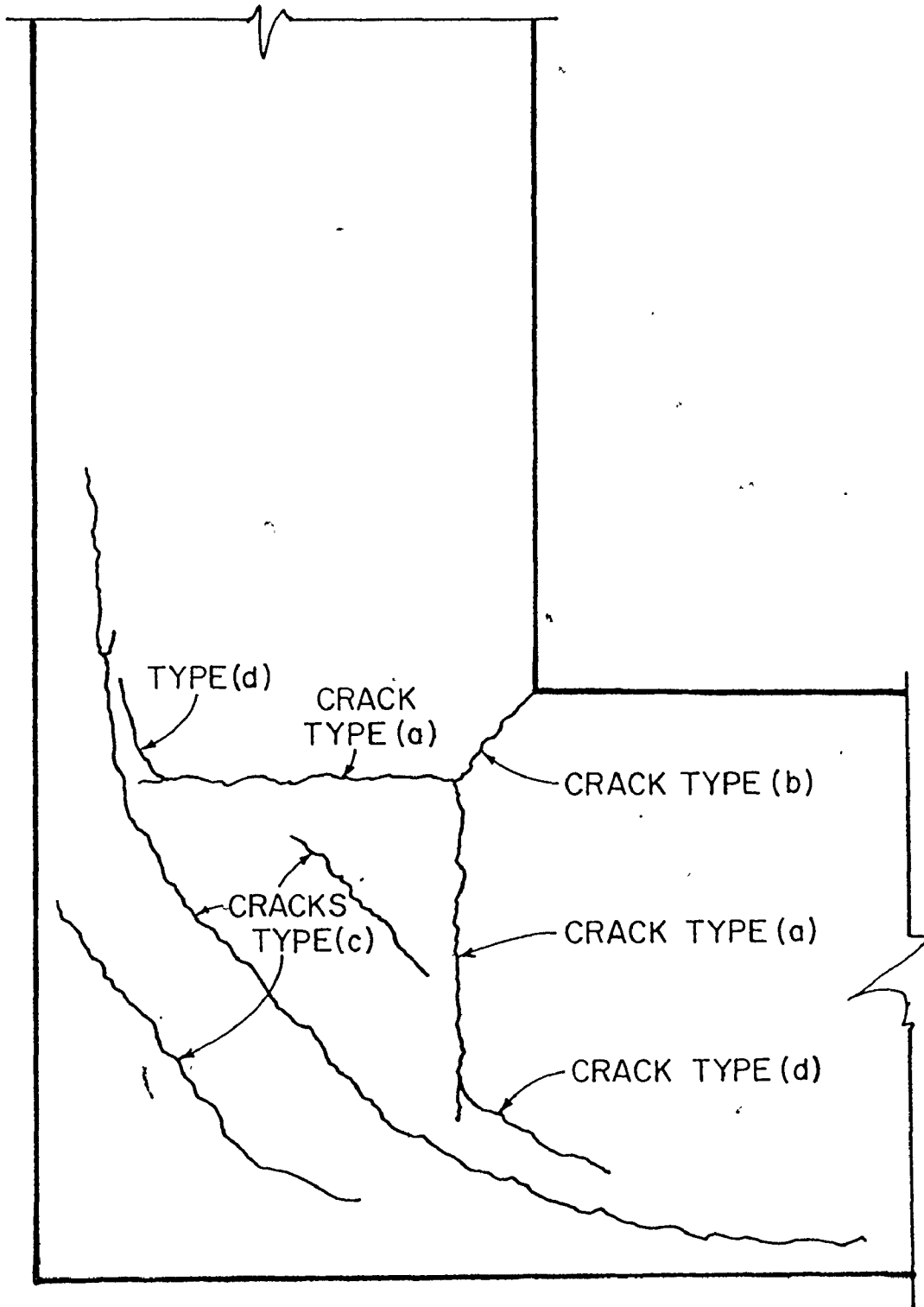


Fig. 4.16 POSSIBLE CRACK TYPES IN JOINT REGION.

in Table 4.2. The experimental ultimate capacity as a ratio of the calculated capacity is also shown in the same table.

Table 4.2 SUMMARY OF JOINT TEST RESULTS

Joint Detail Number	f'_c ksi	Steel Prop. limit f_y , ksi	% Load at crack occurrence calculated ultimate load				Ult. cap. kips	$\frac{\text{exp. ult. cap}}{\text{Cal. ult. cap}}$ %
			C R A C K T Y P E					
			(a)	(b)	(c)	(d)		
(1)	4.98	69	50	40	50	75	10.5	104%
(2)	4.98	69	-	30	20	-	6.5	64%
(3)	5.11	68	30	30	70	50	11.5	114%
(4)	5.11	68	40	30	90	50	12.5	124%
(5)	5.36	71	40	30	70	90	11.6	115%
(6)	5.36	71	24	12	50	50	14.75	88%

NOTE:

The capacities of Details (1) to (4) are the capacities from one cycle load test while these for (5) and (6) are the capacities after 4 cycles of load reversals as previously discussed.

4.6 Observations

In this chapter the test results for the joints were presented and discussed. Further discussions are contained in Chapter 7 where comparisons between experimental and analytical results are made. Discussions of the mode of failure of each specimen is also presented in Chapter 7.

From considerations of just the test results the following observations can be made:

(1) Detail (2) for the quantity of diagonal stirrups used in the test has the least capacity and the lowest overall performance of all the details tested. In Chapter 7 the effect of increasing the amount of diagonal reinforcement shall be discussed.

(2) Details (1) and (3) performed satisfactorily from a capacity and displacement point of view. However, their fabrication required more effort than was required, for Details (4), (5) and (6). The practicality of welding is an important requirement for the fabrication of Detail (3).

(3) Details (4), (5) and (6) were relatively simple to fabricate and generally have a capacity in excess of that required by the design of their intersecting members. The exception is Detail (6) which had a slightly lower capacity than that required. This however, may have been due to the deterioration of the joint during the cyclic loading. This observation and other factors such as size and anchorage of

reinforcement are discussed in Chapter 7.

It is thought, therefore, that a reinforcement layout as shown in Details (4), (5) and (6) may be superior to other widely used details.

The test program studies only a very limited range of variables and, therefore, additional evidence is required to confirm the applicability of any of these details. However, a full experimental study of this nature is beyond the scope of this investigation. Instead, subsequent chapters describe the analytical approach which was developed not only to try to help explain the performance of established joint details but to complement experimental work in the development of other joint details.

CHAPTER 5
ANALYTICAL METHOD AND DESCRIPTION
OF THE COMPUTER PROGRAM

5.1 Introduction

To develop a better understanding of the behaviour of reinforced concrete joints is the primary objective for this research. The use of inadequate joint details may be due to the lack of rigorous explanation for the complex interaction found in joint behaviour. Experimental research can be of great value to assist in the process of developing better joint details. However, development of an analytical method based on rational modelling of concrete and steel and their interactive behaviour is helpful in two ways. It will not only complement the experimental results by facilitating a better understanding of the behaviour of an experimentally developed joint but should also be of great assistance in actually developing satisfactorily performing joints through understanding and analytical testing of their complex behaviour.

This chapter contains the descriptions of the computer program developed by the author to analyse the behaviour of reinforced concrete members. The particular objective for developing this program was to model reinforced concrete beam-column connections and simple beams. The program is applicable only to cases with monotonically increasing loads and a major

feature is the ability to introduce and trace crack growth. Joint elements (linkage elements at steel and concrete interface) are also introduced to permit the modelling of bond-slip and of dowel action. The feature of permitting cracks to develop is very necessary for a proper analysis of reinforced concrete members of the types intended in this investigation. However, this introduces computational complexities such as iterations required for establishing crack stability and the necessity to continuously alter the stiffnesses of the finite elements to allow for this as well as other non-linearities involved in the analysis.

5.2 Idealizations Introduced in the Finite Element Method of Analysis

Some idealizations of the concrete and steel configurations and the nature of their interconnectivity are required since the analysis is limited to being finite and two dimensional.

A plane stress analysis of a reinforced concrete member using the finite element method is possible assuming that

1. Steel reinforcing bars are uniformly distributed across the member.
2. Loads are applied in a plane parallel to the length and depth directions.
3. The length of the member is relatively large as compared to its cross sectional dimensions.

In some instances, to be valid, analysis must account for the

three dimensional nature of the stress and strain fields. For example, this is important in the anchorage zone of a prestressed concrete beam or in beams with large widths and a single reinforcing bar.

The finite element idealization of members reinforced with "m" bars of diameter " ϕ ", distributed over the width "b" of the member is shown in Fig. 5.1. For analytical purposes it is convenient to replace each round bar with an equivalent rectangular bar of the same cross sectional area. The dimension of the equivalent bar in the depth direction is kept the same as " ϕ " to maintain realistic cross sectional geometry which is especially important with complex arrangements of reinforcement. The width of the idealized steel element is modified to

$$S = m \frac{\pi \phi}{4} \dots\dots\dots(5.1)$$

The modified width of concrete elements at the steel level becomes

$$b_{\text{net}} = b - S \dots\dots\dots(5.2)$$

where b = total member width.

The finite element idealization of a continuum is made by subdividing this continuum into a finite member of elements interconnected at a number of discrete nodes. The elements can have various shapes such as triangles, rectangles or quadrilaterals. The shape and the number of elements used in an analysis are usually chosen by the user to suit various contours and to obtain sufficient precision consistent with a reasonable number of degrees of freedom. Concrete and steel elements are

idealized by using constant stress triangles in this investigation. Triangular elements best suit the complicated reinforcing steel arrangements used in this study. Due to the large number of elements required for the tracing of crack growth in concrete elements, the use of more than two degrees of freedom per node was not possible with the available computer facilities.

The complex interaction between concrete and steel at their interface is idealized by special discrete elements called, hereinafter, "joint elements". These joint elements were developed by Goodman et.al. (46), to permit deformations in the directions parallel and perpendicular to their lengths. These special linkages have no thickness, therefore, they eliminate the introduction of a non-realistic concrete or steel configuration. Section 5.3.3 is devoted to the description of this type of element.

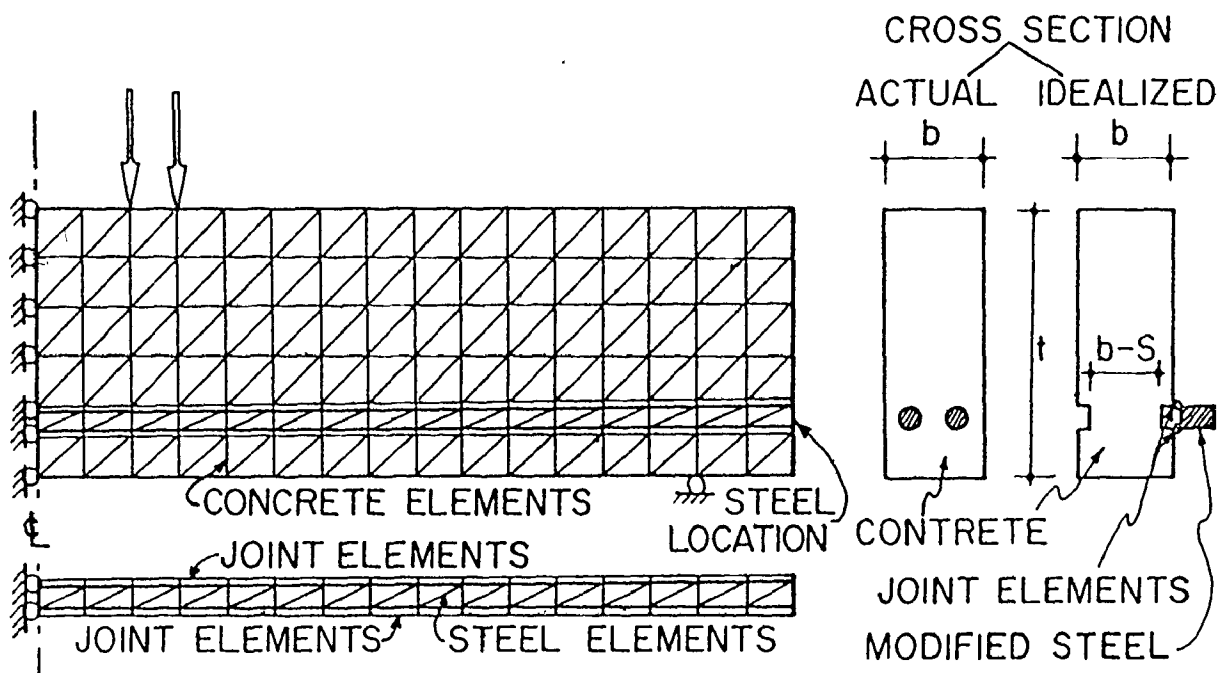


Fig. 5.1 FINITE ELEMENT IDEALIZATION OF A SIMPLE BEAM.

5.3 Mathematical Formulation

5.3.1 Concrete and Steel Element

The finite nature of the connectivity between the elements makes possible the formulation of simultaneous algebraic equations relating the nodal forces to the nodal displacements in each element. These equations are equal in number to the number of degrees of freedom chosen. In the present analysis of plane stress cases, two degrees of freedom per node are incorporated. In matrix notation the equations are as follows:

$$\{P_e\} = [k_e] \{\delta_e\} \dots\dots\dots(5.3)$$

where,

- $\{P_e\}$ = nodal force vector
- $\{\delta_e\}$ = nodal displacement vector
- $[k_e]$ = element stiffness matrix

The description of the derivation of the stiffness characteristics of plane stress elements used in this investigation can be found in many finite element method text books. (37, 59, 80).

The element stiffness matrix

$$[k] = t [B]^T [D] [B] dA \dots\dots\dots(5.4)$$

where, $[B]$ = strain matrix

$[D]$ = elasticity matrix

The strain matrix $[B]$ relates the strain vector $\{\epsilon\}$ to the nodal displacement vector $\{\delta_e\}$ hence,

$$\{\epsilon\} = [B] \{\delta_e\} \dots\dots\dots(5.5)$$

where,

$$[B] = \left\{ \frac{\partial u}{\partial x} \quad \frac{\partial v}{\partial y} \quad \frac{\partial u}{\partial y} + \frac{\partial v}{\partial x} \right\} \quad (5.6)$$

and u and v are the displacement functions in the form of polynomials with the number of coefficients equal to the number of the degrees of freedom chosen for the element. A closed form solution of the integrals in the stiffness matrix can readily be obtained for constant or linear strain triangles as well as for rectangular elements.

In the case of a general quadrilateral element, Zienkiewicz (37), reported that "It will, however, be evident on inspection that integration of the various expressions required for the formulation of the stiffness and strain matrices will present difficulties which are almost insurmountable if closed form expressions are desired. This is due to the inverse of the Jacobian matrix, in which polynomials occur in the denominator of various expressions. It seems essential, therefore, to apply numerical integration procedures. Application of Gauss' rule or other similar techniques will permit numerical evaluation of the appropriate integrals. Computer programs, however, become longer now, and it is perhaps problematical whether the improved accuracy would not be better achieved by the use of a finer subdivision in the simpler formulation of triangular elements."

The elasticity matrix $[D]$ relating stresses to strains should incorporate the biaxial stress state which is often present in reinforced concrete members. Because concrete does not behave elastically, the values of the elastic moduli included

in the elasticity matrix are actually variable quantities depending on the strain level. Thus this nonlinearity can be incorporated in an inelastic analysis when an incremental loading technique is used. The orthotropic elasticity matrix can be written (37) as:

$$[D] = \begin{bmatrix} \frac{E_x}{1-\nu_x \nu_y} & \frac{E_x \nu_y}{1-\nu_x \nu_y} & 0 \\ \frac{E_y \nu_x}{1-\nu_x \nu_y} & \frac{E_y}{1-\nu_x \nu_y} & 0 \\ 0 & 0 & G \end{bmatrix} \quad (5.7)$$

where E_x and E_y = elastic moduli in orthogonal x and y directions.

ν_x and ν_y = Poisson's ratio in the x and y directions

G = Shear modulus of elasticity

In this investigation ν_x and ν_y were set equal and constant throughout the analysis. ($\nu_{\text{concrete}} = 0.2$, $\nu_{\text{steel}} = 0.3$)

In equation 5.7, the increase in effective stiffness in either direction in the presence of normal compressive stress is due only to the Poisson's ratio effect. With Poisson's ratio for concrete assumed to be 0.20, and ratio of principal stresses equal to 1.0, a stiffness increase for 20% higher than the uniaxial stiffness was calculated by Liu et.al. (86). They observed experimentally that in the presence of biaxial compression, a stiffness increase greater than that which can be

explained by Poisson's effect alone, existed, They also concluded (87) that the main cause of this supplementary stiffness is the confinement of potential microcracking in the presence of biaxial compression. The supplementary stiffness was estimated to be 15% for a ratio of principal compressive stresses equal to 1.0. To account for both Poisson's effect and microcracking confinement, Liu et.al. (86), proposed, in uncoupled form, the following constitutive relationship

$$\{\sigma\} = \begin{bmatrix} E_{xb} & 0 & 0 \\ 0 & E_{yb} & 0 \\ 0 & 0 & G_b \end{bmatrix} \{\epsilon\} \quad (5.8)$$

where E_{xb} and E_{yb} are the effective moduli in directions x and y , respectively, obtained from their proposed stress-strain relationship for concrete submitted to biaxial compression. G_b is the shear modulus for biaxially-stressed concrete. Good agreement was reported between the proposed biaxial stress-strain relationship and the experimental data of Kupfer et.al. (56) who noted that the strength increase for equal compressive stresses in the two principal directions is approximately 16% above the uniaxial strength. No experimental data were found (86) to check the shear modulus, G_b . For biaxial tension and tension compression cases, uniaxial stress-strain relations were found to be adequate, (87).

In the present investigation, the elasticity matrix equation (5.7) is used with the assumption that $E_x = E_y$. The value of the Modulus of Elasticity $E = E_x = E_y$ is found from the stress-strain equation of concrete in uniaxial compression.

The minimum principal strain in an element under biaxial stresses is used to find the modulus of elasticity of the element. The modulus of elasticity of the element in compression is continuously changed according to the non-linear stress-strain relationship of concrete in uniaxial compression.

A constant modulus of elasticity equal to the initial tangent of the stress-strain curve in axial compression is incorporated in the analysis for elements in tension until the failure criterion in tension is met.

5.3.2 Cracked Concrete Elements

Concrete elements in tension will crack when they meet their failure criterion. In this investigation a concrete element in tension is considered to crack when the maximum principal stress exceeds the modulus of rupture of concrete. Exact modelling of cracking is difficult because of the different problems associated with crack formation.

To accurately simulate cracks in elements new nodes should be introduced in the cracked element and this element should then be subdivided into new elements. This technique has great complexities because of the creation of new irregular shapes of elements, the solution of which are much more complex than triangular or rectangular elements. The introduction of new nodes may also cause problems with the computer core storage. Increasing the number of degrees of freedom of the structure shall also result in a much higher cost per run.

An alternative to subdividing the element into two new elements which may have irregular shapes is to separate the nodes of existing elements at their interface. However, this

solution, besides confining crack paths to element boundaries, creates the same problem with increasing the number of nodes and consequently increasing the number of degrees of freedom incorporated in the analysis as discussed above.

Another alternative, which may replace dividing the cracked elements or separating the nodes, is to reduce the stiffness, of the element in the direction normal to the crack according to the technique reported by Zienkiewicz (37): This technique which was developed for stratified materials is incorporated in the analysis. This assumption, although, it may not be the most realistic, was thought to be a definite improvement over the relatively crude process which have been used by many other investigators by totally deleting the element from the global matrix when cracked.

One of the complex phenomena created upon cracking of concrete is the aggregate interlock which was described in Chapter 2. Simulation of aggregate interlock can be done using one of the two following techniques:

1. Introduction of new nodes at cracks can be used to transfer shear across the crack. This can be accomplished by joining the corresponding concrete nodes with joint elements which have stiffnesses representing the aggregate interlock action. This, however, complicates the computer programming to a great extent considering the unrestricted growth of cracks which is incorporated in this analysis. The predefinition of cracks to overcome this difficulty nullifies the significance

of this technique for tracing growth of cracks. The increase in the required computer core storage associated with any method which involved an increase in the number of degrees of freedom normally made that method impractical.

2. The use of shear retention techniques have been recently developed and used by some investigators (105) to overcome the problems of core storage when other methods of modelling aggregate interlock were used. In this method, of shear retention, the shear modulus, G , in cracked elements is reduced to a smaller value. Since it is known that aggregate interlock depends on the crack width, this shear retention factor should be a function of crack width. However, it was found (105) that in many cases a constant value of reduced G gave better results. The reliability of this technique and the necessary factors required for its use have not yet been developed.

In this investigation the inclusion of the aggregate interlock phenomena was neglected. This was thought to be an appropriate assumption, because aggregate interlock may only be effective in beams with a limited range of shear span to depth (a/d) ratios. The inclusion of the effects of aggregate interlock phenomenon in the present analysis was not possible for joints because of computer core storage limitations. To study the effects of including shear retention factors, to simulate aggregate interlock, on the behaviour of a joint is beyond the scope of this study.

The reduced stiffness of a cracked element $[k_c]$ and the stresses and strains in this element are found as follows:

For a cracked element as shown in Fig. 5.2, the following assumptions are made:

1. The element has no stiffness in the direction normal to the crack (i.e. $E'_y \rightarrow 0$)
2. Poisson's effect is neglected in the cracked element (i.e. $\nu \rightarrow 0$)
3. The shear stiffness of a cracked element is significantly reduced (i.e. $G \rightarrow 0$)

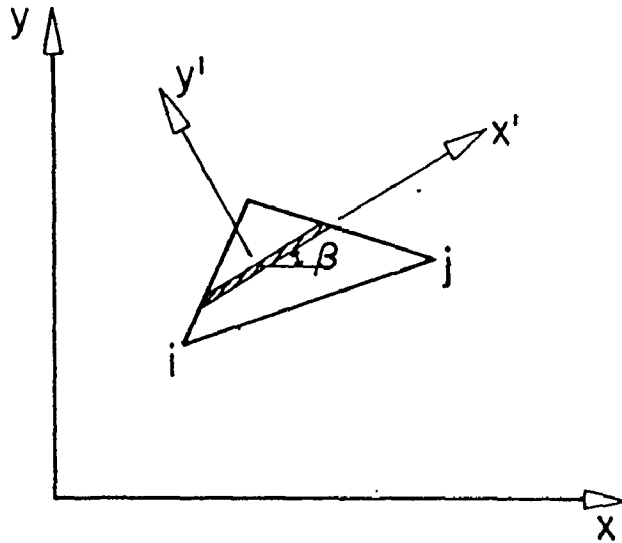


Fig. 5.2 IDEALIZATION OF A CRACKED CONCRETE ELEMENT.

Then, where $[D']$ is the elasticity matrix in local coordinates (x', y') ,

$$[D'] = \frac{1}{1 - \nu^2} \begin{bmatrix} E'_x & \nu E'_x & 0 \\ \nu E'_y & E'_y & 0 \\ 0 & 0 & G(1-\nu^2) \end{bmatrix} \dots(5.9)$$

Therefore, for the cracked element, $[D']$ reduces to

$$[D'] = \begin{bmatrix} E'_x & 0 & 0 \\ 0 & 0 & 0 \\ 0 & 0 & 0 \end{bmatrix} \dots(5.10)$$

and if $[D] = [T][D'] [T]^T \dots(5.11)$

where

$[D]$ = elasticity matrix --global coordinates.

$[T]$ = strain transformation matrix.

$$[T] = \begin{bmatrix} \cos^2\beta & \sin^2\beta & -2\sin\beta\cos\beta \\ \sin^2\beta & \cos^2\beta & 2\sin\beta\cos\beta \\ \sin\beta\cos\beta & -\sin\beta\cos\beta & \cos^2\beta - \sin^2\beta \end{bmatrix} \dots(5.12)$$

where,

β = angle of inclination of the crack with the global x axis.

then, $[k_c]$ the stiffness matrix of the cracked element becomes

$$[k_c] = [B]^T [D] [B] t \dots(5.13)$$

or

$$[k_c] = [B]^T [T] [D] [T]^T [B] t \cdot \Delta \dots(5.14)$$

where,

t = thickness of the element

Δ = area of the element

and for plane stress elements the strain matrix [B] becomes:

$$[B] = \begin{bmatrix} 0 & 1 & 0 & 0 & 0 & 0 \\ 0 & 0 & 0 & 0 & 0 & 1 \\ 0 & 0 & 1 & 0 & 1 & 0 \end{bmatrix} \dots\dots\dots(5.15)$$

to find the stress in the cracked element

$$\{\sigma\} = \{\epsilon\}^T [D] \dots\dots\dots(5.16)$$

$$\{\sigma\} = \{\epsilon\}^T [T] [D'] [T]^T$$

where $\{\sigma\}$, $\{\epsilon\}$ are the stress and strain vectors respectively.

5.3.3. Stirrup Elements

The idealization and modelling of stirrups to accurately describe their effect on the behaviour of a reinforced concrete structure is relatively difficult to achieve using a two dimensional analysis. Conventional stirrups, either closed or U-shaped, confine a portion of the concrete and, where closely spaced, increase the ductility of the member and its rotational capacity (18). However, this was not of great significance for the problems analyzed in this investigation, since the few stirrups provided in the joints tested were not closely spaced. Furthermore, the analyzed beams had no web reinforcement.

During the development of the computer program it was evident that a three dimensional analysis was impossible for practical considerations associated with the available

computer facilities (core storage and computational time),

In this investigation segments of stirrups are represented by four-degree of freedom bar elements, Fig. 5.3, described by a stiffness matrix:

$$[k]_{st} = \frac{E_s A_{st}}{L_s} \begin{bmatrix} \cos^2 \theta & \cos \theta \sin \theta & -\cos^2 \theta & \cos \theta \sin \theta \\ \cos \theta \sin \theta & \sin^2 \theta & \cos \theta \sin \theta & -\sin^2 \theta \\ \cos^2 \theta & \cos \theta \sin \theta & \cos^2 \theta & \cos \theta \sin \theta \\ -\cos \theta \sin \theta & \sin^2 \theta & \cos \theta \sin \theta & \sin^2 \theta \end{bmatrix} \quad (5.17)$$

where,

θ = angle of inclination of local x-axis to global x-axis

E_s = Modulus of Elasticity of stirrup steel

A_{st} = Cross sectional area of stirrup

L_s = Length of the stirrup

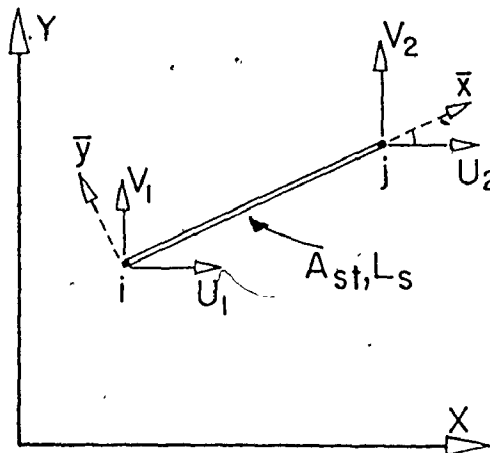


Fig. 5.3 IDEALIZATION OF STIRRUP ELEMENTS.

These stirrup elements can be connected between any two concrete or steel nodes directly or with the use of joint elements, depending upon whether or not relative slip displacement is expected.

If large steel forces and large relative displacements between the steel and concrete are anticipated, joint elements should be introduced. If the stirrup is located so that no large deformations or end slip are expected the stirrups can be connected directly to steel nodes. This procedure will tend to minimize computer core storage; which is usually a problem with a finite element analysis of the nature intended in this investigation.

5.3.4 Joint Elements

Mathematical representations of bond-slip, aggregate interlock and dowel action relationships are not easy to produce. An idealization was introduced in 1967 by Ngo and Scordelis (39) using four-degree of freedom spring linkages. These links connected corresponding nodes on concrete and steel elements at their interface to simulate bond-slip and dowel action, and they were used to connect corresponding nodes of concrete on either side along a crack to simulate aggregate interlock. This idealization has been used by Ngo and Scordelis (68), Nilson (48) Spolowski (88), Houde and Mirza (99) and others to predict the behaviour of reinforced concrete structures. The only drawback of this technique is that it only insures compatibility conditions at the nodes. This concept was broadened in 1968 by Goodman et.al.(46) when they introduced joint elements in an application to jointed rock masses.

The joint element as shown in Fig. 5.4, has a finite length "L" but zero thickness as the nodal pairs (1,4) and (2,3) initially have identical coordinates. In this figure, the joint elements is in a local coordinate system with the x-axis along

the length, and the origin taken at the centroid of the joint element.

The relative displacement vector of the top and bottom of the joint element is given by

$$W = \begin{Bmatrix} W_s^{\text{top}} - W_s^{\text{bottom}} \\ W_n^{\text{top}} - W_n^{\text{bottom}} \end{Bmatrix} \dots\dots\dots(5.18)$$

where W_s^{top} and W_s^{bottom} are the displacements in the tangential direction of the top and bottom parts of the joint element, respectively, and W_n^{top} and W_n^{bottom} are the displacements in the normal direction of the top and bottom parts of the joint element, respectively. This relative displacement vector is related to the external applied forces by

$$\{P\} = [K]_{jt} \{W\} \dots\dots\dots(5.19)$$

where

$\{P\}$ is defined as

$$\{P\} = \begin{Bmatrix} P_s \\ P_n \end{Bmatrix} \dots\dots\dots(5.20)$$

where P_s and P_n are the forces per unit length in the tangential and normal directions respectively.

$[K]_{jt}$ is defined as

$$[K]_{jt} = \begin{bmatrix} k_s & 0 \\ 0 & k_n \end{bmatrix} \dots\dots\dots(5.21)$$

where K_n is the normal force per unit length, required to produce a unit deformation in the direction normal to the joint, and similarly K_s applies to the direction tangent to the joint.

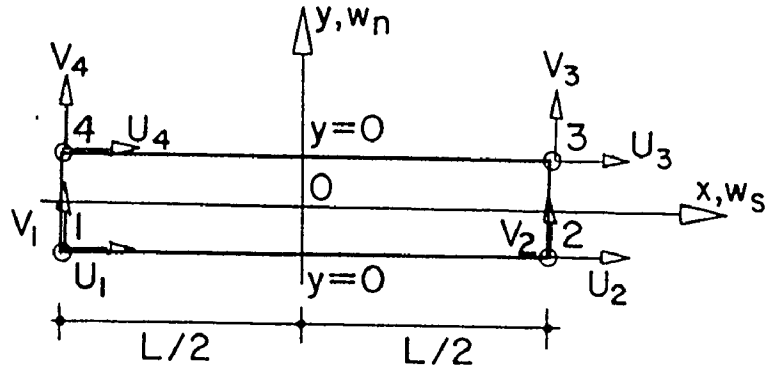


Fig. 5.4 JOINT ELEMENT REPRESENTATION⁽⁴⁶⁾

In terms of the local coordinates the energy stored in a joint element due to applied forces per unit length acting through the displacements is:

$$\phi = \frac{1}{2} \int_{L/2}^{L/2} \{w\}^T [P] dx \dots\dots\dots(5.22)$$

If the displacements $\{w\}$ were replaced by the nodal point displacements $\{U\}$ through a linear interpolation formula the energy is:

$$\phi = \frac{1}{2} L \{U\}^T [K] \{U\} \dots\dots\dots(5.23)$$

where $[K]$ is the joint element stiffness per unit length. Development of $[K]$ is given in full detail in reference (46).

The structural (global) stiffness matrix for the entire system of elements and joints is then assembled by

properly adding corresponding terms of elements contributing stiffness at each nodal point.

Once the solution is obtained, the joint forces (or stresses) are calculated from the nodal displacements. Derivation of the joint stresses in terms of displacements is also given in the reference (46).

5.4 Program Description

5.4.1 General

A computer program utilizing the finite element technique has been developed to study the behaviour of reinforced concrete members. The program was of a general nature regarding the shapes and types of structures it can handle. However, it was written mainly to analyze simple reinforced concrete beams and joints and has not been tested for other types of elements.

In the course of developing the program, numerous problems were encountered. Some of these problems were related to the nature of the analysis and the expected inaccuracies accompanying a discrete solution to a problem of a continuous nature. The other type of problems was due to the limited computer core storage available and to finally trying to reduce the cost per run to a feasible amount. The nature of some of the problems and how they were tackled shall be discussed in Section 5.4.4. This might be helpful to future investigators who are working in the same field.

5.4.2 Function of the Main Program and the Subroutines:

The program was written to run on the CDC-6400 computer available at the McMaster University Computing Centre. Due to core storage limitations (124 K maximum) it was necessary to convert the program to run also on the IBM-370 computer, available at McMaster University for administrative use. The IBM-370 has a core storage capacity of 700K, however, double precision is necessary for any problem where solution of ill-conditioned matrices is expected. The introduction of joint elements and the imposition of cracks in concrete elements usually results in an ill-conditioned matrix which requires double precision. The CDC-6400 computers' single precision was almost equivalent to double precision on the IBM-370.

All of the simple R.C. beam runs were made on the CDC-6400 Computer because it was more accessible than the IBM-370. Also beam runs could be handled with reasonable accuracy using the available CDC-6400 core storage capacity. Analysis of joints were all made on the IBM-370 computer.

The Program consists of a main Routine (MAIN) and 17 subroutines. The organization of the main program, of the subroutines and the auxiliary storage files is shown in Fig. 5.5. The functions of the subroutines are to formulate the "Global Stiffness Matrix of the Structure", to solve for the displacements, strains, and stresses corresponding to the applied loads, to check the failure criteria of the different elements and modify their stiffness accordingly, and to store information regarding the cracking history.

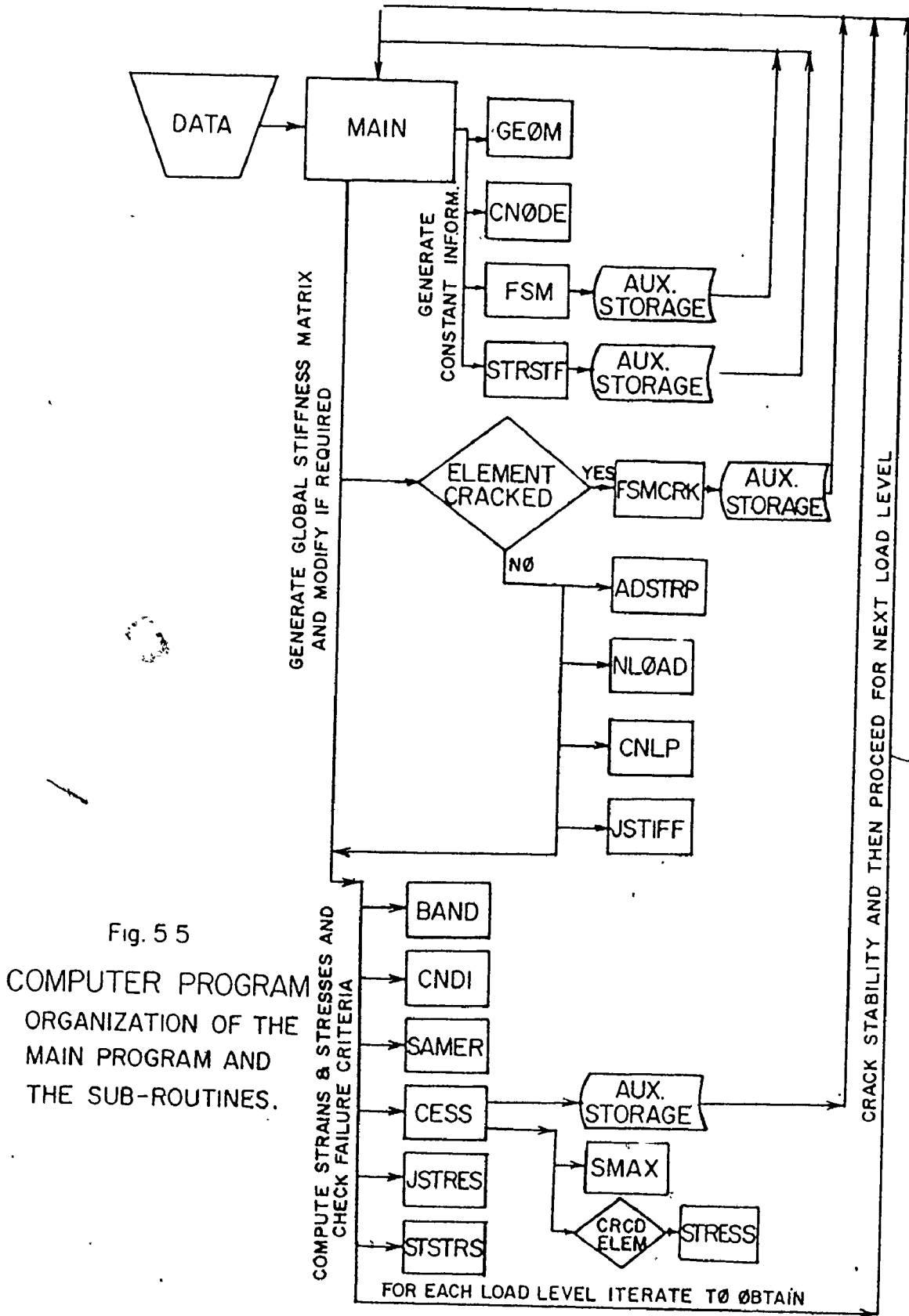


Fig. 5 5
 COMPUTER PROGRAM
 ORGANIZATION OF THE
 MAIN PROGRAM AND
 THE SUB-ROUTINES.

Appendix A contains a detailed description of the function of each subroutine and a listing of the computer program.

5.4.3 Program Logic and Operation

One of the interesting features of the program is its ability to predict crack patterns. During the development, the general trend of the crack patterns predicted by the analysis agreed in a very encouraging fashion with crack patterns from experimental work. Therefore, the logic of the program was changed from the usual application of pre-selected load increments on the structure to a logic which allows the analysis to predict crack growth in a more realistic manner.

To more accurately predict crack patterns in reinforced concrete structures, it was necessary to let only one element crack at a time. The element in the structure which is stressed the most is the only element that should be allowed to crack at any particular iteration for crack stability. Even when there is more than one element in the structure which meets the failure criterion, the most highly stressed one is the only one that should be allowed to crack. Modification of the stiffness of the cracked element is then performed according to the direction of the crack (normal to the maximum principal tensile stress) and re-entered in the global stiffness matrix. This technique allows the redistribution of stresses to take place before any other element is allowed to crack. This results, in most cases, in relieving

some of the surrounding elements which were overstressed and prevents the occurrence of an unnecessary crack. The topology of the structure will then be the same as that of an actual structure with a crack in the process of propagation.

Although this technique greatly increased the computer time required, it was found in earlier trials that allowing several overstressed elements to crack at one time created discrepancies (especially for cracking patterns) which were not justified for the sake of the reduced cost of running the program.

After crack stability is achieved for a certain load level (i.e. no elements are overstressed for this particular load level), the next load increment is not imposed on the solution but rather is automatically determined within the program based on the level of stress in the next most highly stressed element which did not exceed the failure criteria. However, if this increment is larger than a predetermined limiting size of increments, it is then set at the smaller value to minimize divergence resulting from the nonlinear material properties used in this analysis.

During the iterations for crack stability, all concrete elements, steel elements and joint elements are constantly modified to include the effects of the nonlinear relationships of concrete in compression, bond-slip and of the strain hardening of steel. Convergence was normally obtained fairly readily and in most cases no further iterations for material properties were required. However, divergence occurs in some elements which are near failure because of the extra sensitivity due to more pronounced nonlinear

material behaviour.

The convergence to a correct solution despite all of the involved nonlinearities can be achieved by iterating around material properties until the errors are within acceptable limits. This is not included in the present analysis, however, because of the extra cost involved in running the program and since this slight divergence was only noticed quite near failure and in relatively few elements.

Although the expression "incrément" was used in the above discussion, in this analysis the total load is applied on the structure rather than the easier to employ but less accurate method of superimposing incremental effects. The possibility of employing an incremental technique or a mixed procedure utilizing a combination of the incremental and total load schemes, although not used in this investigation, was also incorporated in the computer program for future studies.

The reliability and suitability of the program has been documented by comparison with some of the available experimental data. This is reported and discussed in the following chapters.

Although the title of this thesis is "Behaviour of Reinforced Concrete Joints", the program's accuracy was tested and developed first by using simple reinforced concrete beams. There has been much more experimental work done in this area and researchers are more familiar with their general behaviour so that visual comparison and simplified mathematical calculations can more easily reveal discrepancies in the analysis than would be the case for joints. Beam

results are included in Chapter 6, whereas the results for joints are introduced in Chapter 7.

5.4.4 Some Problems Associated with Finite Element Analysis of Reinforced Concrete

a. Element Size

"There is no doubt that the solution to plane elasticity problems is, in the limit of subdivision, an exact solution. Indeed at any stage of a finite subdivision it is an approximate solution.

The total strain energy obtained during any stage of approximation will be below the true strain energy of the exact solution. In practice it will mean that the displacements, and hence also the strains and stresses, will be underestimated by the approximation, in its general picture. However, this is not necessarily true at every point of the continuum individually; hence the value of such a bound in practice is not great" (37).

What is important to the engineer is to know the order of accuracy achievable for typical problems using a certain fineness, of element subdivision. In any particular case the error can be assessed by comparison with known, exact solutions or by a study of the convergence, using two or more stages of subdivision.

In a stress field which varies either linearly or nonlinearly, the basic assumption of constancy of stress within elements means that the solution will be approximate

only. In the case of a beam subjected to constant bending moment with a fairly coarse subdivision of elements, the axial stress given by the element straddles the exact values and, in fact, if the constant stress values are associated with centroids of the elements the best fit line, Fig. 5.6, reproduced from reference (37) should be close to the exact stresses. The stresses perpendicular to the axis of the

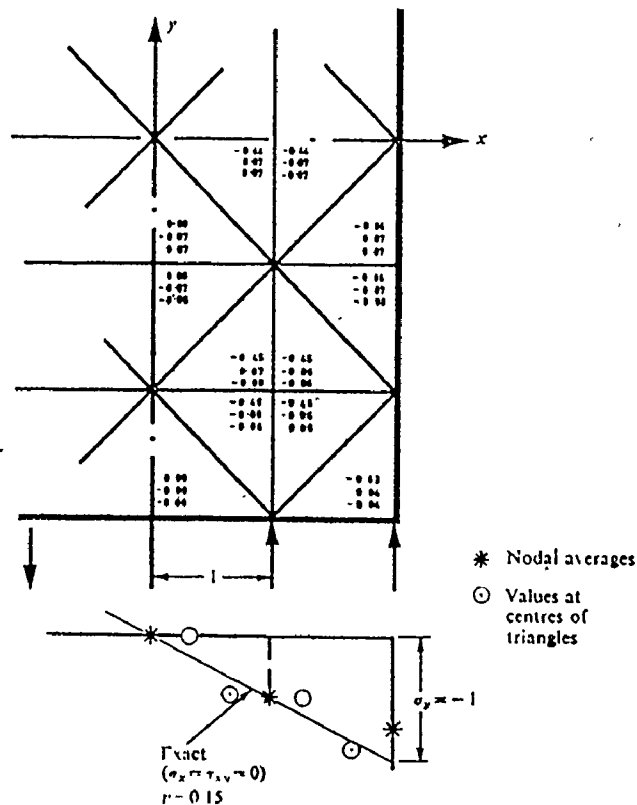


Fig. 5.6 Pure bending of a beam solved by a coarse subdivision into elements of triangular shape. (Values of σ_y , σ_x , and τ_{xy} listed in that order)

(Reproduced From Reference 37)

member and the shear stress components also differ from the exact values, which are simply zero. However, it is noted that they will oscillate by equal and in most cases small

amounts around the exact values. At internal nodes, if the average of stresses of surrounding elements is taken, it will be found that the exact stresses are very closely represented. The average at external faces however, is not so close. Figure 5.6 shows that σ_y obtained from the nodal averages is very close to the exact solution at the internal nodes while it is underestimated at the external face. Weighting of the averages near the faces of the structure can be used as a further refinement.

Representation of the stresses by nodal averages is a definite improvement of the approximation. However, it is preferable to use a finer subdivision wherever possible and when the accuracy requires it.

In this investigation reasonably fine subdivisions were always used whenever the core storage permitted. When the computer core storage capacity limited the desired fineness, averaging of the stresses at the nodes was applied. When this averaging technique is employed the deflections of the analyzed structure are usually considered a reliable indication for the degree of precision achieved in the cases where the accuracy of the calculated strains and stresses cannot be verified.

It is worthwhile noting again that, because of the lower bound nature of the solution obtained from the finite element method of analysis, for a coarser mesh, the underestimation of the computed deflections, strains and stresses

will increase.

b. Efficient Use of Core Storage:

Minimizing the band width of the global stiffness matrix is necessary for finite element analyses using the "Choleski" technique in solving the banded matrix. As mentioned before, accuracy increases with fineness of the element mesh. The band width reduction or minimization becomes then a matter of great importance to save on the required computer core storage. To get the minimum possible band width for a structure such as the corner joints, (i.e. members with a sudden bend) it was found very useful to number the nodes in diagonal or fan-type fashion rather than using a vertical or horizontal numbering scheme.

c. Data Generation

To generate the large amount of data required to drive the program, especially for joints, development of automatic and semi-automatic data generators, data checkers, and routines for optimization of the band width were found to be quite helpful.

5.5 Additional Information

The cost of running the program was found to be relatively reasonable for beams (i.e. between 8 and 20 CP minutes execution time on the CDC-6400 computer). However analysing corner or other types of joints which require much larger core storage and a larger number of nodes and elements was expensive. The amount of data available from these runs,

however, justified the higher cost in a satisfactory way. (The approximate average time on the IBM-370 computer was around 100 CP minutes for execution). In terms of time, information obtained and actual cost, this compares favourably with experimental work.

The current rapid development in the speed and storage capacities of modern computers should make this analytical tool even more economically feasible in the near future.

In the next two chapters the analytical results are presented analysed and compared with experimental data. Final conclusions are presented in Chapter 8. A complete listing of the computer program is included in Appendix A.

CHAPTER 6
APPLICATION OF THE FINITE ELEMENT METHOD TO
SIMPLE REINFORCED CONCRETE BEAMS

6.1 Introduction

A great deal of work has been done on simply supported reinforced concrete beams by numerous investigators (28, 33, 38, 44, 49, 64, 67). Simple beams were thought of as a reliable means of developing the proposed method of analysis. Their well documented behaviour allowed the performance of visual and rough mathematical checks which were easier to formulate and more readily revealed any discrepancies in the analysis than would be the case for joints. They were also much more economical to analyze using the computer. All the same programming features for joints were also required for beams, therefore no major programming modification were required to analyze the joints. This is not to say that the results of the beam analyses are not useful in themselves. In fact as will be shown, the results reproduce cracking behaviours and failures in a fashion which documents observed phenomena.

In this chapter comparisons with results for beams tested by Leonhardt and Walther (28), are made. Load-deflection, ultimate capacity, type of failure, stress distributions,

and crack patterns from the analyses are presented and where possible compared with the test results.

Five beams were analyzed and are discussed in this chapter. The choice of beams from Leonhardt and Walther's (28) test data was made so that the reliability of the method of analysis could be assessed and so that the sensitivity to the following variables could be tested.

1. The effects of different a/d (shear span/depth) ratios.
2. The effects of bond-slip characteristics.
3. The effects of different material properties.
4. The effects of cracking on the overall behaviour of simple reinforced concrete beams.

In the next chapter, the joint test results are compared with the analytical results obtained from the developed computer program.

6.2 Test Data and Description of the Analyzed Beams

In 1962, Leonhardt and Walther (28), tested a series of beams to investigate the influence of the moment versus shear relationship. This relationship has been established as a very important criterion for the shear carrying capacity, for beams with point loads and uniform loads. All the beams were rectangular with the same 19 cm by 32 cm (7.48 in x 12.6 in) cross section and were reinforced with two 26 mm diameter (1.024 in) Bst IIIb steel bars in the longitudinal direction. To avoid anchorage failure rather long cantilevered beam

ends with stirrups as reinforcing were employed, although stirrups were not used in the main parts of the beams. Figure 6.1.a shows a sketch of the test set-up and the dimensions used.

In the case of beams with point loads, the a/d ratio was changed so that the distance between the symmetric load points and the supports was different. The distance "a" between the two point loads was chosen to be small and to be the same for most of the beams. Thus different span lengths resulted and also different slenderness ratio for the beams. The left load distribution plate (3.0 inch wide) was made smaller than the right one (5.0 inch wide) to find out if different local pressures had any influence. No influence was found and hence the size of the loading plate was neglected in this investigation and all of the comparisons are made for a constant point loading pattern. No beams with uniform loads were considered in this investigation.

The beams were kept moist and tested without any time for drying to avoid shrinkage influences. The material properties, exact dimensions and the type of steel reinforcing bars used for the five analysed beams are included in Table 6.1. The concrete was proportionately sandrich (60% from 0-7 mm (9/32 in.) with a cement content of 290 kg/m^3 (490 lbs/ yd^3) cement type 475 and a water-cement ratio = 0.68.

Deflections were measured in the middle of the beam and crack patterns were recorded at every loading step. The widths of cracks were not measured for the beams analysed here.

Beam	l in.	a in.	a' in.	t in.	d in.	b in.	a/d	cube strength psi	f' _c psi	Steel type
4	66.93	26.38	14.17	12.6	10.6	7.48	2.5	5050	4290	
7/1	122.00	53.15	15.70	12.6	10.6	7.48	5.0	5290	4500	Rippentor stahl
9/1	228.35	74.4	79.55	12.6	10.75	7.48	6.92	5430	4620	Bst IIIb
EAI	78.74	29.5	19.74	12.6	10.6	7.48	2.78	3570	2860	Rippentor- stahl
EB1	78.74	29.5	19.74	12.6	10.6	7.48	2.78	3570	2860	Blankerstah st 37 k

Table 6.1 Dimensions and Material Properties.

*f'_c values are calculated as 80% of the cube strength for concrete strengths under 5,000 psi and 85% of the cube strength for concrete strengths higher than 5,000 psi. The above values were arbitrarily chosen with guidance from the tables and equations developed by Evans and L'Hermite both referenced in the text, "Properties of Concrete" by Neville, (98).

To find the influence of the bond of the longitudinal reinforcing on the shear carrying capacity for rectangular beams without shear reinforcing, Leonhardt and Walther (28) tested four beams under two point loading with the same span lengths, cross-section areas, concrete strengths and reinforcing ratio, where only the quality of the bond of the longitudinal reinforcing, was changed. The beams contained no shear reinforcing, but beam ends protruded far over the supports to avoid anchorage failures. The anchorage zone did not have any stirrups. The quality of the bond was changed either by changing the number and diameter of the reinforcing bar or by varying the condition of the surface of the reinforcement. It is known that bond is better for smaller diameter reinforcement because the ratio between circumferential area and cross-sectional area becomes greater.

Beam EA1 was reinforced with 2, 24 mm (.945 in) diameter and 1, 6 mm (.236 in.) diameter bars having ribbed surfaces (Rippentorstahl BST 1116). Beam EB1 was reinforced with 2, 25 mm (.984 in.) diameter cold drawn machine steel (St 37 k). This steel is round and has a very smooth mirror like surface. In order to anchor the smooth rods adequately at their ends ribbed pieces of rod were welded on. The a/d ratio for all of these tests for influence of bond was 2.78.

The concrete used had a normal composition with 251 kg/m^3 (423 lbs/yd^3) of Pz 375 cement with a water-cement ratio of 0.75. The cube strength had an average value of

252 kg/cm² (3584 psi). The tensile strength under bending averaged 41.4 kg/cm² (589 psi). The stress-strain curves for both types of steel used in specimens EA1 & EB1 did not show any noticeable difference in the range of steel stresses which coincided with shear failure. With the exception of beams EA1 and EB1, the cracking patterns for the beams analyzed in this chapter were clear but the numbers on the photographs were not readable even with the use of a magnifying glass. Therefore, it was not possible to compare the sequence of crack occurrence and crack propagation with the predicted behaviour for any beams but EA1 and EB1. However, the crack patterns are compared for these other beams.

The stress-strain diagram for concrete was not included in Leonhardt and Walther results, however, the information provided was adequate for the use of Saenz's (24) equations which are employed in this investigation.

The stress-strain curves for the reinforcing steel used in the beam tests are shown in Fig.6.1.b. However, an idealized elastic-plastic stress-strain relationship was employed in the analysis, since post-yielding did not have any influence on the behaviour of the tested beams.

For all deformed bars, (ribbed bars) used in the beam tests, the bond-stress slip characteristics have been assumed to be represented by the equations developed by Houde and Mirza (99) which were described earlier in Chapter 2. Also the dowel action equations described in Chapter 2

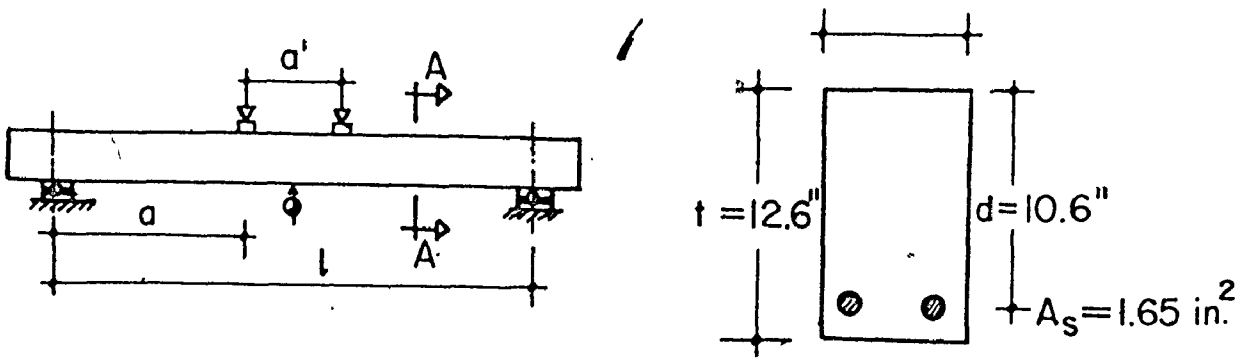


Fig. 6.1a DIMENSIONS OF THE ANALYSED BEAMS.

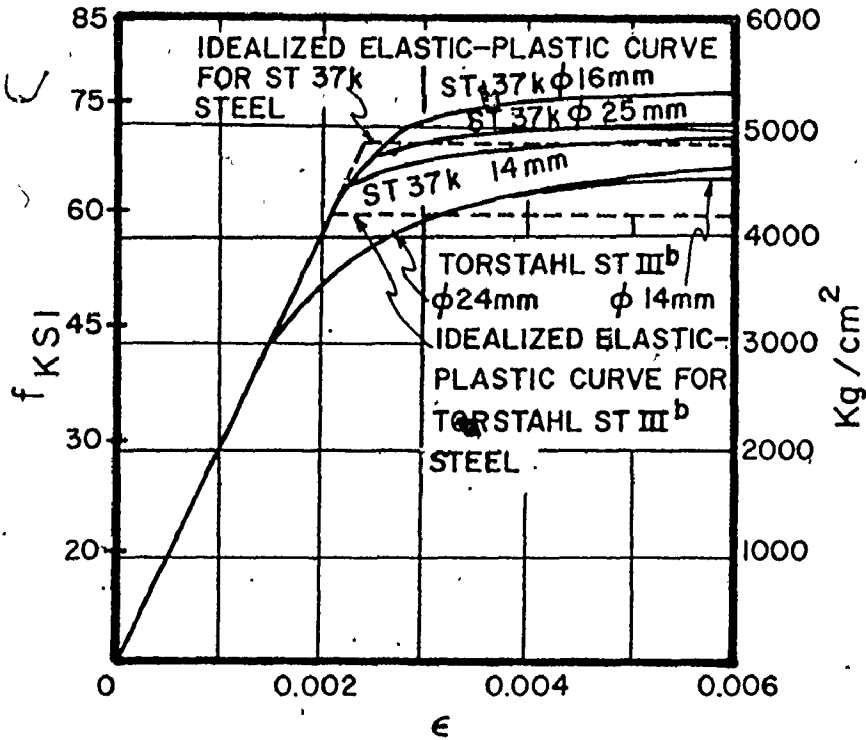


FIG. 6.1b STRESS-STRAIN DIAGRAM FOR STEEL USED IN LEONHARDT AND WALTHERS' BEAMS REPRODUCED FROM REFERENCE (28)

are used in the analyses.

6.3 Summary of Test Results

In this section the test results (28) for all of the beams tested with point loads are summarized, even though only five of these beams were analysed in this chapter. The pictures shown in Fig. 6.2 were reproduced from reference (28) and show the crack patterns after failure for beams with different a/d ratios. For the shortest beam, beam (1), the diagonal crack is steep because of the stress components, F_y , between load and the support allow the directions of the principal tensile stresses to become flatter than 45° . For beams (2) and (3), the shear cracks which led to failure, extended under the load into the zone of pure bending because the concrete compressive strength in bending is increased directly under the load because of the local confinement due to the load. Although the concrete actually crushed in the zone of pure bending, this must be considered a shear failure because of the depth of the compression zone for bending was decreased much more by the shear crack than by the flexural cracks.

For beams (1) to (4), the shear cracks developed beyond the flexural cracks only at relatively high loads. In beams (5) to (8) shear cracks sometimes developed out of the bending cracks and at other times they were new cracks which formed at an angle right across existing flexural cracks. In the top region they were very flat, due to the presence of the high longitudinal compressive stresses.

Beam	l	a	M/O - A
	m	m	
1	0.90	0.27	1.0
2	1.15	0.40	1.5
3	1.45	0.54	2.0
4	1.70	0.67	2.5
5	1.95	0.81	3.0
6	2.35	1.10	4.0
7/1	3.10	1.35	5.0
8/1	3.60	1.48	6.0
10/1	4.70	2.16	8.0
9/1	5.80	2.89	7.0

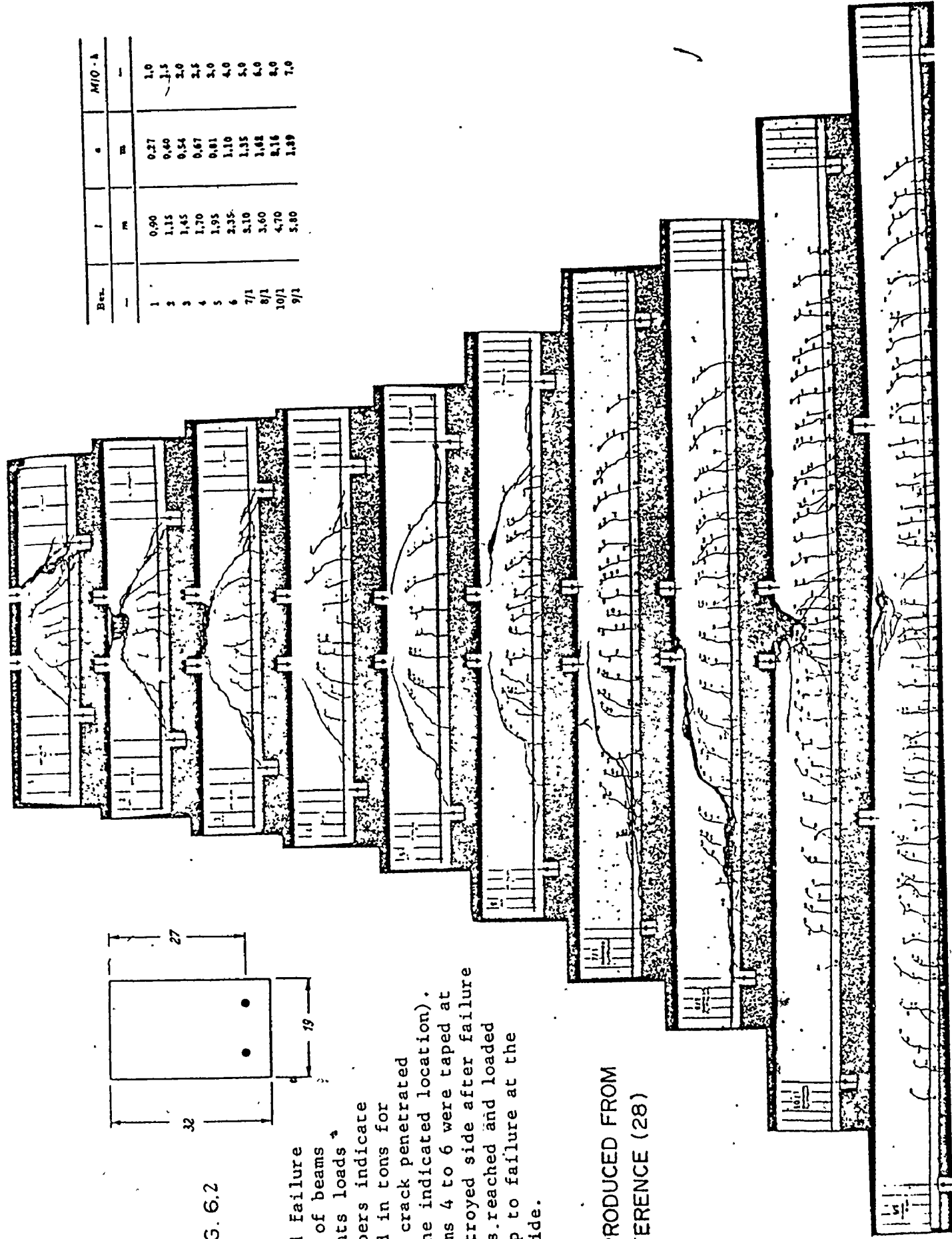


FIG. 6.2

Crack and Failure pictures of beams with points loads (the numbers indicate the load in tons for which a crack penetrated up to the indicated location). The Beams 4 to 6 were taped at the destroyed side after failure load was reached and loaded again up to failure at the other side.

REPRODUCED FROM REFERENCE (28)

In general as shear cracks open at higher loads a greater part of the shear force is transferred through the lower reinforcing bars. Because of this the concrete cracks and splits along or below the reinforcing with the crack possibly extending up to the supports. Extension of cracking of this type is generally a near failure or post failure phenomena.

The location of failure is always close to the loading point, where $\frac{M}{Vd}$ reaches its maximum value. Where,

M = external moment applied to beam

V = Vertical total shear due to external loading

d = distance between the centroidal axes of the steel bars and the top concrete face.

For $\frac{M}{Vd} \geq 7$, the beam pairs (9) and (10) were reported to have failed in bending and in this case because of crushing of the concrete before the yield stress of the reinforcing steel was reached.

For beams (1) to (6) the critical cracks propagated gradually over several load increments until finally the compression zone was destroyed. For the beam pairs (7) and (8), the sudden failure was typified by rapid development of a flat shear crack. The lack of warning of shear failure was more pronounced in the case of point loads far from the support compared to loads close to the support (smaller a/d ratios).

Nonetheless, they found that less reinforcing was required to avoid shear failures in slender beams than for shorter beams where the ratio of shear capacity to flexural capacity is lower when no shear reinforcing is used.

Flexural and shear stress distributions along the beams were not included in the test results. However, some discussion of analytical flexural and shear stress distributions will be presented in the following section for beam (7) even though no corresponding experimental data was provided.

6.4 Failure Criteria for Beams:

6.4.1 General

The various modes of failure for simple R.C. beams include cracking or crushing of concrete under complex states of stress, as for example, when diagonal tension cracking, shear compression failure, or splitting occurs. Other modes of failure also include yielding of reinforcing steel, breakdown of bond or end anchorage, breakdown of aggregate interlock, and breakdown of dowel action.

All of the above mentioned failure modes and the failure criterion adopted for each mode are included in the present analysis either explicitly or implicitly, with the exception of aggregate interlock. Although, relatively easy to incorporate in the analysis, the inclusion of aggregate interlock creates computer core storage difficulties and requires a special node numbering scheme which was not practical with the available computing facilities.

6.4.2 Criteria of Failure for Concrete in Compression:

The development of a failure criterion for concrete subjected to combined states of stress is a complex subject. Although, the formulation of such a criterion has received considerable attention in the past, this did not result in the development of a well established or widely recognized single failure criterion.

It is not intended here to attempt a review of the different theories for concrete failure criteria. The subject is documented in several publications (12, 54, 56, 87) and many others not included in the Bibliography.

Some of the existing theories are:

1. The maximum strain theory.
2. The maximum stress theory (Rankine).
3. The maximum shear (internal friction) theory by Coulomb.
4. Mohr's failure envelope theory.
5. Cowan failure envelope theory.
6. Modified Cowan theory by Zia.

The maximum strain theory, although it may not be the most accurate, was successfully used by several investigators (39, 51, 68, 89) using the finite element method of analysis to study the behaviour of reinforced concrete structures.

The maximum strain theory states that failure occurs when the maximum compressive strain in a concrete element reaches a limiting strain (this strain was set at 0.003 as

described in Chapter 3). It was felt that this theory can provide a rational basis for the study of the behaviour of reinforced concrete members of the nature intended in this investigation. This theory can be changed within the computer program to any other theory with no major effort.

6.4.3 Failure Criteria for Concrete in Tension:

For concrete in tension a crack is introduced when the maximum tensile stress in an element exceeds a predetermined tensile strength. The tensile strength for all concretes used in the analysis of beams was taken as the modulus of rupture represented by the following expression recommended by the Comité Européen du Béton

$$f_t = 9.5 (f'_c)^{1/2} \dots\dots\dots(6.1)$$

The above expression is in better agreement with the values reported by Leonhardt and Walther (28) than the following expression suggested at the University of Illinois:

$$f_t = \frac{3,000}{4 + \frac{12,000}{f'_c}} \dots\dots\dots(6.2)$$

Both expressions are reported and referenced in the text book "Properties of Concrete" by Neville (98). As was mentioned in Chapter 3, although there is some indication in the literature that some small amount of yielding may occur prior to failure (98), the stress-strain relationship of concrete in tension can be represented by a straight line without serious loss of

accuracy (32). A modulus of elasticity in tension equal to the initial tangent modulus of concrete in compression is used in this investigation up to the value of the ultimate tensile strength.

The direction of a crack in an element is the direction perpendicular to that computed for the maximum principal tensile stress exceeding the ultimate strength of concrete in tension.

Although it was noticed in the early stages of developing the computer program, that some cracked elements tended to close at loads near failure, this feature was not included in the final analyses used in this thesis. When this feature was included in the development of the analysis it caused cracking instability, in some instances, in those elements (i.e. cracks opening and closing several times) because of the difficulty involved in determining their new moduli of elasticity after crack closure.

6.4.4 Failure Criteria for Bond Elements:

Bond elements (Joint elements) joining the steel and concrete elements at their interface behave non-linearly according to the equation developed by Houde and Mirza (99) which was discussed in Chapter 2. Equation (2.4.5) best represents the bond-slip relationship before the peak bond stress value is reached (93). The bond-slip behaviour past the peak point, shown in Fig. 2.14, was reported (93) to be dependent on the distance from the end face of loading

(representing crack location). For points at some distance from the end face (3 to 4 inches and more) the bond stress was almost constant for all slip values. For smaller distances, bond stresses decreased progressively with increasing slips. This loss of bond transfer capacity near the end faces was explained by Houde (93) to be a result of the splitting cracks observed. Since the normal cracks spacing for the particular concrete cover and the type of reinforcing used in this analysis ranged between 3.0 to 6.0 inches, the use of a progressive decrease of bond stresses with increasing slips is more appropriate, than a constant stress for all slips.

Houde and Mirza's equation (2.4.5) was examined for slips beyond the peak bond stress value and it was found that nearly half of the peak bond stress value was obtained at a slip = 0.002 inches. Houde and Mirza did not suggest a specific maximum slip in their study. However, the values suggested by Nilson (78, 92) ranged between 0.0008 and 0.003 inch for different distances from the crack face.

In this investigation the failure of a bond linkage (joint element failure in the direction parallel to its length) is considered to occur when a slip value of .002 inch is reached.

When several bond elements fail, the reinforcement bar usually depends on the bond elements near its ends to provide end anchorage. If these latter elements also fail the whole beam will very likely fail immediately due to bond

breakdown.

6.4.5 Failure Criteria for Dowel Elements:

Two failure criteria were considered for joint elements representing dowel action. These were for failure in tension or failure in compression. When shear is transferred across a crack through the steel bars the dowel force in the joint elements on the top at the L.H.S. of the beam are in tension as shown in Fig. 6.3, and the bottom elements are in compression.

When the tensile stress in the elements reaches the direct adhesion strength between steel and concrete the two surfaces separate. However, the compressive forces at the bottom can still transfer the shear force from the right to the left of the crack until finally a concrete tension crack forms along the reinforcement, as a result of the tensile stresses caused by the pressure on the concrete cover. Therefore, the failure of the joint elements in tension is usually of no great significance whereas the elements in compression cause tension cracks in neighbouring concrete element. Hence the breakdown of dowel action is implicitly determined from the failure of the concrete elements along the steel bar and not explicitly from the failure of the joint elements.

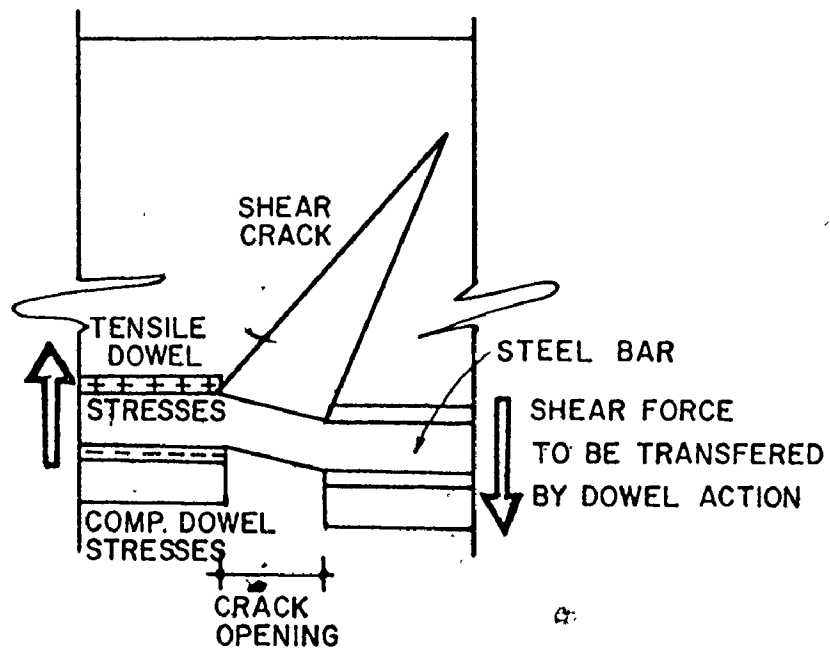


Fig. 6.3 DOWEL STRESSES IN BEAMS.

The stiffnesses which represent dowel action of the joint elements were discussed in Chapters 2 and 5.

The tension failure criterion of the joint elements employed in the analysis was:

$$f_{t_j} = f_t \dots\dots\dots(6.3)$$

f_{t_j} = the maximum tensile strength of the joint elements normal to their axes.

f_t = modulus of rupture of concrete as defined in equation (6.1)

6.4.6 Definition of Modes of Failure for Beams:

The possible modes of failure for a beam can be described as follows:

1. Flexural failure occurs when the beam attains its full flexural capacity.

This type of failure is either caused by excessive yielding of steel reinforcement followed by crushing of the concrete, or by compression failure of the fully effective compression zone (i.e. not reduced by any type of cracking other than the flexural cracks). For the case where steel yields first, the failure is accompanied by large deflections.

2. Shear failure can be a reason for the beam not attaining its full flexural capacity as defined in (1). Shear failures can be subdivided into two main divisions. These are diagonal tension failure and shear-compression failure. In the first case, the failure crack develops from a normal flexural crack and travels very rapidly towards the load point.

At the same time, a splitting crack usually develops along the line of the steel reinforcement and propagates towards the support. In the second case, the crack is straighter and steeper and develops also fairly rapidly as the beam splits into halves. Fenwick (49) describes these two kinds of behaviour as "beam action" in the former case and "arch action"

in the latter. The beam capacity is reduced by the formation of either one of the two types of shear cracks. Diagonal tension failures are usually sudden with very few or no signs of failure. Differentiation between diagonal failure and shear compression failure is not an easy task using a numerical analysis of the type proposed in this investigation. However, shear-compression failure and diagonal tension failure were detected analytically for beams (4) and (7/1) respectively as shall be discussed later in this chapter.

3. Bond or end anchorage failures are not as difficult to detect by the analysis as they sometimes are from test observations. As discussed previously in section 6.4.4, end anchorage or bond failure is identified once all the bond elements fail due to excessive slippage. This includes the elements provided for end anchorage, if any, and the beam is not able to carry any more load. This, of course, is true only if the beam did not fail in the previous steps for some other reason such as flexural or shear failures and exhibit apparent bond failure as a post-failure phenomenon. Interpretation requires examination of the sequence of occurrence of failures of different types of elements.

4. Dowel failure is usually considered to be another type of shear failure which is caused by the extension of a horizontal crack along the reinforcing steel from the point of an existing shear crack toward the support. Failure of this type may also be easily detected using the proposed analysis after studying the sequence of events and when the picture of the predicted crack pattern is completed.

5. The aggregate interlock type of failure which is another form of shear failure was not included in the analysis of the beams for the reasons mentioned in section 6.4.1. The exclusion of aggregate interlock phenomena from the analysis may affect the results. However, varied opinion in this matter especially considering beams with wide shear cracks supported the decision not to try to include this effect in the analysis. It was thought that these effects would not have any sizeable influence on failure loads for the problems considered in this study. The decision not to include it was also based on practical limitations of computer storage capacity as discussed previously.

6.5 Comparison of Experimental and Analytical Results

6.5.1 General:

In this section the results obtained using the analytical model described in Chapter 5 are presented and compared with the results of the tests conducted by Leonhardt and Walther (28), which were summarized earlier in this chapter.

Crack patterns, load-deflection curves and ultimate capacities are compared. Comments, explanations of results and presentations of some stress distributions are also included in the following sections of this chapter.

6.5.2 General Observations on Load-Deflection Results:

The experimental and analytical load-deflection curves are presented and discussed in this section. Figures 6.4 to 6.7 show the load-deflection results from the analysis and tests for beams (7/1), (9/1), EA1, and EB1 respectively. The experimental load-deflection curve for beam (4) was not available for comparison. As can be noted, the computer analysis generally tends to slightly underestimate the deflections. This tendency is natural because the analysis is a lower bound solution which tends to underestimate deformation values for any given load when the finite element mesh is not fine enough. As was discussed in Chapter 5, the degree of fineness of the mesh is the main factor that determines the cost of running the program. However, it was considered that the degree of accuracy obtained is acceptable from the engineering point of view and for the purposes of this investigation.

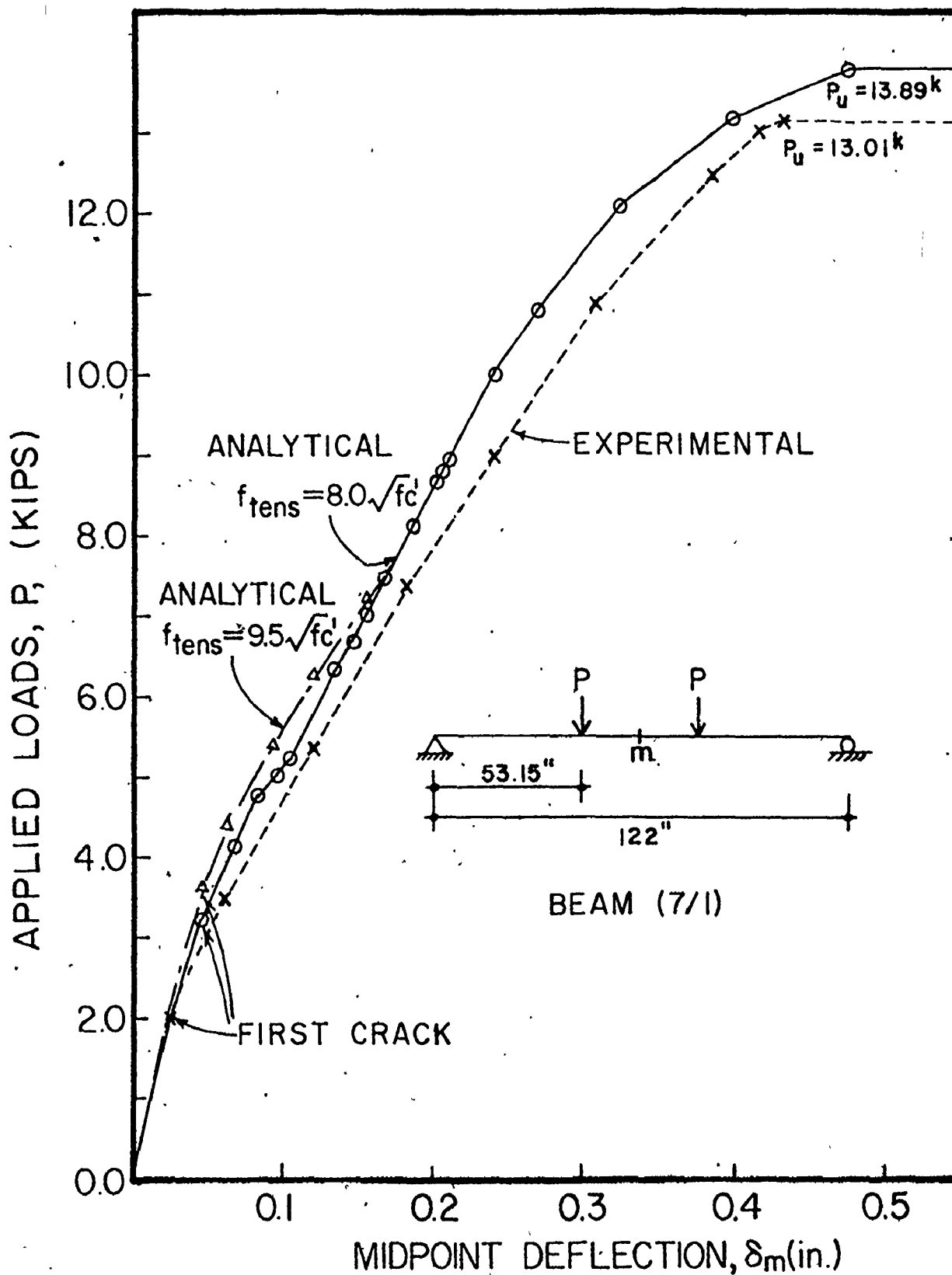


Fig. 6.4 LOAD-DEFLECTION RESULTS FOR BEAM (7/1).

$$a/d = 5.0$$

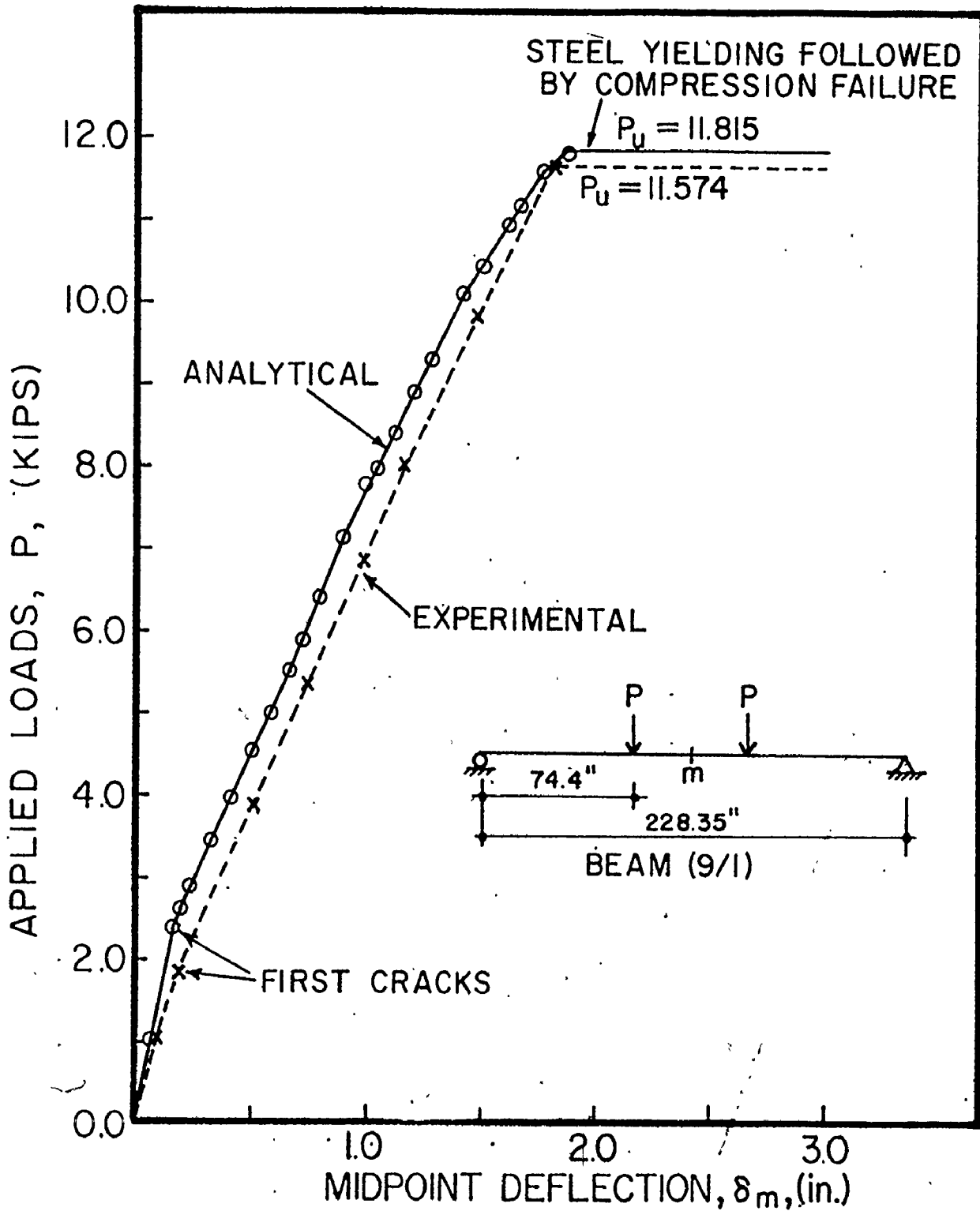


Fig. 6.5 LOAD-DEFLECTION RESULTS FOR BEAM (9/1)

$$a/d = 7.0$$

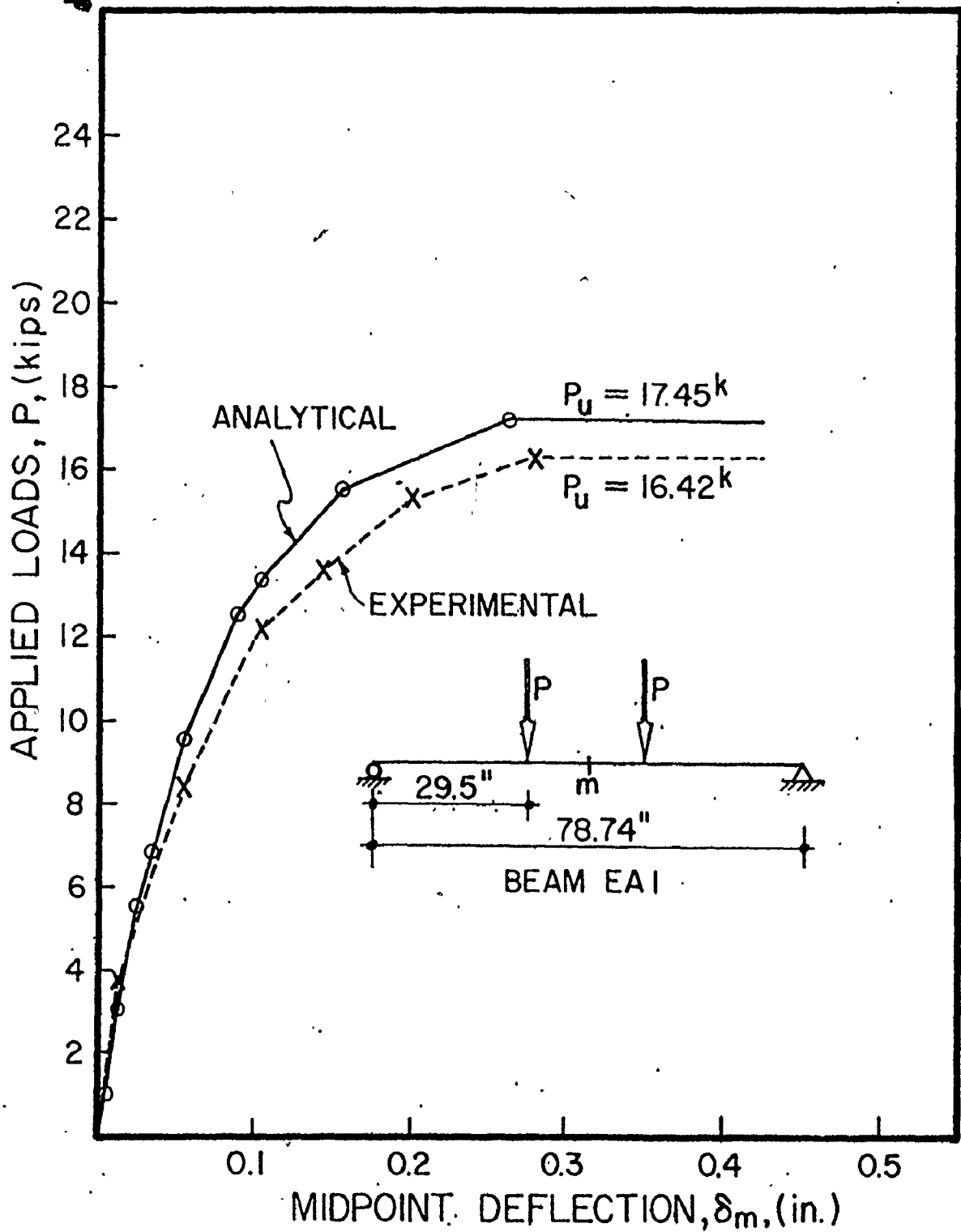


Fig. 6.6 LOAD DEFLECTION RESULTS FOR BEAM EA I
 NORMAL BOND $-a/d = 2.78$

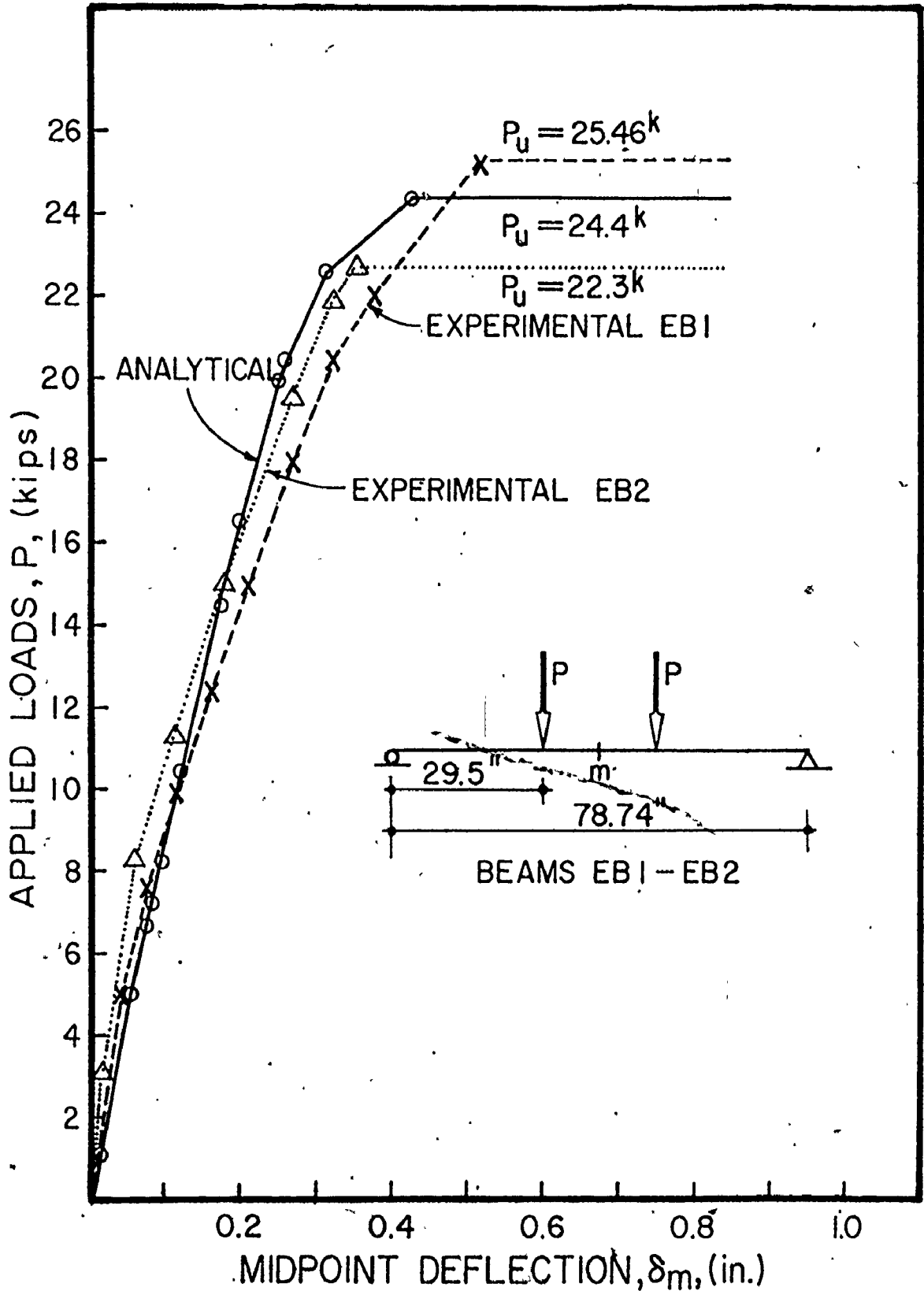


Fig. 6.7 LOAD DEFLECTION RESULTS FOR BEAMS EB1-EB2
 POOR BOND, $a/d = 2.78$

In Figure 6.4, two curves from the analysis are compared with the experimental curve. One analysis was done using a modulus of rupture, f_t , of $9.5\sqrt{f'_c}$ and the other using $8.0\sqrt{f'_c}$. This comparison permitted the study of the sensitivity of the analysis to a change in the value of the modulus of rupture which determines the failure criterion for concrete in tension. As can be seen the analytical load-deflection curves were slightly apart in the first loading stages, and the load at first cracking was proportionately smaller for the smaller value of f_t . However, when the height of flexural cracking stabilized at a load near 7.0 kips, the two deflection curves coincided.

In conclusion, a generally close agreement between the analyses and the test results was obtained using only a moderately fine finite element mesh.

6.5.3 Cracking Patterns and Failure Modes:

In this section predicted crack patterns from the proposed method of analysis are compared with the crack patterns taken from pictures of test specimens in Reference 28. The crack patterns shown in Fig. 6.2 were scaled up in Figs. 6.8 to 6.12 to facilitate comparison with predicted cracks. Figures 6.8 to 6.12 are for beams (4), (7/1), (9/1), EA1 and EB1 respectively. The sequence of test crack occurrence is only shown for beams EA1 and EB1 since for the remainder, this information was not readable. The results for each beam are discussed separately in more detail below.

6.5.3.1 Beam (4)

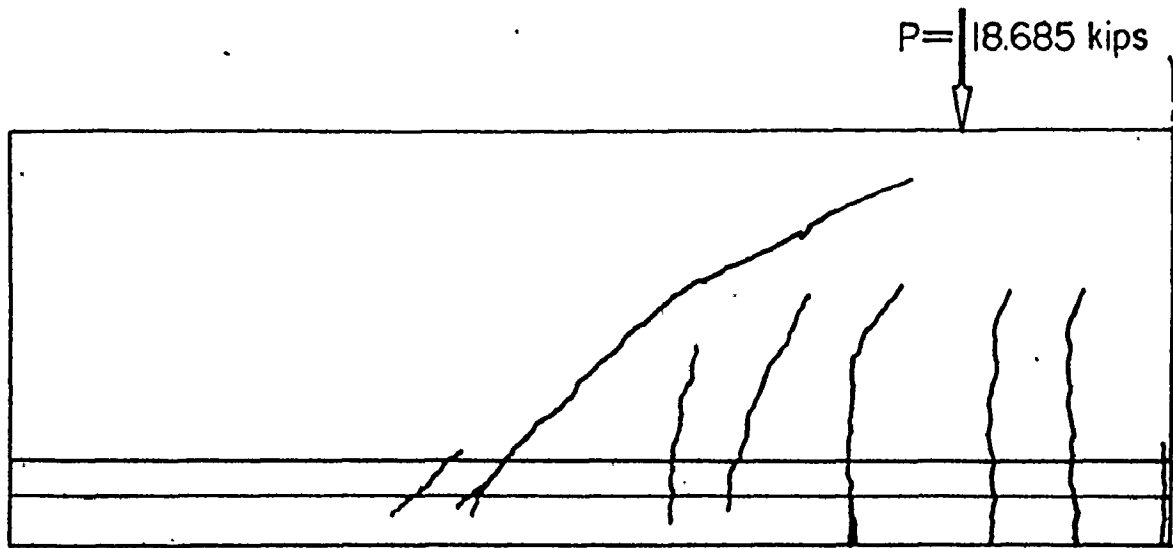
The experimental crack patterns for the left and right hand sides of the beam shown in Figures 6.8a and 6.8b respectively. The predicted crack pattern is superimposed on the finite element mesh used as shown in Fig. 6.8c. The failure loads are shown for both the test and the analysis. These loads and the first cracking loads are included in Table 6.2.

The two sides of the tested beam are shown to illustrate the degree of variation of cracking patterns and crack locations for supposedly identical conditions.

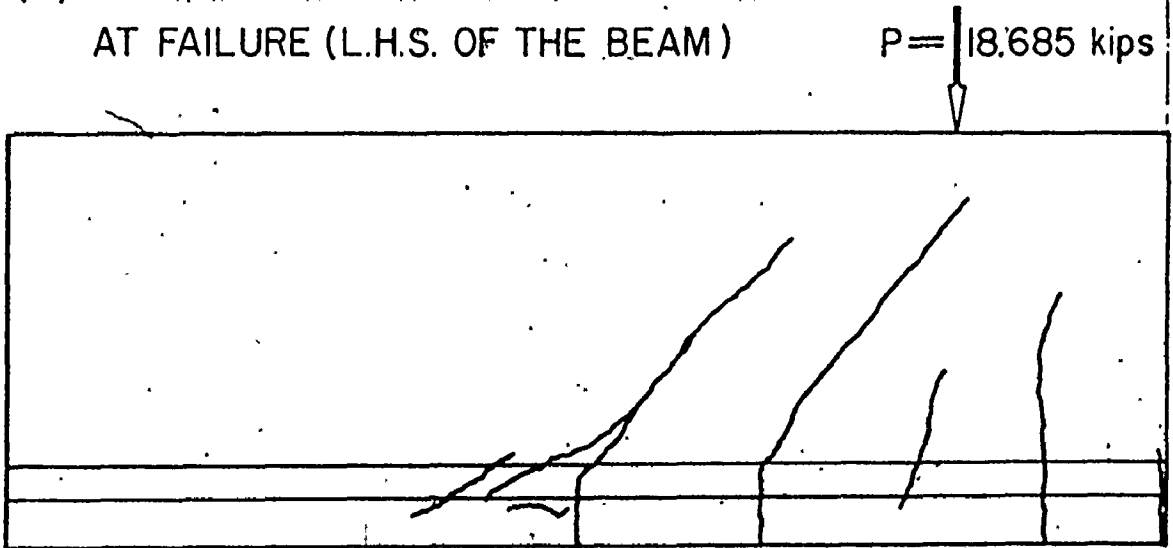
The numbers shown in Fig. 6.8c indicate the sequence of the crack occurrence predicted by the analysis. The load levels corresponding to these numbers were listed in Table 6.3 for all beams.

As can be seen from Fig. 6.8c not all of the elements in the constant moment region are cracked even at failure and the effect of the bond-slip phenomenon on the spacing and sequence of the cracking can be noticed. More detailed discussion on this effect is included for Beam (9/1).

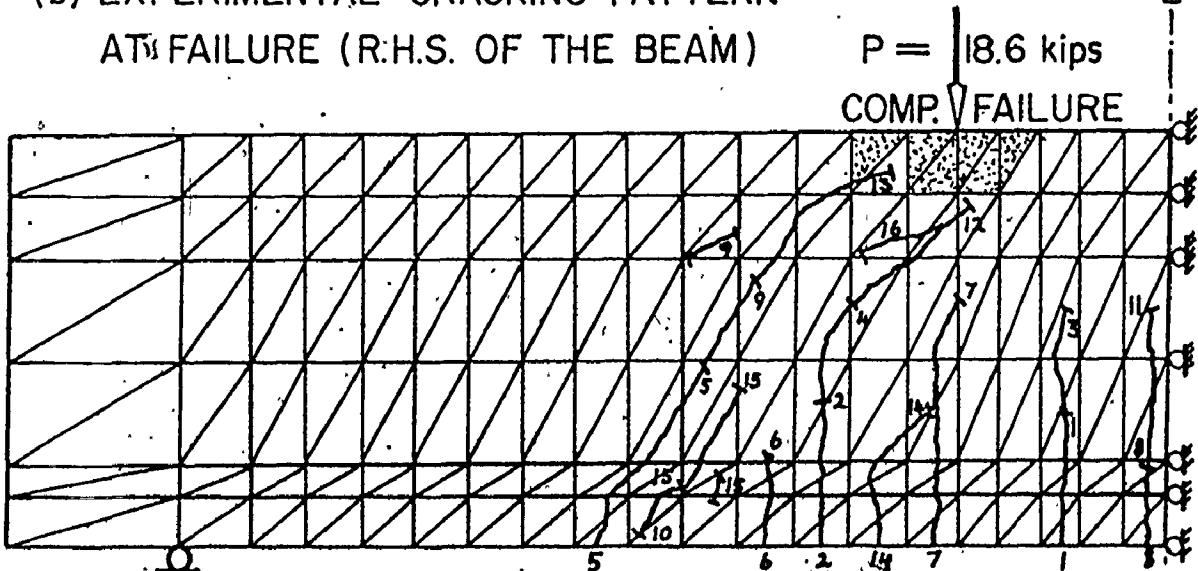
Shear-compression failure occurred when the crack closest to the support (which was the fifth crack to occur) had propagated during load step 13, and substantially reduced the compression zone near the load location. The second major crack identified by load steps 2, 4, and 12 may also have had some influence on a reduced compression zone. When shear



(a) EXPERIMENTAL CRACKING PATTERN AT FAILURE (L.H.S. OF THE BEAM)



(b) EXPERIMENTAL CRACKING PATTERN AT FAILURE (R.H.S. OF THE BEAM)



(c) PREDICTED CRACKING PATTERN AT FAILURE.

Table 6.2 Beam Cracking and Failure Loads.

BEAM	First Cracking Load			Ultimate Failure Load		
	Experi- mental (kips)	Analytical (kips)	Analysis Experiment	Experi- mental (kips)	Analytical (kips)	Analysis Experiment
4	-	5.64	-	18.685	18.60	0.99
7/1	-	2.89	-	13.01	13.887	1.067
9/1	-	2.44	7	11.574	11.815	1.021
EAI	5.12	5.42	1.062	16.42	17.45	1.059
EB1	4.80	5.02	1.046	25.46	24.4	0.96

Load Step No.	Beam (4)	Beam (7/1)	Beam (9/1)	Beam EA1	Beam EB1	Load Step No.	Beam (9/1)
1	5640	2886	2440	5423	5020	30	8101
2	7510	3443	2493	6837	5253	31	8165
3	8960	4332	2536	9491	6662	32	8211
4	9430	4433	2809	10041	7137	33	8312
5	12470	4887	3465	10226	8069	34	8440
6	12492	5560	3507	12223	10225	35	8689
7	13475	5855	3714	12583	14394	36	8825
8	14528	5864	3728	13517	16506	37	9187
9	15370	6163	3885	15777	19957	38	9270
10	15381	6428	4001	15984	20460	39	9299
11	15695	6703	4099	16782	22703	40	9665
12	18196	6962	4149	17451	24400	41	9712
13	18600	6988	4194			42	9976
14	18600	7906	4278			43	10056
15	18600	8525	4439			44	10097
16	18600	9625	4523			45	10151
17		9637	4778			46	10309
18		10344	5033			47	10480
19		11083	5160			48	10695
20		11162	5309			49	10877
21		12038	5508			50	10949
22		12973	5826			51	11105
23		13887	6397			52	11263
24		13887	6545			53	11349
25		13887	7114			54	11407
26		13887	7357			55	11449
27		13887	7738			56	11572
28			7789			57	11689
29			8035			58	11815

Table 6.3 Loads in lbs. Corresponding to load step numbers

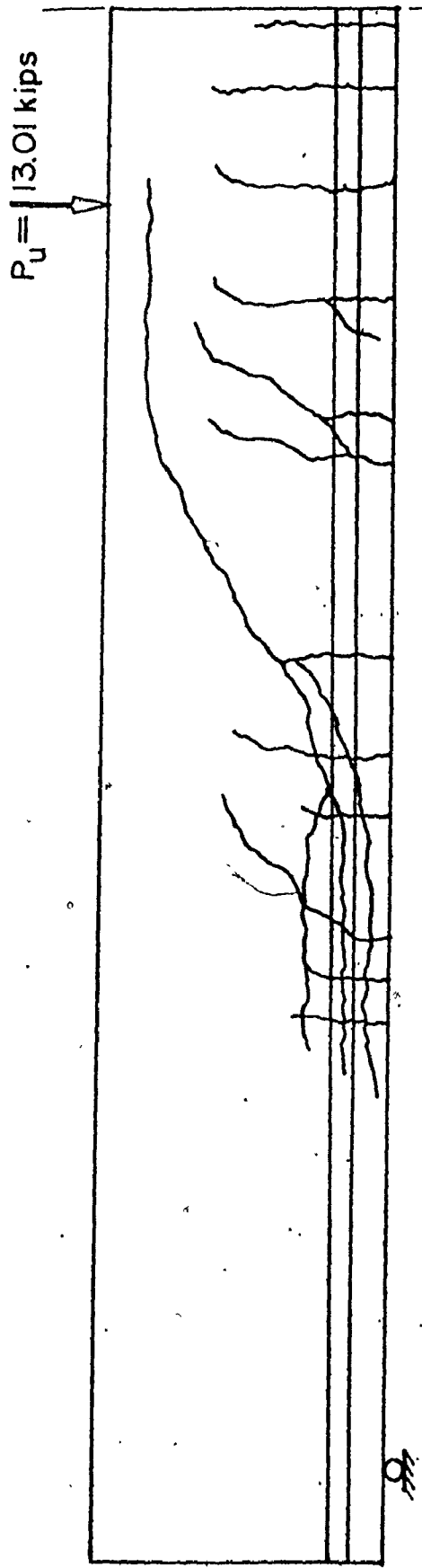
compression failure occurred, post-failure cracks 14-14, 15-15 and 12-16 developed. No bond break down or anchorage failure occurred because proper end anchorage was provided.

There was very close agreement between the test and the analysis results for the cracking patterns (spacing, height, shape and location) and the failure loads. Also, the mode of failure reported from the test (shear-compression failure) was predicted by the analysis.

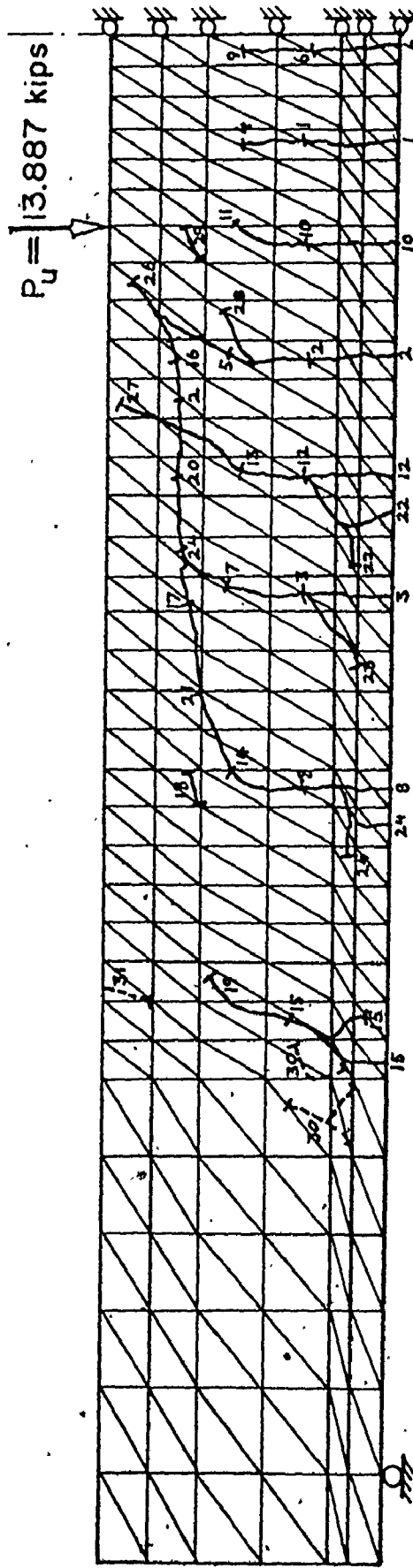
(6.5.3.2) Beam (7/1)

Beam (7/1) was chosen to be analyzed in this thesis because ~~its~~ a/d ratio (5.0) was in the middle range for diagonal tension failure. More detailed analytical results for this beam than for the others are included for this reason. Detailed drawings showing crack propagation at different loading steps are included, along with stresses in concrete and steel reinforcement. Also, the bond stresses along the reinforcement for different load levels are presented and discussed in the next section.

A sudden diagonal tension failure of beam (7/1) was reported by Leonhardt and Walther (28). It was significant to see the same type of distinct crack propagation and failure detected by the analysis. As can be seen in Figure 6.9 the crack associated with failure is very flat compared with the corresponding cracks shown in Fig. 6.8 for beam (4). This flat crack was initiated from the flexural-shear crack, 8-14-21 and several other cracks which opened near the top of



(a) EXPERIMENTAL CRACKING PATTERN AT FAILURE.



(b) PREDICTED CRACKING PATTERN AT FAILURE.

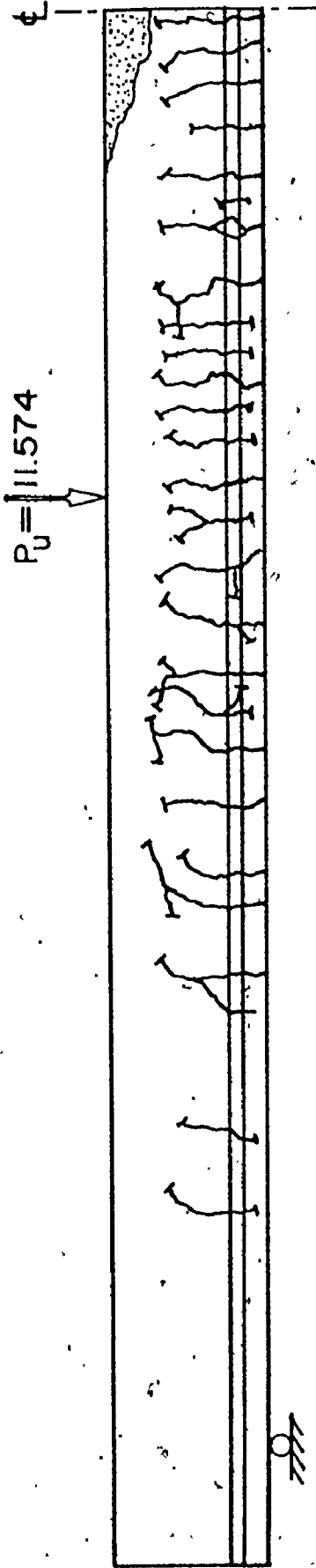
Fig. 6.9 CRACKING PATTERN RESULTS FOR BEAM 7/1 ($a/d = 5.0$)

existing flexural cracks at very flat angles and at different stages of loading. All of these small flat cracks, designated by 16, 17 and 20, were joined by crack 8-14-21 at load step 26 to form a diagonal tension crack which extended to near the loading point and which caused the beam to fail by crushing of the compression zone around the loading point. The same observation regarding the cracking pattern discussed for beam (4) apply here.

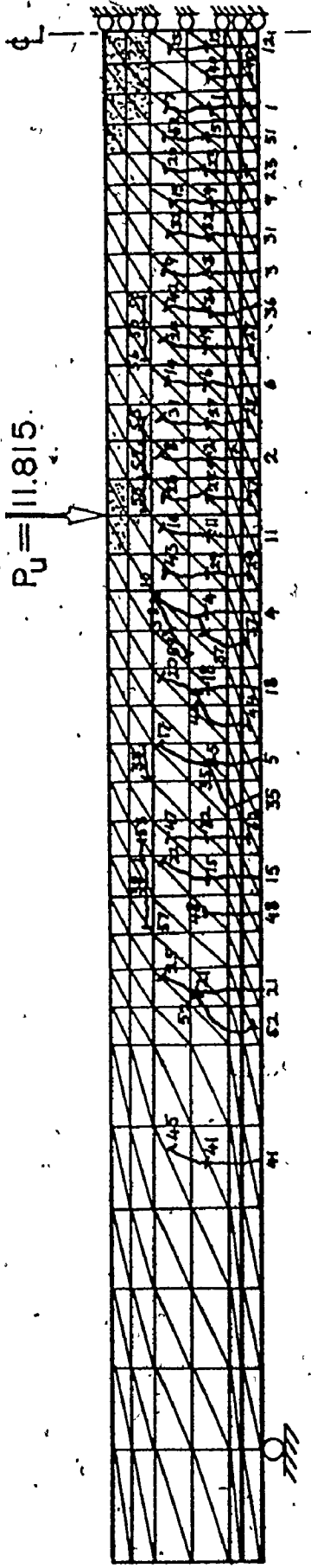
It is also very interesting to observe that dowel cracks have occurred in the shear span at loads near failure, steps (22, 23, and 24) and after initial failure. The excessive post-failure dowel cracking which cannot be prevented in tests was not predicted by the analysis. The analysis was stopped at a preselected limiting deflection before the rest of the dowel cracks along the reinforcement had the chance to form.

6.5.3.3 Beam (9/1)

Experimental results have shown that Beam (9/1) with an a/d ratio near 7, should fail in flexure for normal loading conditions and normal bond-slip characteristics. The reported test failure load of 11.57 kips is very close to the theoretical ultimate flexural capacity of the beam. Flexural failure can be identified from observation of the cracking pattern shown in Fig. 6.10 at failure of the beam. Although some short flat cracks appear near the top of some of the flexural cracks in both the shear span and the constant moment region, no diagonal cracks can be seen in the crack pattern



(a) EXPERIMENTAL CRACKING PATTERN AT FAILURE.



(b) PREDICTED CRACKING PATTERN AT FAILURE.

Fig. 6.10 CRACKING PATTERN RESULTS FOR BEAM 9/I ($a/d = 6.92$)

at failure. Yielding of the steel followed by crushing of the concrete in compression was predicted from the analysis. This does not exactly agree with the test result, where concrete in compression crushed prior to yielding of the steel. This disagreement may be partly due to the closeness of the steel amount used compared to the balanced steel of the section, and partly due to the idealization of the stress-strain relationship by an elastic-plastic curve. (Percentage of steel was 2.2, and balanced steel is 2.3%).

As can be seen from Fig. 6.10b almost every row of elements is cracked. This is due to the coarse mesh used for this beam which was necessary because it was fairly long. The size of the elements is almost equal to the crack spacing found in the experimental work and reproduced in the analysis of other beams using a finer element mesh. The cracks did not occur simultaneously and the sequence of crack occurrence followed the theory of cracking (27). Cracking would usually begin with large spacing. The the distance between two cracks, (usually called primary cracks) would normally be halved by another crack which is usually termed a secondary crack. The secondary crack may or may not propogate fully depending on its location relative to all other cracks. This process of halving the crack spacing continues until a typical minimum crack spacing for the particular geometry is reached.

Although a fairly coarse element mesh size was used as compared to the other beams analysed, this did not affect the degree of accuracy of the analysis to any appreciable

extent as can be judged from comparisons of ultimate load, the load-deflection results, and the cracking patterns.

6.5.3.4 Beams EA1 & EB1

Beams EA1 & EB1 were analysed to demonstrate the effect of the bond-slip relationship on the behaviour of simply supported R.C. beams. Beams EA1 & EB1 have the same a/d ratio of 2.78. In this range of a/d ratios, reduction of capacity from flexural strength due to shear type failure is most marked. Beam EA1 had deformed reinforcing bars with normal bond while Beam EB1 had all the same physical qualities of beam EA1 except that the steel bars were very smooth and had a mirror like surface. Therefore, the bond would be expected to be very poor.

Figure 6.6 shows the load-deflection curves for beam EA1 obtained from the experiment and the computer analysis. Also, the ultimate capacities of the beam is indicated for both. The predicted ultimate load is 6.3% higher than the experimental value. The agreement between the analytical and experimental results can be considered quite acceptable.

The analytical and experimental load-deflection curves for beam EB1 are shown in Fig. 6.7 along with the corresponding ultimate load values. The experimental load deflection curve for beam EB2 which is another beam similar to beam EB1 except that it had slightly better bond, is also shown. This slightly better bond was obtained by using smaller but still

smooth bars, having the same total cross-sectional area as for beam EB1. Small values for stiffness were assigned to the bond elements in the computer program where zero stiffness would cause an error in the stiffness matrix solution. No specific values for bond-slip were given for these beams. However, the adhesion between the bars and the concrete can provide some bond resistance. Three arbitrary values of 1%, 5% and 10% of the normal bond stiffness were analyzed. The 10% value gave the most realistic result. Therefore it was used in the analysis with the same failure criterion as that for normal bond.

The analytical load-deflection curve lies very close to both the EB1 and EB2 experimental curves, however, the predicted ultimate load was 4.2% lower than the experimental load for beam EB1 & 9.8% higher than the experimental load for beam EB2. This discrepancy may indicate that the bond-slip values used in the computer program did not accurately represent the actual characteristics of either beam EB1 or beam EB2.

Comparison of the crack patterns on Figures 6.11 and 6.12 shows the dramatic difference in behaviour due to different bond-slip characteristics for otherwise identical beams.

Figure 6.11a shows the experimental cracking pattern at failure for beam EA1, while Fig. 6.11b shows the analytically predicted cracking pattern for the same beam. The crack occurrence sequence is shown for both the test and the analysis.

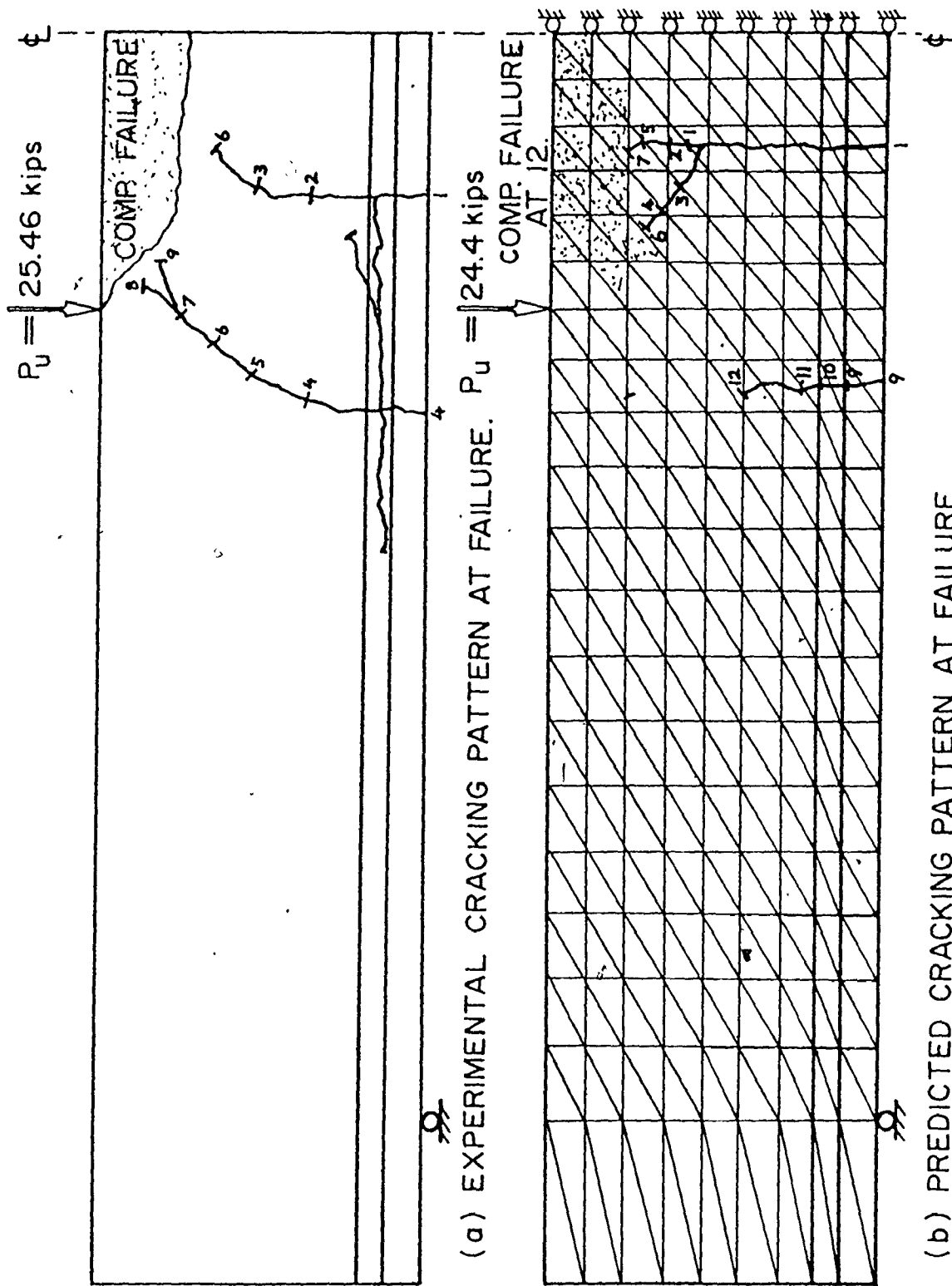


Fig. 6.12 CRACKING PATTERN RESULTS FOR BEAM EB1 (POOR BOND, $a/d = 2.78$)

It can be seen that the agreement between crack sequences, crack locations (crack spacing) and the general crack pattern at failure is quite close. The same agreement can be observed for beam EB1 from Figs. 6.12a and 6.12b. Only two cracks occurred in both the experimental and predicted cracking patterns. For this latter beam, failure occurred, experimentally and analytically due to compressive crushing of the concrete at loads just below the theoretical flexural capacity of the beams. The difference between the modes of failure for beams EA1 and beam EA2 can be easily visualized from the predicted cracking patterns. Beam EA1 failed in a shear-compression mode whereas beam EB1 failed in a flexural-compression mode.

From the experimental and the analytical ultimate failure loads for beams EA1 and EB1, it can be concluded that, contrary to the general notion of stronger being better, stronger bond causes premature shear-compression or diagonal tension failures in beams with a/d ratios in this range. Also failure loads have been shown to be quite near their flexural capacity when reinforced with low bond bars provided that they are adequately anchored at their ends. However, the widths of cracks will be much larger than those for better bonded reinforcement. Larger crack widths occur due to the concentration of all the reinforcing elongations at relatively fewer crack locations when bond is poor.

6.5.4 Detailed behaviour of Beam (7/1) at different loading

Steps:

Figures 6.13 to 6.35 show the extent of cracking at different loading steps as predicted by the analysis: Also, the longitudinal and shear stresses in the concrete are shown for selected sections at several load steps. The longitudinal steel stresses are shown for all load steps and bond stresses along the bar are shown at several intervals upto near failure. [Please note: The stresses shown in these figures are drawn to different scales for each loading step. Shear stresses have their own scale which is shown for every figure. The steel stresses for the elements along the bar length are joined in the figures to show continuous stress curves for the longitudinal steel reinforcing bars. However, bond stresses are shown as discrete values. When bond is broken, (i.e. when a joint element fails in the direction parallel to the bar axis) an X mark is made to indicate the failure of this particular joint element].

This series of figures illustrates how the flexural cracks initiated and propagated until they stabilized in height around the 8,000 lbs. load level. At the load level of 9,625 lbs. flat cracks occurring immediately above some of the existing flexural cracks started to appear and flexural cracks started to branch at the bottom forming another crack. Failure occurred suddenly, at the 13,887 lbs. load level, when the flat cracks were all joined with an inclined crack in the shear span as shown with the dotted line, in Figure 6.35.

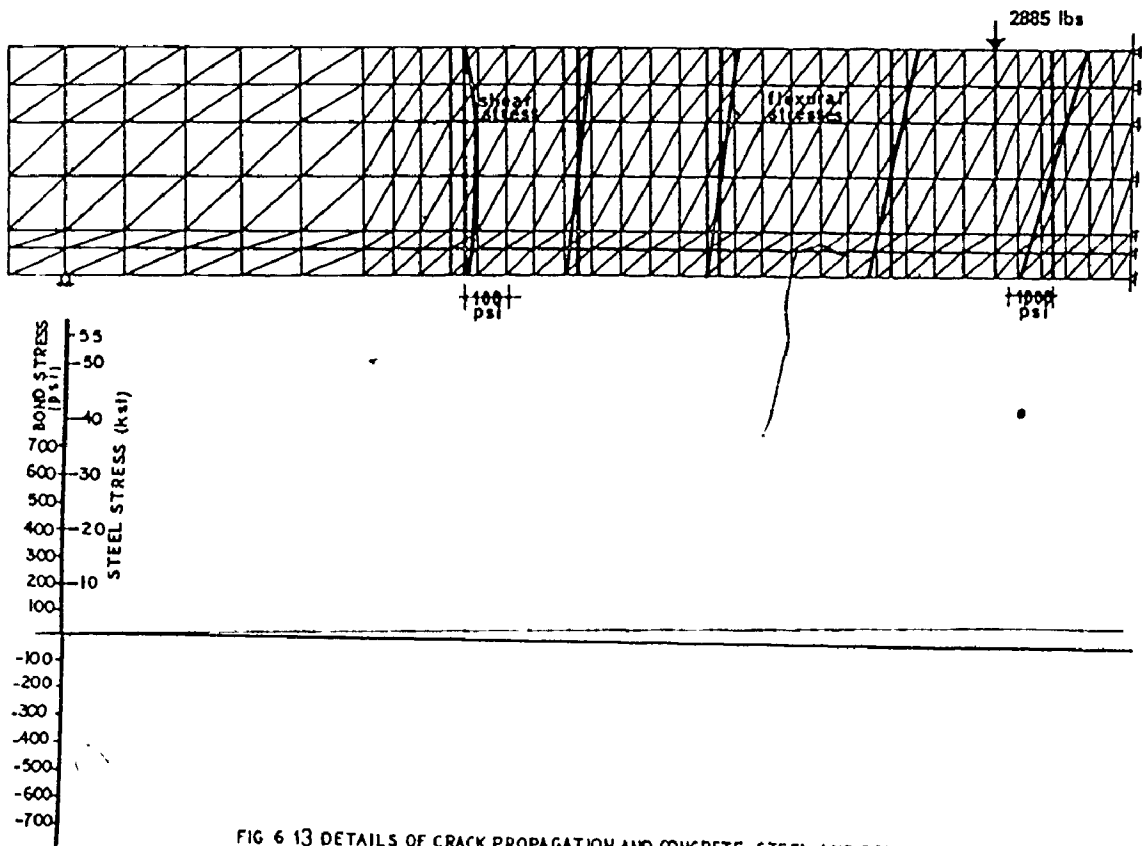


FIG 6 13 DETAILS OF CRACK PROPAGATION AND CONCRETE, STEEL AND BOND STRESS DISTRIBUTIONS FOR BEAM(7/1)

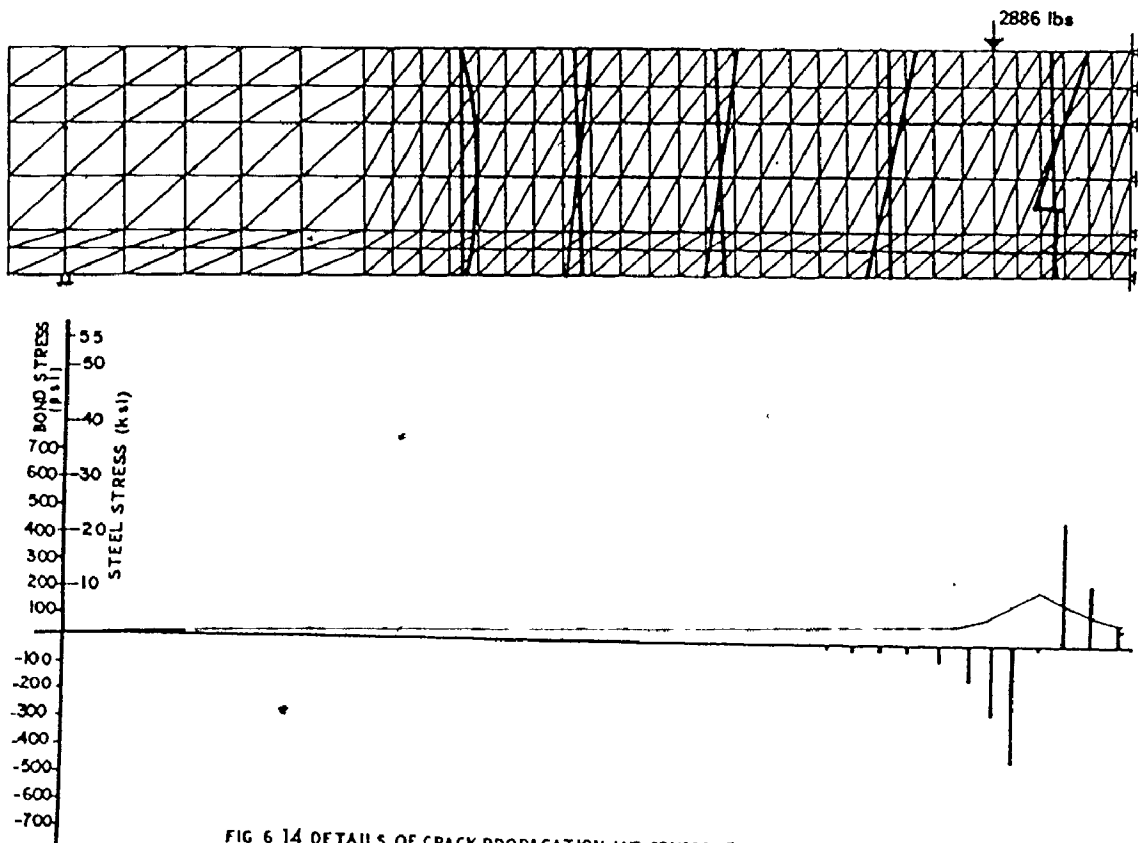


FIG 6 14 DETAILS OF CRACK PROPAGATION AND CONCRETE, STEEL AND BOND STRESS DISTRIBUTIONS FOR BEAM(7/1)

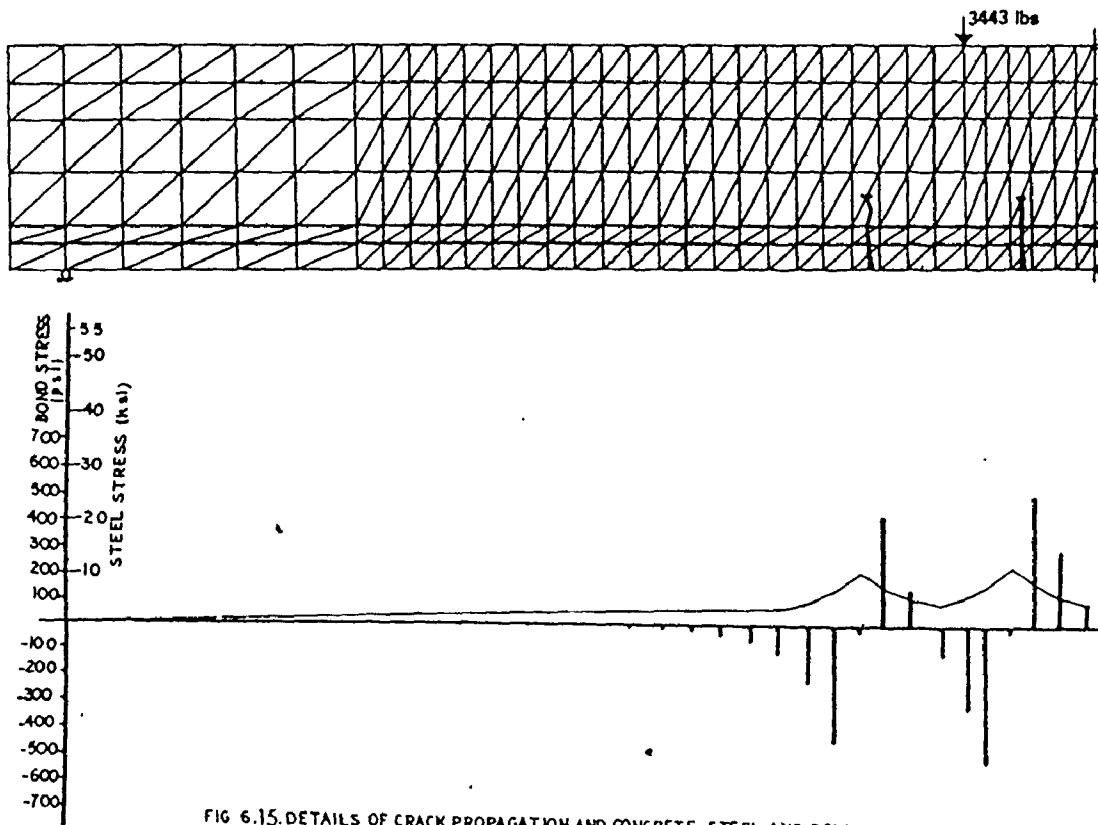


FIG 6.15. DETAILS OF CRACK PROPAGATION AND CONCRETE, STEEL AND BOND STRESS DISTRIBUTIONS FOR BEAM(7/1)

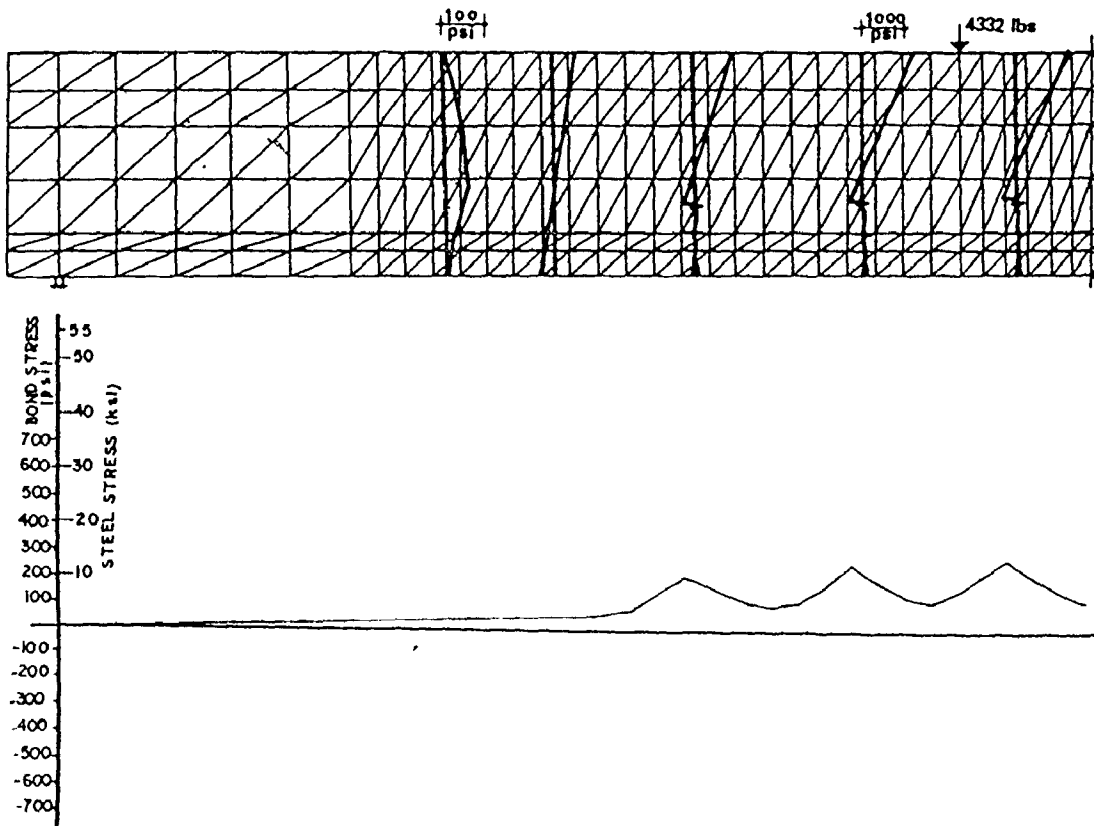


FIG 6.16 DETAILS OF CRACK PROPAGATION AND CONCRETE, STEEL AND BOND STRESS DISTRIBUTIONS FOR BEAM(7/1)

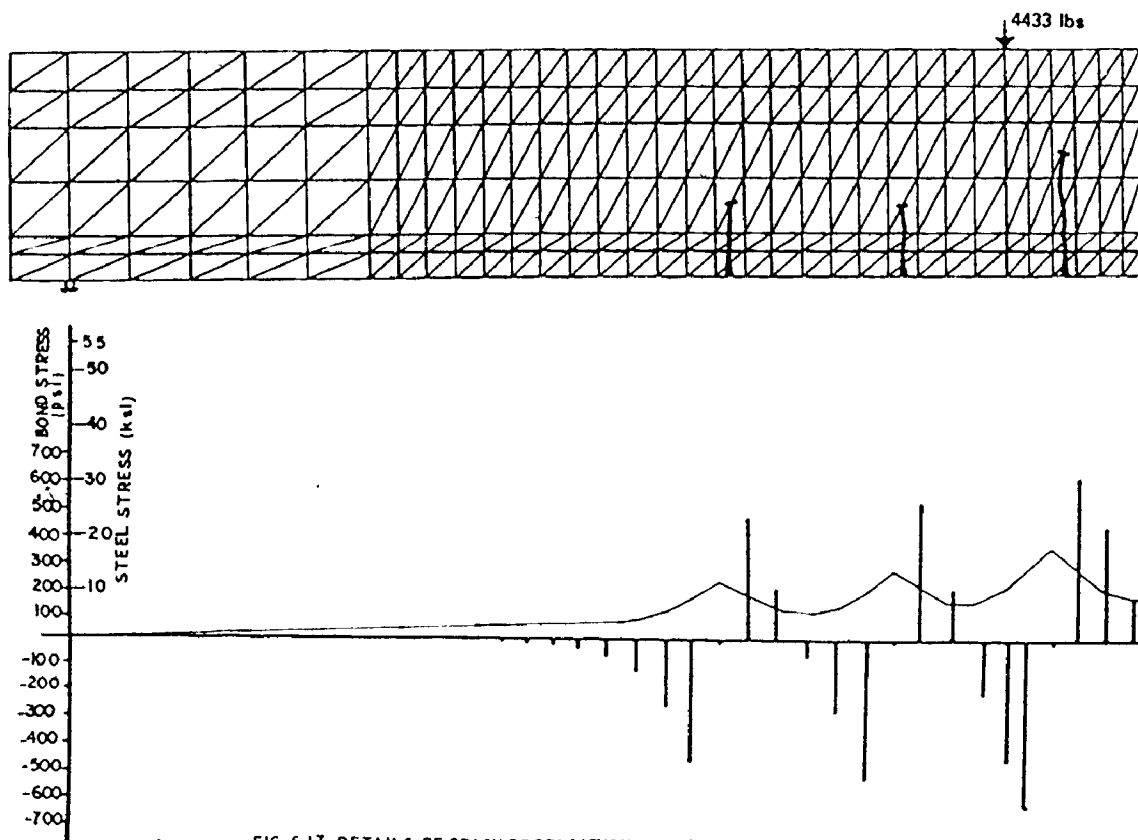


FIG 6 17 DETAILS OF CRACK PROPAGATION AND CONCRETE, STEEL AND BOND STRESS DISTRIBUTIONS FOR BEAM(7/1)

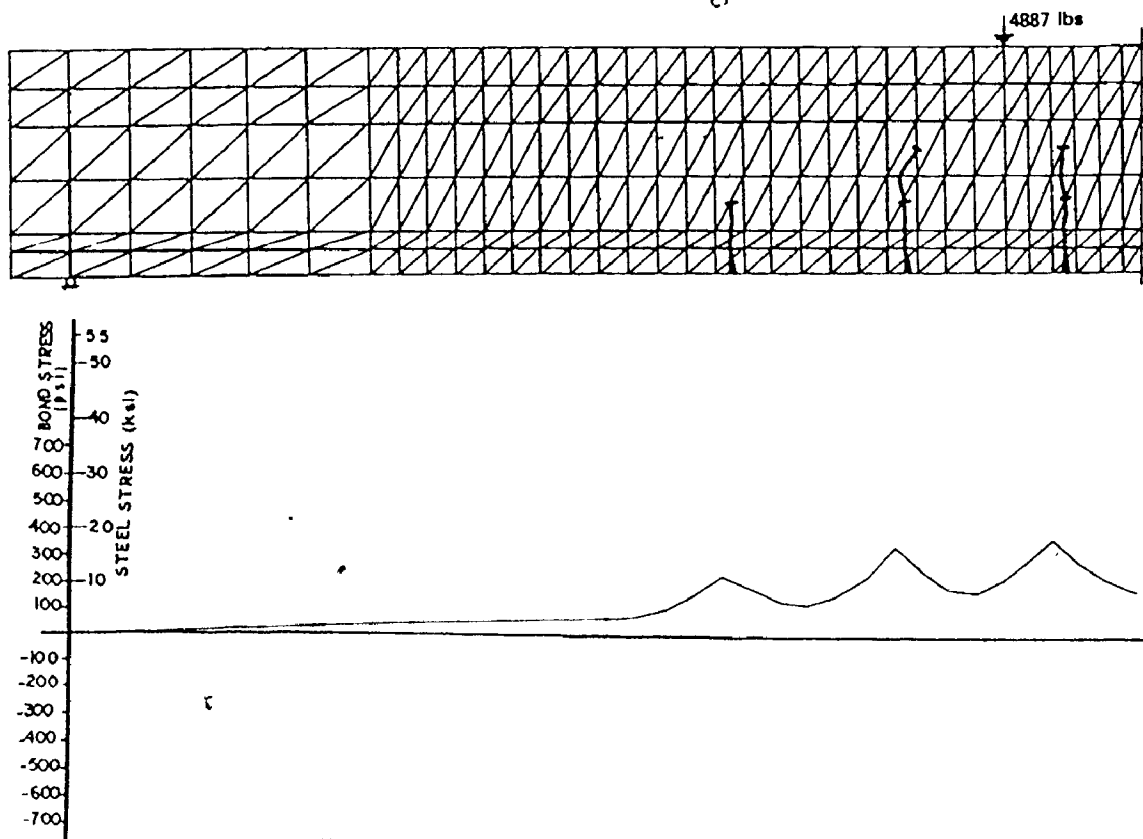


FIG 6 18 DETAILS OF CRACK PROPAGATION AND CONCRETE, STEEL AND BOND STRESS DISTRIBUTIONS FOR BEAM(7/1)

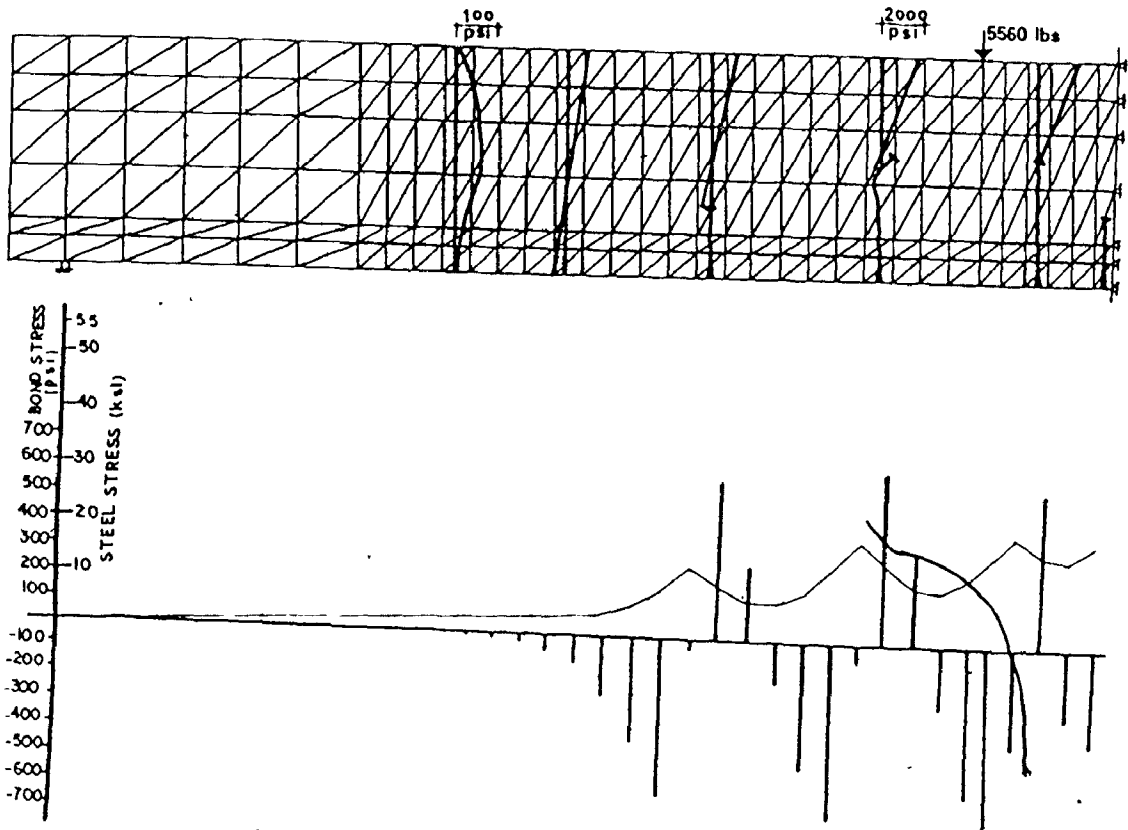


FIG 6 19. DETAILS OF CRACK PROPAGATION AND CONCRETE, STEEL AND BOND STRESS DISTRIBUTIONS FOR BEAM(7/1)

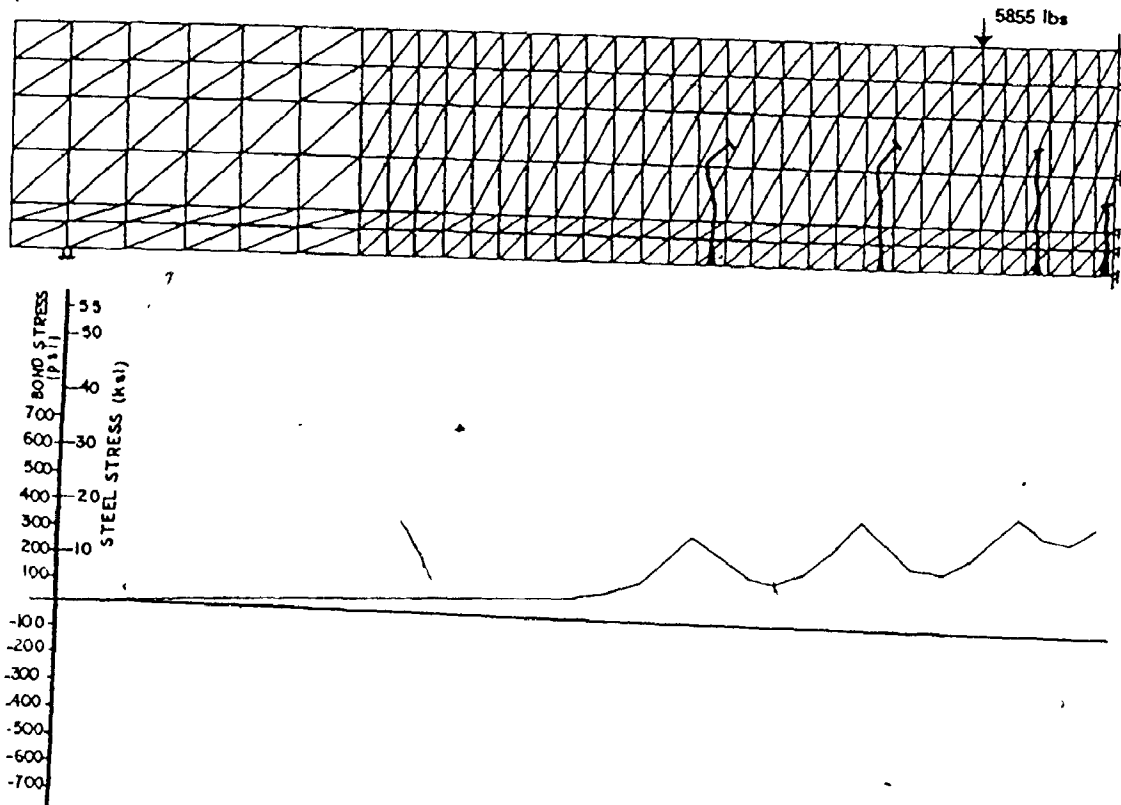


FIG 6 20 DETAILS OF CRACK PROPAGATION AND CONCRETE, STEEL AND BOND STRESS DISTRIBUTIONS FOR BEAM(7/1)

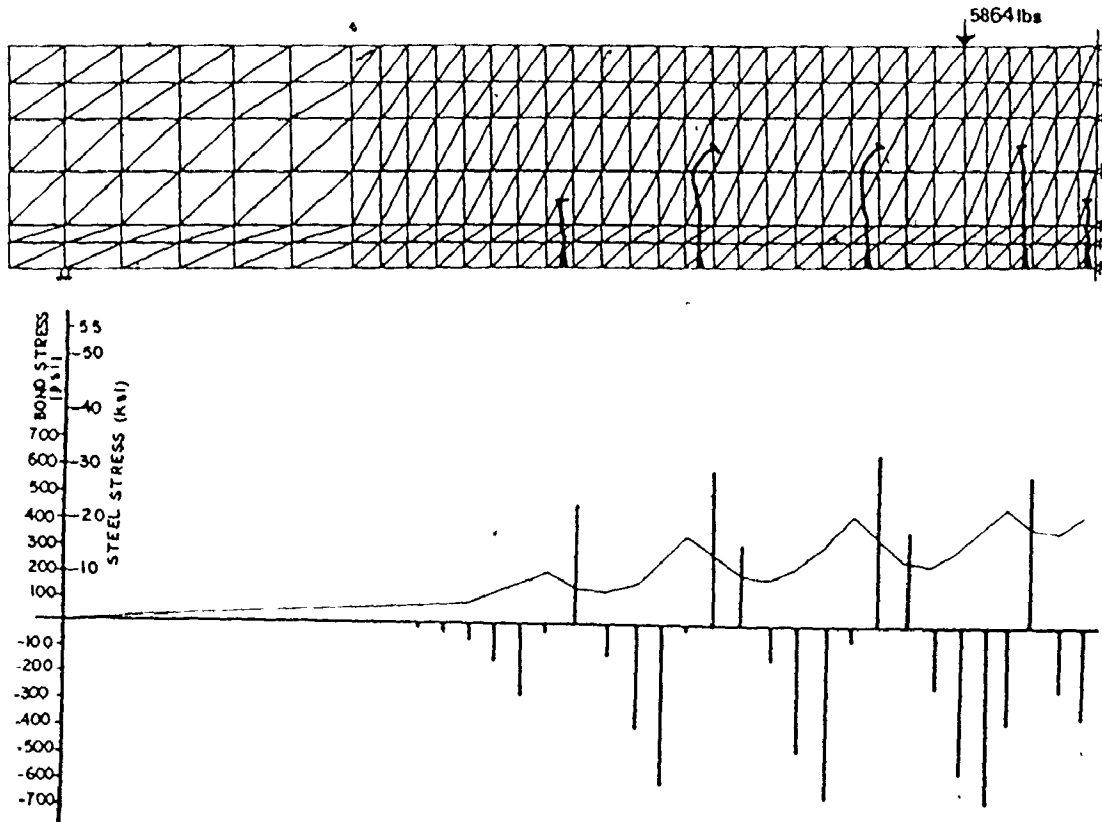


FIG 6 21 DETAILS OF CRACK PROPAGATION AND CONCRETE, STEEL AND BOND STRESS DISTRIBUTIONS FOR BEAM(7/1)

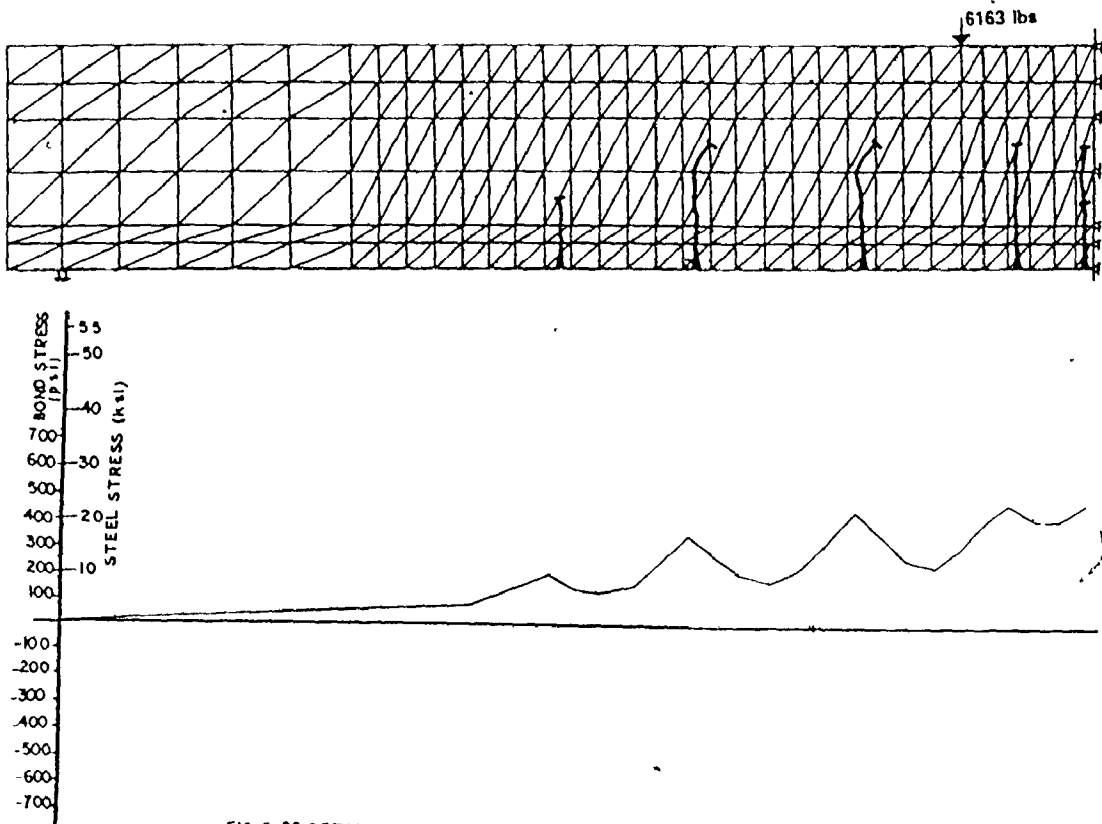


FIG 6 22. DETAILS OF CRACK PROPAGATION AND CONCRETE, STEEL AND BOND STRESS DISTRIBUTIONS FOR BEAM(7/1)

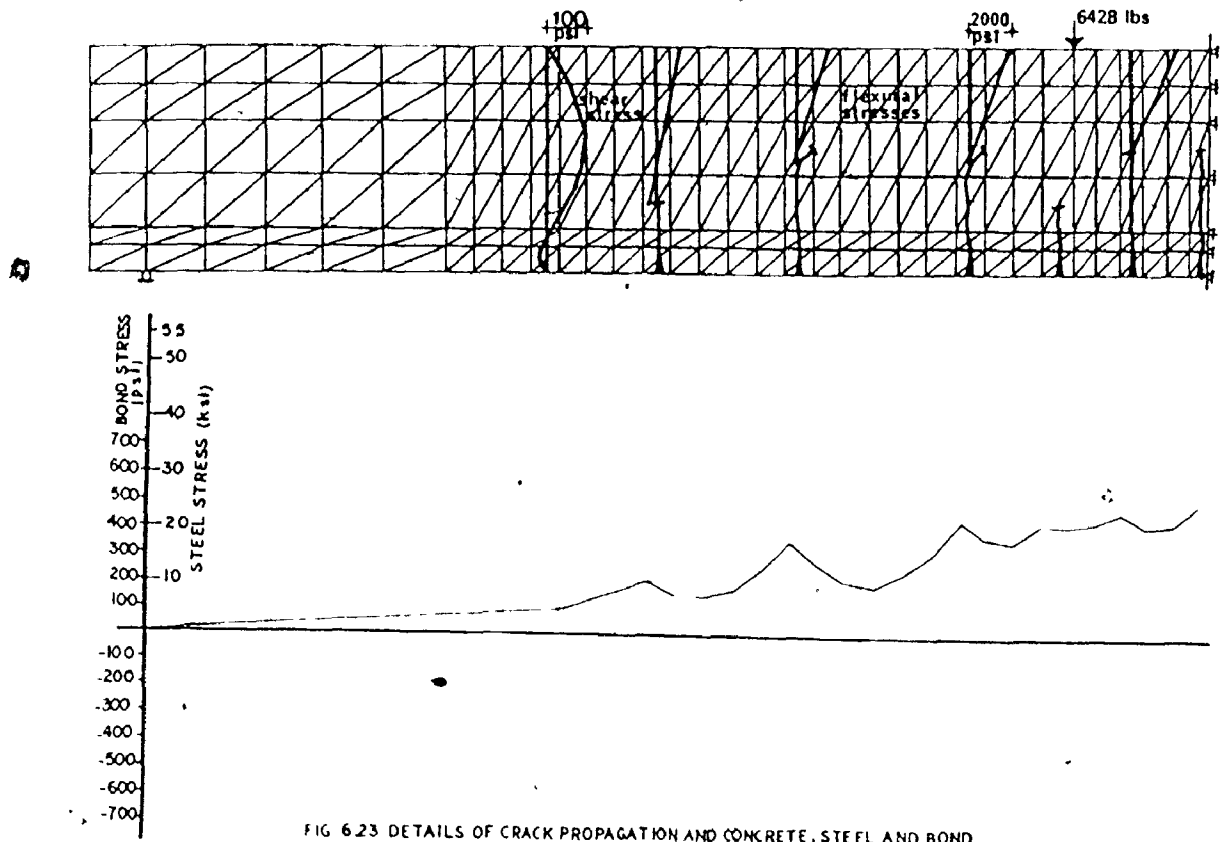


FIG 6.23 DETAILS OF CRACK PROPAGATION AND CONCRETE, STEEL AND BOND STRESS DISTRIBUTIONS FOR BEAM(7/1)

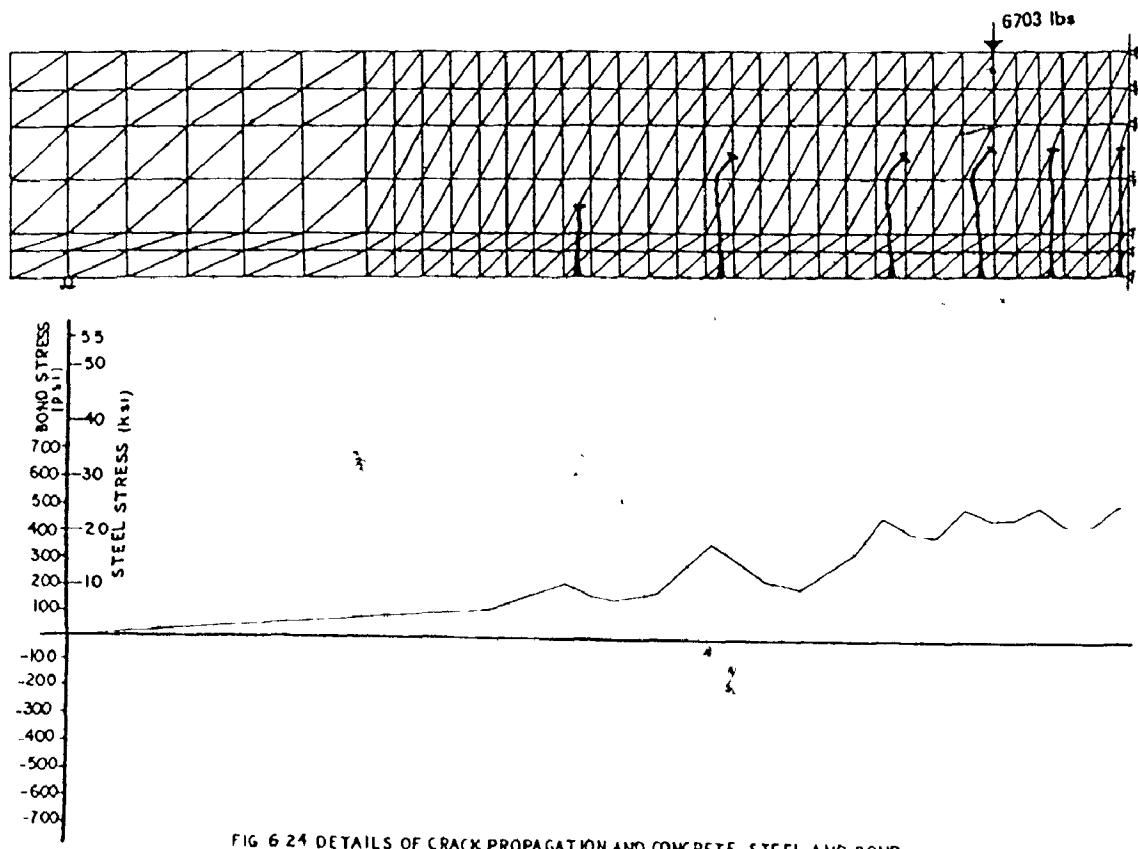


FIG 6.24 DETAILS OF CRACK PROPAGATION AND CONCRETE, STEEL AND BOND STRESS DISTRIBUTIONS FOR BEAM(7/1)

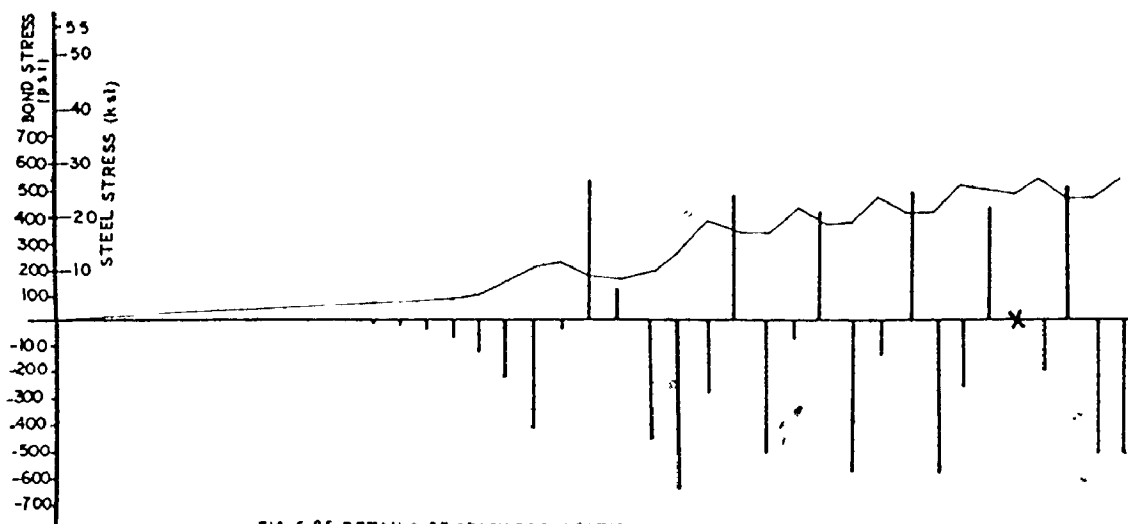
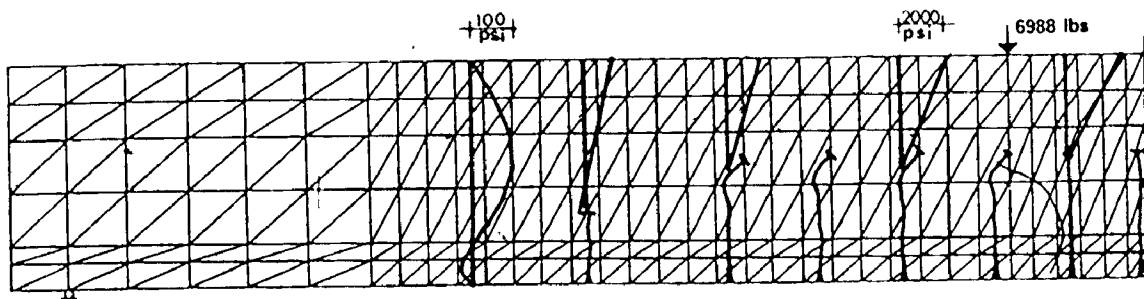


FIG 6 25 DETAILS OF CRACK PROPAGATION AND CONCRETE, STEEL AND BOND STRESS DISTRIBUTIONS FOR BEAM(7/1)

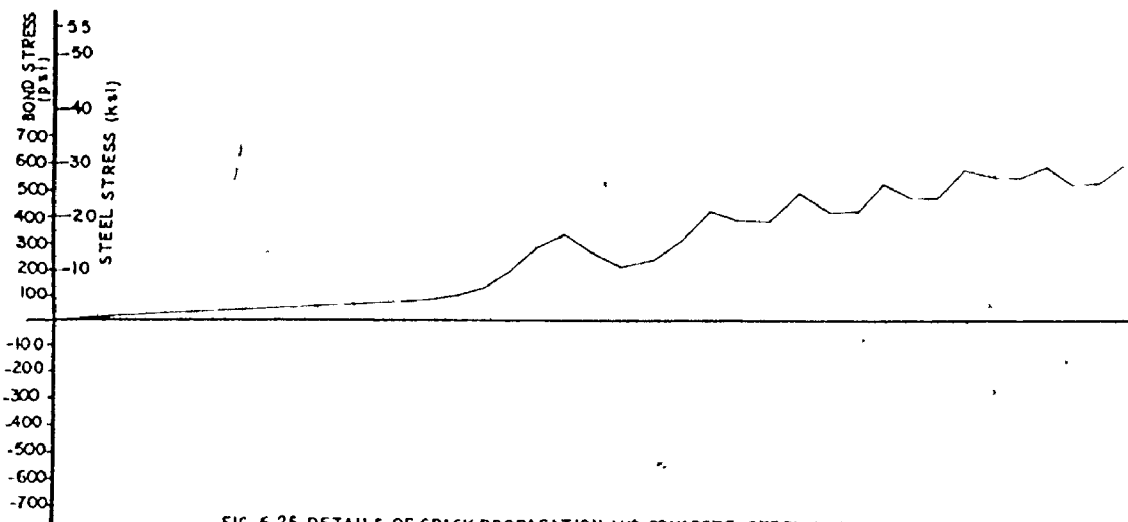
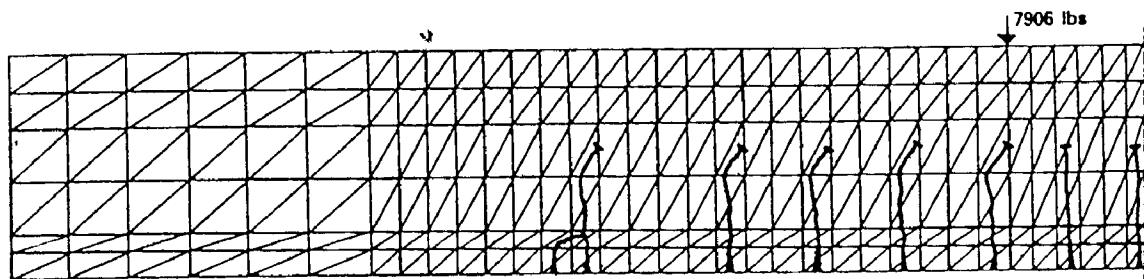


FIG 6 26 DETAILS OF CRACK PROPAGATION AND CONCRETE, STEEL AND BOND STRESS DISTRIBUTIONS FOR BEAM(7/1)

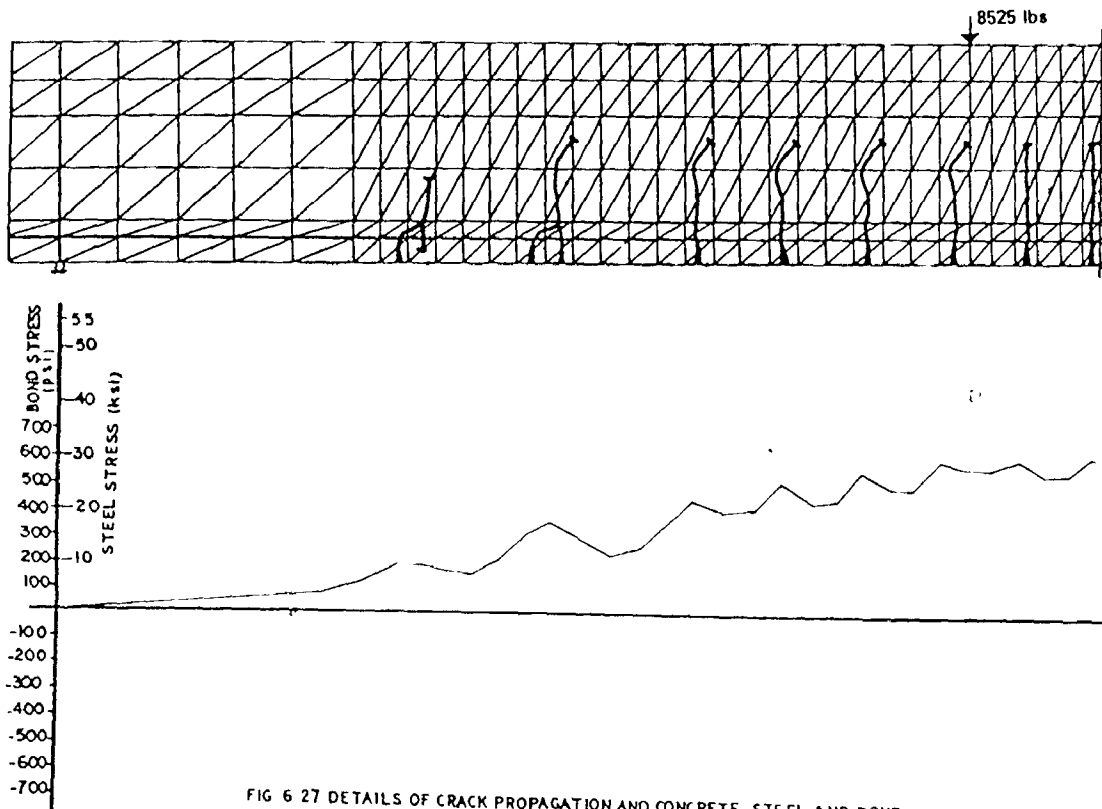


FIG 6 27 DETAILS OF CRACK PROPAGATION AND CONCRETE, STEEL AND BOND STRESS DISTRIBUTIONS FOR BEAM(7/1)

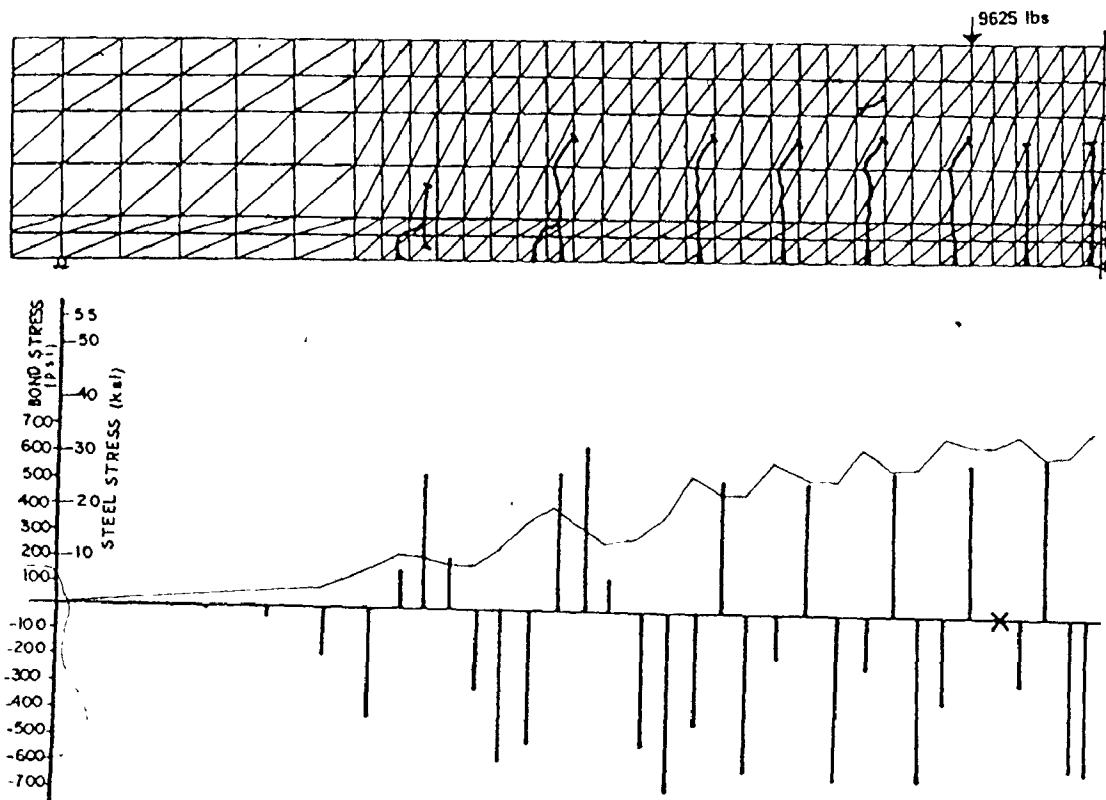


FIG 6 28 DETAILS OF CRACK PROPAGATION AND CONCRETE, STEEL AND BOND STRESS DISTRIBUTIONS FOR BEAM(7/1)

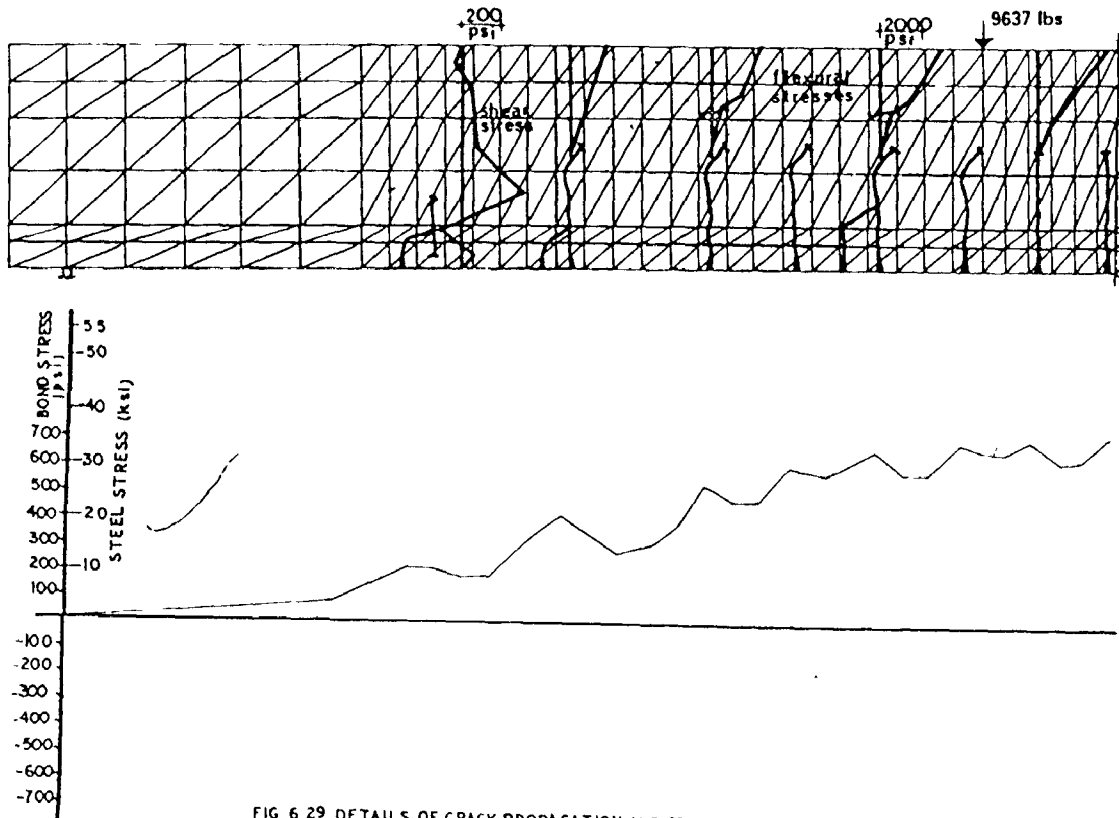


FIG 6.29 DETAILS OF CRACK PROPAGATION AND CONCRETE, STEEL AND BOND STRESS DISTRIBUTIONS FOR BEAM(7/1)

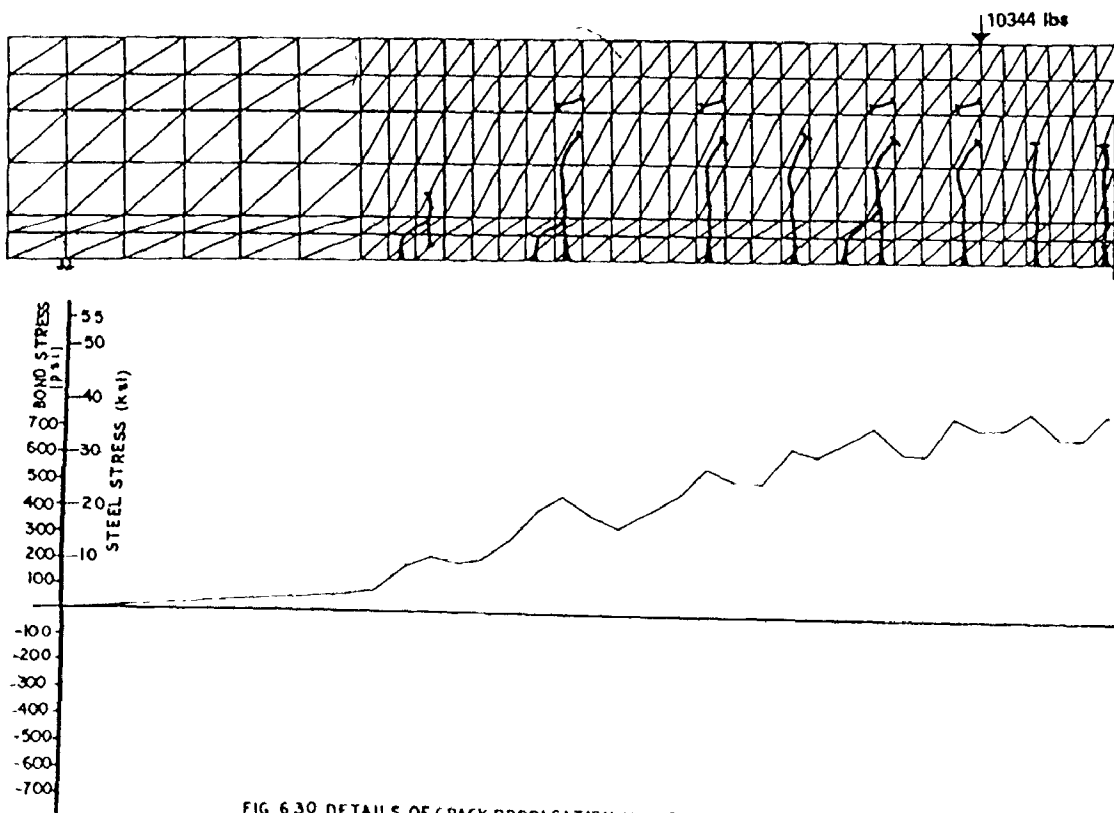


FIG 6.30 DETAILS OF CRACK PROPAGATION AND CONCRETE, STEEL AND BOND STRESS DISTRIBUTIONS FOR BEAM(7/1)

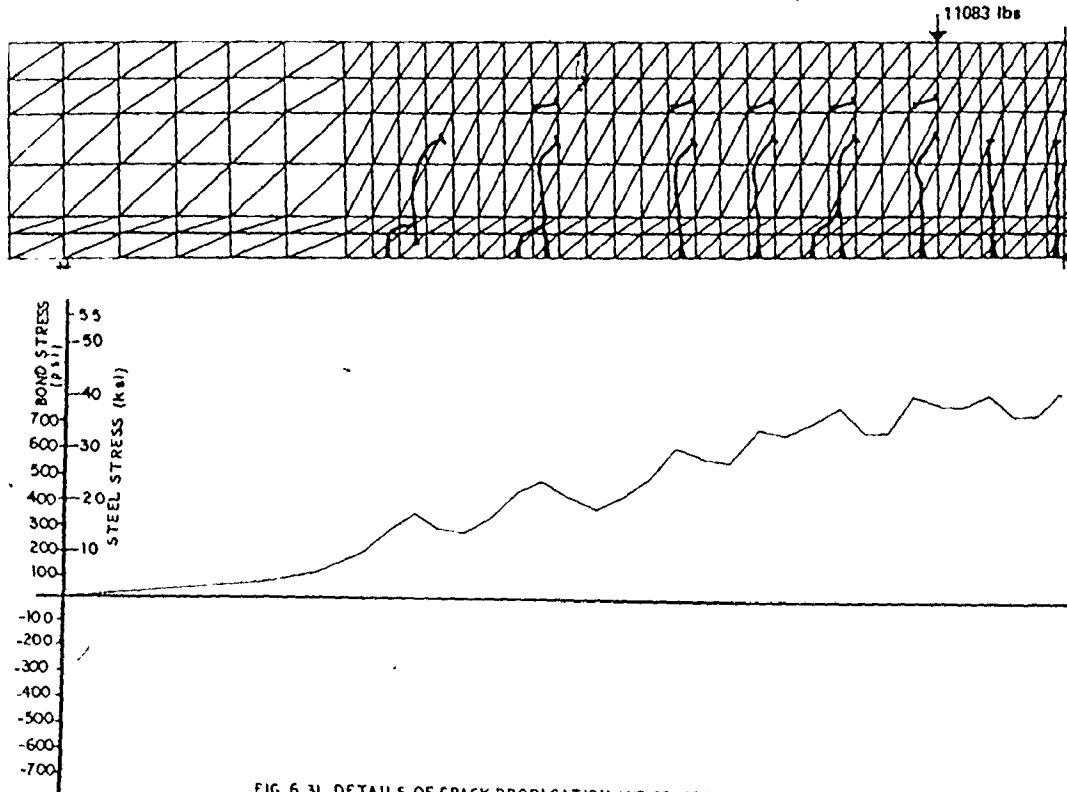


FIG 6 31 DETAILS OF CRACK PROPAGATION AND CONCRETE, STEEL AND BOND STRESS DISTRIBUTIONS FOR BEAM(7/1)

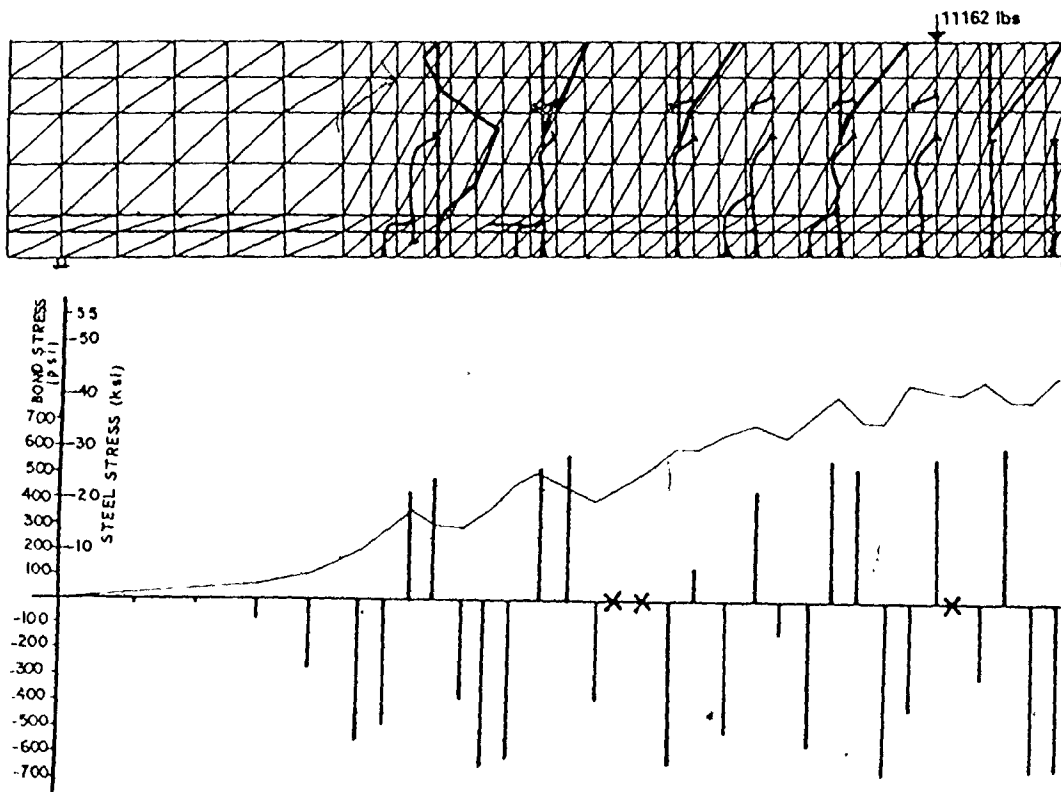


FIG 6 32 DETAILS OF CRACK PROPAGATION AND CONCRETE, STEEL AND BOND STRESS DISTRIBUTIONS FOR BEAM(7/1)

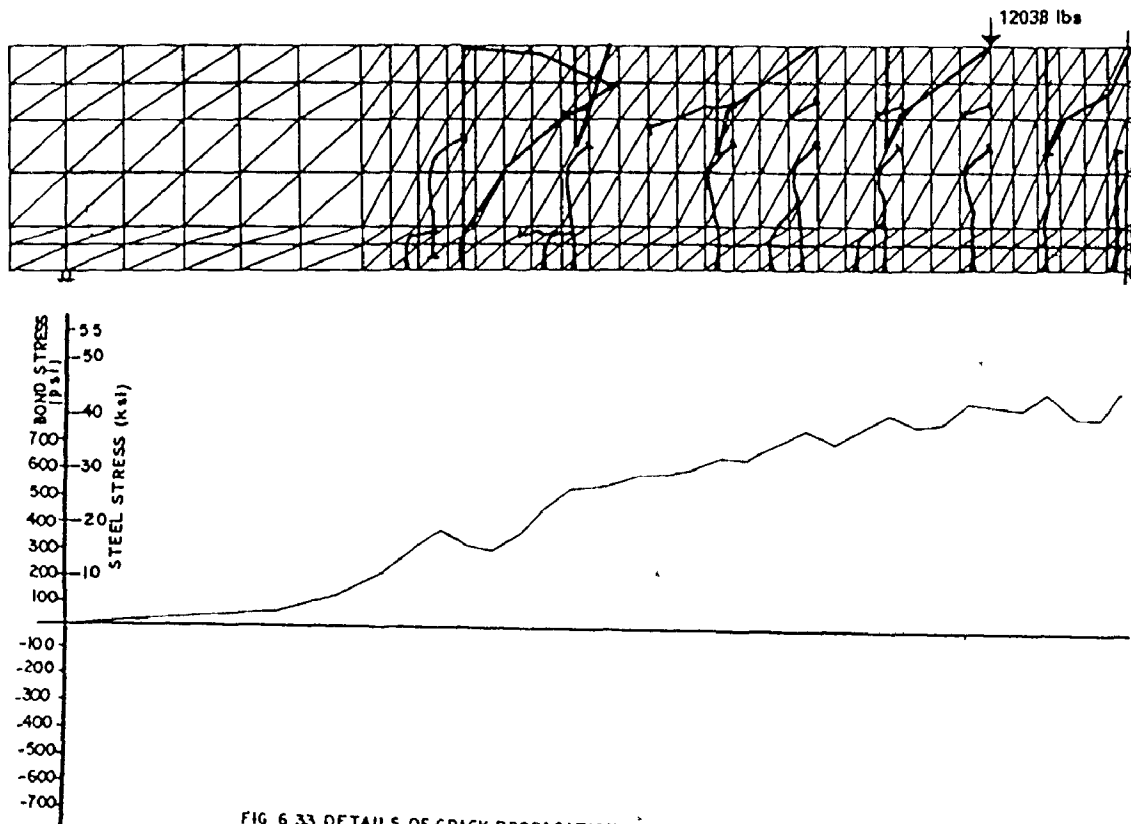


FIG 6 33 DETAILS OF CRACK PROPAGATION AND CONCRETE, STEEL AND BOND STRESS DISTRIBUTIONS FOR BEAM(7/1)

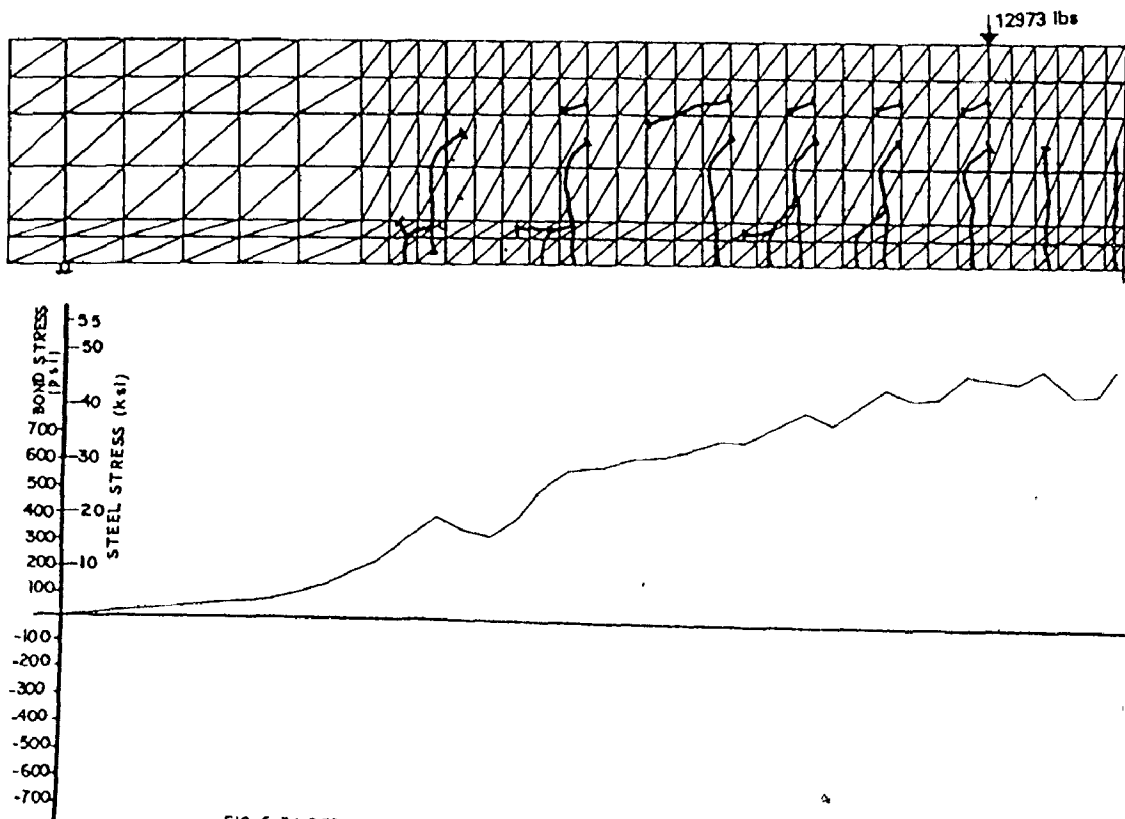


FIG 6 34 DETAILS OF CRACK PROPAGATION AND CONCRETE, STEEL AND BOND STRESS DISTRIBUTIONS FOR BEAM(7/1)

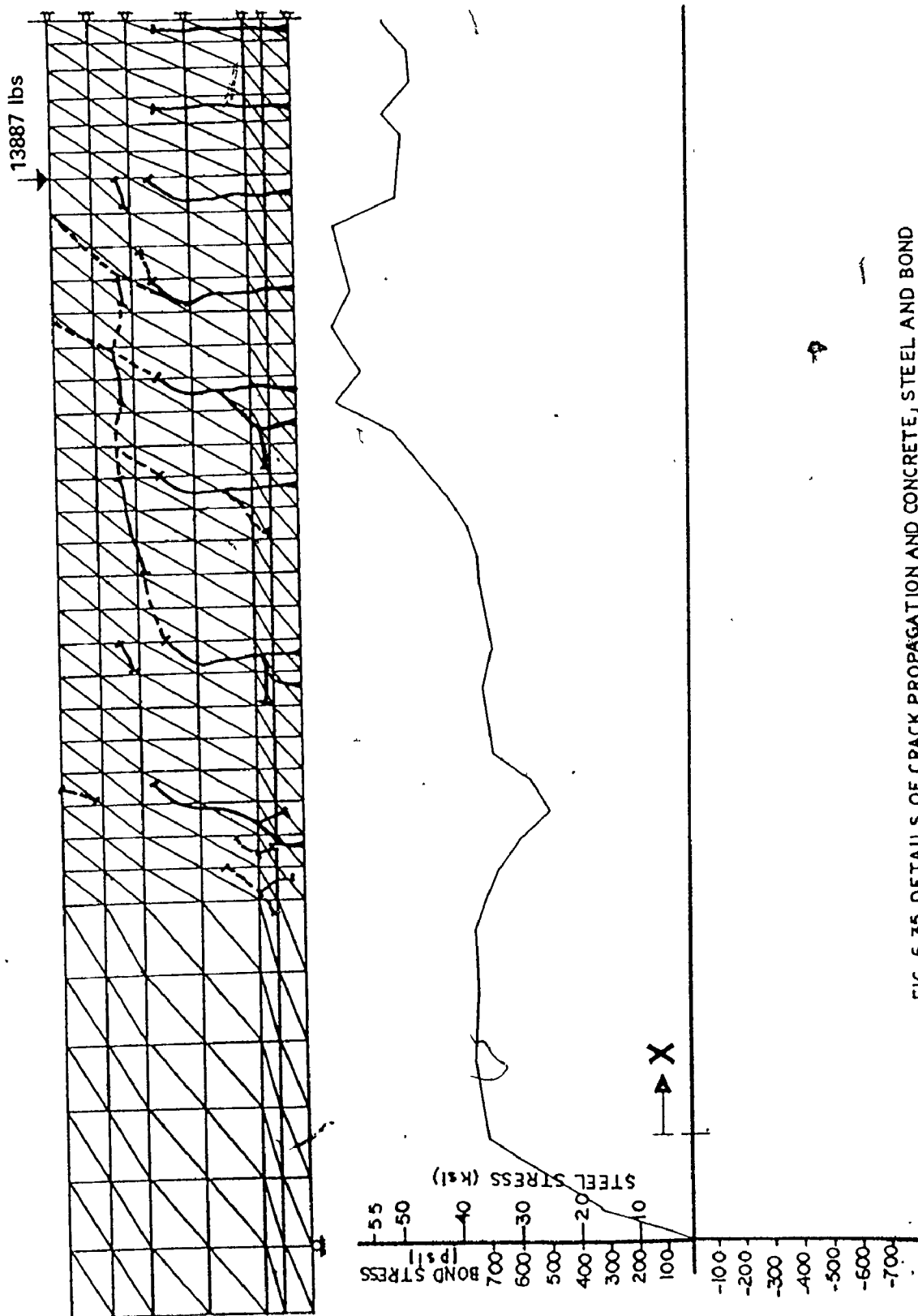


FIG. 6.35. DETAILS OF CRACK PROPAGATION AND CONCRETE, STEEL AND BOND STRESS DISTRIBUTIONS FOR BEAM (7/1)

The steel and the concrete stresses were still well below their failure limits at the iteration prior to the crack formation. Once the diagonal crack began to join with the existing flat cracks, no further stable load level was found and the crack propagated to failure in a manner similar to the sudden failure which is observed in tests. Dowel cracks formed after the diagonal crack formed, but these are not reliable because of the reported instability.

6.6 Conclusion

In this chapter five beams tested by Leonhardt and Walther (28) were described and their results were compared with the analytical results found using the proposed method of analysis. These five beams had different a/d ratios and different bond-slip characteristics.

Load-deflection results and cracking patterns were presented and discussed for all the beams. Concrete and steel stresses, and bond stresses were presented for one beam. The good agreement between the analytical and the experimental results was considered to provide evidence of the validity and the reliability of the analytical method proposed in this investigation.

The results presented and discussed in this chapter provided a rational explanation of the behaviour of some of the most interesting types of failures of simply supported reinforced concrete beams. The crack patterns reported here are believed to reproduce observed phenomena in a fashion which has not been reported previously in the literature.

CHAPTER 7
APPLICATION OF THE FINITE ELEMENT METHOD TO
REINFORCED CONCRETE JOINTS

7.1 Introduction

In the previous chapter, the analysis of simply supported reinforced concrete beams were presented and discussed. In this chapter the more complex subject of reinforced concrete joints is investigated. The behaviours of joints with different steel reinforcing details are studied. The McMaster University joint test results are compared with the analytical results obtained from the computerized method of analysis.

Of the six joints tested (see Fig. 4.1), Details (4) and (5) were almost identical, and Detail (6) had the same arrangement but with a higher percentage of steel. Analyses were done for the exact arrangements used in the tests of Details (1), (2), (3), (5) and (6). Also Detail (2) was studied using two different amounts of diagonal stirrup reinforcing steel and additional analyses and discussions were done for Detail (3) using three different end anchorage conditions.

Details of the McMaster University joint testing program were discussed in Chapter 4. In this section a brief summary of the test results is given.

Details (1), (3), (4), (5) and (6) had overall capacities of nearly equal to or exceeding the theoretical section capacities of the intersecting members, whereas Detail (2) had a much lower capacity. Details (4), (5) and (6) which had essentially the same steel arrangements were judged to be superior to the others. These had higher capacities and were easier to fabricate.

Experimental load-deflection and moment-rotation results along with cracking patterns for the tested joints were shown in Figs. 4.2 to 4.11 in Chapter 4. In this chapter, analytical and experimental load-deflection results are presented only for joints (2) and (3) which illustrate representative behaviours.

The load-deformation characteristics used in the analytical method for the joint analyses were previously discussed in Chapters 3, 5 and 6. These characteristics and the equations representing them are the same as those used for the beam analyses discussed in Chapter 6 with the exception being the stress-strain relationship for the steel reinforcing bars. The idealized stress-strain curve for steel reinforcing bars in tension and compression shown in Fig. 3.3 was employed

in the analysis. This curve has a very short flat yield plateau followed by a sloping part representing the actual strain hardening for the steel.

7.2 Failure Modes for Joints

Failure modes for reinforced concrete joints are probably not as well known as they are for beams. However, most of the failure modes discussed for beams in the previous chapter are also applicable to joints.

Flexural failure with its two distinctive modes of excessive yielding of steel in tension and/or crushing of concrete in compression are possible causes of joint failure whether it occurs in the joint or in an intersecting member. Crushing of the concrete in the joint region may not necessarily be considered as flexural failure, in some instances, since this feature can be triggered by some other cause such as excessive cracking of the joint region or diagonal cracks which can reduce the compression zone in one or each of the two intersecting members. Another possible mode of failure of the joint may be diagonal tension failure which is caused by the extension of a type (c) crack as was shown in Figure 4.16. and which was discussed in Chapter 4. Bond failure and/or end anchorage breakdown are common causes of failure in joints. Similarly the yielding of diagonal bars or stirrups may cause the joint to fail immediately.

Distinct failure modes were difficult to identify from the test results. Although characteristic diagonal tension cracks were formed in some of the specimens, this did not mean that the failure mode was necessarily diagonal tension. Some failures, such as a premature yielding of the diagonal stirrups, may cause cracks quite similar to diagonal tension cracks to occur. If one is not aware that the diagonal stirrups have yielded prior to the propagation of the crack, the failure could mistakenly be classified as diagonal tension failure. However, this confusion is avoided with the use of the proposed methods of analysis.

Compressive crushing of the concrete, yielding of the main or the secondary reinforcement and diagonal tension failures are readily detected using the analysis by studying the detailed information on element behaviour at the stages of loading near failure. Bond and/or end anchorage breakdown failures are also fairly easily identified by examining the status of the joint elements which simulate bond-slip and dowel action phenomena.

Of all the possible joint failure modes, flexural failure can be considered as the only desirable type of failure. In fact the ultimate goal of a joint designer should be to ensure that the capacity is controlled by flexure rather than any other type of capacity reducing failure.

7.3 Presentation of Analytical Results and Comparison With Test Results:

7.3.1 , General

In this section, the results obtained from the computerized method of analysis described in Chapter 5 are presented and compared where possible with the results of the tests described in Chapter 4 which were conducted by the author at the McMaster University research facilities.

Predicted crack patterns, load-deflection curves, moment-rotation curves and ultimate capacities of the analysed joints are compared with test results. Concrete stress distributions, bond stresses and steel stresses in some sections for a representative joint are also presented for different stages of the loading procedure. Failure modes and failure causes for each joint detail are discussed.

7.3.2 Load-Deflection Results

Load-deflection comparisons are only valid for experimental and analytical results obtained for the same conditions. Details (2) and (3) were analysed using the complete member lengths and the loading closely simulated the testing conditions. This necessitated using a very large number of elements and a relatively coarse mesh. Details (1), (5) and (6) were analysed using different conditions. Nearly one half of the length

of each of the two intersecting members were included in the analyses. This approach was adopted to permit a finer element mesh size with the same number of finite elements as used in the analyses of Details (2) and (3). The finer mesh gives more accurate results and is more reliable for understanding the detailed behaviour of the joint region. However, the use of a finer mesh was not possible for the full member lengths due to computer core storage limitations.

Equivalent bending moments and shearing forces were applied at the ends of reduced member lengths and thus were away from the critical joint region. Hence, this application of equivalent actions in place of the actual applied forces would not have any appreciable effects on the area of interest.

Due to using this analytical procedure for joints (1), (5) and (6), no predicted deflections are available for the extremities of the members. However, moment-rotation relationships which were not affected by this reduction in the intersecting members' lengths are presented for all the joints.

Figures 7.1, 7.2 and 7.3 show the finite element mesh configurations used for Detail (2), Detail (3) and Details (1, 5 and 6) respectively. These figures are presented separately without superimposing the cracking pattern results to avoid crowding at the reduced size shown in this thesis.

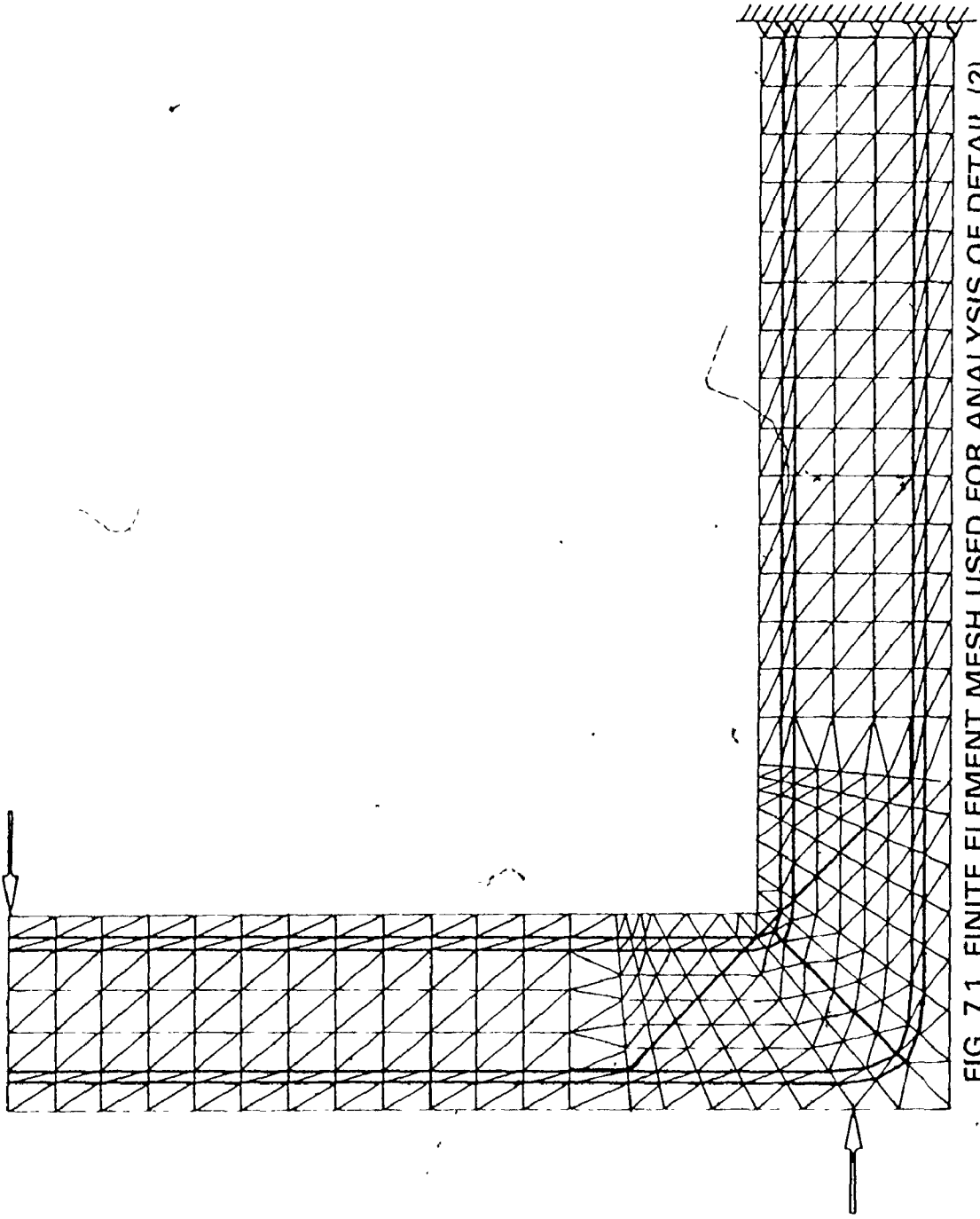


FIG. 7.1. FINITE ELEMENT MESH USED FOR ANALYSIS OF DETAIL (2)

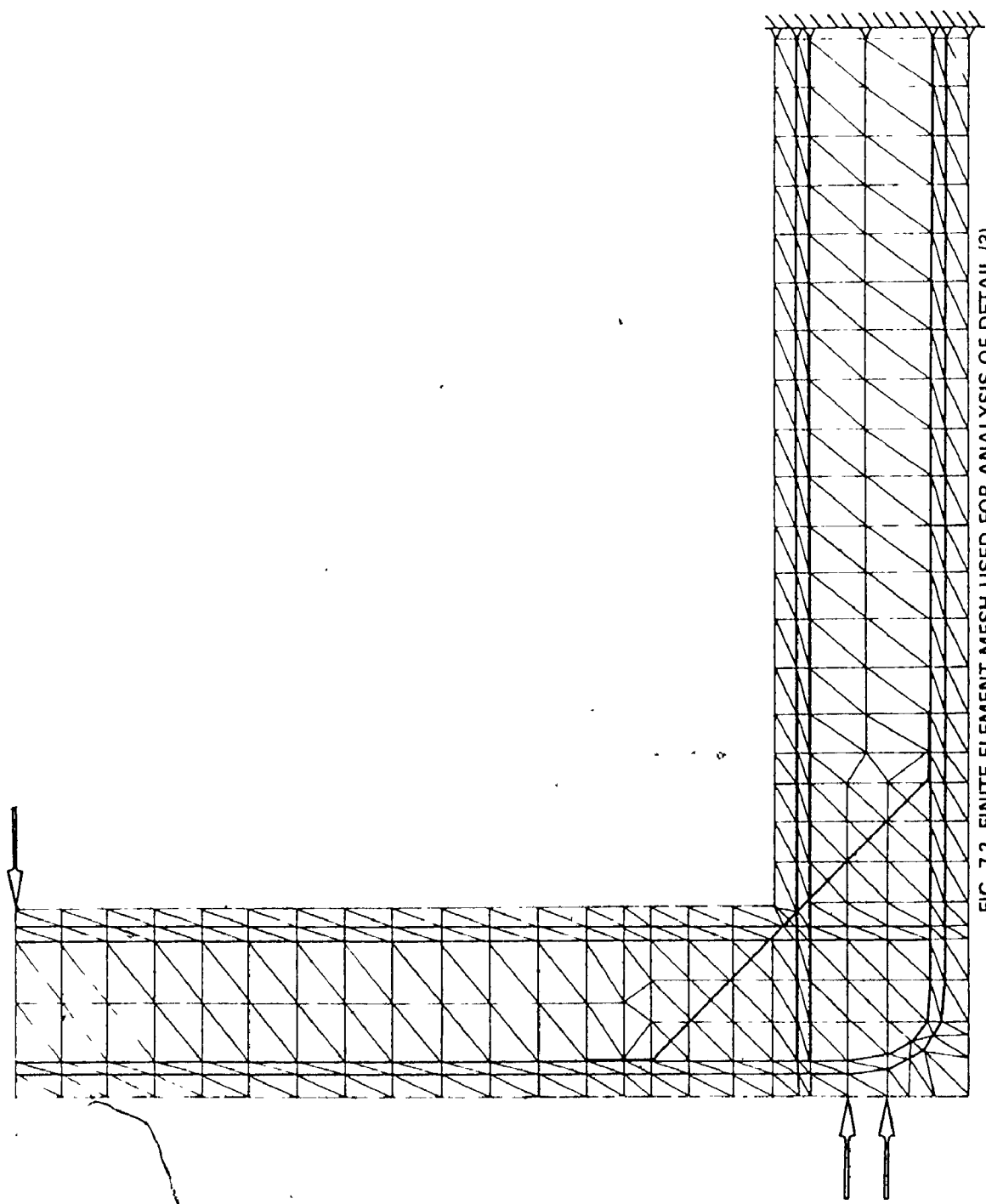


FIG. 7.2. FINITE ELEMENT MESH USED FOR ANALYSIS OF DETAIL (3)

10

[Handwritten scribble]

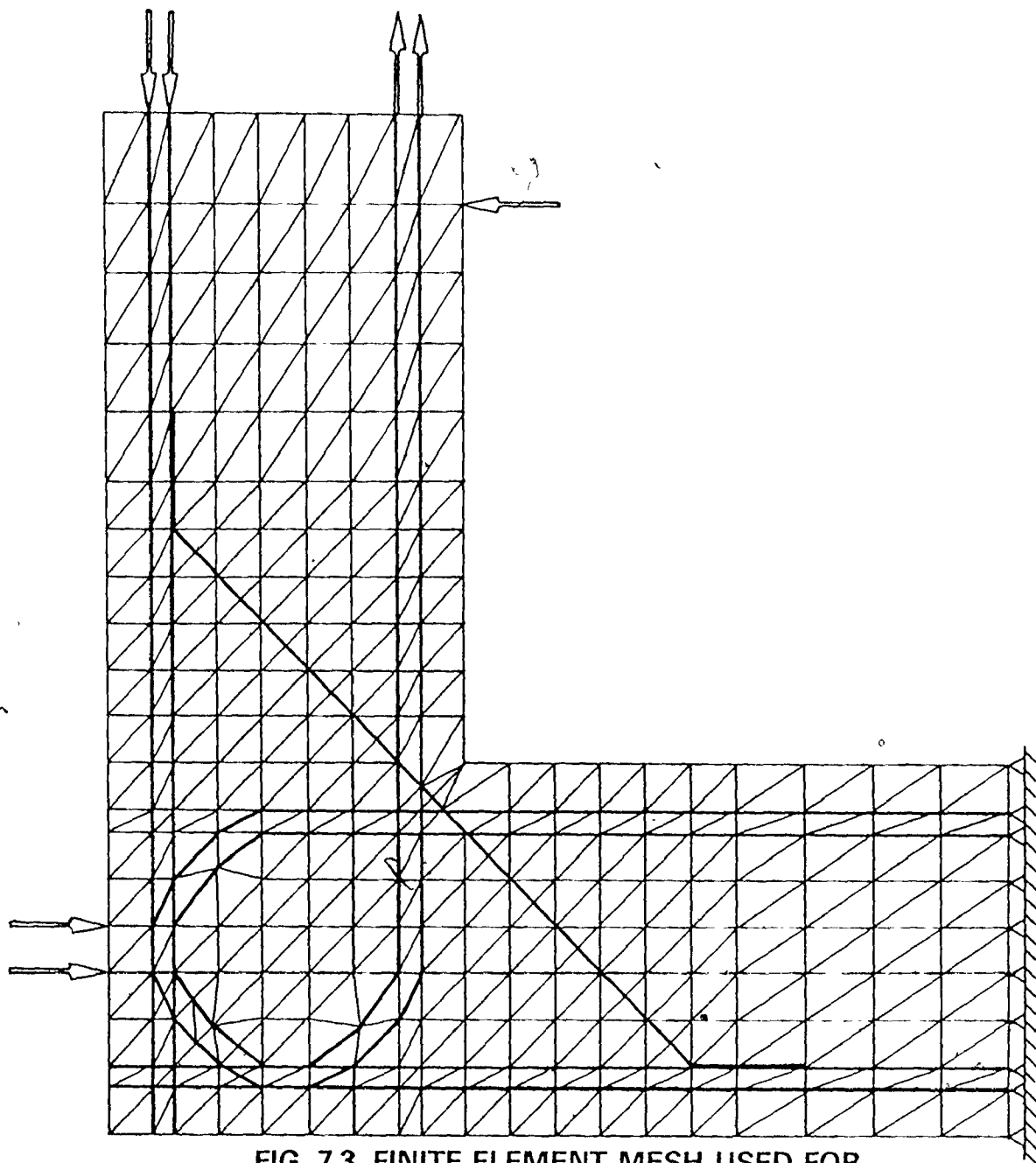


FIG. 7.3. FINITE ELEMENT MESH USED FOR ANALYSIS DETAILS, (1), (5) & (6)

Figure 7.4 shows the load-deflection results obtained experimentally and analytically for Detail (2). It can be easily seen that a very close agreement in the shape (path) of the curves was obtained. However, due to the lower bound nature of the solution and the slight delay of cracking predicted by the analysis for this Detail, the deflection values would be expected to be underestimated for the same load level. In this case computed deflection values ranged between 5% and 30% less. The same detail was analysed twice as can be seen from Fig. 7.4. The analysis of the beam with the same amount of diagonal stirrups used in the experiment showed general agreement with the results obtained experimentally. The failure of the joint was initiated by yielding of the diagonal stirrups at a load 7.5% higher than that obtained experimentally. When the amount of diagonal stirrup steel was increased from 2 No. 3 bars, 2 branch stirrups, (having a ratio of stirrup area to main steel area of $A_{st}/A_s = .5$) to 2 No. 5 bar, 2 branch stirrups (with $A_{st}/A_s = 1.40$), the capacity increased from 69% to 87% of the theoretical capacity of the intersecting members. The failure mode changed to a diagonal tension failure which was detected by the analysis. Further discussions concerning failure modes and cracking patterns are presented in following sections.

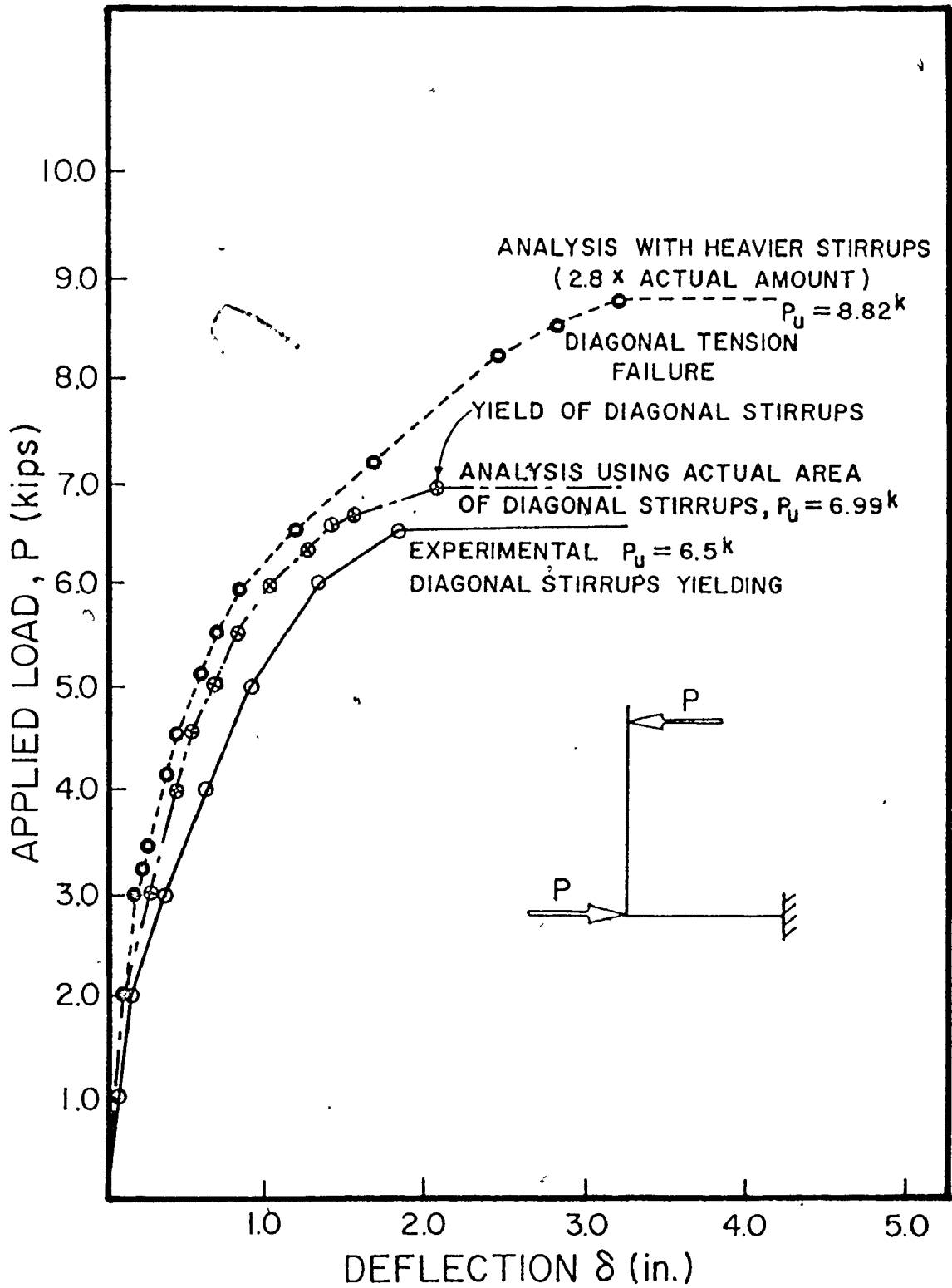


Fig. 7.4 LOAD-DEFLECTION RESULTS FOR DETAIL (2) FROM TEST AND ANALYSIS.

Figure 7.5 contains the load-deflection results for Detail (3). Four curves are shown in Fig. 7.5, where curve D represents the experimental results and A, B and C are the results of the analyses using three different end anchorage conditions for the diagonal bar. Curve A is for the analysis of Detail (3) with an imposed condition of poor end anchorage for the diagonal bar. This condition was created by not extending the diagonal bar parallel to the main reinforcement in the compression zones of each of the two intersecting members. Failure occurred in this case at 92% of the theoretical design capacity. End anchorage breakdown of the diagonal bar occurred at 79% of the theoretical capacity. Redistribution of the forces in the diagonal bar to the strongly welded main steel reinforcing arrangement enabled the joint to carry additional loads up to the failure load when diagonal cracks extended into the compression zone.

The end anchorage of the diagonal bar was then made far stronger by rigidly connecting its ends to the steel reinforcement which would be in compression. The rigid attachment resulted in overstressing the diagonal bar which was forced to carry more load than what it would have if some slip had been allowed. This resulted in yielding of the diagonal bar and consequently failure of the joint because there was no reserve capacity for the redistribution of forces. This was the only case

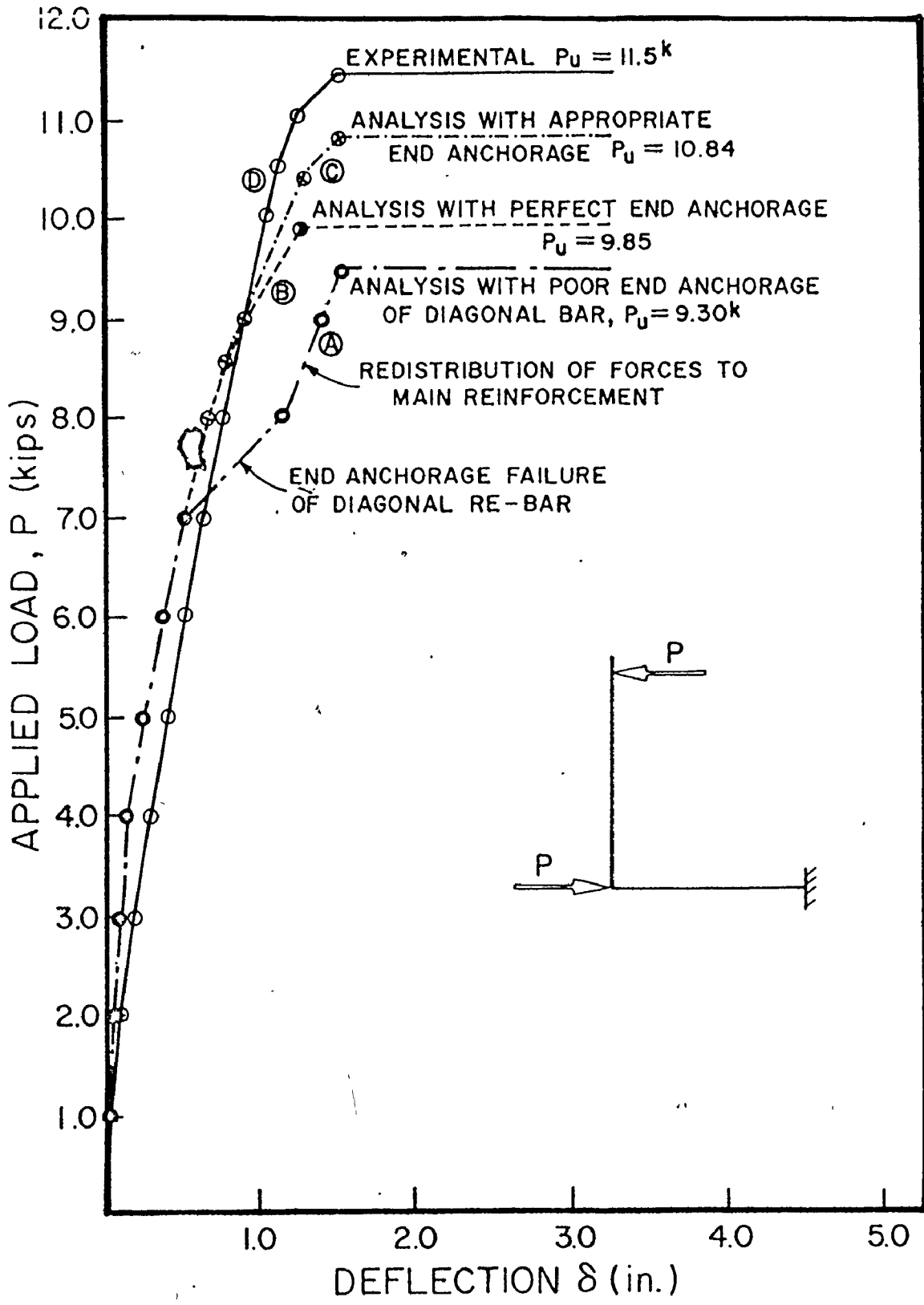


Fig. 7.5 LOAD-DEFLECTION RESULTS FOR DETAIL (3) FROM TEST AND ANALYSIS.

where overstressing of the diagonal bars was observed. In all other cases the diagonal bar stress at failure of the joint ranged from 40% to 65% of its yield strength. The analysis predicted that this arrangement would be able to withstand 97% of the theoretical ultimate capacity of the intersecting members. Curve B shows the load deflection characteristics for this case. The actual end anchorage condition of the diagonal bar was modelled in the analysis by extending the bar ends parallel to the main reinforcement in the compression zones of the intersecting members as shown in the sketch in Fig. 7.8. As illustrated in Fig. 7.5 by curve C, this resulted in an increase in the ultimate capacity. As can be seen from all the curves in Fig. 7.5 the analytical curves cross the experimental one. This may be explained by considering the original underestimation of deformations inherent in the method of analysis, and then the influence of a slight over estimation of the cracking effects which results from reducing the stiffnesses of the cracked element in the direction normal to the crack. The two inaccuracies may tend to balance at a stage of loading which depends among other things on the mesh size chosen for the analysis.

7.3.3 Moment-Rotation Results:

Moment-rotation values reported in this investigation were obtained indirectly from deflection values. The rate of change of the deflection over a short length was adopted as the criterion for the calculation of member rotations both experimentally and analytically. Although a high accuracy for rotations is not guaranteed, they are adequate to provide a reasonable and consistent basis for discussion of the general moment-rotation characteristics of the analysed joints. The results obtained from both the experiments and the analyses are based on the same lengths and deflection locations for calculation of the rotations.

Figures 7.6 to 7.10 illustrate the moment-rotation relationships obtained both experimentally and analytically for all of the analysed joints. It can be seen from these figures that the discrepancies between the rotation results vary considerably from one detail to another. Detail (1) involved the largest discrepancies, while Detail (6) had the least discrepancies. These variations reflect the complexities involved when the several factors which affect joint rotations are considered. A slight delay of a crack growth or the alteration of a crack path or location may affect the rotation values obtained at a particular

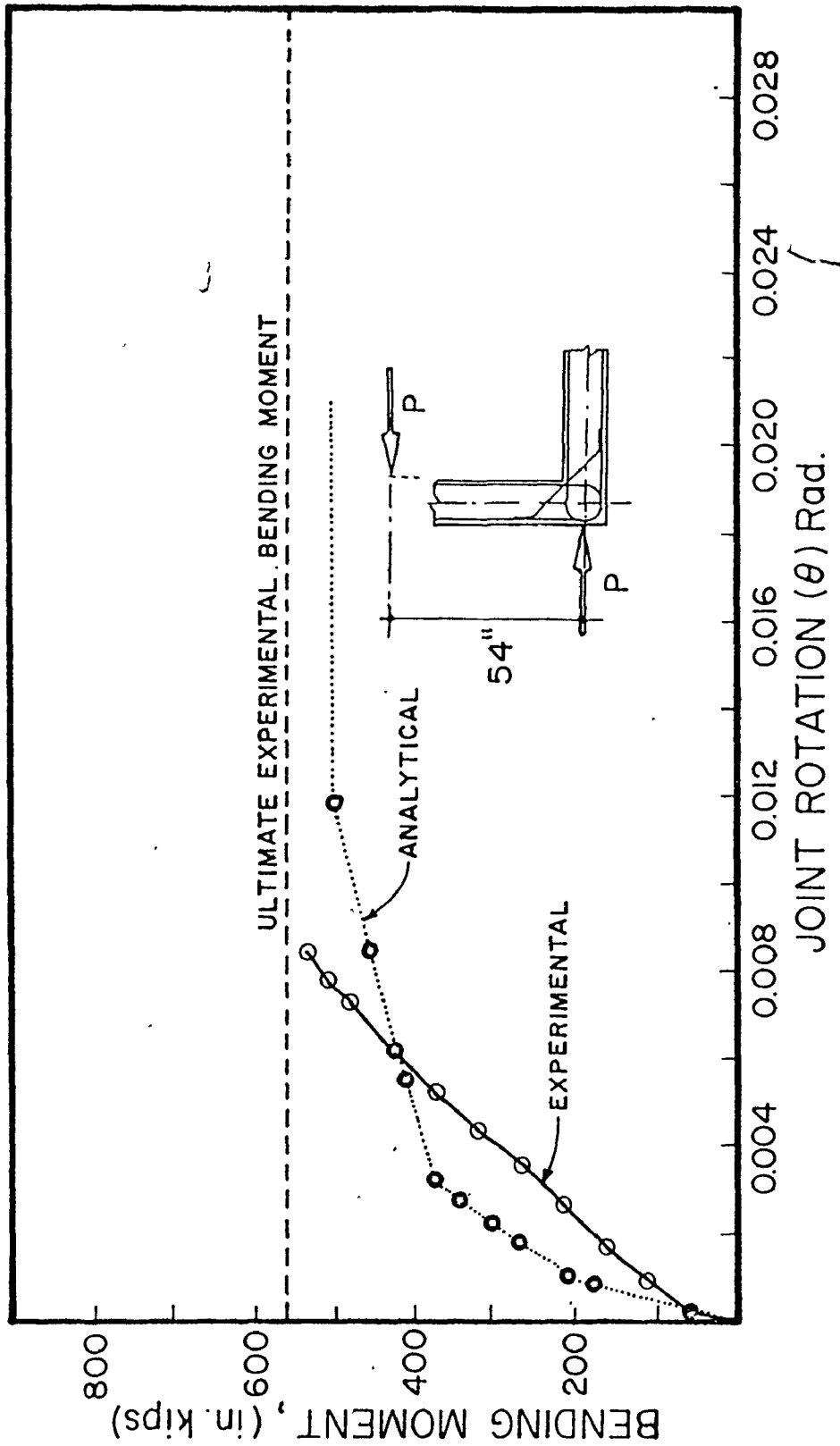


Fig. 7.6 EXPERIMENTAL AND ANALYTICAL MOMENT-ROTATION RESULTS FOR DETAIL (I)

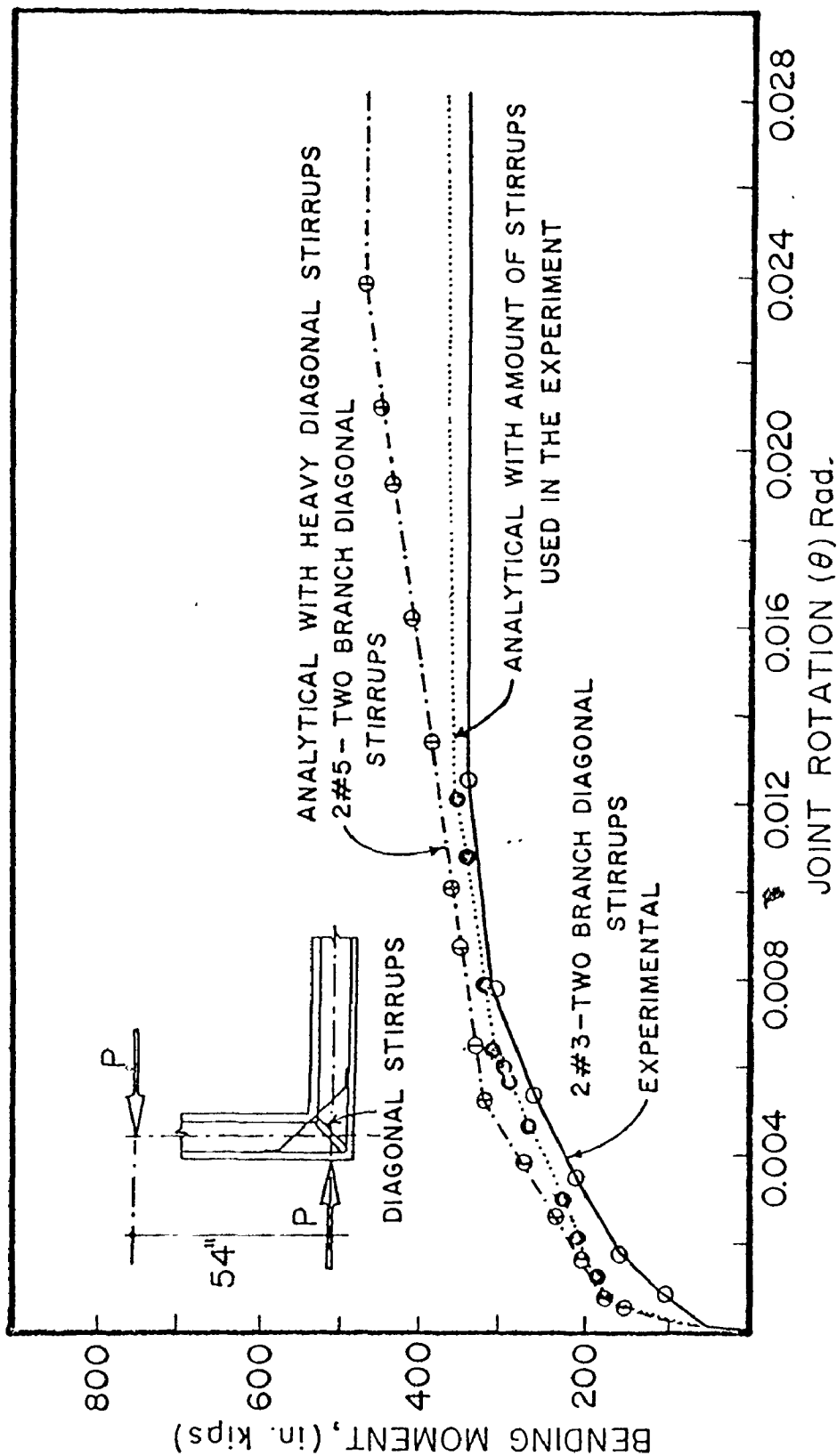


Fig. 7.7 EXPERIMENTAL AND ANALYTICAL MOMENT-ROTATION RESULTS FOR DETAIL (2).

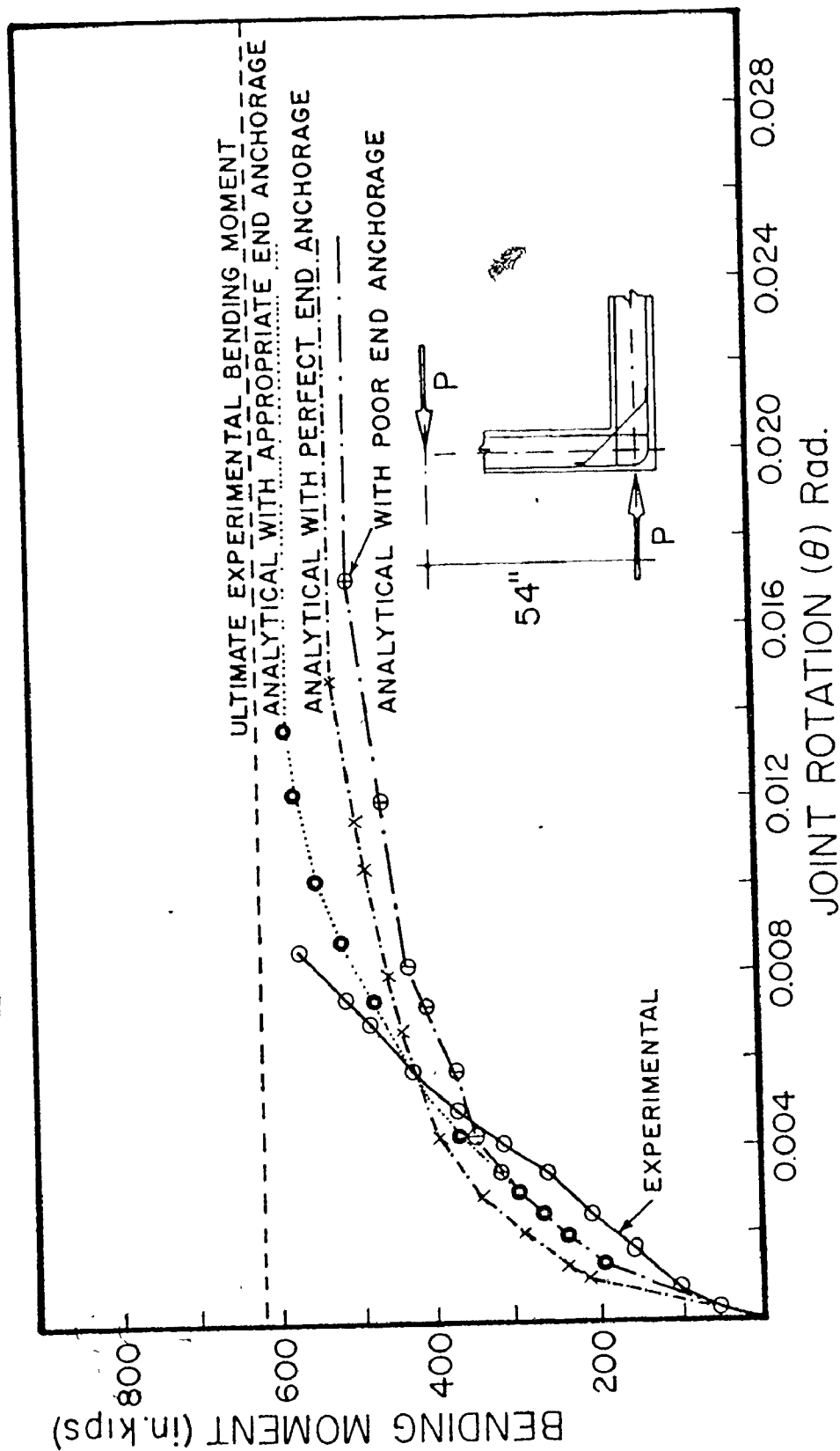


Fig. 7.8 EXPERIMENTAL AND ANALYTICAL MOMENT-ROTATION RESULTS FOR DETAIL (3)

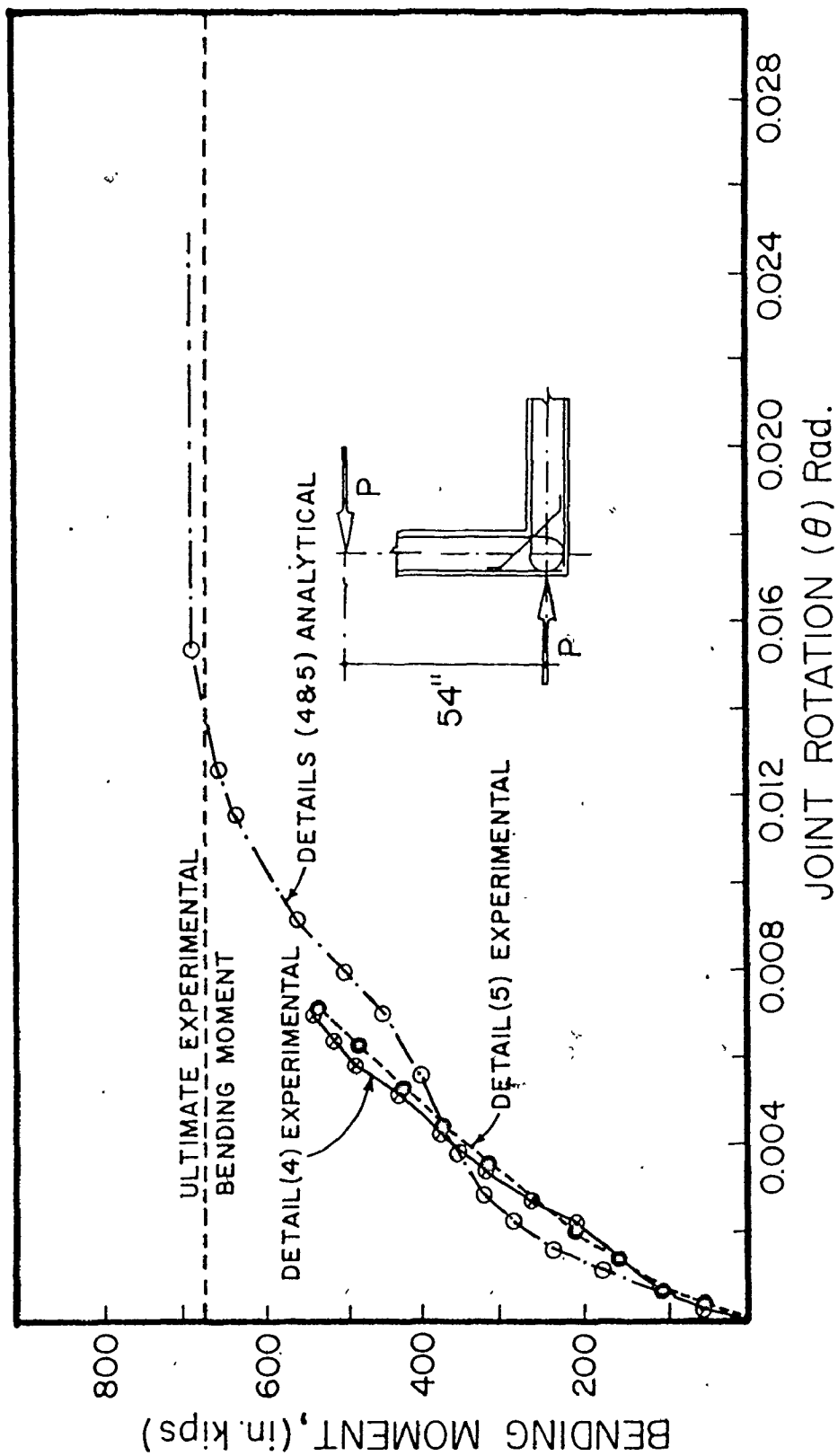


Fig. 7.9 EXPERIMENTAL AND ANALYTICAL RESULTS OF MOMENT-ROTATION FOR DETAILS (4) AND (5).

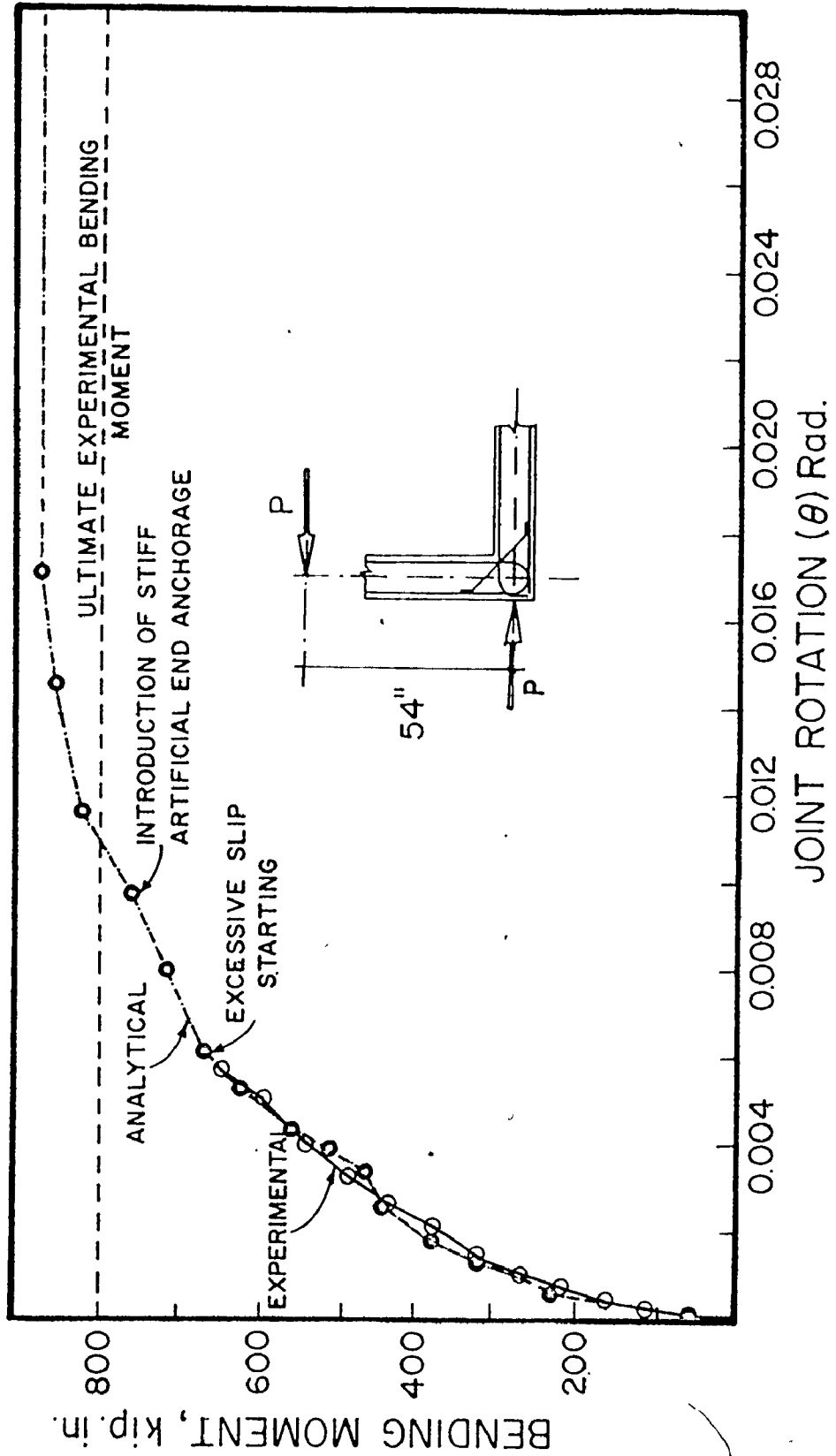


Fig. 7.10 EXPERIMENTAL AND ANALYTICAL MOMENT-ROTATION RESULTS FOR DETAIL (6).

load level. This, however, may not have any appreciable effects on the overall behaviour of the joint. Another possible reason for the observed differences in the moment-rotation curves could be due to inaccuracies involved in modelling the intricate interaction between steel and concrete at their interface. Overestimated or underestimated values of slip between steel and concrete can very easily alter the rotation values, especially in the more highly stressed joint region.

With the exception of the curves in Fig. 7.7, all the remaining analytical curves shown in Figures 7.6 to 7.10 underestimate the rotation values up to a point where the analytical curves cross the experimental ones with the result being generally overestimated deformations. It is suggested that the reasons for this behaviour are mainly the same as those discussed for the deflections. It is also suggested that this typical crossing did not occur for Detail (2), shown in Fig. 7.7 because this detail failed in a premature fashion due to yielding of the diagonal stirrups. This resulted in larger experimental joint deformations at lower loads than were observed for any other detail. The yielding of the diagonal stirrups was predicted by the analysis to start at a load 7.5% higher than that obtained experimentally. This overestimation in the capacity directly resulted in keeping the analytical curve above the experimental one.

7.3.4 Discussion of Behaviour of Each Detail

In this section cracking patterns predicted from the analyses are compared with crack patterns traced from the test specimens. The modes of failure for each analysed joint are also discussed.

Table 7.1 is presented to facilitate an overall comparison between the experimental and analytical results for all the joint details. The predicted first cracking and the failure loads are listed along with the corresponding experimental values. The ratio of the analytical to experimental first cracking load varied from 0.84 to 1.22 for Details (1) to (5) and it was 1.82 for Detail (6). However, the early formation of the corner crack at a load of 2.0 kips, as shown in Fig. 4.11, is likely due to local material weakness in the tested joint. The loads at which subsequent cracks formed were much closer to the predicted values. The ratio between the analytical and experimental ultimate load capacities showed better agreement than that obtained for initial crack formation. The ratios of predicted to experimental ultimate load varied from 0.88 to 1.08.

The scatter is considered to be acceptable and demonstrates the validity of the analysis. This acceptance is based primarily upon the consideration of two aspects. The first being that the variation between test results for similar joints has about the same range of scatter (97).

The second aspect is that the idealization of reinforced concrete as a homogeneous material can by itself account for a large portion of this scatter.

Table (7.1) Beam Cracking and Failure Loads

Joint Detail	First Cracking Load (kips)			Ultimate Failure Load (kips)			
	Exp.	Anal.	av. $\frac{\text{Anal.}}{\text{Exp.}}$	Exp.	Anal.	av. $\frac{\text{Anal.}}{\text{Exp.}}$	$\frac{\text{Anal.}}{\text{Theory}}$
1	4.0	3.35	.84	10.5	9.22	.88	.91
2	3.0	2.84	.95	6.5	6.99	1.08	.69
3	3.0	3.65	1.22	11.5	10.84	.94	1.07
4	3.0	3.34	.95	12.5	11.86	.98	1.17
5	4.0			11.6			
6	2.0	3.63	1.82	14.75	12.89*	1.07*	.97
					14.02	.95	
					16.22*	1.10*	

* Values are for analyses after main steel anchorage break down and the introduction of strong artificial anchorage.

Table 7.2 shows the analytical crack spacing results in the two intersecting members outside the joint region for all the analysed joints. Average, minimum and maximum crack spacings are given for each joint detail. The mean and standard deviation for the crack spacings are only for the joints indicated which had the same amounts of steel reinforcement.

Table (7.2)
Crack Spacings for Analysed Joint Details

Crack Spacing (inches)			
Joint Detail	Average	Maximum	Minimum
(1)	6.8	8.7	4.4
(2)	6.71	9.6	5.0
(2')	6.92	9.6	5.0
(3)	6.87	9.6	1.8
(3')	9.22	12.4	5.4
(4,5)	7.94	8.8	7.6
(6)	8.04	9.1	7.6
Mean* = 7.08		Standard deviation* = .58	

*For (1), (2), (3), (4&5) only

It can be seen from comparing Tables 4.1 and 7.2, representing the experimentally measured and the analytically predicted crack spacings respectively, that a reasonable agreement is achieved. The analysis tends to overestimate the spacing. However, the experimental and analytical means are close with the analytical being 13% higher than the experimental, which is acceptable, considering the normal range of variation in experimental work. The analytical standard deviation is lower than that obtained from the experimental results which as expected indicates

that the analytical results were more consistent than the experimental data.

Although Detail (1) had the greatest difference between the experimental and analytical capacities, the general trend of the results obtained from the analyses of the different joints remained unchanged from the experimental data. The detail which had the least capacity by testing remained the least when analysed, and the best performing detail also maintained its rank using the analysis. This trend can easily be seen from Table 7.1, in fact this agreement in the general trend along with the tendency of the analysis to generally underestimate the ultimate capacities of the joints, gives confidence and sound basis for comparison between different details.

In the next subsections the behaviour of each joint detail is discussed in more detail.

Table 7.3 lists the loads corresponding to the analytical loading step numbers for the analyses. These loading step numbers are shown on Figures 7.11 to 7.17 and indicate the points to which cracks had propagated at those particular loading steps. The joint detail numbers designated by a prime in Table 7.3 are for special joint conditions having the same general configurations as those for corresponding numbers without

Table (7.3) Loads Corresponding to Load Step Numbers (lbs.)

Load Step No.	Detail (1)	Detail (2)	Detail (3)	Detail (4,5)	Detail (6)	Detail (3')	Detail (3)	Detail (4,5)	Detail (6)	Detail (3)	Detail (2)	Detail (3)	Detail (3')
1	3351	2843	2973	3654	3339	3630	32	3283	6727	6491	11856	10361	63
2	3890	2960	3170	4265	3888	3698	33	5403	6827	6540	12014	11473	64
3	4006	3034	3185	4315	4269	3914	34	5403	6958	6627	12363*	12416	65
4	4263	3088	3221	4339	4332	4163	35	5403	7035	6945	12890	12478	66
5	4331	3091	3221	4304	4335	4191	36	5516	7472	7030	13223	13223	67
6	4362	3157	3224	4516	4495	4610	37	5516	7582	7377	14018	14018	68
7	4818	3190	3481	4597	4518	4711	38	5706	7729	7436	14169	14169	69
8	4919	3191	3481	4630	4887	4847	39	5771	8099	7754	14926	14926	70
9	4960	3192	3483	4707	4635	4907	40	5796	8213	7978	15359	15359	71
10	5231	3378	3533	4712	4709	4980	41	5796	8514	8005	16220	16220	72
11	5712	3405	3533	4810	5008	4990	42	5925	8669	8265			73
12	5761	3541	3765	4890	5569	5120	43	5925	8906	8668			74
13	5799	3612	3765	5065	4911	5674	44	6429	9235	8913			75
14	6101	3768	3765	5147	5068	6068	45	6429	9383	9159			76
15	6362	3921	3765	5343	6023	6232	46	6429	9498	9303			77
16	6498	4326	3765	5390	6055	6246	47	6536	9846				78
17	6513	4690	3869	5511	6149	6282	48	6536	10271				79
18	6829	4864	4174	5535	6198	6302	49	6536	10842				80
19	6961	4988	4174	5568	6250	6358	50	6536					81
20	7390	5019	4344	5723	6299	7070	51	6536					82
21	7873	5520	4344	5830	6719	7224	52	6536					83
22	8577	5640	4344	5887	7383	8000	53	6536					84
23	9224	5693	4770	5920	7548	8081	54	6536					85
24		5932	5138	6010	7637	8232	55	6536					86
25		6060	5138	6038	7793	8310	56	6536					87
26		6075	5138	6141	8471	8373	57	6536					88
27		6310	5138	6196	9293	8718	58	6536					89
28		6370	5138	6283	9432	9316	59	6536					90
29		6631	5138	6283	9817	9516	60	6536					91
30		6990	5283	6285	10533	10282	61	6606					92
31			5283	6461	11682	10282	62	6606					93
													94
													9303

10842

the primes. These special conditions are discussed in the appropriate subsections dealing with these particular details.

7.3.4.1 Detail (1)

Detail (1) was developed by Nilsson (97) and was tested by the author in the experimental part of this investigation. The experimental results were reported in Chapter 4. This detail, when tested, had an overall satisfactory performance and an ultimate capacity in excess of that required by design of the two intersecting members.

The predicted and experimental cracking patterns at failure for Detail (1) are shown in Fig. 7.11. The numbers shown beside the cracks are those corresponding to the load step numbers listed in Table 7.3.

A comparison between the flexural cracks outside the joint region obtained from testing and the analysis shows very good agreement with respect to the crack lengths and the load levels at the occurrence of such cracks. Crack spacings, however, were overestimated by the analysis as was discussed previously. Crack types (a), (b), (c) and (d) as defined in Fig. 4.16 were observed in both the test and the analysis. Crack type (b) was the first crack to occur in both cases. Cracks of type (c) were

observed experimentally to start at a load level of 5.0 kips while this load was predicted to be 6.5 kips. The propagation of types (c) and (d) cracks was the main cause of failure in the analytical model and the test specimen where failure occurred by reduction of the compressive zone of the horizontal member at a distance approximately equal to the depth of the member from the inner face of the joint's vertical member. Several additional cracks of type (c) predicted by the analysis were not observed experimentally. These analytically obtained cracks occurred because of a successive failure of some of the bond elements along the bend of the main reinforcement. These failures may not have occurred in the actual specimen. The bond-slip relationship could not account for the effect of the compression confinement on the inside of the bend. This aspect along with other observations discussed in the next sections leads the author to believe that the failure criterion chosen for bond linkages in this investigation was conservative. This aspect when added to the effect of neglecting the aggregate interlock phenomena may very well be the cause of the general underestimation of ultimate capacities of this detail and the details discussed in the following subsections.

The failure mode of this detail may be classified as shear-compression failure caused by the propagation of

crack types (c) and (d) into the compression zones of the intersecting members. The ultimate capacity of this detail can be considered satisfactory regardless of the fact that the analytical capacity was only 91% of the theoretical ultimate capacity, since the analysis generally underestimates these capacities and since the experimental result was higher than the theoretical requirement.

7.3.4.2 Detail (2)

Detail (2) was developed by Mayfield et.al.(91) and was tested by the author to confirm the results obtained. The experimental results for this detail which were discussed in Chapter 4, indicated very poor overall performance and unacceptable capacity (64% efficiency). In Chapter 4, the great loss in capacity was attributed to the possibility of yielding of the diagonal stirrups. The same cause of failure was obtained analytically. Crack spacings and load levels at crack propagation points obtained from the computer analysis were again in general agreement with the test results. As can be visualized from observation of Figure 7.12, the stirrups did not provide effective confinement for the joint core. This resulted in the early appearance of type (c) cracks which were observed to occur at a later loading stage in all of the other specimens tested.

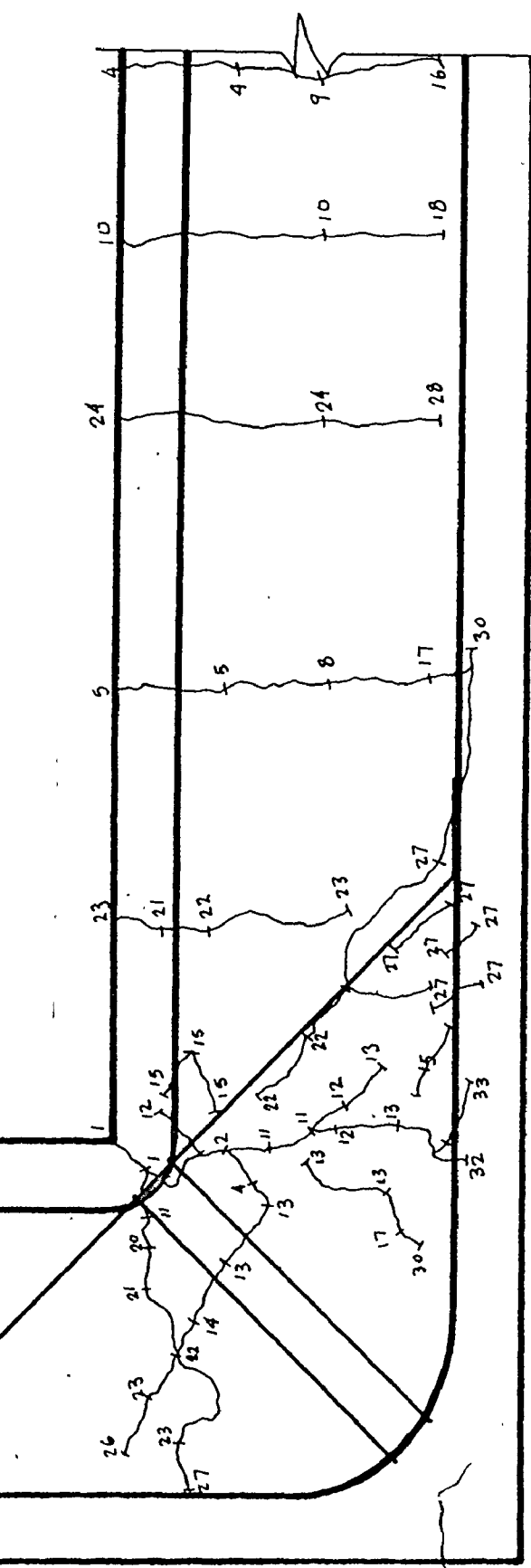
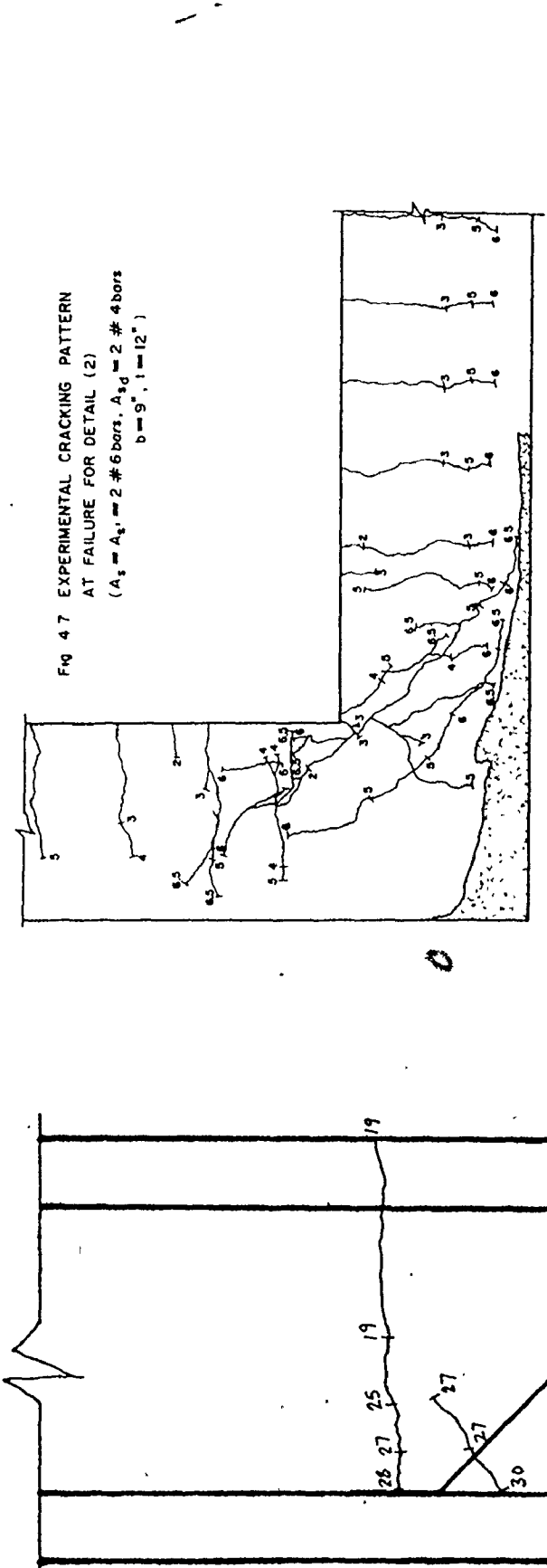


Fig. 7.12 PREDICTED CRACKING PATTERN FOR DETAIL (2), USING THE SAME AMOUNT OF DIAGONAL STIRRUPS AS THAT FOR THE TEST.

To investigate the effect of the amount of diagonal stirrup steel on the overall performance of the joint, another computer analysis was made. The area of diagonal stirrups was increased from 0.44 in² to 1.23 in² with ratios A_{st}/A_s of 0.5 and 1.4, respectively. As was discussed in Section 7.3.2, the analytical ultimate capacity of the joint increased from 69% to 87% of ultimate theoretical capacity.

Fig. 7.13 shows the predicted cracking pattern at failure of the joint specimen. It can be seen that all (a), (b), (c) and (d) types of cracks appeared in this case. Although the diagonal stirrups used in this analysis did not yield at the ultimate capacity of the joint, the joint failed to reach the desired 100% efficiency. This failure was caused by the continuous propagation of crack types (c) and (d) into the compression zones of both intersecting members. The failure modes can be classified as either diagonal tension or shear compression.

The final evidence of failure predicted by the analysis was compressive failure of the concrete elements in the compression zone of the horizontal member. However, this failure occurred only because of the propagation of the diagonal cracks into the compression zone. Diagonal tension failure, with its characteristic sudden extension of the diagonal cracks to the outermost

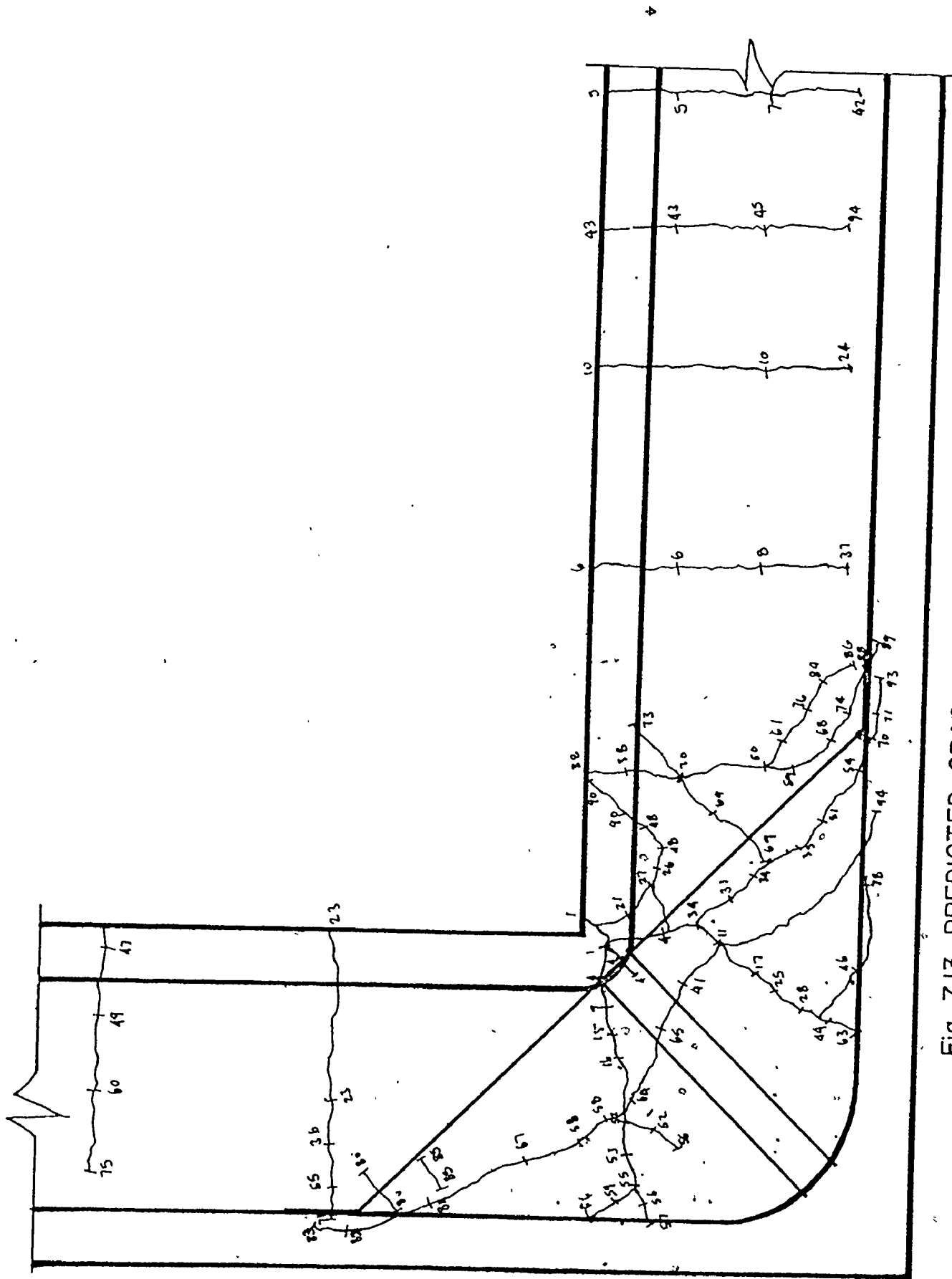


Fig. 7.13 PREDICTED CRACKING PATTERN FOR DETAIL (2), SAME AS
DETAIL (2) BUT USING HEAVIER DIAGONAL STIRRUPS.

compression face, was prevented due to the presence of web reinforcement in both the vertical and horizontal members.

The performance of this joint detail was not satisfactory. However, this conclusion is not in direct contradiction with Mayfield et.al.'s (74,91) results. Although they reported that this method of reinforcing joints is a promising one, the efficiency of the detail dramatically dropped from the range of 99% to 130% for a reinforcement percentage of 0.52% to an efficiency of 38% for a reinforcement percentage of 1.34%. Therefore, the test results of this study and the analytical confirmation of these results should not be surprising. Although the author's results seem to be in direct opposition to Mayfield et.al., it is in effect in opposition to their conclusion and not their test results.

7.3.4.3 Detail (3)

As was discussed in Chapter 4, Detail (3) was the first attempt by the author to overcome the fabrication difficulties encountered with Detail (1) and the apparent deficiencies found in Detail (2). This detail developed 114% of the theoretical ultimate capacity when tested. Figures 7.14 and 7.15 show the predicted cracking patterns for two of the three analysed cases which were described in Section 7.3.2 for Detail (3). These two cases are for the properly and for the inadequately anchored diagonal

bar respectively. The third case with the diagonal bar rigidly connected to the main steel reinforcement in the compression zone of the intersecting members was not shown because it was predicted to be essentially the same as that shown in Fig. 7.14 up to the load level corresponding to the yielding of the diagonal bar which caused the joint to fail as was discussed in Section 7.3.2.

The failure predicted by the analysis when the diagonal bar was properly anchored, by extending its ends into the compression zone of the intersecting members, was eventually caused by the diagonal cracks types (c) and (d) reducing the compression zones in the two intersecting members. Although this detail developed over 100% efficiency, the ultimate propagation of the diagonal cracks was primarily due to the lack of adequate web reinforcement (stirrups) near the outer face of the joint. It can be seen from Fig. 7.14 that the growth of the diagonal cracks was controlled in a desirable fashion. These cracks in the joint region did not develop until the applied loads reached nearly 93% of its theoretical ultimate capacity.

For the case when poor end anchorage was imposed on the diagonal bar (Detail (3')), serious cracking occurred. The excessive cracking which can be seen in Fig. 7.15 was caused by the progressive loss of bond along the diagonal bar. However, when the end anchorage

broke down at approximately 79% of the theoretical capacity, the forces carried by the diagonal bar were redistributed to the main reinforcement. After this stage, the cracking occurred at a much faster rate and joint finally failed by diagonal tension at 92% efficiency.

The above discussion illustrates the decisive role of the diagonal bar on the overall behaviour of the joint. It indicates that for the same joint detail not only does the presence of this bar effect the behaviour and the ultimate capacity of the joint, but also that proper anchorage of this bar is extremely important.

It is also evident that a rigid main reinforcement cage such as the welded arrangement used for this detail can be of great help to provide reserve capacity as was shown when the end anchorage of the diagonal bar broke down.

7.3.4.4 Details (4&5)

Details (4&5) had practically identical reinforcing arrangements. As was discussed in Chapter 4 and in Section 7.3.3 of this chapter, these two details exhibited the best overall behaviour of all the joint details studied. The experimental and analytical capacities were both in excess of the theoretical ultimate capacity.

In this subsection not only is the cracking pattern shown in Fig. 7.16 discussed, but also some stress distribution in the steel and concrete along with bond stresses at different locations and loading stages are presented.

Figure 7.16 illustrates the predicted cracking pattern for Details (4&5) at failure of the joint. The ultimate capacity of this detail was predicted to be limited by bond failure (end anchorage breakdown) of the main tensile reinforcement at the joint region. However, to get more information about the behaviour of the joint beyond the initial failure, an ability of introducing strong artificial end anchorage upon bond breakdown was built into the computer program. When this was incorporated in the analysis, the joint was able to develop the yield stresses in the main tension reinforcement.

The analytical results confirmed the results obtained from testing Details (4) and (5). The joint was able to develop the theoretical ultimate capacity without any loss due to diagonal cracking or shear failure. When the anchorage of the main reinforcement was arbitrarily increased, increased capacity was obtained to take advantage of some of the steel strain hardening.

Improved anchorage of the main tensile reinforcement may be provided mechanically by welding of end plates to the ends of all of the tension bars. If possible, the inclusion of concrete stubs beyond the joint to complement the anchorage development length can also be helpful (95).

The extension of the tension reinforcement far into the outer corner of the joint seems to be beneficial. This seems to provide the same confinement of the joint's core as that for Detail (1) developed by Nilsson (97) which helps in delaying the diagonal tension cracks. However, excessive bar slippage, especially for heavily reinforced joints, may cause the concrete cover in the joint region over the ends of the tension reinforcing bars to be pushed off (concrete spalling failure). This may be avoided with provision of the mechanical end anchorage or the concrete stubs mentioned above.

From comparison between Figure 7.16 and both Figures 4.9 and 4.10 for joint Details (4) and (5) respectively, it can be seen that the agreement between the tests and the analysis is closer than for any of the details discussed previously. Crack spacing and the extent of crack propagation at certain levels are in very good agreement.

Although comparisons between experimentally measured and analytically computed strains might not

be reliable for a single joint detail because of the limited number of tested specimens, the elastic strains measured before cracking should be fairly consistent for all specimens with different details but with equal percentage of reinforcement.

Figure 7.17 shows the average strains measured for specimen Details (1), (2), (3), (4) and (5) versus the analytical values. In this figure two sets of analytical strains were obtained for the joint region. Since the measured strains were obtained using an 8 inch gauge length, the average strains over 8 inches as well as the localized strains obtained analytically are plotted. It can be seen that the average strains obtained analytically slightly underestimate the experimental values. This is mainly due to the coarse finite element mesh used in the analysis. The localized strains are higher than average, and since there is no experimental counterpart, no direct comparison can be made.

Diagrams of strains found analytically at different sections in the constant moment region of the horizontal member are shown in Fig. 7.18 for different load levels. Figure 7.18 (a), (b) & (c) illustrates the strains at the location of a primary crack (section I-I), at an uncracked section (section II-II) and at the location of a secondary crack (section III-III) respectively.

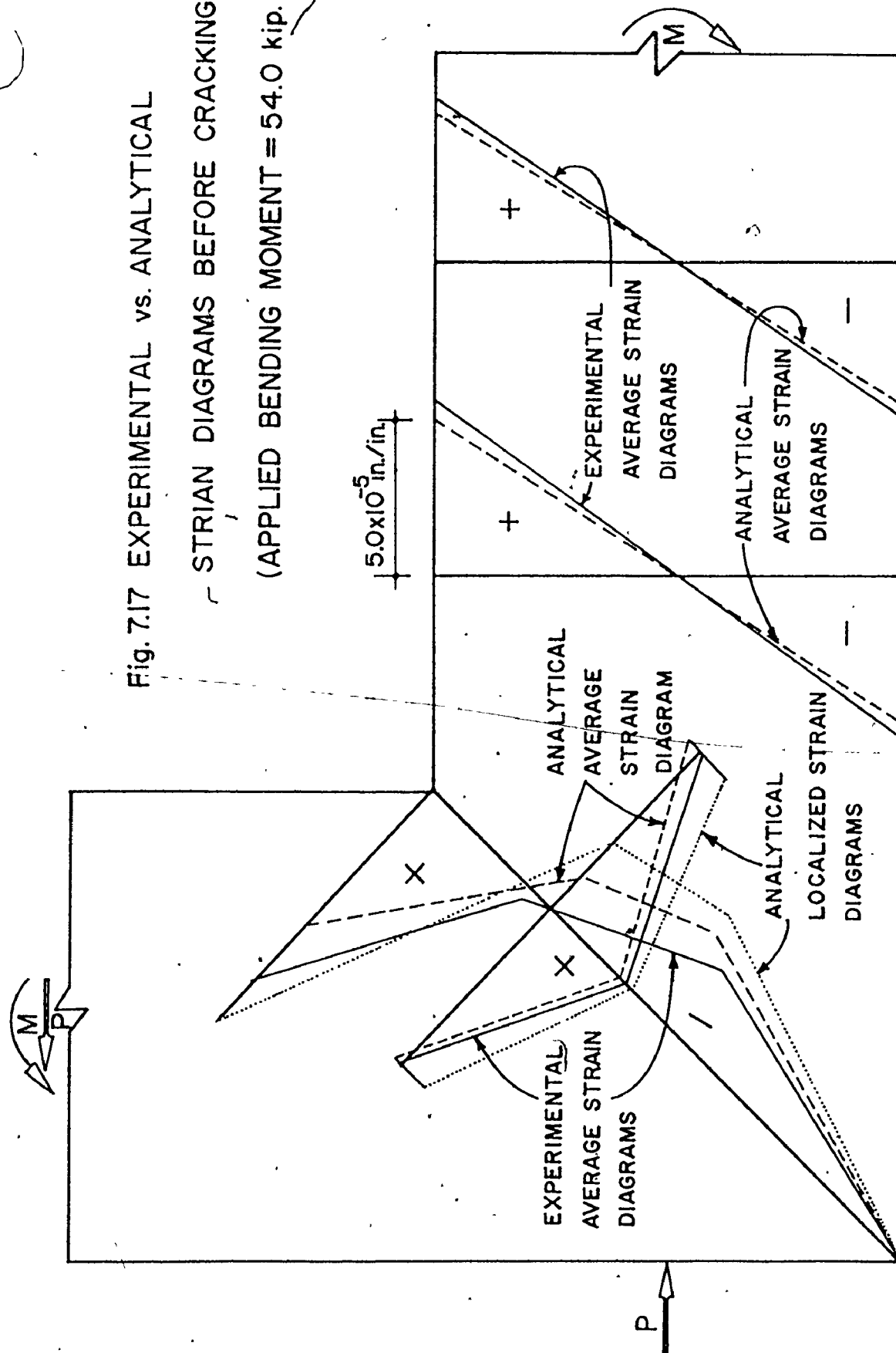


Fig. 7.17 EXPERIMENTAL vs. ANALYTICAL

STRAIN DIAGRAM BEFORE CRACKING.

(APPLIED BENDING MOMENT = 54.0 kip.in.)

It can be seen from the three diagrams that the strains were linear before cracking. After the occurrence of the first crack at section I-I, the tensile strains tapered off in the vicinity of the crack as can be seen for section II-II. The compressive strains, however, remained very close for sections I-I and II-II. These compressive strains were slightly lower for section III-III and the sections farther from the joint region. Tensile strains increased continuously but in a non-linear fashion in section III-III until a crack occurred.

Stability of crack height was achieved for section I-I at a load level of 8.47 kips, as illustrated in Fig. 7.18(a), when it reached the existing neutral axis. This was not the case for sections II-II or III-III. Section II-II remained uncracked until joint failure occurred. Section III-III was cracked but the crack height was stabilized at an earlier stage than for section I-I. The tensile strains decreased after the further propagation of the two surrounding primary cracks at sections I-I and IV-IV. This decrease in tensile strains (and the tensile stresses) is one of the reasons which causes the fairly realistic crack spacing obtainable using the analytical method presented in this investigation. The primary reasons which cause the concrete tensile strains to decrease in the immediate vicinity of existing cracks are the decreasing stiffnesses of the cracked concrete

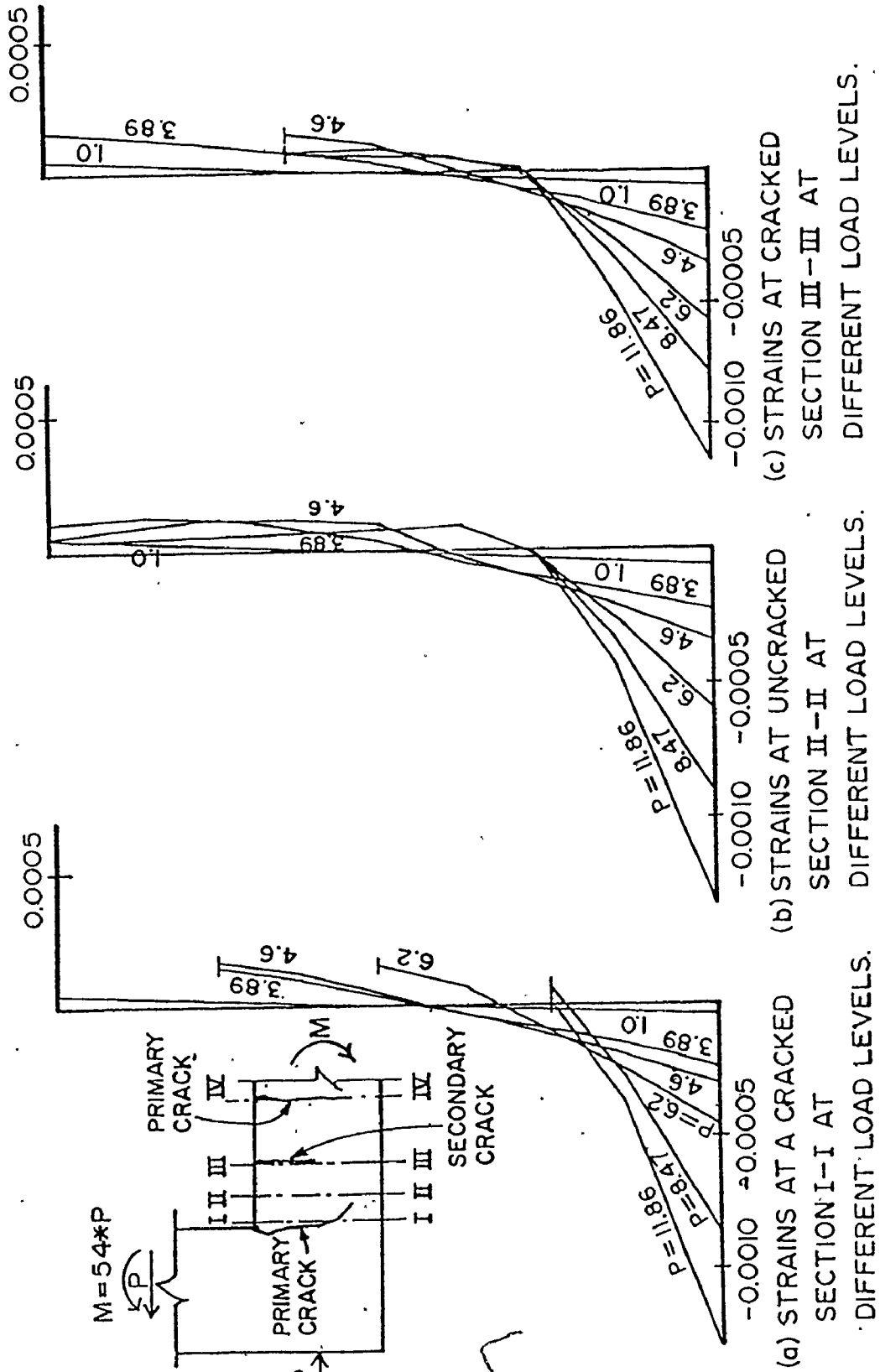


Fig. 7.18 STRAIN DIAGRAMS AT DIFFERENT SECTIONS IN THE CONSTANT MOMENT REGION OF DETAILS (4 & 5).

elements and the destruction of the bond elements adjacent to the faces of the crack. The distance between the cracks is determined by the ability of the bond linkages to accumulate large enough forces to cause the concrete to crack. At a particular stage, and for a certain crack spacing, the forces accumulated by the bond elements should not be able to produce a crack in the concrete and this is when crack spacing stability is achieved.

Figure 7.19 illustrates the analytical distribution of the strains which are normal and tangential to the diagonal line joining the inside and the outside corners of the joint. The strain distributions are plotted for different loading stages of the analysis. The load levels indicated on Figures 7.19(a) and 7.19(b) are the same as those shown in Figure 7.18. It can be visualized from the strain diagrams that tensile strains which cause cracks of types (b), (c) and (d) were present and were able to produce the three crack types at different stages of loading. However, the compressive strains in the normal direction, ϵ_x , which existed in the joint core were effective in delaying the occurrence of cracks of types (c) and (d) until a later stage of loading (at nearly 80% of the ultimate capacity).

Fig. 7.19 CONCRETE STRAIN DISTRIBUTION
IN THE NORMAL AND TANGENT
DIRECTIONS TO THE CORNER
DIAGONALS OBTAINED FROM
THE ANALYSIS OF
DETAILS (4 & 5)

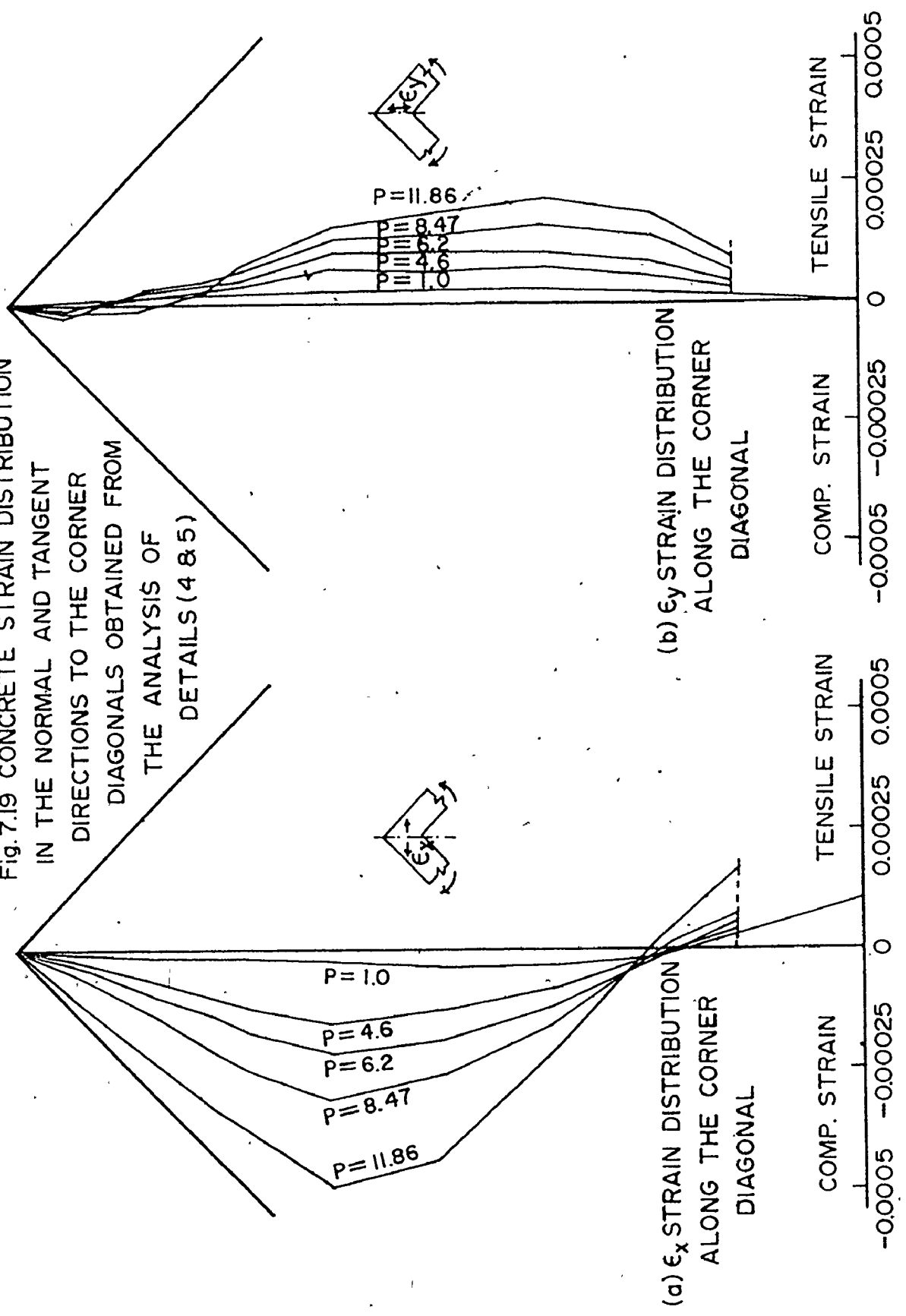


Figure 7.20 demonstrates the history of stress distribution along the main tensile reinforcement. The effects of cracking on stress concentrations in the steel reinforcement, discussed in Chapter 6 for beams, can be seen by observing the correspondence between crack locations and peak steel stresses shown in this figure. While the yielding stresses were obtained for this detail when the artificial end anchorage was introduced after end anchorage breakdown, this was not observed for any of the other details and the other joints failed with steel stresses less than their yield stresses.

To illustrate the adequacy of the amount of steel used for the diagonal bar, steel stresses at three different points as shown in Fig. 7.21 were plotted for different loading stages up to failure of the joint. It can be concluded that the amount of steel used was adequate (50% of the main steel), since the maximum stress in the bar reached at failure of the joint was less than 50% of the yield stress. The compressive stresses in the steel at points (1) and (3) all the way to failure, indicate adequate anchorage.

Bond stresses in some selected bond elements along the main steel reinforcing bars were plotted in Figure 7.22 for different loading stages up to failure.

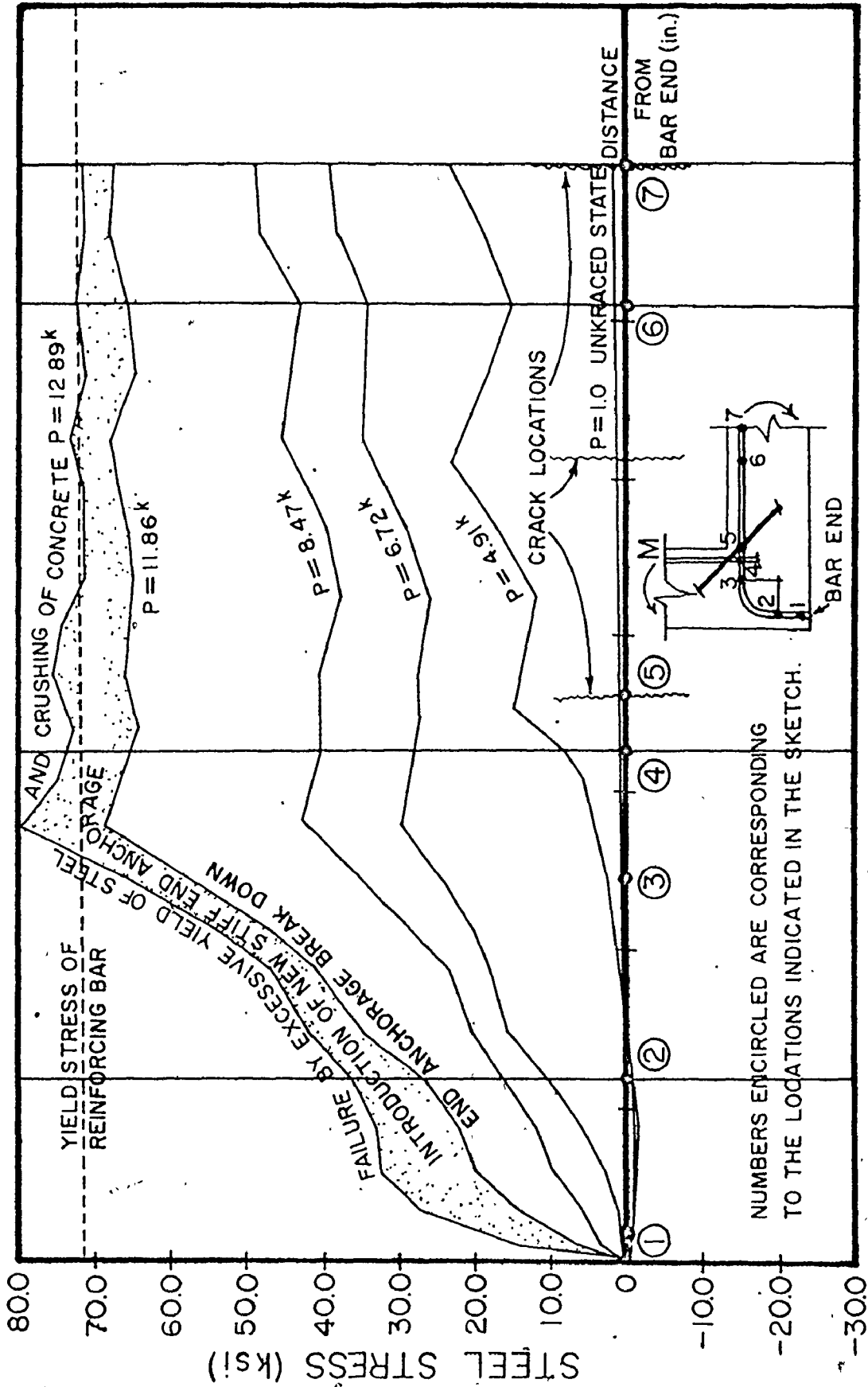


Fig. 7.20 LOCALIZED STEEL STRESSES AT DIFFERENT LOAD LEVELS FROM THE ANALYSIS OF DETAILS (4 & 5).

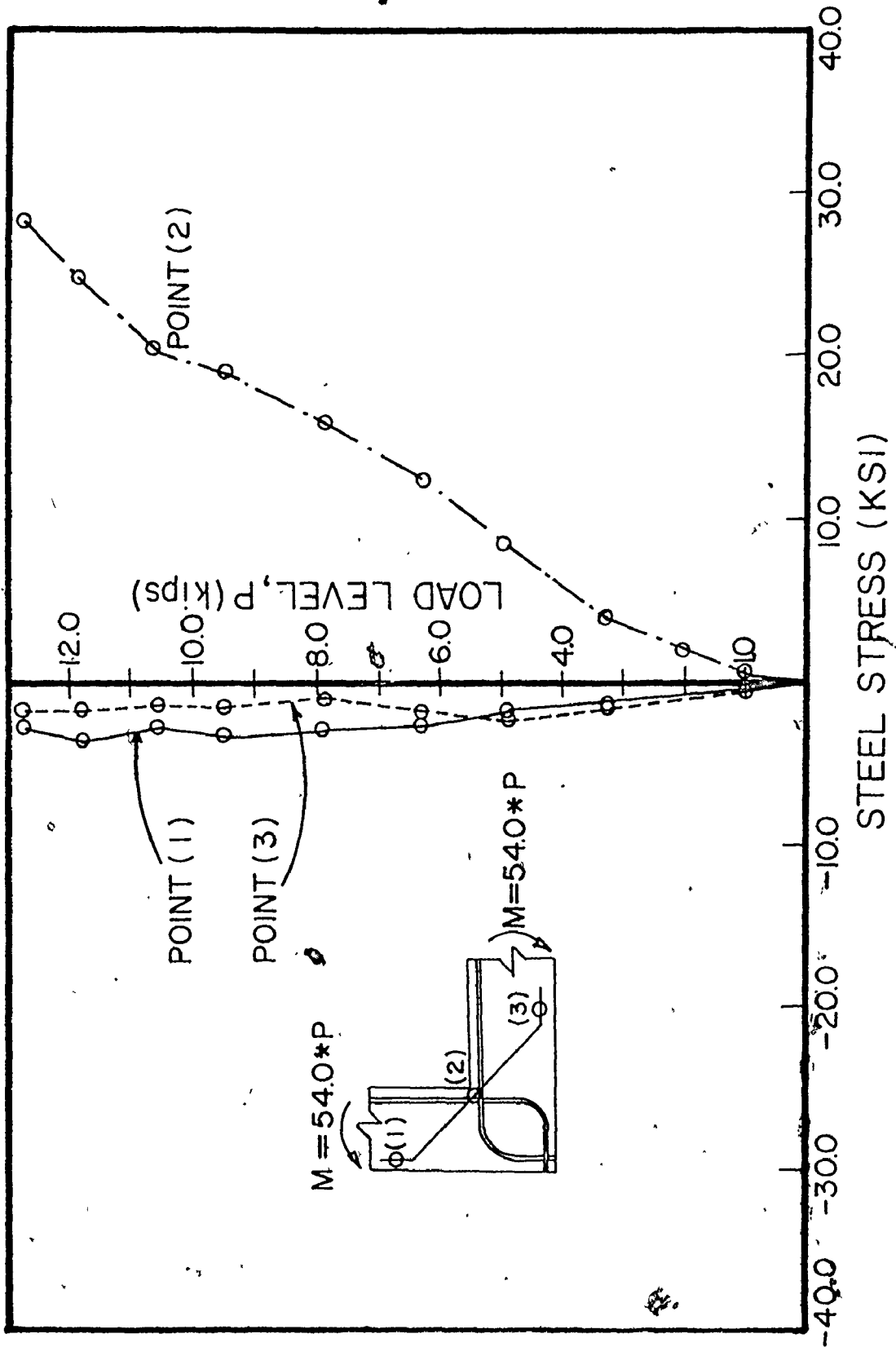


Fig. 7.21 STRESSES IN DIAGONAL BAR AT DIFFERENT LOAD LEVELS FROM THE ANALYSIS OF DETAILS (4 & 5)

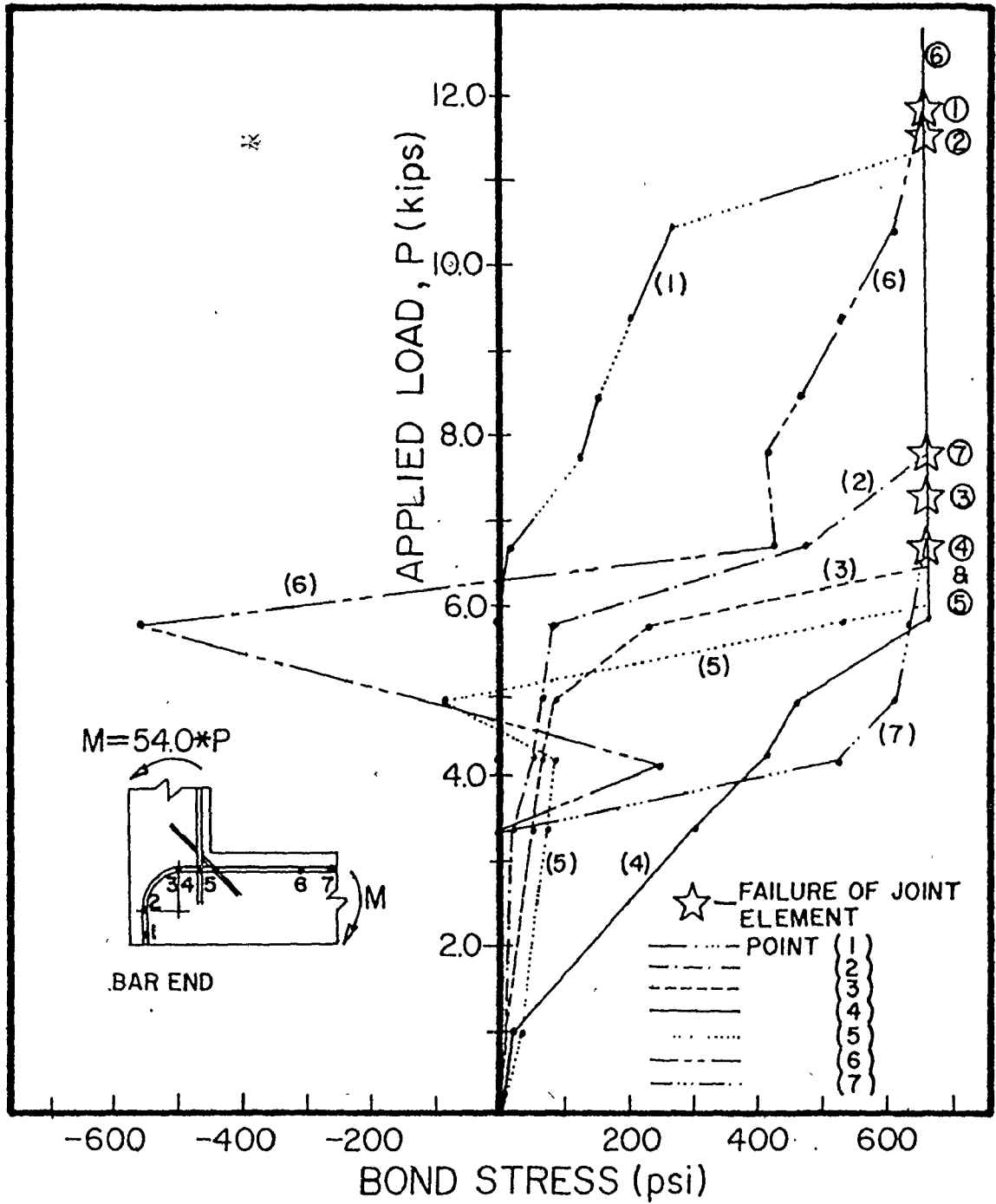


Fig. 7.22 BOND STRESSES AT DIFFERENT LOADING STAGES ALONG THE MAIN REINFORCEMENT FOR DETAILS(485)

The progressive bond failures which finally led to end anchorage breakdown can be observed considering the load levels at which the different bond elements have failed. Bond elements at locations 4 and 5 were the first to fail almost simultaneously. The element at position 3 followed shortly thereafter, and the element at position 7 was the next to fail but it did not contribute to the end anchorage problem because it was located in the constant moment region of the specimen. The bond element at position 2 followed these failures at a higher load level. When finally the bond element located at point 1 near the bar end failed at a load level of 11.86 kips, the bar would have slipped with no further bond resistance. This, however, was avoided in the analysis by artificially introducing stiff end anchorages which helped the joint to reach its maximum capacity which was controlled by the yielding of the steel.

7.3.4.5 Detail (6)

Detail (6) was the last of the details tested and analysed in this investigation. As was shown in Table 7.1, this detail failed by end anchorage breakdown at 95% of the theoretical ultimate capacity. The introduction of the artificial end anchorages as was discussed for Details (4 & 5), enabled the joint to develop the yielding stresses in the steel reinforcement.

From the analysis, the general behaviour of this detail was essentially the same as that for Details (4&5) with the exception of the cracking pattern. As shown in Fig. 7.23, more cracks were predicted for this detail than for Details (4&5). This should not be surprising, because of the larger steel and bond forces present which resulted from the higher percentage of reinforcement. The agreement between the predicted cracking pattern shown in Fig. 7.23 and that obtained experimentally is very good.

7.4 Summary

In this chapter the analytical results for joints subjected to positive bending moment were presented and discussed. All of the joints which were tested in the experimental program were analysed using the proposed method of analysis. Additional special cases which investigated the influence of the amount of diagonal stirrups and the degree of anchorage of the diagonal bars were also discussed. Cracking patterns, load-deflection curves and moment-rotation curves were illustrated. For Details (4) and (5), stress and strain distributions in the steel and concrete elements in addition to bond stresses along the reinforcing bars were also presented.

Generally very good agreement between the experimental and analytical results was found. Further

explanations of the behaviour of the joint details, which were not fully understood from the tests, were possible by using the proposed method of analysis. In addition, it was shown that other aspects and influence of variables could be investigated without companion experimental work.

In the next chapter, the summary and conclusions of this study, together with recommendations for future research are presented.

CHAPTER 8

SUMMARY AND CONCLUSIONS

8.1 Introduction

The main purpose of the investigation reported in this dissertation was to provide additional information to aid in understanding reinforced concrete joint behaviour. The specific area of interest was the behaviour of corner joints subjected to positive bending moment tending to open the corner.

Very little analytical information was found in the literature relating to the behaviour of reinforced concrete, beam-column connections. Little attention was given to the theoretical modelling and explanation of the behaviour of such a vital region in any reinforced concrete structure. A relatively few experimental results for different shapes of joints are available in the literature, primarily as a result of two major research programs in Sweden (97) and Britain (74, 91). Special problems in detailing, designing and understanding corner joints have been reported in several publications (74, 91, 97, 103). It was therefore, felt that a contribution to the subject would be made by providing better explanation to help understand the behaviour of corner or knee joints.


A brief summary of the research program along with final conclusions and recommendations for future research are

given in the following sections. More detailed discussions for both the experimental and the analytical parts of this research program have already been presented in the pertinent chapters.

8.2 Summary of the Experimental Investigation

An aim of the experimental investigation was to develop joint details which would perform in a satisfactory fashion. In addition, the results, of the experimental program were to provide data to test the reliability of the mathematical model.

Six tests of joints were performed, where four different details were tested, two of which reproduced arrangements previously reported in the literature. Three of the four details, of which two were developed by the author, were considered satisfactory in terms of attaining joint capacities equal to or exceeding the theoretical capacities, of the intersecting members. One of these details was considered to be superior to all the others. Two more tests were done on this detail; one to confirm the original results and the other to examine the influence of an increased ration of steel reinforcement on the behaviour of the joint. Although the behaviour of these joints under load reversals was not a major aim of this research, the last two tests were subjected to 4 cycles of load reversals before being loaded to failure. The test results indicated satisfactory performance.



8.3 Summary of the Analytical Investigation

A computer program utilizing the finite element technique was developed to study the behaviour of reinforced concrete structures. In the course of developing the program numerous problems were encountered. One of the most challenging problems was the modelling of cracking, so that realistic crack patterns could be predicted. It was found to be necessary to let only one concrete element crack at a time. The element which was stressed the most was the only element which was allowed to crack at any particular cycle of crack stability iterations. Modification of the stiffness of the cracked element was then performed according to the direction of the crack and the new stiffness was entered in the global matrix. This technique allowed for the redistribution of stresses to take place before any other element was allowed to crack. This resulted, in most cases, in relieving some of the elements which were previously overstressed and hence prevented the occurrence of unnecessary cracks.

After crack stability was achieved for a certain load level, the next load increment was automatically determined within the program according to the level of stress in the next most highly stressed element which did not exceed the failure criteria. However, if this increment was larger than a predetermined size of increment, it was then set at the smaller value to avoid divergence due to the non-linear material properties used in this analysis.

The reliability and suitability of the program was verified by comparison with well documented experimental data. The program's accuracy was tested and developed first for simply supported reinforced concrete beams. Compared to joints, they were more easily represented by finite elements much more economical to analyze, and they had the advantage of being more familiar to investigators so that visual and standard mathematical checks would more easily reveal any discrepancies in the analysis.

Comparisons with the beams tested by Leonhardt and Walther (28) were made. The agreement found between the tests and the analyses confirmed the reliability of the method of analysis. Comparisons of data obtained from the analysis with the results of the joint details tested by the author showed very good agreement and provided additional information which assisted in understanding the behaviour of joints.

Analytically predicted crack patterns agreed with the experimental results in a fashion which had not been found previously in the literature.

8.4 Final Conclusions

The analytical results presented in this dissertation documents the behaviour of simply supported reinforced concrete beams subjected to two-point loading. The demonstrated ability to predict cracking patterns and failure modes

which closely resemble those observed for shear and bending type failures in beams is a significant achievement even though the study of reinforced concrete beams was not the central topic of this investigation.

The experimental and analytical results for joints subjected to positive moments provide data in a relatively unexplored area. Considering only the experimental results, the acceptability of previously recommended details and merit of proposed modifications to detailing was examined. It was shown that not all recommended details are adequate. The proposed modified details facilitated fabrication and were capable of developing capacities in excess of that required.

The analytical results reproduced the experimental results with reasonable accuracy and also revealed behavioural characteristics which could not be observed or measured experimentally. The complex interactions in bondslip relationships, cracking, dowel action, and material nonlinearities were incorporated in a manner which could not be aspired to using simpler analytical techniques. In terms of cost and access to relevant information, it is suggested that this research provides a capability for extended studies for further development of joints. In this way, a wider range of variables than was investigated in this dissertation may be included as well as other ideas for joint details.

The analytical model developed in this investigation was applied to only two components of reinforced concrete

structures.

8.5 Suggestions for Future Research

It is recommended that joints incorporating a wider range of variables be included in future studies. Much more experimental and analytical work will be needed before the problems associated with joint detailing are completely documented. In the course of this investigation, several areas where more research is required were noted. These are listed below:

1. More research on the intricate interaction of steel and concrete is required. Data for bond-slip and dowel action is relatively scarce.
2. The ability to model the response of concrete to biaxial states of stress is required which in turn requires more basic information.
3. More testing of joints is required with the following variables as suggested guide lines:
 - a. effects of the unequal dimensions of the intersecting members on joint behaviour,
 - b. effect of steel percentage on joint efficiency,
 - c. influence of anchorage and development lengths of steel bars in the joint region,
 - d. effectiveness of stirrups in the joint region, and
 - e. effects of using different material properties.

4. It is suggested that the present finite element program be improved and extended to include the aggregate interlock phenomenon. Also, the presently used method of modifying the stiffness of elements to take cracking effects into considerations can be replaced more accurately by sub-dividing the cracked element into two new elements. Both of these proposals will require extensive additional computer core space and computing time.

It is also suggested that iterations for nonlinear material properties can be included in the analysis when faster generations of computers become available or when the economy permits to do so.

APPENDIX A

The listing of the computer program used in this investigation is given in this appendix along with the following descriptions of the functions of the Main Program and the Subroutines.

The program consists of a main program (MAIN) and seventeen Subroutines. These subroutines are

1. Subroutine (GEOM) computes the areas of elements and the Transformation matrix relating strains and displacements.
2. Subroutine (CNODE) determines code numbers for degrees of freedom, Bandwidth of the global matrix and nodal gravity loading for each element if required.
3. Subroutine (FSM) formulates the stiffness matrix of each individual element (Steel and Concrete).
4. Subroutine (NLOAD) is a subroutine to determine nodal loads including externally applied loads and add gravity loads if desired.
5. Subroutine (CNLP) prints out nodal loads at loaded nodes only.
6. Subroutine (JSTIFF) calculates the stiffness

of every joint element in the structure and modifies the necessary joint element stiffnesses to conform with the given bond-slip, dowel action, or aggregate interlock relationships.

It also, adds the joint element stiffnesses to the global matrix in the appropriate location.

7. Subroutine (BAND) is a subroutine which utilizes the Choleski technique to solve for nodal displacements in terms of nodal loads.
8. Subroutine (CNDI) prints nodal deflections at prechosen locations only or at all nodes if required.
9. Subroutine (CESS) checks steel and concrete elements against failure criteria and decides if some particular elements need modification to their stiffness. The checks made are that for tension cracking in the concrete, changes in the modulus of elasticity of concrete elements in compression to follow the non-linear stress-strain curve, and for yielding of the main steel bars. Several subroutines are called upon from (CESS) to find the principal strains and stresses in an element and to determine the stresses in a cracked element.
10. Subroutine (SMAX) determines the principal strains and stresses and the direction of potential and existing cracks.

11. Subroutine (JSTRES) is a subroutine which computes the stresses and strains (or displacements) of joint elements parallel and perpendicular to their lengths. The stresses and displacements in the direction parallel to the length of joint element linking concrete and steel represents the bond stress and slip respectively. The forces and displacements in the direction normal to the length of the elements represent the dowel forces and dowel displacements. In the case of elements joining corresponding concrete nodes the forces and displacements can represent the aggregate interlock phenomena. The failure criteria of these joint elements are also examined in this subroutine and their stiffnesses are modified accordingly for the next iteration.
12. Subroutine (STRSTF) is a subroutine to compute stiffnesses of stirrup elements (bar type elements) and transfer them to another subroutine to have them added to the global stiffness matrix in their appropriate locations.
13. Subroutine (ADSTRP) adds stirrup stiffnesses that were computed in (STRSTF) to the global stiffness matrix.
14. Subroutine (STSTRS) computes stirrup strains and stresses in terms of nodal displacements

- and checks the failure criteria for stirrups.
15. Subroutine (FSMCRK) is called upon from the main program to find the modified stiffness of a cracked element. It substitutes the original stiffness of a cracked element with the new stiffness computed using Zienkiewicz's technique for stratified materials.
 16. Subroutine (STRESS) calculates the stresses and strains of cracked element.
 17. Subroutine (SMAER) is a subroutine that finds the stresses and strains in concrete and steel elements and averages the stresses of surrounding elements if required, (68).
 18. Program (MAIN) controls and links all of the above mentioned subroutines. It decides on the convergence criteria and performs iterations, if convergence is not satisfied. It also generates the global stiffness matrix with the aid of the calculated individual element stiffness. The program also increases the applied loads when crack stability is achieved, and finally stops the run when completed or when any trouble is identified.

This program requires four disc files for auxiliary storage and uses around 550-700K core storage capacity for corner joints on the IBM-370 computer using double

precision.

The Chart shown in Fig. 5.5 illustrates the organization of the Main Program and the Subroutines.

```

C          P R O G R A M A I N                               IN  10
C          COMPUTER PROGRAM UTILIZING THE FINITE ELEMENT METHOD. IN  20
C          PREDICTS THE BEHAVIOURAL CHARACTERISTICS OF REINFORCED CONCRETE IN  30
C          MEMBERS.                                         IN  40
C          TAKES THE FOLLOWING INTO ACCOUT,                 IN  50
C          (1) BOND -SLIP RELATIONSHIP                     IN  60
C          (2) DOWEL ACTION                                 IN  70
C          (3) NON-LINEAR MATERIAL PROPERTIES.             IN  80
C          (4) STRAIN HARDENING OF STEEL REINFORCEMENT.   IN  90
C          (5) CRACKING AND CRACK PROPAGATION EFFECTS.     IN 100
C          (6) INCLUSION OF STIRRUPS.                     IN 110
C                                                         IN 120
C                                                         IN 130
C          IMPLICIT REAL*8(A-H,O-Z)                       IN 140
C          COMMON SM(58000)                                IN 150
C          DIMENSION EI(20),FF(2),FC(1124),FN(1124),DX(562),DY(562),P(6,6) IN 160
C          1,PT(9),NP(8),R(6,6),S(6,6),UI(20),UNI(20),ND(562,2) IN 170
C          2,EX(818),EY(818),EXY(818),SEX(818),SEY(818),SEXY(818) IN 180
C          3, NIJ(3),NNPR(562),F(1124)                    IN 190
C          DIMENSION KK(200),XII(200),YII(200),XJJ(200),YJJ(200),JM(200,4) IN 200
C          S ,SJ(8,8),ENS1(200)                            IN 210
C          S ,MFLAG(818),BRA(2),WIDE(818)                 IN 220
C          S ,FACTOR(818,2),NEAN(20)                      IN 230
C          S ,CSJ(200),TITLE(10)                          IN 240
C          DIMENSION SKS(4,4),STS(150),RAT(150)           IN 250
C          DIMENSION BETA(818),INDC(818)                  IN 260
C          S KOW(16)                                       IN 270
C          COMMON/BLK1/ENS1                                IN 280
C          COMMON/BLK2/RAT                                  IN 290
C          COMMON/BLOK3/DIA1,DIA2,DIA3,N1,N2,N3           IN 300
C          COMMON/BLK7/RATIO,NSWICH,IBM1,NT1,JOB,NCYCLE   IN 310
C          COMMON/BLK9/IPP                                  IN 320
C          READ(5,52) TITLE                                IN 330
52          FORMAT(10A8)                                    IN 340
53          FORMAT(1H1,2X,10A8,/,3X,100(' '),//)          IN 350
C          WRITE(6,53) TITLE                               IN 360
C          WRITE(3,53) TITLE                               IN 370
C          WRITE(6,28)                                     IN 380
C                                                         IN 390
C          NN= NO. OF NODAL POINTS                        IN 400
C          NE= NO. OF FINITE ELEMENTS.                   IN 410
C          NUE= NO. OF DIFFERENT MATERIALS.              IN 420
C          NCI= GRAVITY LOADING IDENTIFIER               IN 430
C          NLC=NO. OF ALLOWABLE LOAD CASES               IN 440
C          KV=ALLOWABLE TOTAL NUMBER OF UNKOWNS.        IN 450
C          NJE=NO. OF JOINT ELEMENTS                     IN 460
C          NBOUN= NO. OF NODES HAVING BOUNDARY CONDITIONS OTHER THAN FREE IN 470
C          NLINE= NO. OF NODAL LINES FOR BEAMS(USED FOR AUTO. DATA GENERATION IN 480
C          NJPLN= NO. OF NODAL POINTS PER LINE           IN 490
C          KOW IS THE NOS. OF NODES THE DEFL. OF WHICH ARE TO BE PRINTED IN 500
C          NSTR=NUMBER OF STIRRUP ELEMENTS               IN 510
C          NIK=NO. OF NODES TO SUPPLY THEIR ORDINATES    IN 520
C          NCRTCL= THE NODE NO. CONTROLLING DEFLECTION   IN 530
C          NAXY=1 IF DEFLXION IS IN THE X DIRN.          IN 540
C          NAXY=2 IF DEFLXION IS IN THE Y DIRN.          IN 550
C          NSWICH IS A PRINTING SWITCH LEAVE BLANK IF STATE IF CRACKED IN 560
C          ELEMENTS IS NOT DESIRED TO BE PRINTED ,SET TO ANY NO. OTHERWISE. IN 570
C                                                         IN 580
C          READ (5,3) NN,NE,NUE,NCI,NLC,KV ,NSTR ,NJE,NBOUN,NLINE,NJPLN IN 590
C          S ,NIK,NCRTCL,NAXY,NSWICH                      IN 600
C          READ(5,3) (KOW(I),I=1,16)                     IN 610
C          IF(NCRTCL.EQ.0)NCRTCL=NN                       IN 620
C          IF(NAXY.EQ.0) NAXY=1                           IN 630
C                                                         IN 640
C          NANCH= TOTAL NUMBER OF ELEMENTS WELL ANCHORD  IN 650
C          NEAN = THE NUMBERS OF THE ANCHORD ELEMNTS IN ORDER IN 660
C                                                         IN 670
C          READ(5,3) NANCH                                  IN 680
C          READ(5,3) (NEAN(KA),KA=1,NANCH)                IN 690
C                                                         IN 700
C          BRA(1)= WIDTHS OF ELEMENTS CORRESPONDING TO DIFFERENT MATERIALS. IN 710
C                                                         IN 720
C          READ(5,5) (BRA(KIN),KIN=1,NUE)                IN 730

```

```

C          IN 740
C FTENS= ALLOWABLE TENSILE FACTOR FOR THE CONCRETE TO BE MULTIPLIED IN 750
C BY CYLINDER CONC STRENGTH**0.5 IN 760
C FPC=CONC CYLINDER STRENGTH IN 770
C EPSYLD= STEEL YIELDING STRAIN IN 780
C BNDSLP= IN INITIAL SLOPE OF BOND -SLIP CURVE, IF ZERO DEFAULTS IN 790
C TO ROUDE AND MIRZAS RELATIONSHIP IN 800
C DOWEL = INITIAL DOWEL STIFF. ,SET=0.0 TO DEFAULT TO IN C10
C ROUDE AND MIRZA'S IN C20
C ALDEFL = MAXIMUM ALLOWABLE DEFL. AFTER WHICH THE PROC. STOPS. IN 830
C          IN 840
C READ(5,6) FTENS, FPC ,EPSYLD ,BNDSLP, DOWEL, ALDFL IN 850
C IF(BNDSLP.EQ.0.) BNDSLP=1.95E+06 IN 850
C IF(ALDFL.EQ.0.0) ALDFL=3.0 IN 870
C IF(FTENS.EQ.0.0) FTENS=9.5 IN 880
C IF(FTENS.GT.10.0) FTENS=9.6 IN 890
C FTENS=FTENS*DSQRT(FPC) IN 900
C DO 11 KIKI=1, NJE IN 910
C KK(KIKI)=0 IN 920
911 CONTINUE IN 930
C EC=57620.0*(FPC**0.5) IN 940
C BNET=BRA(1)-BRA(2) IN 950
C IF(DOWEL.EQ.0.0) DOWEL=BNET*EC IN 960
C          IN 970
C          IN 980
C CALCULATE CONSTANTS FOR CONCRETE STRESS-STRAIN CURVE(SAENZ'S) IN 990
C          IN 1000
C EPS0=1.0E-05*(FPC**0.25)*(31.5-FPC**0.25) IN 1000
C FFC=0.94*FPC IN 1010
C EPSF=0.0025 IN 1020
C EPSC=-EPSF IN 1030
C ENOD=FPC/EPSC IN 1040
C REC=EC/ENOD IN 1050
C RFC=FPC/FFC IN 1050
C RSE=EPSF/EPSC IN 1070
C RCAP=REC*(RFC-1.0)/((RSE-1.0)**2)-1.0/RSE IN 1080
C C1=2.0*RCAP-1.0 IN 1090
C C2=RCAP IN 1100
C C3=RCAP+REC-2.0 IN 1110
C DO 2 I=1, NN IN 1120
C DO 2 J=1, 2 IN 1130
C ND(I, J)=1 IN 1140
2 CONTINUE IN 1150
C          IN 1160
C READ NOS. OF NODAL POINTS FIXED IN EITHER ONE OF THE TWO DEGREES IN 1170
C OF FREEDOM(1=FREE, 0=FIXED) IN 1180
C          IN 1190
C          IN 1200
C          IN 1210
12 CONTINUE IN 1220
C DO 13 I=1, NN IN 1230
C WRITE (6,79) I, ND(I, 1), ND(I, 2) IN 1240
13 CONTINUE IN 1250
C WRITE(6,4) IN 1260
C REWIND 1 IN 1270
C REWIND 2 IN 1280
C REWIND 4 IN 1290
C NT1=1 IN 1300
C NT2=4 IN 1310
C NU = 1 IN 1320
C DO 1 II = 1, NN IN 1330
C DO 1 JJ = 1, 2 IN 1340
C IF(ND(II, JJ).EQ.0) GO TO 1 IN 1350
C ND(II, JJ) = NU IN 1360
C NU = NU + 1 IN 1370
1 CONTINUE IN 1380
C NU = NU - 1 IN 1390
C          IN 1400
C          IN 1410
C          IN 1420
C          IN 1430
C          IN 1440
C          IN 1450
C          IN 1460
102 IN

```

	DO 14 J=1,NLINE	IN 1420
	READ (5,3) (MFLAG(I),I=1,NJPLN)	IN 1420
	DO 14 I=1,NJPLN	IN 1500
	IF(MFLAG(I).EQ.0) GO TO 14	IN 1510
	KX=2*MFLAG(I)-1	IN 1520
	KY=2*MFLAG(I)	IN 1530
	IF(J.GT.13) GO TO 15	IN 1540
	SH(KX)=FACTOR(I,1)+XII(J)	IN 1550
	SH(KY)=FACTOR(I,2)+YII(J)	IN 1560
	GO TO 14	IN 1570
15	SH(KX)=FACTOR(I,2)+XII(J)	IN 1580
	SH(KY)=FACTOR(I,1)+YII(J)	IN 1590
14	CONTINUE	IN 1600
23	IF(NIK.EQ.0) GO TO 19	IN 1610
C		IN 1620
C	READ NODAL POINT COORDINATES IF NO AUTO. GENERATION WAS USED	IN 1630
C		IN 1640
	DO 18 IZIB=1,NIK	IN 1650
	READ(5,23000) MFD,XEX,YEX	IN 1660
23000	FORMAT(15,2F10.0)	IN 1670
	KX=2*MFD-1	IN 1680
	KY=2*MFD	IN 1690
	SH(KX)=XEX	IN 1700
	SH(KY)=YEX	IN 1710
18	CONTINUE	IN 1720
19	CONTINUE	IN 1730
	DO 16 L2=1,NJE	IN 1740
	XII(L2)=0.0	IN 1750
	YII(L2)=0.0	IN 1760
16	CONTINUE	IN 1770
	DO 2000 LI=1,NE	IN 1780
	FACTOR(LI,1)=1.0	IN 1790
	FACTOR(LI,2)=1.0	IN 1800
2000	CONTINUE	IN 1810
	DO 104 I=1,NUE	IN 1820
C		IN 1830
C	READ MATERIAL CONSTANTS FOR CONC. AND STEEL RESP. E,POISSON'S RATIO	IN 1840
C	0 ASSUMED .2 AND .3 RESP.)	IN 1850
C		IN 1860
	READ(5,6)EI(1),UI(1),UNI(1)	IN 1870
	EI(1)=1000.0*EI(1)	IN 1830
	EI(1)=EC	IN 1890
104	CONTINUE	IN 1900
	SARR = 0.0	IN 1910
	IPO=0	IN 1920
	IPP=1	IN 1930
	NB = 0	IN 1940
	JC = 0	IN 1950
	NCYCLE=0	IN 1960
	ISEE=1	IN 1970
	NNDX=2	IN 1980
	RATIO=0.0	IN 1990
	LC=0	IN 2000
	IBH1=0	IN 2010
	DO 10202 JER =1,NU	IN 2020
	F(JER) =0.0	IN 2030
10202	CONTINUE	IN 2040
	INDEED=ND(NCRTCL,NAXY)	IN 2050
C		IN 2060
C	READ NO. OF EACH ELEM., I, J, K NODES AND MATERIAL IDENTIFIER(1 FOR	IN 2070
C	CONCRETE, 2 FOR STEEL)	IN 2080
C		IN 2090
	DO 105 J=1,NE	IN 2100
	READ(5,3) NOM,NI,NJ,NK,MET	IN 2110
	IF(NOM.NE.J)STOP	IN 2120
	E = EI(MET)	IN 2130
	U = UI(MET)	IN 2140
	UN = UNI(MET)	IN 2150
	XI = SH(2*NI-1)	IN 2160
	YI=SH(2*NI)	IN 2170
	XJ=SH(2*NJ-1)	IN 2180
	YJ=SH(2*NJ)	IN 2190
	XK=SH(2*NK-1)	IN 2200
	YK=SH(2*NK)	IN 2210

```

C * SUBROUTINE GEOM DETERMINES THE ELEMENT AREA AND TRANSPOSE MATRIX P IN 2220
C * SUBROUTINE GEOM REQUIRES NO INPUT DATA. IN 2230
CALL GEOM(XI,XJ,XK,YI,YJ,YK,PT,A,ARR) IN 2240
ARR = (UN*ARR)/6. IN 2250
ARR = ARR/2. IN 2260
SARR = SARR + ARR IN 2270
WIDTH=BRA(MET) IN 2280
WIDE(J)=WIDTH IN 2290
WRITE(6,0) J,MET,NI,NJ,NK,XI,XJ,XK,YI,YJ,YK,E,U,UN,ARR,WIDTH IN 2300
C SUBROUTINE CNODE DETERMINES CODE NOS. , BARD WIDTH , AND IN 2310
C NODAL GRAVITY LOADING FOR EACH ELEMENT IN 2320
CALL CNODE (J,ND,NP,NB,NU ,FG,NI,NJ,NK,ARW) IN 2330
C SUBROUTINE FSM DETERMINES EACH ELEMENT STIFF MATRIX S. IN 2340
C SUBROUTINE FSM REQUIRES NO INPUT DATA. IN 2350
CALL FSM (P,S,R,PT,E,U,ARR ,WIDTH) IN 2360
WRITE(1) (NP(I) , I=1,6) , ((S(MI,IN) , IN=1,6) , MI=1,6) , (PT(K) , K=1,9) , IN 2370
I A,E,U , NI,NJ,NK,ARR IN 2380
105 CONTINUE IN 2390
REWIND 1 IN 2400
IF(NSTR.LE.0) GO TO 2010 IN 2410
SDIAM=0.01 IN 2420
WRITE(6,65) IN 2430
65 FORMAT(5X,'STIRRUP INFORMATION',/,5X,20('+'),/,5X, IN 2440
S' IS JS XIS YIS XJS YJS AREA LENGTH',/) IN 2450
DO 2040 NG=1,NSTR IN 2460
RAT(NS)=1.0 IN 2470
2020 FORMAT(3I5,2F10.0) IN 2480
C IN 2490
C IBX =NO. OF STIRRUP ELEMENT IN 2500
C IS,JS SHOULD BE CHOSEN SO THAT THE POSTIVE LOCAL MEMBER X-AXIS IN 2510
C DOES NOT MAKE MORE THAN 180 DEG WITH THE GLOBAL X-AXIS. IN 2520
C SDIA= DIAMETER OF STIRRUP IN 2530
C BRACH= NO. OF STIRRUP BRANCHES. IN 2540
C IN 2550
C READ(5,2020) IBX,IS,JS,SDIA ,BRANCH IN 2560
C IF(BRANCH.EQ.0.0) BRANCH=2.0 IN 2570
C IF(SDIA.EQ.0.0) SDIA=SDIAM IN 2580
C SDIAM=SDIA IN 2590
C SAREA=BRANCH*.7854*SDIA**2 IN 2600
C IN 2610
C STSTF IS A SUBROUTINE WHICH DETERMINES STIRRUP STIFFNESSES. IN 2620
C IN 2630
C CALL STRTF(IS,JS,ANG,SAREA,SKS,ALS,EI) IN 2640
NP(1)=ND(IS,1) IN 2650
NP(2)=ND(JS,1) IN 2660
NP(3)=ND(IS,2) IN 2670
NP(4)=ND(JS,2) IN 2680
WRITE(2) IS,JS,ANG,SAREA,((SKS(KI,MI) , KI=1,4) , MI=1,4) , IN 2690
S (NP(I) , I=1,4) ,ALS IN 2700
MAX=0 IN 2710
MIN=3000 IN 2720
DO 402 J=1,4 IN 2730
IF(NP(J).EQ.0) GO TO 402 IN 2740
IF(NP(J)-MAX) 403,403,404 IN 2750
404 MAX=NP(J) IN 2760
403 IF(NP(J)-MIN) 405,402,402 IN 2770
405 MIN=NP(J) IN 2780
402 CONTINUE IN 2790
NB2=MAX-MIN IN 2800
IF(NB2.GT.NB) NB=NB2 IN 2810
2040 CONTINUE IN 2820
REWIND2 IN 2830
2010 CONTINUE IN 2840
IBI=0 IN 2850
DO 142 KIM=1,NE IN 2860
INDC(KIM)=0 IN 2870
142 NFLAG(KIM)=0 IN 2880
IF(NJE ,EQ. 0) GO TO 41 IN 2890
C IN 2900
C READ JOINT ELEMENT NOOS. , I,J,K,L NODAL CODE NUMBERS. IN 2910
C IN 2920
DO 10300 I=1,NJE IN 2930
, J=1,4) IN 2940
IN 2950

```

C		IN 2960
C	READ THE NUMBERS OF JOINT ELEMENTS JOINING DIFFERENT DIAMETERS	IN 2970
C	OF STEEL, UP TO THREE DIAMS. .	IN 2980
C	N(I) IS THE STARTING NO. OF THE JOINT ELEMS.	IN 2990
C	DIA IS THE BAR DIAM. CORRESPONDING TO THE ABOVE JT. ELEM. NO.	IN 3000
C	CNN IS THE FACTOR FOR DOWEL STIFF. ALWAYS SET TO 1.0 OR ALTER	IN 3010
C	TO STUDY EFFECT OF DOWEL STIFF. ON THE BEHAVIOUR.	IN 3020
C		IN 3030
	READ(5,62) N1,N2,N3,DIA1,DIA2,DIA3,CNN	IN 3040
	CSS1=3.14159*BNDSLP*DIA1	IN 3050
	CSS2=3.14159*BNDSLP*DIA2	IN 3060
	CSS3=3.14159*BNDSLP*DIA3	IN 3070
	CNN=DOWEL*CNN	IN 3080
	CSSF=0.0	IN 3090
	WRITE(6,70)	IN 3100
	WRITE(6,71) ((1,(JM(I,J),J=1,4)),I=1,NJE)	IN 3110
	WRITE(6,72) CSS1,CNN,CSSF,CSS2,CSS3,N1,N2,N3	IN 3120
	WRITE(6,73)	IN 3130
C		IN 3140
C	COMPUTE AND STORE JOINT ELEM. CONSTANTS.	IN 3150
C		IN 3160
	DO 63 I=1,NJE	IN 3170
	ENS1(I)=.00	IN 3180
	CSJ(I)=CSS1	IN 3190
	IF(I.GT.N1.AND.I.LE.N2) CSJ(I)=CSS2	IN 3200
	IF(I.GT.N2.AND.I.LE.N3) CSJ(I)=CSS3	IN 3210
	II = JM(I,1)	IN 3220
	JJ = JM(I,2)	IN 3230
	IL = JM(I,3)	IN 3240
	JL = JM(I,4)	IN 3250
	XII(I) = SM(2*II-1)	IN 3260
	YII(I) = SM(2*II)	IN 3270
	XJJ(I) = SM(2*JJ-1)	IN 3280
	YJJ(I) = SM(2*JJ)	IN 3290
	WRITE(6,76) I,XII(I),YII(I),XJJ(I),YJJ(I)	IN 3300
	NP(1) = ND(II,1)	IN 3310
	NP(2) = ND(JJ,1)	IN 3320
	NP(3) = ND(IL,1)	IN 3330
	NP(4) = ND(JL,1)	IN 3340
	NP(5) = ND(II,2)	IN 3350
	NP(6) = ND(JJ,2)	IN 3360
	NP(7) = ND(IL,2)	IN 3370
	NP(8) = ND(JL,2)	IN 3380
	MAX = 0	IN 3390
	MIN = 3000	IN 3400
	DO 42 J = 1,8	IN 3410
	IF(NP(J) .EQ. 0) GO TO 42	IN 3420
	IF(NP(J) - MAX) 43,43,44	IN 3430
44	MAX = NP(J)	IN 3440
43	IF(NP(J) - MIN) 45,42,42	IN 3450
45	MIN = NP(J)	IN 3460
42	CONTINUE	IN 3470
	NB1 = MAX - MIN	IN 3480
	IF(NB1 .GT. NB) NB = NB1	IN 3490
63	CONTINUE	IN 3500
41	CONTINUE	IN 3510
	NB1 = NB + 1	IN 3520
	NV = NB1*NU	IN 3530
	WRITE(6,999) NB,NV	IN 3540
	IF(NV.LE.KV) GO TO 122	IN 3550
	WRITE(6,17) NV	IN 3560
C		IN 3570
C	IF NO. OF UNKOWNS IS .GT.ALLOWED STOP EXECUTION.	IN 3580
C		IN 3590
	STOP	IN 3600
122	CONTINUE	IN 3610
	IPX=IPO	IN 3620
	IPO=IPP	IN 3630
	IPP=IPX	IN 3640
	NCYCLE=NCYCLE+1	IN 3650
	IF(NCYCLE.GT.1) MFLAG(JOB)=0	IN 3660
	IF(NCYCLE.EQ.1.AND.LC.NE.0) IBM=IBM+1	IN 3670
	WRITE(6,75) NCYCLE	IN 3680
		IN

C	GENERATES MAIN STIFFNESS MATRIX	IN 3700
C	DO 40 JL=1,NV	IN 3710
	SM(JL)=0.0	IN 3720
40	CONTINUE	IN 3730
	DO 20 KJJ = 1,NE	IN 3740
	READ(NT1)(NP(I),I=1,6),((S(MM,MN),MN=1,6),MM=1,6),(PT(J),J=1,9),	IN 3750
	1 A,E,U,NI,NJ,NK,ARR	IN 3760
	IF(MFLAG(KJJ).NE.1.OR.INDC(KJJ).NE.0) GO TO 1010	IN 3770
	BATA=BETA(KJJ)	IN 3780
	WIDTH=WIDE(KJJ)	IN 3790
	E1=E*FACTOR(KJJ,NNDX)	IN 3800
C		IN 3810
C	IF ELEMENT IS CRACKED FIND ITS MODIFIED STIFFNESS.	IN 3820
C		IN 3830
	CALL FSHCRK(S,PT,E1,U,ARR,WIDTH,BATA,INDC,KJJ)	IN 3840
1010	CONTINUE	IN 3850
	WRITE(NT2)(NP(I),I=1,6),((S(MM,MN),MN=1,6),MM=1,6),(PT(J),J=1,9),	IN 3860
	1 A,E,U,NI,NJ,NK,ARR	IN 3870
	IF(MFLAG(KJJ).EQ.1.AND.INDC(KJJ).EQ.1) GO TO 149	IN 3880
	IF(MFLAG(KJJ).EQ.2) FACTOR(KJJ,NNDX)=.001	IN 3890
	IF(FACTOR(KJJ,NNDX).EQ.1.0) GO TO 47	IN 3900
	DO 49 JIM=1,6	IN 3910
	DO 49 JEM=1,6	IN 3920
	S(JIM,JEM)=FACTOR(KJJ,NNDX)*S(JIM,JEM)	IN 3930
49	CONTINUE	IN 3940
	GO TO 47	IN 3950
149	INDC(KJJ)=2	IN 3960
47	DO 7 JJ=1,6	IN 3970
	IF(NP(JJ).EQ.0) GO TO 7	IN 3980
	DO 11 II=JJ,6	IN 3990
	IF(NP(II).EQ.0) GO TO 11	IN 4000
	IF(NP(JJ)-NP(II))9,10,10	IN 4010
10	K=(NP(II)-1)*NB+NP(JJ)	IN 4020
	SM(K)=SM(K)+S(JJ,II)	IN 4030
	GO TO 11	IN 4040
9	K=(NP(JJ)-1)*NB+NP(II)	IN 4050
	SM(K)=SM(K)+S(JJ,II)	IN 4060
11	CONTINUE	IN 4070
7	CONTINUE	IN 4080
20	CONTINUE	IN 4090
	REWIND NT1	IN 4100
	REWIND NT2	IN 4110
	NTX=NT2	IN 4120
	NT2=NT1	IN 4130
	NT1=NTX	IN 4140
C	ADD STIRRUP STIFFNESSES TO MAIN STIFFNESS MATRIX	IN 4150
	IF(NSTR.LE.0) GO TO 2050	IN 4160
	CALL ADSTRP(NSTR,NB)	IN 4170
2050	CONTINUE	IN 4180
	IF(ISEE.EQ.1) GO TO 3100	IN 4190
	IF(IBM.CT.0) COTO 494	IN 4200
3100	CONTINUE	IN 4210
	IF(NGI.EQ.1) GO TO 31	IN 4220
C	DETERMINE NOADAL LOADS	IN 4230
C	SUBROUTINE NLOAD DETERMINES NOADAL LOADS	IN 4240
C	SUBROUTINE NLOAD REQUIRES DATA.	IN 4250
	IF(RATIO.GT.1.0) GO TO 144	IN 4260
	CALL NLOAD(ND,FG,FF,NU,NGI)	IN 4270
	GO TO 22	IN 4280
31	CONTINUE	IN 4290
	IF(NLC.EQ.0) GO TO 22	IN 4300
	CALL NLOAD(ND,FG,FF,NN,NGI)	IN 4310
22	CONTINUE	IN 4320
494	CONTINUE	IN 4330
	GO TO 143	IN 4340
144	DO 145 JAS=1,NU	IN 4350
	FG(JAS)=(RATIO-1.0)*F(JAS)	IN 4360
145	CONTINUE	IN 4370
143	CONTINUE	IN 4380
	DO 124 JJ = 1,NU	IN 4390
	F(JJ) = F(JJ) + FG(JJ)	IN 4400
	IF(NNDX.EQ.1)FN(JJ)=FG(JJ)	IN 4410
	IF(NNDX.EQ.2)FN(JJ)=F(JJ)	IN 4420
		IN 4430

```

124 CONTINUE                               IN 4440
    WRITE (6,21)                             IN 4450
C   SUBROUTINE CNLP PRINTS OUT NODAL LOADS    IN 4460
    CALL CNLP (F, FN, ND, NN, NNPR, IPP)      IN 4470
331 IF(NJE .EQ. 0) GO TO 64                  IN 4480
    CALL JSTIFF(SJ, JH, KK, ND, XII, XJJ, YII, YJJ, CSJ, CNW, NB, NJE, CSSF
    S, HANCH, NEAN)                           IN 4490
333 CONTINUE                               IN 4500
64 CONTINUE                                IN 4510
    WRITE(6,24)                               IN 4520
C   * SUBROUTINE BAND SOLVES FOR DISPLACEMENTS USING THE CHOLESKI SQUARE IN 4530
C   METHOD.                                    IN 4540
    DET = 1.E-8                               IN 4550
    CALL BAND (SH, FN, NU, NB1, 1, DET)        IN 4560
    IF(DET) 125, 126, 127                     IN 4570
125 WRITE(6,25)DET                          IN 4580
    GO TO 1003                                 IN 4590
126 WRITE(6,26)DET                          IN 4600
    GO TO 1003                                 IN 4610
127 CONTINUE                                IN 4620
    DFLXN=DABC(FN(INDEED))                    IN 4630
    IF(DFLXN.GT.ALDFL) STOP                   IN 4640
    DO 495 JJ=1,NU                            IN 4650
    FG(JJ)=0.0                                IN 4660
495 CONTINUE                                IN 4670
C   SUBROUTINE CNDI REQUIRES NO INPUT DATA  IN 4680
C   SUBROUTINE CNDI PRINTS OUT NODAL DEFLECTIONS IN 4690
    CALL CNDI(FN, ND, NN, DX, DY, KOW, JC)    IN 4700
    IF(NCYCLE.EQ.1) WRITE(3,3000)            IN 4710
3000 FORMAT(1X,100('-'))                     IN 4720
    WRITE(3,75) NCYCLE                         IN 4730
    IF(IPP.EQ.1) GO TO 707                    IN 4740
    WRITE(3,29)                               IN 4750
707 CONTINUE                                IN 4760
C   FIND STRESSES AND STRAINS USING THE AVERAGING TECHNIQUE. IN 4770
C   CALL SAMER(FN, EX, EY, EXY, SEX, SEY, SEXY, NN, FACTOR, UI, NV IN 4780
    S , NT1, NE, MFLAG, FTENS)                IN 4790
C   * SUBROUTINE CESS DETERMINES AND PRINTS OUT THE ELEMENT STRAINS IN 4800
C   AND STRESSES.                            IN 4810
C   * SUBROUTINE CESS REQUIRES NO INPUT DATA. IN 4820
    CALL CESS(FN, EX, EY, EXY, SEX, SEY, SEXY, NE, JC, UI, IPP, FG, ND, IN 4830
    1 WIDE, NN, IDW, MFLAG, FTENS, EPSC, EPSYLD, C1, C2, C3, EPSO, FACTOR, EC, BETA IN 4840
    S , INDC)                                 IN 4850
    IF (NJE .EQ. 0) GO TO 128                 IN 4860
    IF(IPP.EQ.1) GO TO 708                    IN 4870
    WRITE(6,59)                               IN 4880
708 CONTINUE                                IN 4890
C   FIND BOND AND DOWEL STRESSES AND DISPLACEMENTS IN JT. ELEMS. IN 4900
C   CALL JSTRES (JH, DX, DY, XII, YII, XJJ, YJJ, KK, NJE, CSS1, CNW, CSSF IN 4910
    S, CSJ)                                   IN 4920
128 CONTINUE                                IN 4930
    IF(NSTR.LE.0) GO TO 2060                  IN 4940
    IF(IPP.EQ.1) GO TO 709                    IN 4950
    WRITE(6,2070)                             IN 4960
709 CONTINUE                                IN 4970
C   FIND STRAINS AND STRESSES IN STIRRUPS    IN 4980
C   CALL STSTRS(JC, EI, EPSYLD, FN, NSTR)     IN 4990
2060 CONTINUE                                IN 5000
    IF(NCYCLE.EQ.1.AND.LC.EQ.0) GO TO 81      IN 5010
    KAM=IBW-IBW0                              IN 5020
    IF(KAM.EQ.1.AND.NCYCLE.EQ.1) GO TO 1004  IN 5030
    IF(KAM.GT.0) GO TO 1002                   IN 5040
1004 LC=LC+1                                  IN 5050
    IF(LC.GE.NLC) STOP                        IN 5060
C   NNDX=1 IS FOR THE OPTION OF COMBINED INC.+TOTAL IN 5070
    NNDX=1                                     IN 5080
    NCYCLE=0                                   IN 5090
    IN 5100
    IN 5110
    IN 5120
    IN 5130
    IN 5140
    IN 5150
    IN
    IN

```

```

NNDX=2 IN 5180
C JC=1 IF INC+TOTAL PROCEDURE IS REQUIRED. IN 5190
  IBMO=IBM IN 5200
  GO TO 122 IN 5210
1002 IF(NCYCLE.GT.65) STOP IN 5220
  JC=0 IN 5230
81 CONTINUE IN 5240
  IBMO=IBM IN 5250
  ISEE=2 IN 5260
  NNDX=2 IN 5270
  IF(IBM.GT.0) GOTO 122 IN 5280
  IF(IBM.EQ.0) GO TO 1004 IN 5290
3 FORMAT(16I5) IN 5300
  4 FORMAT(1X,'INPUT DATA DESCRIBING THE FINITE ELEMENTS.'//1X, IN 5310
  1' NO. MET NI NJ NK XI XJ XK YI YJ YK IN 5320
  2 E U UNWT AREA WIDTH'//) IN 5330
5 FORMAT(12F5.2) IN 5340
6 FORMAT(8F10.0) IN 5350
8 FORMAT(1X,5I6,6F6.1,1E12.4,1F6.2,1F6.2,2F6.2) IN 5360
17 FORMAT(1X,'SIZE OF THE PROBLEM IS. ',16,' PROGRAM CAPACITY EXCEED IN 5370
  1ED. ') IN 5380
21 FORMAT(1X,' LOAD INCREMENT TOTAL LOAD'/1X'NODE IN 5390
  1 NO. X FORCE Y FORCE X FORCE Y FORCE'//) IN 5400
24 FORMAT(1X,' DEFLECTION INCREMENT TOTAL DE IN 5410
  1FLECTION'/1X,'NODE NO. X DEFLECTION Y DEFLECTION X DEFLEC IN 5420
  2TION Y DEFLECTION'//) IN 5430
25 FORMAT(1X,'MATRIX SM IS NOT POSITIVE DEFINITE. DET=',E15.7) IN 5440
26 FORMAT(1X,'DETERMINANT IS ZERO. DET=',E15.7) IN 5450
28 FORMAT(6X,'NODE NUMBER DEGREES OF FREEDOM',//) IN 5460
29 FORMAT(1X,'(FIRST LINE GIVES INCREMENT, SECOND LINE GIVES TOTAL.)' IN 5470
  1/1X,'(THIRD LINE GIVES THE TOTAL CHANGE IN STRESS WHEN DESIRED.)' IN 5480
  2//4X,'NO.XSTRAIN YSTRAIN XYSTRAIN XSTRESS YSTRESS XYSTRESS IN 5490
  3MAXSTRESS MINSTRESS MINSTRAIN MAX XY STRN DIRN E ERROR IN 5500
  4'//) IN 5510
  59 FORMAT(1X,'JOINT ELEMENT STRAINS AND STRESSES'/7X,' N STRAIN IN 5520
  1S STRAIN N STRESS S STRESS') IN 5530
61 FORMAT(12I5) IN 5540
62 FORMAT(3I5,6F10.0) IN 5550
70 FORMAT(1X,' NODE NUMBERS OF JOINT ELEMENTS',//,12X,'NI NJ NK IN 5560
  1 NL',//) IN 5570
71 FORMAT(1X,5I6) IN 5580
72 FORMAT(1X,'JOINT CONSTANTS',//,6X,'CSS1= ',E12.5,6X,'CNN = ',E12.5 IN 5590
  1,6X,'CSSF = ',E12.5,'CSS2=',E12.5,'CSS3=',E12.5,3I5) IN 5600
73 FORMAT(//,1X,'COORDINATES OF JOINT NODES',//,9X,'XXI YII XJJ IN 5610
  1 YJJ',//) IN 5620
75 FORMAT(1X,'ITERATION NUMBER',15,/,1X,23('-')) IN 5630
76 FORMAT(115,4F10.2) IN 5640
78 FORMAT(3I5) IN 5650
79 FORMAT(2X,3I10) IN 5660
  999 FORMAT(//,1X,'HALF BAND WIDTH = ',16,/,1X,'TOTAL UNKNOWNNS = ',16) IN 5670
1003 WRITE(6,60) NNDX IN 5680
2070 FORMAT(1X,'STIRRUP STRAINS AND SRESSES',/,1X,29('-'),/,4X, IN 5690
  6'ST. NO. STRAIN INC STRESS INC TOTAL STRAIN TOTAL STRESS ANG IN 5700
  6LE OF INCL.',//) IN 5710
60 FORMAT(2X,15) IN 5720
  STOP IN 5730
  END IN 5740

```

SUBROUTINE GEOM(XI,XJ,XK,YI,YJ,YK,PT,A,ARR,J)	GEO 10
IMPLICIT REAL*8(A-H,O-Z)	GEO 20
DIMENSIONPT(9)	GEO 30
A=(XI-XJ)*(YI-YK)-(XI-XK)*(YI-YJ)	GEO 40
ARR= DABS(A)	GEO 50
PT(1)=XJ*YK-XK*YJ	GEO 60
PT(2)=XK*YI-XI*YK	GEO 70
PT(3)=XI*YJ-XJ*YI	GEO 80
PT(4)=YJ-YK	GEO 90
PT(5)=YK-YI	GEO 100
PT(6)=YI-YJ	GEO 110
PT(7)=XK-XJ	GEO 120
PT(8)=XI-XK	GEO 130
PT(9)=XJ-XI	GEO 140
RETURN	GEO 150
END	GEO 160

	SUBROUTINE CNODE(J,ND,NP,NB,NU ,FG,NI,NJ,NK,ARW)	CNO 10
	IMPLICIT REAL*8(A-H,O-Z)	CNO 20
	DIMENSION FG(1)	CNO 30
	DIMENSION ND(562,2),NP(6)	CNO 40
	IF(J.NE. 1) GO TO 13	CNO 50
	NB = 0	CNO 60
	DO 12 IJ=1,NU	CNO 70
	FG(IJ)=0.0	CNO 80
12	CONTINUE	CNO 90
13	CONTINUE	CNO 100
	NP(1) = ND(NI,1)	CNO 110
	NP(2) = ND(NJ,1)	CNO 120
	NP(3) = ND(NK,1)	CNO 130
	NP(4) = ND(NI,2)	CNO 140
	NP(5) = ND(NJ,2)	CNO 150
	NP(6) = ND(NK,2)	CNO 160
C	COMPUTE NODAL LOADS DUE TO GRAVITY.	CNO 170
	IF(ND(NI ,2).EQ.0)GO TO 10	CNO 180
	IK=ND(NI ,2)	CNO 190
	FG(IK)=FG(IK)-ARW	CNO 200
10	CONTINUE	CNO 210
	IF(ND(NJ ,2).EQ.0)GO TO 11	CNO 220
	IK=ND(NJ ,2)	CNO 230
	FG(IK)=FG(IK)-ARW	CNO 240
11	CONTINUE	CNO 250
	IF(ND(NK ,2).EQ.0)GO TO 25	CNO 260
	IK = ND(NK,2)	CNO 270
	FG(IK)=FG(IK)-ARW	CNO 280
25	CONTINUE	CNO 290
	MAX=0	CNO 300
	MIN=3000	CNO 310
	DO 5 KK=1,6	CNO 320
	IF(NP(KK).EQ.0) GO TO 5	CNO 330
	IF(NP(KK)-MAX)6,6,7	CNO 340
7	MAX=NP(KK)	CNO 350
6	IF(NP(KK)-MIN)8,5,5	CNO 360
8	MIN=NP(KK)	CNO 370
5	CONTINUE	CNO 380
	NB1=MAX-MIN	CNO 390
	IF(NB1.GT.NB) NB=NB1	CNO 400
	RETURN	CNO 410
	END	CNO 420

	SUBROUTINE FSM (P,S,R,PT,E,U,ARR,WIDTH)	FSM 10
	IMPLICIT REAL*8(A-H,O-Z)	FSM 20
	DIMENSION P(6,6),S(6,6),R(6,6),PT(9)	FSM 30
	DO 1 II=1,6	FSM 40
	DO 1 JJ=1,6	FSM 50
	S(II,JJ)=0.0	FSM 60
	P(II,JJ)=0.0	FSM 70
1	CONTINUE	FSM 80
	DO 110 II=1,3	FSM 90
	DO 110 JJ=1,3	FSM 100
	KK=3*(II-1)+JJ	FSM 110
	P(II,JJ)=PT(KK)	FSM 120
	MJJ=II+3	FSM 130
	NJJ=JJ+3	FSM 140
110	P(MJJ,NJJ)=P(II,JJ)	FSM 150
	CONTINUE	FSM 160
	EU=E*WIDTH/(1.0-U**2)	FSM 170
	S(2,2)=EU	FSM 180
	S(3,3)=EU*(1.0-U)/2.0	FSM 190
	S(5,5)=S(3,3)	FSM 200
	S(6,6)=S(2,2)	FSM 210
	S(2,6)=EU*U	FSM 220
	S(6,2)=S(2,6)	FSM 230
	S(3,5)=S(3,3)	FSM 240
	S(5,3)=S(3,3)	FSM 250
	AR=4.*ARR	FSM 260
	DO 4 JJ=1,6	FSM 270
	DO 4 II=1,6	FSM 280
	R(JJ,II)=0.0	FSM 290
	DO 4 KK=1,6	FSM 300
	R(JJ,II)=R(JJ,II)+S(JJ,KK)*P(KK,II)	FSM 310
4	CONTINUE	FSM 320
	DO 5 JJ=1,6	FSM 330
	DO 5 II=1,6	FSM 340
	S(JJ,II)=0.0	FSM 350
	DO 5 KK=1,6	FSM 360
	S(JJ,II)=S(JJ,II)+P(KK,JJ)*R(KK,II)/AR	FSM 370
5	CONTINUE	FSM 380
	RETURN	FSM 390
	END	FSM 400

```

SUBROUTINE NLOAD(ND,FC,FF ,NU,NGI)
IMPLICIT REAL*8(A-H,O-Z)
DIMENSION FF(2),FC(1),ND(562,2)
IF (NGI .EQ. 1) GO TO 21
DO 20 KK = 1,NU
  FC(KK) = 0.0
20 CONTINUE
21 CONTINUE
  READ(5,3) NNL
  DO 2 11 = 1,NNL
    READ(5,3) JNU,FF(1),FF(2)
    DO 6 JJ=1,2
      IF(ND(JNU,JJ).EQ.0) GO TO 6
      IK = ND(JNU,JJ)
      FC(IK) = FC(IK)+FF(JJ)
  6 CONTINUE
  2 CONTINUE
3  FORMAT(115,2F10.0 )
  RETURN
  END
NLO 10
NLO 20
NLO 30
NLO 40
NLO 50
NLO 60
NLO 70
NLO 80
NLO 90
NLO 100
NLO 110
NLO 120
NLO 130
NLO 140
NLO 150
NLO 160
NLO 170
NLO 180
NLO 190
NLO 200
```

	SUBROUTINE CNLP(F, FN, ND, NN, NNPR, IPP)	CNL 10
	IMPLICIT REAL*8(A-H, O-Z)	CNL 20
	DIMENSION F(1), FN(1), ND(562, 2), NNPR(1)	CNL 30
	DO 1 JJ=1, NN	CNL 40
	IF(ND(JJ, 1).NE.0) GO TO 4	CNL 50
	FX1=0.0	CNL 60
	FX2=0.0	CNL 70
	GO TO 5	CNL 80
4	IK=ND(JJ, 1)	CNL 90
	FX1=FN(IK)	CNL 100
	FX2=F(IK)	CNL 110
5	CONTINUE	CNL 120
	IF(ND(JJ, 2).NE.0) GO TO 6	CNL 130
	FY1=0.0	CNL 140
	FY2=0.0	CNL 150
	GO TO 7	CNL 160
6	IK=ND(JJ, 2)	CNL 170
	FY1=FN(IK)	CNL 180
	FY2=F(IK)	CNL 190
7	CONTINUE	CNL 200
	IF(FX1.NE.0.0.OR.FY1.NE.0.0) GO TO 3	CNL 210
	IF(FX2.NE.0.0.OR.FY2.NE.0.0) GO TO 3	CNL 220
	GO TO 1	CNL 230
3	CONTINUE	CNL 240
	WRITE(6, 8) JJ, FX1, FY1, FX2, FY2	CNL 250
	WRITE(3, 8) JJ, FX1, FY1, FX2, FY2	CNL 260
1	CONTINUE	CNL 270
8	FORMAT(1X, 16, 4F11.2)	CNL 280
	RETURN	CNL 290
	END	CNL 300


```

SUBROUTINE JSTIFF(SJ, JM, KK, ND, XI, XJ, YI, YJ, CSJ, CNN, RB, NJE, CSSF) JST 10
C
C COMPUTE JOINT ELEMENT STIFFNESSES JST 20
C JST 30
C JST 40
S, NANCH, NEAN) JST 50
IMPLICIT REAL*8(A-H, O-Z) JST 60
COMMON SM(58000) JST 70
DIMENSION XI(1), XJ(1), YI(1), YJ(1), KK(1), NP(8), SJ( 8, 8), JM(200, 4 JST 80
S), ND(562, 2), NEAN(1), CSJ(1) JST 90
DO 1 I=1, NJE JST 100
CSS=CSJ(I) JST 110
DL = ((XJ(I)-XI(I))**2+ (YJ(I)-YI(I))**2)**.5 JST 120
A = (XJ(I)-XI(I))/DL JST 130
B = (YJ(I)-YI(I))/DL JST 140
CSSB=CSS JST 150
CNNB=CNN JST 160
IF(KK(I).EQ.2.OR.KK(I).EQ.4) CNNB=0.0001*CNN JST 170
IF(KK(I).GT.2) CSSB=0.0001*CSS JST 180
A1=(CSSB*A**2+CNNB*B**2)*DL/6. JST 190
A2=(CSSB*B**2+CNNB*A**2)*DL/6. JST 200
A3=(CNNB-CSSB)*A*B*DL/6. JST 210
C ANCORD JOINTS *ARE GIVEN HIGH STIFFNESS VALUES JST 220
DO 22 JL=1, NANCH JST 230
IF(I.NE.NEAN(JL)) GO TO 22 JST 240
A1=50.*A1 JST 250
A2=50.*A2 JST 260
A3=50.*A3 JST 270
22 CONTINUE JST 280
SJ( 1, 1) = 2.*A1 JST 290
SJ( 2, 1) = A1 JST 300
SJ( 2, 2) = 2.*A1 JST 310
SJ( 3, 1) = -1.*A1 JST 320
SJ( 3, 2) = -2.*A1 JST 330
SJ( 3, 3) = 2.*A1 JST 340
SJ( 4, 1) = -2.*A1 JST 350
SJ( 4, 2) = -1.*A1 JST 360
SJ( 4, 3) = A1 JST 370
SJ( 4, 4) = 2.*A1 JST 380
SJ( 5, 1) = -2.*A3 JST 390
SJ( 5, 2) = -1.*A3 JST 400
SJ( 5, 3) = A3 JST 410
SJ( 5, 4) = 2.*A3 JST 420
SJ( 5, 5) = 2.*A2 JST 430
SJ( 6, 1) = -1.*A3 JST 440
SJ( 6, 2) = -2.*A3 JST 450
SJ( 6, 3) = 2.*A3 JST 460
SJ( 6, 4) = A3 JST 470
SJ( 6, 5) = A2 JST 480
SJ( 6, 6) = 2.*A2 JST 490
SJ( 7, 1) = A3 JST 500
SJ( 7, 2) = 2.*A3 JST 510
SJ( 7, 3) = -2.*A3 JST 520
SJ( 7, 4) = -1.*A3 JST 530
SJ( 7, 5) = -1.*A2 JST 540
SJ( 7, 6) = -2.*A2 JST 550
SJ( 7, 7) = 2.*A2 JST 560
SJ( 8, 1) = 2.*A3 JST 570
SJ( 8, 2) = A3 JST 580
SJ( 8, 3) = -1.*A3 JST 590
SJ( 8, 4) = -2.*A3 JST 600
SJ( 8, 5) = -2.*A2 JST 610
SJ( 8, 6) = -1.*A2 JST 620
SJ( 8, 7) = A2 JST 630
SJ( 8, 8) = 2.*A2 JST 640
DO 20 J = 1, 8 JST 650
IF(J.EQ.8) GO TO 20: JST 660
JJ = J+1 JST 670
DO 21 K = JJ, 8 JST 680
SJ( J, K) = SJ( K, J) JST 690
21 CONTINUE JST 700
20 CONTINUE JST 710
II = JH(1, 1) JST 720
JJ = JH(1, 2) JST 730

```

IL = JM(1,3)	JST 740
JL = JM(1,4)	JST 750
NP(1) = ND(11,1)	JST 760
NP(2) = ND(JJ,1)	JST 770
NP(3) = ND(IL,1)	JST 780
NP(4) = ND(JL,1)	JST 790
NP(5) = ND(11,2)	JST 800
NP(6) = ND(JJ,2)	JST 810
NP(7) = ND(IL,2)	JST 820
NP(8) = ND(JL,2)	JST 830
DO 4 JK = 1,8	JST 840
IF(NP(JK).EQ. 0) GO TO 4	JST 850
DO 5 IK = JK,8	JST 860
IF(NP(IK).EQ. 0) GO TO 5	JST 870
IF(NP(JK) - NP(IK)) 9,10,10	JST 880
10 K = (NP(IK)-1)*NB + NP(JK)	JST 890
SM(K) = SH(K) + SJ(JK,IK)	JST 900
GO TO 5	JST 910
9 K = (NP(JK)-1)*NB + NP(IK)	JST 920
SM(K) = SH(K) + SJ(JK,IK)	JST 930
5 CONTINUE	JST 940
4 CONTINUE	JST 950
1 CONTINUE	JST 960
RETURN	JST 970
END	JST 980

	SUBROUTINE BAND(A, B, N, M, LT, DET)	BAN 10
C	SOLVE THE BANDED STIFF. MATRIX FOR DISPLACEMENTS.	BAN 20
C	IMPLICIT REAL*8(A-H, O-Z)	BAN 30
C	DIMENSION A(2), B(1)	BAN 40
	MM=M-1	BAN 50
	NM=N*M	BAN 60
	NM1=N-MM	BAN 70
	IF (LT.NE.1) GO TO 53	BAN 80
	MP=M+1	BAN 90
	KK=2	BAN 100
	FAC=DET	BAN 110
	A(1)=1./DSQRT(A(1))	BAN 120
	BIGL=A(1)	BAN 130
	SML=A(1)	BAN 140
	A(2)=A(2)*A(1)	BAN 150
	A(MP)=1./DSQRT(A(MP)-A(2)*A(2))	BAN 160
	IF(A(MP).GT.BIGL)BIGL=A(MP)	BAN 170
	IF(A(MP).LT.SML)SML=A(MP)	BAN 180
	MP=MP+M	BAN 190
	DO 62 J=MP, NM1, M	BAN 200
	JP=J-MM	BAN 210
	MZC=0	BAN 220
	IF(KK.GE.M) GO TO 1	BAN 230
	KK=KK+1	BAN 240
	II=1	BAN 250
	JC=1	BAN 260
	GO TO 2	BAN 270
1	KK=KK+M	BAN 280
	II=KK-MM	BAN 290
	JC=KK-MM	BAN 300
2	DO 65 I=KK, JP, MM	BAN 310
	IF(A(I).EQ.0.)GO TO 64	BAN 320
	GO TO 66	BAN 330
64	JC=JC+M	BAN 340
65	MZC=MZC+1	BAN 350
	ASUM1=0.	BAN 360
	GO TO 61	BAN 370
66	MZC=MM*MZC	BAN 380
	II=II+MZC	BAN 390
	KI=KK+MMZC	BAN 400
	A(KI)=A(KI)*A(JC)	BAN 410
	IF(KI.GE.JP)GO TO 6	BAN 420
	KJ=KI+MM	BAN 430
	DO 5 I=KJ, JP, MM	BAN 440
	ASUM2=0.	BAN 450
	IM=I-MM	BAN 460
	II=II+1	BAN 470
	KI=II+MMZC	BAN 480
	DO 7 K=KI, IM, MM	BAN 490
	ASUM2=ASUM2+A(KI)*A(K)	BAN 500
7	KI=KI+MM	BAN 510
5	A(I)=(A(I)-ASUM2)*A(KI)	BAN 520
6	CONTINUE	BAN 530
	ASUM1=0.	BAN 540
	DO 4 K=KM, JP, MM	BAN 550
4	ASUM1=ASUM1+A(K)*A(K)	BAN 560
61	S=A(J)-ASUM1	BAN 570
	IF(S.LT.0.)DET=S	BAN 580
	IF(S.EQ.0.)DET=0.	BAN 590
	IF(S.GT.0.)GO TO 63	BAN 600
	NROW=(J+MM)/M	BAN 610
	WRITE(6,99) NROW	BAN 620
99	FORMAT(35H0ERROR CONDITION ENCOUNTERED IN ROW,16)	BAN 630
	RETURN	BAN 640
63	A(J)=1./DSQRT(S)	BAN 650
	IF(A(J).GT.BIGL) IROW=(J+MM)/M	BAN 660
	IF(A(J).GT.BIGL)BIGL=A(J)	BAN 670
	IF(A(J).LT.SML) IROW=(J+MM)/M	BAN 680
	IF(A(J).LT.SML)SML=A(J)	BAN 690
62	CONTINUE	BAN 700
	IF(SML.LE.FAC*BIGL)GO TO 54	BAN 710
		BAN 720
		BAN 730

	CO TO 53	BAN 740
54	DET=0.	BAN 750
	ZIG=SML/BIGL	BAN 760
	WRITE(6,100) ZIG,MROW,IROW	BAN 770
100	FORIAT(2X,'SML/BIGL=',E15.7,2X,'SML AT',16,2X,'BIGL AT',16)	BAN 780
	RETURN	BAN 790
53	DET=SML/BIGL	BAN 800
55	B(1)=B(1)*A(1)	BAN 810
	KK=1	BAN 820
	K1=1	BAN 830
	J=1	BAN 840
	DO 8 L=2,N	BAN 850
	BSUM1=0.	BAN 860
	LM=L-1	BAN 870
	J=J+M	BAN 880
	IF(KK.GE.M)GO TO 12	BAN 890
	KK=KK+1	BAN 900
	GO TO 13	BAN 910
12	KK=KK+M	BAN 920
	K1=K1+1	BAN 930
13	JK=KK	BAN 940
	DO 9 K=K1,LM	BAN 950
	BSUM1=BSUM1+A(JK)*B(K)	BAN 960
	JK=JK+M	BAN 970
9	CONTINUE	BAN 980
8	B(L)=(B(L)-BSUM1)*A(J)	BAN 990
	B(N)=B(N)*A(NM1)	BAN1000
	NM1=NM1	BAN1010
	NN=N-1	BAN1020
	ND=N	BAN1030
	DO 10 L=1,NN	BAN1040
	BSUM2=0.	BAN1050
	NL=N-L	BAN1060
	NL1=N-L+1	BAN1070
	NMM=NM1-M	BAN1080
	NJ1=NMM	BAN1090
	IF(L.GE.M)ND=ND-1	BAN1100
	DO 11 K=NL1,ND	BAN1110
	NJ1=NJ1+1	BAN1120
	BSUM2=BSUM2+A(NJ1)*B(K)	BAN1130
11	CONTINUE	BAN1140
10	B(NL)=(B(NL)-BSUM2)*A(NM1)	BAN1150
	RETURN	BAN1160
	END	BAN1170

	SUBROUTINE CNDI (FN,ND,NN,DX,DY,KOW,JC)	CND 10
C	PRINTOUT NODAL DISPLACEMENTS.	CND 20
C	IMPLICIT REAL*8(A-H,O-Z)	CND 30
	DIMENSION FN(1),DX(1),DY(1),ND(562,2)	CND 40
	DIMENSION KOW(1)	CND 50
	NEK=1	CND 60
	DO 1 JJ=1,NN	CND 70
	IF(ND(JJ,1).NE.0) GO TO 3	CND 80
	DXX=0.0	CND 90
	GO TO 4	CND 100
5	IK=ND(JJ,1)	CND 110
	DXX = FN(IK)	CND 120
4	CONTINUE	CND 130
	IF(ND(JJ,2).NE.0) GO TO 6	CND 140
	DYY=0.0	CND 150
	GO TO 9	CND 160
6	IK=ND(JJ,2)	CND 170
	DYY = FN(IK)	CND 180
9	CONTINUE	CND 190
	IF(JC .NE. 0) GO TO 100	CND 200
	DX(JJ) = 0.	CND 210
	DY(JJ) = 0.	CND 220
100	CONTINUE	CND 230
	DX(JJ)=DX(JJ)+DXX	CND 240
	DY(JJ)=DY(JJ)+DYY	CND 250
	KOW=KOW(NEK)	CND 260
	IF(JJ.NE.KOW) GOTO 1	CND 270
	NEK=NEK+1	CND 280
	WRITE(6,8) JJ,DXX,DYY,DX(JJ),DY(JJ)	CND 290
8	FORMAT(1X,18,4(1PE16.5))	CND 300
1	CONTINUE	CND 310
	RETURN	CND 320
	END	CND 330
		CND 340
		CND 350

	SUBROUTINE CESS(FN, EX, EY, EXY, SEX, SEY, SEXY, NE, JC, UI, IPP, FG, ND,	CES	10
	1 WIDE, NN, IBM, MFLAG, FTENS, EPSC, EPSYLD, C1, C2, C3, EPSO, FACTOR, EC, BETA	CES	20
	S , INDC)	CES	30
	IMPLICIT REAL*8(A-H, O-Z)	CES	40
	COMMON SM(58000)	CES	50
	DIMENSION FN(1), EX(1), EY(1), EXY(1), SEX(1), SEY(1), SEXY(1), UI(6)	CES	60
	3, NIJ(3), MFLAG(1), FACTOR(818,2), INDC(1)	CES	70
	DIMENSION NP(6), PT(9), S(6,6), WIDE(1), FG(1), FF(2), BETA(1)	CES	80
	DIMENSION SIXYN(1)	CES	90
	DIMENSION IFLG(100)	CES	100
	COMMON/BLK7/RATIO, NSWICH, IBM1, NT1, JOB, NCYCLE	CES	110
	XMAX=0.0	CES	120
	ZHAX=0.0	CES	130
	IKOUNT=1	CES	140
	DO 202 JAN=1,100	CES	150
202	IFLG(JAN)=0	CES	160
	DO 1 KJ=1,NE	CES	170
	IM=0	CES	180
	J=KJ	CES	190
	READ(NT1)(NP(I), I=1,6), ((S(MM, MN), MN=1,6), MM=1,6), (PT(JKL), JKL=1,9	CES	200
	1), A, E, U, NI, NJ, NK, ARR	CES	210
C		CES	220
C	FIND AVERAGE STRESSES AND STRAINS IN ELEMENTS	CES	230
C		CES	240
	SEX(J)=(SM(4000+NI)+SM(4000+NJ)+SM(4000+NK))/3.0	CES	250
800	CONTINUE	CES	260
	SEY(J)=(SM(5000+NI)+SM(5000+NJ)+SM(5000+NK))/3.0	CES	270
801	CONTINUE	CES	280
	SEXY(J)=(SM(6000+NI)+SM(6000+NJ)+SM(6000+NK))/3.0	CES	290
802	CONTINUE	CES	300
	IF(MFLAG(J).EQ.1) SEXY(J)=0.0	CES	310
	EU=E*FACTOR(J,2)/(1.0-U**2)	CES	320
	EX(J)=(SEX(J)-U*SEY(J))/(EU*(1.0-U**2))	CES	330
803	CONTINUE	CES	340
	EY(J)=(SEY(J)-U*SEX(J))/(EU*(1.0-U**2))	CES	350
804	CONTINUE	CES	360
	EXY(J)=2.0*SEXY(J)/(EU*(1.0-U))	CES	370
805	CONTINUE	CES	380
	IF(U.GT.0.21) GO TO 113	CES	390
	E1=E*FACTOR(J,2)	CES	400
113	CONTINUE	CES	410
	XS=EX(J)	CES	420
	YS=EY(J)	CES	430
	XYS=EXY(J)	CES	440
	IF(JC.NE.0) GO TO 20	CES	450
	EX(J)=0.	CES	460
	EY(J)=0.	CES	470
	EXY(J)=0.	CES	480
20	CONTINUE	CES	490
	EX(J)=EX(J)+XS	CES	500
	EY(J)=EY(J)+YS	CES	510
	EXY(J)=EXY(J)+XYS	CES	520
	CALL SMAX(XS, YS, XYS, EM1, EM2, EM3, EM4)	CLS	530
	IF(EM1.GT.0.0.AND.EM2.GT.0.0) GO TO 50	CES	540
	EM1=EM1	CES	550
	IF(EM2.LT.EM1) EM1=EM2	CES	560
50	CONTINUE	CLS	570
	CALL SMAX(EX(J), EY(J), EXY(J), EM1, EM2, EM3, EM4)	CES	580
	FACTOR(J,1)=1.0	CES	590
	FACTOR(J,2)=1.0	CES	600
	IF(U.GT.0.21) GO TO 139	CES	610
	IF(EM1.GT.0.0.AND.EM2.GT.0.0) GO TO 129	CES	620
	EM=EM1	CES	630
	IF(EM2.LT.EM1) EM=EM2	CES	640
51	IF(EM.GT.0.0) GO TO 119	CES	650
	IF(U.GT.0.21.AND.IM.GT.0) GO TO 1	CLS	660
C		CES	670
C	FIND NEW TANGENT AND SECANT MODULI FOR CONC.USING SAENZ'S EQN.	CES	680
C		CES	690
	EMR=DABS(EM/EP50)	CES	700
	FACT=(1.0+C1*(EMR**2)-2.0*C2*(EMR**3))/((1.0+C3*EMR-C1*(EMR*	CES	710
	S**2)+C2*(EMR**3))**2)	CES	720
	IF(FACT.LE.0.0) FACT=.01	CES	730

	FACTOR(J,1)=FACT	CES 740
	BACT =1.0/(1.0+C3*EMR-C1*EMR**2+1.0*C2*EMR**3)	CES 750
	FACTOR(J,2)=BACT	CES 760
129	IF(U.LT..21) GO TO 119	CES 770
139	AH=DABS(EM1)	CES 780
	BH=DABS(EM2)	CES 790
	CM=AM	CES 800
	IF(BM.GT.CM) CM=BM	CES 810
C		CES 820
C	INCLUDE STRAIN HARDENING EFFECTS FOR STEEL ELEMS.	CES 830
C		CES 840
	IF(CM-EPSYLD) 120,120,121	CES 850
120	FACTOR(J,1)=1.0	CES 860
	FACTOR(J,2)=1.0	CES 870
	GO TO 119	CES 880
121	FACTOR(J,1)=0.056	CES 890
	CKFH=0.30E+08*EPSYLD	CES 900
	CKOC=0.168E+07*(CM-EPSYLD)	CES 910
	FACTOR(J,2)=(CKFH+CKOC)/(CM*E)	CES 920
119	CONTINUE	CES 930
	IF(M.GT.0) GO TO 1	CES 940
	E=E*FACTOR(J,2)	CES 950
	IF(U.GT..21) E1=E	CES 960
	EROR=(E1-E)/E1	CES 970
	IF(MFLAG(KJ).GT.0) EROR=0.	CES 980
	SIX=SEX(J)*E/E1	CES 990
	SIY=SEY(J)*E/E1	CES1000
	SIXY=SEXY(J)*E/E1	CES1010
	IF(MFLAG(J).NE.1) GO TO 300	CES1020
	IF(INDC(J).EQ.3) GO TO 302	CES1030
	BATA=BETA(J)	CES1040
C		CES1050
C	FOR CRACKED ELEMENTS CALL STRESS TO COMPUTE CORRESPONDING	CES1060
C	STRESSES AND STRAINS.	CES1070
C		CES1080
	CALL STRESS(XS,YS,XYS,SIX,SIY,SIXY,BATA,E,U)	CES1090
	GO TO 300	CES1100
302	SIX=0.	CES1110
	SIY=0.	CES1120
	SIXY=0.	CES1130
300	IF(JC.NE.0) GO TO 30	CES1140
	SEX(J)=0.	CES1150
	SEY(J)=0.	CES1160
	SEXY(J)=0.	CES1170
30	CONTINUE	CES1180
	SEX(J)=SEX(J)+SIX	CES1190
	SEY(J)=SEY(J)+SIY	CES1200
	SEXY(J)=SEXY(J)+SIXY	CES1210
C	CALL SMAX(SIX,SIY,SIXY,XM1,XM2,XM3,XM4)	CES1220
C	WRITE(3,5)KJ,XS,YS,XYS,SIX,SIY,SIXY,XM1,XM2,XM3,XM4	CES1230
	CALL SMAX(SEX(J),SEY(J),SEXY(J),XM1,XM2,XM3,XM4)	CES1240
	IF(MFLAG(J).EQ.1) GO TO 301	CES1250
	BETA(J)=XM4*.01745329	CES1260
301	IF(MFLAG(KJ).EQ.0) GO TO 31	CES1270
	IF(NSWICH.EQ.0) GO TO 9	CES1280
	WRITE(3,16) MFLAG(KJ)	CES1290
31	CONTINUE	CES1300
	IF(IPP.EQ.1) GOTO 707	CES1310
	WRITE(3,6) KJ,EX(J),EY(J),EXX(J),SEX(J),SEY(J),SEXY(J),XM1,XM2,EM2	CES1320
	S, XM3, XM4, E, EROR	CES1330
707	CONTINUE	CES1340
C		CES1350
C	CHECK FAILURE CRITERIA FOR CONCRETE AND STEEL ELEMENTS.	CES1360
C		CES1370
	MER=0	CES1380
C	IF(MFLAG(J).EQ.1.AND.EX(J).LT.0.0.AND.EY(J).LT.0.0) GO TO 91	CES1390
	IF(MFLAG(J).GT.0) GO TO 9	CES1400
	IF(U-0.21) 3,3,4	CES1410
3	IF(MH.GT.FTENS.OR.XM2.GT.FTENS) MER=1	CES1420
	IF(FM1.LT.-0.003.OR.EM2.LT.-.003) MER=2	CES1430
	GO TO 8	CES1440
4	IF(EM1.GT.EPSYLD.OR.EM2.GT.EPSYLD) MER=3	CES1450
8	IF(MER.EQ.0) GO TO 22	CES1460
	IF(MER-2) 10,11,12	CES1470

C	WRITE(3, 13)	CES1480
10	CONTINUE	CES1490
	IFLG(IKOUNT)=J	CES1500
	IKOUNT=IKOUNT+1	CES1510
	IF(IKOUNT.GT.100) GO TO 200	CES1520
	GO TO 19	CES1530
11	WRITE(3, 14) J, EM1, EM2	CES1540
	GO TO 19	CES1550
12	WRITE(3, 15) J, EM1, EM2	CES1560
19	IBM=IBM+1	CES1570
22	MFLAG(KJ)=MER	CES1580
	IBM1=IBM	CES1590
	GOTO 123	CES1600
91	MFLAG(KJ)=0	CES1610
	WRITE(3, 17)	CES1620
	IBM1=IBM1-1	CES1630
C	CALL ELEMED(WIDE, PT, SEX, SEY, SEXY, NI, NJ, NK, ND, FC, J)	CES1640
	GO TO 123	CES1650
9	CONTINUE	CES1660
	IF(MFLAG(J).EQ.1.AND.XM1.GT.FTENS) XM1=0.0	CES1670
	IF(MFLAG(J).EQ.1.AND.XM2.GT.FTENS) XM2=0.0	CES1680
	IF(MFLAG(J).EQ.1.AND.EM1.LT.-.0038) GO TO 122	CES1690
	IF(MFLAG(J).EQ.1.AND.EM2.LT.-.0038) GO TO 122	CES1700
	GO TO 123	CES1710
122	INDC(J)=3	CES1720
	WRITE(3, 13) J, XM1, XM2, XM4	CES1730
	IFLG(IKOUNT)=J	CES1740
	IKOUNT=IKOUNT+1	CES1750
	IBM=IBM+1	CES1760
123	CONTINUE	CES1770
	IF(IBM1.GE.NE) STOP	CES1780
13	FORMAT(5X, 'NEW TENSILE CRACK')	CES1790
14	FORMAT(5X, 'COMPRESSIVE FAILURE', 15, 2E20.7)	CES1800
15	FORMAT(5X, 'STEEL YIELDED', 15, 2E20.7)	CES1810
16	FORMAT(5X, 'ELEMENT FAILED PREVIOUSLY, TYPE OF FAILURE=', 13)	CES1820
17	FORMAT(5X, 'CRACK IS CLOSING')	CES1830
18	FORMAT(5X, 'ELEMENT CRACKED IN TWO DIRECTIONS', 15, 2E20.7, 2X, F6.1)	CES1840
	NIJ(1)=NI	CES1850
	NIJ(2)=NJ	CES1860
	NIJ(3)=NK	CES1870
	IM=1	CES1880
	IF(U.GT..21) GO TO 1	CES1890
	FIS=0.7	CES1900
	IF(JC.EQ.0) FIS=0.1	CES1910
	EM=EM+FIS*EMI	CES1920
	IF(MFLAG(J).EQ.1) GOTO 149	CES1930
	IF(XM1.LE.XMAX) GO TO 159	CES1940
	XMAX=XM1	CES1950
	JOB=J	CES1960
	GO TO 159	CES1970
149	CONTINUE	CES1980
	IF(XM1.LT.ZMAX) GO TO 159	CES1990
	ZMAX=XM1	CES2000
	JAK=J	CES2010
159	GO TO 51	CES2020
1	CONTINUE	CES2030
	IF(XMAX.LT.FTENS) GOTO 610	CES2040
	WRITE(3, 611) XMAX	CES2050
611	FORMAT(2X, 'ERROR IN MAX TENSILE STRESS IN THE FIELD', F10.5)	CES2060
610	RATIO=FTENS/XMAX	CES2070
	MFLAG(JOB)=1	CES2080
	JEB=JOB	CES2090
	WRITE(3, 21) JOB, RATIO	CES2100
21	FORMAT(2X, 'ELEMENT NO.', 15, 'IS PREDICTED TO CRACK AT', F5.2, 'TIMES	CES2110
	3 THE APPLIED LOAD', /, 2X, 'IF ANOTHER CYCLE OF ITERATION IS REQUIRED	CES2120
	3 THIS PREDICTION IS VOID', /)	CES2130
	DO 201 JAN=1, 100	CES2140
	KI=IFLG(JAN)	CES2150
	IF(KI.LE.0) GO TO 201	CES2160
	IF(KI.EQ.JAK) GO TO 204	CES2170
	WRITE(3, 203) KI	CES2180
	MFLAG(KI)=0	CES2190
	IF(INDC(KI).EQ.3) MFLAG(KI)=1	CES2200
	IBM1=IBM1-1	CES2210

	GO TO 201	CES2220
204	CONTINUE	CES2230
	IF(INDC(KI).EQ.3) FACTOR(KI,1)=0.001	CES2240
	IF(INDC(KI).EQ.3) FACTOR(KI,2)=0.001	CES2250
	ANGLE =BETA(KI)/.01745329	CES2260
	WRITE(3,205) KI,ANGLE	CES2270
205	FORMAT(1X,'XXXXX ELEM. NO.',15,' IS CRACKED NOWXXXXX ANGLE OF CRACK	CES2280
	S=',F6.1)	CES2290
203	FORMAT(2X,'CRACK IN ELEMENT NO.',15,' IS POSTPONED FOR NOW')	CES2300
201	CONTINUE	CES2310
	IBM=IBMI	CES2320
	WRITE(3,609) IBM1	CES2330
609	FORMAT(1X,'TOTAL NUMBER OF CRACKED ELEMENTS=',15,/,1X,40(' '))	CES2340
	LEWIND NT1	CES2350
5	FORMAT(1X,14,6E12.4,3E13.4,F6.1)	CES2360
6	FORMAT(1X,14,10E10.3,F6.1,E10.3,F10.4)	CES2370
1601	FORMAT(1X,40X,3E12.4)	CES2380
	RETURN	CES2390
200	WRITE(3,612)	CES2400
612	FORMAT(5X,'ERROR--- NO. OF CRKD ELEMS AT THIS CYCLE.GT.100',/)	CES2410
	STOP	CES2420
	END	CES2430

	SUBROUTINE SMAX(XM, YM, XYM, XM1, XI2, XM3, XM4)	SMA 10
C		SMA 20
C	FINDS PRINCIPAL STRAINS OR STRESSES IN ANY ELEMENT.	SMA 30
C		SMA 40
	IMPLICIT REAL*3(A-H, O-Z)	SMA 50
	XI1=.5*((XM+YM)+ DSQRT((XM-YM)**2+4.*XYM**2))	SMA 60
	XI2=.5*((XM+YM)- DSQRT((XM-YM)**2+4.*XYM**2))	SMA 70
	XM3=0.5*(XM1-XI2)	SMA 80
	IF(DABS(XYID).GT.0.00001) GO TO 1	SMA 90
	XM4=0.00	SMA 100
	XI4=XI4+90.	SMA 110
	RETURN	SMA 120
1	DIR= DATAN2(2.*XYM, XM-YM)	SMA 130
	XM4=(0.5/0.0174533)*DIR	SMA 140
	XI4=XI4+90.	SMA 150
	RETURN	SMA 160
	END	SMA 170

```

SUBROUTINE JSTRES (JM,DX,DY,XI,YI,XJ,YJ,KK,NJE,CSS1,CNN,CSSF,CSJ) JST 10
C FINDS JOINT ELEMENT STRESSES AND DISPL. JST 20
C JST 30
C JST 40
  IMPLICIT REAL*8(A-H,O-Z) JST 50
  DIMENSION KK(1), JH(200,4), XI(1), XJ(1), YI(1), YJ(1), DX(1), DY(1) JST 60
  S, CSJ(1), ENS1(200) JST 70
  COMMON/BLK1/ENS1 JST 80
  COMMON/BLOK3/ DIA1, DIA2, DIA3, N1, N2, N3 JST 90
  COMMON/BLK9/IPP JST 100
  FTENS=600. JST 110
  FCOMP=-5000.0 JST 120
  DO 2 I=1,NJE JST 130
  CSS=CSJ(I) JST 140
  IT = JH(I,4) JST 150
  JT = JH(I,3) JST 160
  IB = JH(I,1) JST 170
  JB = JH(I,2) JST 180
  DL = ((XJ(I)-XI(I))**2+ (YJ(I)-YI(I))**2)**.5 JST 190
  A = (XJ(I)-XI(I))/DL JST 200
  B = (YJ(I)-YI(I))/DL JST 210
  UXI = DX(IT) - DX(IB) JST 220
  UYI = DY(IT) - DY(IB) JST 230
  UXJ = DX(JT) - DX(JB) JST 240
  UYJ = DY(JT) - DY(JB) JST 250
  UXID = UXI *A + UYI *B JST 260
  UYID = (-1.)*B*UXI + UYI *A JST 270
  UXJD = UXJ *A + UYJ *B JST 280
  UYJD = (-1.)*B*UXJ + UYJ *A JST 290
  ENS = (.5)*(UXID + UXJD) JST 300
  ENJ = (.5)*(UYID + UYJD) JST 310
  SS=0.002 JST 320
  CNND=CNN JST 330
  IF(KK(I).EQ.2.OR.KK(I).EQ.4) CNND=0.0 JST 340
  IF(ENJ.LT.0.0.AND.KK(I).EQ.2) KK(I)=1 JST 350
  IF(ENJ.LT.0.0.AND.KK(I).EQ.4) KK(I)=3 JST 360
C FIND BOND AND DOWEL DISPLACEMENTS AND STRESSES ALSO CHECK JST 370
C FAILURE CRITERIA JST 380
C JST 390
C JST 400
  SLP=DABS(ENS) JST 410
  IF(SLP.EQ.0.) GO TO 72 JST 420
  SIXS=(ENS/DABS(ENS))*(1.95E+06*SLP-2.35E+09*SLP**2+1.39E+12*SLP**3 JST 430
  S - .33E+15*SLP**4) JST 440
  SIXS=0.0 JST 450
  SIXN=CNND*ENJ JST 460
  IF(KK(I).GT.2) GO TO 70 JST 470
  IF(SLP.EQ.0.0) GO TO 72 JST 480
  SIXS=(ENS/SLP )*(1.95E+06*SLP-2.35E+09*SLP**2+1.39E+12*SLP**3 JST 490
  S - .33E+15*SLP**4) JST 500
  SIK=DIA1 JST 510
  IF(1.GT.N1.AND.1.LE.N2) SIK=DIA2 JST 520
  IF(1.GT.N2.AND.1.LE.N3) SIK=DIA3 JST 530
  CSJS=DABS(SIXS/SLP) *SIK*3.14159 JST 540
  ERR=(CSS-CSJS)/CSS JST 550
72 CONTINUE JST 560
  IF(KK(I).EQ.4) GO TO 71 JST 570
  IF(KK(I).GT.1) GO TO 70 JST 580
  KK(I)=1 JST 590
  IF(SIXN.GT.FTENS) KK(I)=2 JST 600
  IF(SIXN.LT.FCOMP) KK(I)=2 JST 610
  IF(SLP.GT.SS) KK(I)=3 JST 620
70 IF(KK(I).EQ.2.AND.SLP.GT.SS) KK(I)=4 JST 630
  IF(KK(I).EQ.3.AND.SIXN.GT.FTENS) KK(I)=4 JST 640
  IF(KK(I).EQ.3.AND.SIXN.LT.FCOMP) KK(I)=4 JST 650
  FIS=0.3 JST 660
  SLP=DABS(ENS)+FIS*DABS(ENS-ENS1(I)) JST 670
  IF(SLP.GT.002) SLP=.002 JST 680
  IF(KK(I).GT.2) GO TO 71 JST 690
  CSJ(I)=3.14159*SIK*(1.95E+06-2.35E+09*SLP+1.39E+12*SLP**2-.33E+15 JST 700
  S *SLP**3) JST 710
71 CONTINUE JST 720
  IF(IPP.EQ.1) GO TO 1 JST 730

```

```
      KIKI=KK(I)
      GO TO (101,102,103,104),KIKI
101  WRITE(6,11) I,ENJ,ENS,SIXN,SIXS,ERR
      GO TO 1
102  WRITE(6,12) I,ENJ,ENS,SIXN,SIXS,ERR
      GO TO 1
103  WRITE(6,13) I,ENJ,ENS,SIXN,SIXS
      GO TO 1
104  WRITE(6,14) I,ENJ,ENS,SIXN,SIXS
1     ENS1(I)=ENS
2     CONTINUE
11    FORMAT(1X,16,4E12.5,1F12.5)
12    FORMAT(1X,16,4E12.5,1F12.5,' JOINT DOWEL FAILURE')
13    FORMAT(1X,16,4E12.5,' JOINT YIELDED')
14    FORMAT(1X,16,4E12.5,' JOINT FAILED')
      RETURN
      END
```

JST 740
JST 750
JST 760
JST 770
JST 780
JST 790
JST 800
JST 810
JST 820
JST 830
JST 840
JST 850
JST 860
JST 870
JST 880
JST 890
JST 900

	SUBROUTINE STRTF(IS, JS, ANG, SAREA, SKS, ALS, EI)	STR 10
C	COMPUTE STIRRUP STIFF.	STR 20
C	IMPLICIT REAL*8(A-H, O-Z)	STR 30
C	COMMON SM(58000)	STR 40
	DIMENSION EI(2), SKS(4,4)	STR 50
	X=(SM(2*IS-1)-SM(2*JS-1))	STR 60
	Y=(SM(2*IS)-SM(2*JS))	STR 70
	ALS=DSQRT(X**2+Y**2)	STR 80
	STIF=EI(2)*SAREA/ALS	STR 90
	DANG=3.1416/2.0	STR 100
	IF(X.EQ.0.) ANG=DANG	STR 110
	IF(X.EQ.0.) GO TO 2	STR 120
	ANG=ATAN(Y/X)	STR 130
2	CONTINUE	STR 140
	IF(ANG.LT.0./0) ANG=ANG+3.1416	STR 150
	CO=DCOS(ANG)	STR 160
	S=DSIN(ANG)	STR 170
	SKS(1,1)=STIF*CO*CO	STR 180
	SKS(1,2)=-STIF*CO*CO	STR 190
	SKS(1,3)=STIF*CO*S	STR 200
	SKS(1,4)=-SKS(1,3)	STR 210
	SKS(2,1)=SKS(1,2)	STR 220
	SKS(2,2)=SKS(1,1)	STR 230
	SKS(2,3)=-SKS(1,3)	STR 240
	SKS(2,4)=SKS(1,3)	STR 250
	SKS(3,1)=SKS(1,3)	STR 260
	SKS(3,2)=-SKS(1,3)	STR 270
	SKS(3,3)=STIF*S*S	STR 280
	SKS(3,4)=-SKS(3,3)	STR 290
	SKS(4,1)=-SKS(1,3)	STR 300
	SKS(4,2)=SKS(1,3)	STR 310
	SKS(4,3)=-SKS(3,3)	STR 320
	SKS(4,4)=SKS(3,3)	STR 330
	XIS=SM(2*IS-1)	STR 340
	XJS=SM(2*JS-1)	STR 350
	YIS=SM(2*IS)	STR 360
	YJS=SM(2*JS)	STR 370
	WRITE(6,1) IS, JS, XIS, YIS, XJS, YJS, SAREA, ALS	STR 380
1	FORMAT(5X,2I5,6F7.2)	STR 390
	RETURN	STR 400
	END	STR 410
		STR 420
		STR 430

	SUBROUTINE ADSTRP(NSTR,NB)	ADS 10
C		ADS 20
C	ADD STIRRUP STIFFNESSES TO THE GLOBAL STIFFNESS MATRIX	ADS 30
C		ADS 40
	IMPLICIT REAL*8(A-H,O-Z)	ADS 50
	COMMON SM(50000)	ADS 60
	DIMENSION SKS(4,4) ,NP(4) ,RAT(150)	ADS 70
	COMMON/BLK2/RAT	ADS 80
	DO 405 IZ=1,NSTR	ADS 90
	READ (2) IS,JS,ANG,SAREA,((SKS(KI,MI)),KI=1,4),MI=1,4),	ADS 100
	& (NP(I),I=1,4),ALS	ADS 110
	DO 406 IN=1,4	ADS 120
	IF(NP(IN).EQ.0) GO TO 406	ADS 130
	DO 407 IM=IN,4	ADS 140
	IF(NP(IM).EQ.0) GO TO 407	ADS 150
	IF(NP(IN)-NP(IM)) 408,409,409	ADS 160
409	K=(NP(IM)-1)*NB+NP(IN)	ADS 170
	SM(K)=SM(K)+SKS(IN,IM)*RAT(IZ)	ADS 180
	GO TO 407	ADS 190
408	K=(NP(IN)-1)*NB+NP(IM)	ADS 200
	SM(K)=SM(K)+SKS(IN,IM)*RAT(IZ)	ADS 210
407	CONTINUE	ADS 220
406	CONTINUE	ADS 230
405	CONTINUE	ADS 240
	REWIND 2	ADS 250
	RETURN	ADS 260
	END	ADS 270

	SUBROUTINE STSTRS(JC,EI,EP SYLD, FN, NSTR)	STS 10
C		STS 20
C	CALCULATE STIRRUP STRAINS AND STRESSES	STS 30
C		STS 40
C	FIND STRAINS AND STRESSES IN STIRRUPS.	STS 50
	IMPLICIT REAL*8(A-H,O-Z)	STS 60
	DIMENSION STS(150),EI(2),FN(1),SKS(4,4),UI(4),NP(4),RAT(150)	STS 70
	COMMON/BLK2/RAT	STS 80
	COMMON/BLK9/IPP	STS 90
	DO 1 J=1,NSTR	STS 100
	READ(2)IS,JS,ANG,SAREA,((SKS(KI,MI),KI=1,4),MI=1,4),	STS 110
	C(NP(1),I=1,4),ALS	STS 120
	DO 2 K=1,4	STS 130
	UI(K)=0.0	STS 140
	LL=NP(K)	STS 150
	IF(LL.EQ.0) GO TO 2	STS 160
	UI(K)=FN(LL)	STS 170
2	CONTINUE	STS 180
	ANGLE=0.0	STS 190
	IF(ANG.GT.1.57081633) ANGLE=3.14159265	STS 200
	SI=UI(1)*DCOS(ANGLE+ANG)+UI(3)*DSIN(ANGLE+ANG)	STS 210
	SJ=UI(2)*DCOS(ANGLE+ANG)+UI(4)*DSIN(ANGLE+ANG)	STS 220
	STRN=(SJ-SI)/ALS	STS 230
	IF(JC.NE.0) GO TO 20	STS 240
	STS(J)=0.0	STS 250
20	CONTINUE	STS 260
	IF(ANG.GT.1.57081633) STRN=(SI-SJ)/ALS	STS 270
	ANG=ANG*57.29578	STS 280
	ANGLE=ANGLE*57.29578	STS 290
	STS(J)=STS(J)+STRN	STS 300
	STRS=EI(2)*STS(J)	STS 310
	STRINC=EI(2)*STRN	STS 320
	IF(DABS(STS(J)).GT.EPSYLD) GO TO 22	STS 330
	IF(IPP.EQ.1) GO TO 1	STS 340
	WRITE(6,21) J,STRN,STRINC,STS(J),STRS,ANG	STS 350
	GO TO 1	STS 360
22	STRINC=0.0	STS 370
	STRS=EP SYLD*EI(2)	STS 380
	IF(IPP.EQ.1) GO TO 3	STS 390
	WRITE(6,23) J,STRN,STRINC,STS(J),STRS,ANG	STS 400
3	CONTINUE	STS 410
	RAT(J)=.0001	STS 420
21	FORMAT(1X,15,6E14.7)	STS 430
23	FORMAT(1X,15,5E14.7,5X,'STIRRUP YIELDED')	STS 440
1	CONTINUE	STS 450
	REWIND 2	STS 460
	RETURN	STS 470
	END	STS 480

```

SUBROUTINE FSIORR(S,PT,E,U,ARR,WIDTH,DATA,INPC,KJJ)
C
C FIND MODIFIED STIFFNESSES OF CRACKED ELEMENTS.
C
      IMPLICIT REAL*8(A-H,O-Z)
      DIMENSION D(3,3),R(6,6),P(6,6),T(3,3),S(6,6),PT(9),INPC(1)
      DO 1 I=1,3
      DO 1 J=1,3
      D(I,J)=0.0
      R(I,J)=0.0
1     CONTINUE
      EU=E*WIDTH/(1.0-U**2)
      D(1,1)=EU
      D(1,2)=EU *U/1000.
      D(2,1)=U*EU/1000.0
      D(2,2)=EU/1000.0
      D(3,3)=EU*(1.-U)/(2.0*1000.0)
      C=DCOS(DATA)
      SI=DSIN(DATA)
      T(1,1)=C*C
      T(1,2)=SI*SI
      T(1,3)=-2.C*C*SI
      T(2,1)=T(1,2)
      T(2,2)=T(1,1)
      T(2,3)=-T(1,3)
      T(3,1)=SI*C
      T(3,2)=-T(3,1)
      T(3,3)=T(1,1)-T(1,2)
      DO 2 JJ=1,3
      DO 2 II=1,3
      R(JJ,II)=0.0
      DO 2 KK=1,3
      R(JJ,II)=R(JJ,II)+T(JJ,KK)*D(KK,II)
2     CONTINUE
      DO 3 JJ=1,3
      DO 3 II=1,3
      D(JJ,II)=0.0
      DO 3 KK=1,3
      D(JJ,II)=D(JJ,II)+R(JJ,KK)*T(II,KK)
3     CONTINUE
      DO 4 II=1,6
      DO 4 JJ=1,6
      S(JJ,II)=0.0
      P(JJ,II)=0.0
4     CONTINUE
      DO 110 II=1,3
      DO 110 JJ=1,3
      KK=3*(II-1)+JJ
      P(II,JJ)=PT(KK)
      NJJ=JJ+3
      NJJ=JJ+3
      P(IIJ,NJJ)=P(II,JJ)
110    CONTINUE
      S(2,2)=D(1,1)
      S(2,3)=D(1,3)
      S(2,5)=D(1,3)
      S(2,6)=D(1,2)
      S(3,2)=D(3,1)
      S(3,3)=D(3,3)
      S(3,5)=D(3,3)
      S(3,6)=D(3,2)
      S(5,2)=D(3,1)
      S(5,3)=D(3,3)
      S(5,5)=D(3,3)
      S(5,6)=D(3,2)
      S(6,2)=D(2,1)
      S(6,3)=D(2,3)
      S(6,5)=D(2,3)
      S(6,6)=D(2,2)
      ARR=4.0*ARR
      DO 5 JJ=1,6
      DO 5 II=1,6
      R(JJ,II)=0.0
      FSM 10
      FSM 20
      FSM 30
      FSM 40
      FSM 50
      FSM 60
      FSM 70
      FSM 80
      FSM 90
      FSM 100
      FSM 110
      FSM 120
      FSM 130
      FSM 140
      FSM 150
      FSM 160
      FSM 170
      FSM 180
      FSM 190
      FSM 200
      FSM 210
      FSM 220
      FSM 230
      FSM 240
      FSM 250
      FSM 260
      FSM 270
      FSM 280
      FSM 290
      FSM 300
      FSM 310
      FSM 320
      FSM 330
      FSM 340
      FSM 350
      FSM 360
      FSM 370
      FSM 380
      FSM 390
      FSM 400
      FSM 410
      FSM 420
      FSM 430
      FSM 440
      FSM 450
      FSM 460
      FSM 470
      FSM 480
      FSM 490
      FSM 500
      FSM 510
      FSM 520
      FSM 530
      FSM 540
      FSM 550
      FSM 560
      FSM 570
      FSM 580
      FSM 590
      FSM 600
      FSM 610
      FSM 620
      FSM 630
      FSM 640
      FSM 650
      FSM 660
      FSM 670
      FSM 680
      FSM 690
      FSM 700
      FSM 710
      FSM 720
      FSM 730

```



```
DO 5 KK=1,6
R(JJ, II)=R(JJ, II)+S(JJ, KK)*P(KK, II)
5 CONTINUE
DO 6 JJ=1,6
DO 6 II=1,6
S(JJ, II)=0.0
DO 6 KK=1,6
6 S(JJ, II)=S(JJ, II)+P(KK, JJ)*R(KK, II)/AR
CONTINUE
INDC(IJJ)=1
RETURN
END
```

```
FSH 740
FSH 750
FSH 760
FSH 770
FSH 780
FSH 790
FSH 800
FSH 810
FSH 820
FSH 830
FSH 840
FSH 850
```

C	SUBROUTINE STRESS(XS,YS,XYS,SIX,SIY,SIXY,BATA,E,U)	STR 10
C	COMPUTE STRAINS IN CRACKED ELEMENTS.	STR 20
C		STR 30
	IMPLICIT REAL*8(A-H,O-Z)	STR 40
	DIMENSION D(3,3),R(3,3),T(3,3)	STR 50
	DO 1 I=1,3	STR 60
	DO 1 J=1,3	STR 70
	D(I,J)=0.0	STR 80
	R(I,J)=0.0	STR 90
1	CONTINUE	STR 100
	EU=E/(1.0-U**2)	STR 110
	D(1,1)=EU	STR 120
	C=DCOS(BATA)	STR 130
	S=BSIN(BATA)	STR 140
	T(1,1)=C*C	STR 150
	T(1,2)=S*S	STR 160
	T(1,3)=-2.0*C*S	STR 170
	T(2,1)=T(1,2)	STR 180
	T(2,2)=T(1,1)	STR 190
	T(2,3)=-T(1,3)	STR 200
	T(3,1)=S*C	STR 210
	T(3,2)=-T(3,1)	STR 220
	T(3,3)=T(1,1)-T(1,2)	STR 230
	DO 2 JJ=1,3	STR 240
	DO 2 II=1,3	STR 250
	R(JJ,II)=0.0	STR 260
	DO 2 KK=1,3	STR 270
	R(JJ,II)=R(JJ,II)+T(JJ,KK)*D(KK,II)	STR 280
2	CONTINUE	STR 290
	DO 3 JJ=1,3	STR 300
	DO 3 II=1,3	STR 310
	D(JJ,II)=0.0	STR 320
	DO 3 KK=1,3	STR 330
	D(JJ,II)=D(JJ,II)+R(JJ,KK)*T(II,KK)	STR 340
3	CONTINUE	STR 350
	SIX=D(1,1)*XS+D(2,1)*YS+D(3,1)*XYS	STR 360
	SIY=D(1,2)*XS+D(2,2)*YS+D(3,2)*XYS	STR 370
	FIY=D(1,3)*XS+D(2,3)*YS+D(3,3)*XYS	STR 380
	SIXY=FIY	STR 390
	RETURN	STR 400
	END	STR 410
		STR 420

	SUBROUTINE SAHER(FN,EX,EY,EXY,SEX,SEY,SEXY,NR,FACTOR,UI,NV	SAM 10
	,NT1,NE,IFLAG,FTENS)	SAM 20
C	COMPUTE AND STORE NODAL STRESSES AND STRAINS.	SAM 30
C	IMPLICIT REAL*3(A-H,O-Z)	SAM 40
	COMMON SH(5000)	SAM 50
	DIMENSION NP(6),S(6,6),PT(9)	SAM 60
	DIMENSION FN(1),EX(1),EY(1),EXY(1),SEX(1),SEY(1),SEXY(1),UI(6),	SAM 70
	NI(3),IFLAG(1),FACTOR(318,2)	SAM 80
	DIMENSION IO(18)	SAM 90
	DO 1 J=1,7000	SAM 100
	CX(J)=0.0	SAM 110
	CONTINUE	SAM 120
	FTONS=1.2*FTENS	SAM 130
	DO 3 J=1,NE	SAM 140
	READ(NT1)(NP(I),I=1,6),((S(MM,MM),MM=1,6),IEI=1,6),((PT(L),L=1,9),	SAM 150
	I A,E,U,NI,HJ,NK,ARR	SAM 160
	IF(IFLAG(J).GT.0) ARR=0.0	SAM 170
	IF(IFLAG(J).GT.0) U=0.0	SAM 180
	DO 2 K=1,6	SAM 190
	UI(K)=0.0	SAM 200
	LL = NP(K)	SAM 210
	IF(LL.EQ.0) GO TO 2	SAM 220
	UI(K)=FN(LL)	SAM 230
2	CONTINUE	SAM 240
	XS=(UI(1)*PT(4)+UI(2)*PT(5)+UI(3)*PT(6))/A	SAM 250
	EX(J)=XS	SAM 260
	YS=(UI(4)*PT(7)+UI(5)*PT(8)+UI(6)*PT(9))/A	SAM 270
	EY(J)=YS	SAM 280
	XYS=(UI(1)*PT(7)+UI(2)*PT(8)+UI(3)*PT(9)+UI(4)*PT(4)+UI(5)	SAM 290
)*PT(5)+UI(6)*PT(6))/A	SAM 300
	EXY(J)=XYS	SAM 310
	EU=E*FACTOR(J,2)/(1.0-U**2)	SAM 320
	SIX=EU*(XS+U *YS)	SAM 330
	SEX(J)=SIX	SAM 340
	IF(IFLAG(J).EQ.1.AND.SIX.GT.FTONS) SIX=FTONS	SAM 350
	SIY=EU*(U *XS+YS)	SAM 360
	SEY(J)=SIY	SAM 370
	IF(IFLAG(J).EQ.1.AND.SIY.GT.FTONS) SIY=FTONS	SAM 380
	SIXY=EU*(1.0-U)*XYS/2.0	SAM 390
	SEXY(J)=SIXY	SAM 400
	IF(IFLAG(J).GT.0) SIXY=0.0	SAM 410
	HI(1)=NI	SAM 420
	HI(2)=NJ	SAM 430
	HI(3)=NK	SAM 440
	DO 10 NMI=1,3	SAM 450
	IEC=4*HI(NMI)-3	SAM 460
	SH(IEC)=SH(IEC)+ARR	SAM 470
	SH(IEC+1)=SH(IEC+1)+SIX*ARR	SAM 480
	SH(IEC+2)=SH(IEC+2)+SIY*ARR	SAM 490
	SH(IEC+3)=SH(IEC+3)+SIXY*ARR	SAM 500
10	CONTINUE	SAM 510
3	CONTINUE	SAM 520
	DO 20 I=1,NH	SAM 530
40	IEC=4*I-3	SAM 540
	IF(SH(IEC).EQ.0.0) SH(IEC)=1000.0	SAM 550
	SH(4000+I)=SH(IEC+1)/SH(IEC)	SAM 560
	SH(5000+I)=SH(IEC+2)/SH(IEC)	SAM 570
	SH(6000+I)=SH(IEC+3)/SH(IEC)	SAM 580
20	CONTINUE	SAM 590
	REWIND NT1	SAM 600
	RETURN	SAM 610
	END	SAM 620
		SAM 640

BIBLIOGRAPHY

- [1] Georg Wästlund, "Untersuchungen über die Festigkeit von Beton bei Belastungen, welche örtlich auf die Oberfläche sowie an Schleifen und Abbiegungen von Bewehrungseisen wirken;" Dissertation presented to the Royal Institute of Technology (KTH) in Stockholm in fulfillment of the requirements for the Degree of Doctor of Technology. Tryckeri Aktiebolaget Thule, Stockholm. 1934. (97)
- [2] Georg Wästlund, "Om armering av vinkelformade betongkonstruktioner;" (Reinforcement of angle-shaped concrete structures.) Betong, No. 1, Stockholm 1935, pp 22-35. (97)
- [3] Georg Wästlund, "Untersuchungen über die Bewehrung von winkelförmigen Eisenbetonkonstruktionen;" Beton und Eisen, Vol. 35, Heft 13, July 5, Berlin, 1936, pp 222-227. (97)
- [4] D.B. Gumensky, "Concrete Corners in tension", Engineering News Record, Vol. 123, New York, September 1939, p. 57.
- (5) Hrennikoff, A., "Solution of Problems in Elasticity by the Frame Work Method", Journal of Applied Mechanics, 8, No. 4, Dec. 1941.
- (6) C.J. Posey, O. Kofoid, "Reinforced Concrete Corners in Tension", ACI Journal Proceedings, Vol. 40, Detroit, September, 1943, pp. 41-52.
- (7) McHenry, D. "A Lattice Analogy for the Solution of Stress

- Problems", Journal of the Institute of Civil Engineers, Dec. 1943, pp. 59-82.
- [8] Bishara, A., "Etude du Problème de l'adhérence dan le béton armé", Cahier du Centre Scientifique et Technique du Batiment, Cahier 127, Paris, 1951 (93).
- [9] Brice, L.D., "Adhérence des barres d'acier dans le beton", Annales, L'Institut Technique du Bâtiment et des Travaux Publics, Paris, No. 179, 1951, (93).
- [10] University of Illinois, "Engineering Experimental Station Bulletin", No. 399, 1951. (93).
- (11) Mains, R.M., "Measurement of the Distribution of Tensile and Bond Stresses along Reinforcing Bars". ACI Journal, Proc. Vol. 48 No. 3, Nov. 1951, pp. 225-252.
- (12) Cowan, H.J., "The Strength of Plain, Reinforced and Prestressed Concrete Under the Action of Combined Stresses with Particular Reference to the Combined Bending and Torsion of Rectangular Sections." Magazine of Concrete Research, Vol. 5, No. 14, Dec. 1953.
- (13) Hognestad, E., Hanson, N.W., McHenry, D. "Concrete Stress Distribution in Ultimate Strength Design". ACI Journal Proc. Vol. 52, No. 4, Dec. 1955 pp. 456-479.
- (14) ACI-ASCE Committee 327 "Ultimate Strength Design", ACI Journal, Proc. Vol. 52, Jan. 1956, pp. 505-524.
- (15) Turner, M.J., Clough, R.W., Martin, H.C., Top, L.J., "Stiffness and Deflection Analysis of Complex Structures". Journal of the Aeronautical Sciences, Vol. 23, No. 9, Sept. 1956.

- (16) Rüsçh, H., "Researches for a General Flexure Theory for Structural Concrete", ACI Journal, Proc. Vol. 57 No. 1, July 1960, pp. 1-28.
- (17) Clough, R.W., "The Finite Element in Plane Stress Analysis". Proc. of ASCE Second Conference on Electronic Computation, Pittsburgh, Sept. 1960, pp. 345-378.
- (18) Blume, J.A., Newmark, N.M., Corning, L.H., "Design of Multi-Storey Reinforced Concrete Buildings for Earthquake Motions", Published by the Portland Cement Association, 1961, pp. 96-109.
- [19] Östlund, L., "The Influence of the bending Radius and Concrete Cover for Deformed Bars on the Risk of Splitting Failure in Reinforced Concrete Structures". The Royal Institute of Technology (KTH), Stockholm 1963, 92 pp. (97).
- (20) Robinson, J.R., "Piers, Abutments and Formwork for Bridges" Crosby Lockwood & Son Ltd., London 1963, p. 129.
- (21) Clough, R.W., Wilson, E.L., "Stress Analysis of Gravity Dam by the Finite Element Method", Rilem Bulletin No. 19 June 1963.
- (22) Desayi, P., Krishnan, S. "Equation for the stress-strain Curve of Concrete" ACI Journal, Proc. Vol. 61, No. 3, March 1964, pp. 345, 350.
- (23) Sims, F.W., Rhodes, J.H., Clough, R.W., "Cracking on Norfolk Dam". ACI Journal, Proc. Vol. 61, No. 3, March 1964. pp. 265-285.

- (24) Saenz, L.P., Discussion of "Equation for the Stress-Strain Curve of Concrete" by P. Desayi, and S. Krishnan, ACI, Journal, Proc., Vol. 61, No. 9, Sept. 1964, pp. 1227-1248.
- (25) Base, A.F., Przemieniecki, J.S., ed. et al. "Matrix Methods in Structural Mechanics", Proc. of the Conference held at Wright Patterson Air Force Base, Ohio, 1965, AFFDL-TR-66-80.
- (26) Gere, J.M., Weaver, W., "Analysis of Framed Structures" D. Van Nostrand, Princeton, New Jersey, 1965.
- (27) Broms, B.B., "Stress distribution in Reinforced Concrete Members with Tension Cracks", ACI Journal, Proceedings, Sept. 1965, pp. 1095-1108.
- (28) Leonhardt, F., Walther R., "Contribution to the Treatment of Shear in Reinforced Concrete", Technical translation 1172, National Research Council of Canada, Translated by J.P. Vesschuren and J.G. MacGregor, Ottawa, 1965.
- (29) Struman, G.M., Shah, S.P. Winter, G. "Effect of Flexural Strain Gradients on Microcracking and Stress-Strain Behavior of Concrete," ACI Journal, Proc. Vol. 62, No. 7 July 1965, pp. 805-822.
- (30) Bresler, B., Bertero, V., "Reinforced Concrete Prism under repeated Load", Rilem Symposium on the Effects of Repeated Loading on Materials and Structural Elements, Mexico, 1966.

- (31) Rubinstein, M.F., "Matrix Computer Analysis of Structures". Prentice-Hall Inc., Englewood Cliffs, N.J., 1966.
- (32) Hughes, B.P., Chapman, G.P., "The Complete Stress-Strain Curve for Concrete in Tension" Rilem Bull., News Series No. 30, March 1966, pp. 95-97.
- (33) Krefeld, W.J., Thurston, C.W., "Contribution of longitudinal Steel to Shear Resistance of Reinforced Concrete Beams", ACI Journal Proc. Vol. 63, March 1966, pp. 325-344.
- (34) Krefeld, W.J., Thurston, C.W., "Studies on the Shear Diagonal Tension Strength of Simply Supported Reinforced Concrete Beams", ACI Journal, Proc. Vol. 63, April 1966, pp. 451-476.
- (35) Perry, E.S., Thompson, J.N., "Bond Stress Distribution on Reinforcing Steel in Beams and Pull-out Specimens". ACI Journal, Proc. Vol. 63 No. 8, August 1966, pp. 865-875.
- (36) Drysdale, R.G., "The Behaviour of Slender Reinforced Concrete Columns Subjected to Biaxial Bending", Ph.D. Thesis, Department of Civil Eng. University of Toronto, 1967.
- (37) Zienkiewicz, O.C., Cheung, Y.K. "The Finite Element Method in Structural and Continuum Mechanics", McGraw-Hill, Book Co. London, 1967.

- (38) Bresler, B., MacGregor, J.G., "Review of the Structural Division, ASCE, Vol. 93, No. St. 1, February 1967, pp. 343-373.
- (39) Ngo, D., Scordelis, A.C. "Finite Element Analysis of Reinforced Concrete Beams", ACI Journal, Proceeding, Vol. 64, No. 3, March 1967, pp. 152-163.
- (40) Clarck, L.E., Gerstle, K.H., Tulin, L.G., "Effect of Strain Gradient on the stress-strain curve of Mortar and Concrete". ACI Journal, Proc. Vol. 64 No. 9, Sept. 1967, pp. 580-586.
- (41) Hanson, N.W., Connor, H.W. "Seismic Resistance of reinforced concrete beam-column joints", Journal of the structural Division of the American Society of Civil Engineers, Oct. 1967, pp. 533-560.
- [42] Berbe, L. et al ed. "Matrix Methods in Structural Mechanics". Proceedings of the Second Conference held at the Wright-Patterson Air Force Base. Ohio 1968. AFFDL-TR-68-150.
- (43) Przemieniecki, J.S., "Theory of Matrix Structural Analysis". McGraw-Hill Book Co. New York, 1968.
- (44) Taylor, H.P.J., "Shear Stresses in Reinforced Concrete Beams without Shear Reinforcement", C & CA London, Report TRA 407, Feb. 1968.
- (45) Zienkiewicz, O.C., Valliapan, S, King, I.P., "Stress Analysis of Rock as a (No Tension) Material" Geotechnique 18,

March 1968, pp. 56-66.

- (46) Goodman, R.E., Taylor, R.L., Brekke, T.L., "A Model for the Mechanics of Jointed Rocks" Journal of Soil Mechanics and Foundation Division, ASCE, Vol. No. SM3, Proc. paper S329 May 1968, pp. 637-659.
- (47) Nowlen, W.J., "Influence of Aggregate Properties on the Effectiveness of Interlock Joints in Concrete Pavements," PCA Research and Development Bulletin, D 124, Chicago, May 1968.
- (48) Nilson, A.H., "Non-Linear Analysis of Reinforced Concrete by the Finite Element Method", ACI Journal, Proc. Vol. 65 No. 9, Sept. 1968, pp. 757-766.
- (49) Fenwick, R.C., Paulay, T.O., "Mechanism of Shear Resistance of Concrete Beams", Journal of the Structural Division, ASCE, Vol. 94, No. ST10, Oct. 1968, pp. 2325-2350.
- (50) Beaufait, F., Williams, R.R., "Experimental Study of Reinforced Concrete Frames subjected to alternating sway forces", Journal of the American Concrete Institute, Nov. 1968, pp. 980-984.
- (51) Nilson, A.H., "Finite Element Study of Reinforced Concrete", Ph.D. thesis, University of California at Berkeley, Dec. 1968.
- (52) B.N. Boughton, "Reinforced Concrete Detailers' Manual", Crosby Lockwood & Son Ltd., London, 1969.
- (53) Gergely, P. "Splitting Cracks along the Main Reinforcement in Concrete Members", Research Report, Dept. of Structural

Engineering, Cornell University, Ithaca, New York,
April, 1969.

- (54) Newman, K., Newman, J.B., "Failure Theories and Design Criteria for Plain Concrete", International Conference, Southampton, England, Apr. 1969.
- (55) Gallagher, R.H., Yamada, Y., Ojen, J.T., ed., "Recent advances in Matrix Methods of Structural Analysis and Design". Proceedings of the U.S.-Japan Seminar held at Tokyo in August 1969. The University of Alabama Press.
- (56) Kupfer, H., Hilsdorf, H.K., Hüsich, H. "Behaviour of Concrete under Biaxial Stresses" ACI Journal, Proc. Vol. 66, No. 8, Aug. 1969, pp. 656-666.
- (57) Rowan, W.H., Hackett, R.M., ed., "Proceedings of the Symposium on Application of Finite Element Methods in Civil Engineering", Nashville Tennessee Nov. 1969.
- (58) Swann, R.A., "Flexural Strength of Corners of Reinforced Concrete Portal Frames", Technical Report TRA/434, Cement and Concrete Association, London, Nov. 1969, 14 pp.
- (59) Holand, I., Bell, K., "Finite Element Methods in Stress Analysis", Tapir, Technical University of Norway, Trondheim, 1970.
- (60) Franklin, H., "Nonlinear Analysis of Reinforced Concrete Frames and Panels", Ph.D. Thesis, University of California at Berkeley, 1970.
- (61) Loeber, P.J., "Shear Transfer by Aggregate Interlock",

- M.Sc. Thesis, Univ. of Canterbury, Christchurch, New Zealand, 1970.
- (62) Nilsson, I.H.E., "Reinforcement detailing of T-Joints in reinforced concrete, in Swedish" Laborations Program for V3. Internskrift 70-18, 1970, 17 pp.
- (63) "Standard Method of Detailing Reinforced Concrete", Report by the ~~Joint~~ Committee of the Concrete Society and the Institution of Structural Engineers, London 1970, p. 14.
- (64) Taylor, H.P.J., "Further Tests to Determine Shear Stresses in Reinforced Concrete Beams", C & CA, London, Report, TRA 438, Feb. 1970.
- (65) Davis, J.C.D.T., "Detailing of Reinforced Concrete Corners", M.Sc. Thesis, University of Nottingham, England, Sept. 1970, 250 pp.
- (66) Swann, R.A., "The Flexural Strength of Reinforced Concrete Frame Corners", Precast Concrete (London), V. 1, No. 10 Oct. 1970, pp. 268-272.
- (67) Taylor, H.P.J., "Investigation of the Forces carried across Cracks in Reinforced Concrete Beams in Shear Interlock of Aggregate", C & CA, London, Report 42.447, Nov. 1970.
- (68) Ngo, D., Franklin, H.A., Scordelis, A.C., "Finite Element Study of Reinforced Concrete Beams with Diagonal Tension Cracks". Report UC-SESM 70-19, College of Engineering, Office of Research Services, Univ. of California at Berkeley, Dec. 1970.

- (69) American Concrete Institute, "Building Code Requirements for Reinforced Concrete (ACI-318-71)". Detroit, 1971
- (70) Meek, J.L., "Matrix Structural Analysis", McGraw-Hill Book Co., New York, 1971.
- (71) Megget, L.M., "Anchorage of Beam Reinforcement in Seismic Resistant Reinforced Concrete Frames", Master of Engineering Report. University of Canterbury, New Zealand, 1971, 67 pp. (See also Megget, L.M. and Park, R., "Reinforced Concrete Exterior Beam-Column Joints Under Seismic Loading", New Zealand Engineering, Vol. 26, No. 11, 1971, pp. 341-353).
- (72) Mufti, A.A., Mirza, M.S., McCutcheon, J.O., Houde, J., "A Finite Element Analysis of Non-Linear Behaviour of Concrete Members". Proc. Third Canadian Congress of Applied Mechanics, Univ. of Calgary, 1971, pp. 213-214.
- (73) Youssef, A.A., "Inelastic Bending of Rectangular Plates and Prestressed Concrete slabs", M.Eng. Thesis, Structural Concrete Series No. 71-5, Dept. of Civil Engineering and Applied Mechanics, McGill University, 1971.
- (74) B. Mayfield, F.K. Kong, A. Bennison, JCDT. Davis, "Corner Joint Details in Structural Lightweight Concrete" ACI Journal, Proceedings, Vol. 68, No. 5, Detroit, May 1971, pp. 366-372.
- (75) Hanson, N.W., "Seismic Resistance of Concrete Frames With Grade 60 Reinforcement", Proceedings of the American

- Society of Civil Engineers, Vol. 97, ST6, June 1971, pp. 1685-1700.
- (76) Bennison, A., "Strength and Behaviour of R.C. Corners," M.Ph. Thesis University of Nottingham, England, Sept. 1971, 73 pp.
- (77) Burnett, E.F.P., Jajoo, R.P., "Reinforced Concrete Beam Column Connection", Proceedings of the ASCE, structural Div. Sept. 1971, ST9, pp. 2315-2335.
- (78) Nilson, A.H., "Bond Stress-Slip Relations in Reinforced Concrete", Report 345, School of Civil and Environmental Engineering, Cornell University, Ithaca, New York, Dec. 1971.
- (79) Backlund, J., "Limit Analysis of Reinforced Concrete Slabs by a Finite Element Method", Proceedings of the Specialty Conference. McGill University, Eng. Inst. of Canada, Montreal - 1972.
- (80) Desai, C.S., Abel, J.F., "Introduction to the Finite Element Method, A Numerical Method for Engineering Analysis". Van Nostrand Reinhold Company, New York, 1972.
- (81) Edwards, A.D., Picard, A., "Theory of Cracking in Concrete Members", ASCE Journal Proc., Dec. 1972, pp. 2687-2699.
- (82) Renton, G., "The Behaviour of Reinforced Concrete Beam-Column Joints Under Seismic Loading", Master of Engineering Thesis, University of Canterbury, New Zealand, 1972, 163pp.

- (83) Smith, B.J., "Exterior Reinforced Concrete Joints With Low Axial Load Under Seismic Loading", Master of Engineering Report, University of Canterbury, New Zealand, 1972, 86pp.
- (84) Townsend, W.H., "The Inelastic Behaviour of Reinforced Concrete Beam-Column Connections", Doctor of Philosophy Thesis, University of Michigan, 1972, 178pp.
- (85) P.S. Balint, H.P.J. Taylor, "Reinforcement detailing of frame corner joints with particular reference to opening corners", Cement and Concrete Association, Technical Report 42.462, London, February 1972, 16pp.
- (86) Liu, T.C.Y., Nilson, A.H., Slate, F.O., "Stress-Strain Response and Fracture of Concrete in Uniaxial and Biaxial Compression" ACI Journal, Proc. Vol. 69, No. 5, May 1972, pp. 291-295.
- (87) Liu, T.C.Y., Nilson, A.H., Slate, F. O. "Biaxial stress-strain Relations for Concrete" Journal of the Structural Division ASCE, Vol. 98, STS, May 1972, pp. 1025-1034.
- (88) Spokowski, R.W., "Finite Element Analysis of Reinforced Concrete Members" M.Eng. Thesis, Dept. of Civil Eng. and Applied Mechanics, McGill University, May 1972.
- (89) McCutcheon, J.O., Mirza, M.S., Mufti, A.A., ed. "Finite Element Method in Civil Engineering". Proceedings of the Specialty Conference. McGill University-Engineering Institute of Canada, Montreal, June 1972.

- (90) Ural, O. "Finite Element Method--A Versatile Tool for Civil Engineers" Proceedings of the McGill-Engineering Institute of Canada Specialty Conference on Finite Element Methods in Civil Engineering, McGill University, Montreal, June 1972, pp.155-173.
- (91) B. Mayfield, F.K. Kong, A. Bennison, "Strength and Stiffness of Lightweight Concrete Corners", ACI Journal, Proceedings, Vol. 69, No. 6, Detroit, July 1972, pp. 420-427.
- (92) Nilson, A.H., "Internal measurements of Bond-Slip", ACI Journal, Proc. Vol. 69, No. 7, July 1972, pp. 439-441.
- (93) Houde, J., "Study of the Force-Displacement Relationships for the Finite Element Analysis of Reinforced Concrete", Ph.D. Thesis, Dept. of Civil Eng. and Applied Mechanics McGill University, August 1972.
- (94) Loov, R.E., "Finite Element Analysis of Concrete Members Considering the Effects of Cracking and the Inclusion of Reinforcement". Ph.D. Dissertation, Cambridge University Sept. 1972, 125pp.
- (95) R. Park, T. Paulay, "Behaviour of reinforced concrete external Beam-Column Joints under cyclic loading," Vol. I Paper 88, Proceedings of the Fifth World Congress on Earthquake Engineering in Rome, 1973, 10 pages.
- (96) Chu-kia Wang, and Charles G. Salmon, "Reinforced Concrete Design", Second Edition, In text Educational Publishers, New York, 1973, pp. 32-74.

- (97) Ingvar H.E. Nilsson, "Reinforced Concrete Corners and Joints subjected to bending moment" Document 07:1973, National Swedish Building Research, Stockholm, 1973.
- (98) Neville, A.M., "Properties of Concrete", Pitman Publishing London, England, 1973, pp. 474-475.
- (99) Houde, J., Mirza, M.S., "A Finite Element Analysis of Shear Strength of Reinforced Concrete", ACI Special Publication SP 42-5, American Concrete Institute, Detroit, 1974, 965, pp.
- (100) ACI 315-74, "Manual of Standard Practice for Detailing Reinforced Concrete Structures", American Concrete Institute, Detroit, 1974, 965, pp.
- (101) Uzumeri, S.M., Seckin, M., "Behaviour of reinforced concrete beam-column joints subjected to slow load reversals", Publication 74-05, Univ. of Toronto, Dept. of Civil Engineering, March 1974.
- (102) Taylor, H.P.J., "The Behaviour of Insitu Concrete Beam to column Intersections," C & CA London, 1975.
- (103) Park and Paulay, "Reinforced Concrete Structures", John Wiley and Sons, Publishers, 1975.
- (104) ACI-ASCE Committee 352, "Recommendations for Design of Beam-Column Joints in Monolithic Reinforced Concrete Structures" ACI Journal Proc. Volume 73, No. 7, pp. 375-398, July 1976.

- (105) Cedolin, Luigi, and Dei Poli, Sandro, "Finite Element Studies of Shear-critical R/C Beams," Journal of the Engineering Mechanics Division, ASCE, Vol. 103, No. EM3, Proc. Paper 12968, June, 1977, pp. 395-410.

*NOTE: References designated by square brackets were not available to the author. Only summaries of these were read in other references.